



If you have discovered material in AURA which is unlawful e.g. breaches copyright, (either yours or that of a third party) or any other law, including but not limited to those relating to patent, trademark, confidentiality, data protection, obscenity, defamation, libel, then please read our [Takedown Policy](#) and [contact the service](#) immediately

PETROLOGY OF WEATHERED LOWER  
LIAS CLAYS.

A Thesis presented for the degree of Doctor of  
Philosophy in the Faculty of Engineering,  
University of Aston in Birmingham.

JAMES MARK COULTHARD

January 1975

THESIS

552.5 COU

188993 15 MAR 1976

## SYNOPSIS

In weak argillaceous rocks the unweathered strength may be barely sufficient to meet civil engineering requirements and any reduction due to weathering will be critical. This study investigates the weathering of the Lower Lias clays with particular reference to their petrography and engineering properties.

Investigations revealed the Midland Basin of deposition to contain reasonable thicknesses of clay, relatively uniform in nature with a well developed weathered zone. From the available exposures, the weathering zone of the Blockley Clay pit was selected and sampled for laboratory investigations of; Structure, Mineralogy and Chemistry and Engineering Properties.

The nature and orientation of the fissures in the unweathered clay were analysed. A close relationship was found to exist between the major joint set and the ground surface, with stress release due to excavation being almost negligible. Thin sections of the clay, examined for structural data, suggested that there exist layers or areas that have been disturbed as a result of density differences. Shear planes were found in both the unweathered and weathered clay, in the latter case often associated with remoulding of the material. A direct measure of remoulding was obtained from the birefringence ratio.

The fabric was examined in closer detail using the scanning electron microscope. Mineralogy, as revealed by X-ray and optical techniques indicated illite as the dominant clay mineral, with kaolinite subsidiary; quartz, calcite, pyrite, chlorite/vermiculite are present as accessory minerals. Weathering changes this relationship, calcite and pyrite being removed early in the process, with illite being degraded. The cementing action of calcite and

iron oxides was investigated however, this was shown to be negligible.

Quantitative measurements of both fixed (with minerals) and free (oxide coatings) iron were obtained by atomic absorption, with the  $\text{Fe}^{3+}/\text{Fe}^{2+}$  ratio obtained by Mossbauer spectroscopy. Evidence indicates that free iron oxide coatings only become important as a result of weathering with the maximum concentration in the very highly weathered material.

Engineering index properties and shear strength values were taken throughout the profile. Relationships between moisture content and strength, liquid limit and iron (Fe) were obtained and a correlation between the weathering zones and the shear strength/depth curve has been established.

### ACKNOWLEDGEMENTS

The work formed part of a general study being carried out at the University of Aston in Birmingham on Liassic Clay. The author gratefully acknowledges the financial help given by S.R.C. to carry out this project.

The author also wishes to thank the North Cot Brick Company for the use of the Brick Pits and for the help and guidance given by Dr.J.A.Morton and Dr.K.Starzewski. Many helpful discussions were also held with Dr.D.Vaughan, Dr.G.B.Briscoe, and Dr.M.A.Butterworth, for which the author was grateful.

The author is indebted to the technicians of the Geology and Civil Engineering departments in particular Mr.J.Williams and Mr.M.Lyons for all their help.

Special thanks are given to Mrs.P.M.Coulthard for the time and effort given in typing and preparing this thesis.

## CONTENTS

Chapter 1	Introduction	1
	1:1 Object of Study	1
	1:2 Aspects to be Investigated	2
	1:2:1 Structural	3
	1:2:2 Mineralogical and Chemical Changes	4
	1:2:3 Engineering Properties	4
	1:3 Choice of Site	4
	1:4 Previous Work	5
Chapter 2	Liassic Stratigraphy	6
	2:1 Introduction	6
	2:2 Palaeogeography in Lower Jurassic Times	7
	2:3 Basins of Sedimentation	13
	2:4 Liassic Sedimentation	19
	2:5 Cyclic Sedimentation of the Lias	24
Chapter 3	Area of Study	29
	3:1 Introduction	29
	3:2 Description of the Area	30
	3:2:1 Geology	30
	3:2:2 North Cot Brick and Tile Works (Blockley Clay Pit)	38
Chapter 4	Weathering and Soils	45
	4:1 Introduction	45
	4:2 Weathering	47
	4:3 Soils	50
	4:3:1 Soil Horizon Nomenclature	50

4:3:1:1	Organic and Organo-Mineral Surface Horizons	57
4:3:1:2	Sub-Surface Horizons	58
4:4	Engineering Classification	59
4:5	Summary of Classifications	64
4:6	Weathered Profile at Blockley Clay Pit Blockley Series	65
4:7	Honeybourne Clay Pit	71
Chapter 5	Mesostructures	76
5:1	Introduction	76
5:2	Discontinuities	77
5:2:1	Definitions and Observations	77
5:2:2	Origin	80
5:2:3	Classifications	86
5:3	Observation of Data	86
5:3:1	Block Technique	87
5:3:2	Cavity Technique	94
5:4	Presentation of Data and Validity	95
5:5	Joint Analysis at Blockley	97
5:5:1	Cavity Technique Results	98
5:5:2	Block Technique Results	99
5:6	Discussion	100
Chapter 6	Microstructures	107
6:1	Introduction	107
6:2	Preparation of Thin Sections	108
6:2:1	Carbowax 6000	108
6:2:2	Epoxy Resins	112
6:3	Procedure for Impregnation and Cutting	113
6:3:1	Carbowax	113

6:3:2	Epoxy Resins	114
6:4	Preparation of Electron Microscope Samples	117
6:5	Results of Thin Section Analysis	120
6:6	Results of the Scanning Electron Microscope (S.E.M.)	133
6:6:1	Open Structures	138
6:6:2	Denser Structures	139
Chapter 7	Mineralogy	150
7:1	Introduction	150
7:2	Clay Minerals	153
7:2:1	Classification and Identification	153
7:2:2	Sample Preparation	159
7:2:3	Previous Work	159
7:2:4	Clay Mineralogy of the Lias at Blockley	162
7:3	Non-Clay Minerals	172
7:3:1	Quartz	172
7:3:2	Calcite	172
7:3:3	Iron Minerals	175
7:3:3:1	Spheres	175
7:3:3:2	Irregular Veins	180
7:3:4	Organic Material	180
7:3:5	Feldspars	181
Chapter 8	Geochemical Analysis	184
8:1	Introduction	184
8:2	Carbonate Analysis	185
8:2:1	Results and Discussion	186
8:3	Iron Analysis	189
8:3:1	Iron Content Determination and Sample Preparation	189
8:3:2	Removal of Free Iron Oxides	189



8:3:2:1	Procedure	192
8:3:3	Total Iron Determination	192
8:3:3:1	Fusion	192
8:3:3:2	Concentrated Acids	193
8:3:3:3	Procedure for Total Iron Determination	194
8:3:4	Results and Discussion	200
8:3:4:1	Total Iron	200
8:3:4:2	Extractable Iron	202
Chapter 9	Oxidation State and Position of Iron	204
9:1	Mossbauer Spectroscopy Analysis	204
9:2	Source	204
9:3	Apparatus	205
9:4	Application of Spectral Data	208
9:4:1	Isomer Shift (I.S.)	208
9:4:2	Quadrupole Splitting (Q.S.)	209
9:4:3	Hyperfine Magnetic Interactions	211
9:4:4	Relative Intensities	212
9:5	Sample Preparation	213
9:6	Calibration of Equipment	214
9:7	Previous Work	217
9:8	Results	220
9:9	Analysis of Results	222
9:9:1	Spectra at Room Temperature	222
9:9:1:1	Variation with Depth	223
9:9:1:2	Intensity of Peaks	227
9:9:2	Spectra at 77°K	228
9:9:2:1	Intensity of Peaks	231
9:10	Conclusions	231

Chapter 10	Engineering Properties	233
10:1	Introduction	233
10:2	Engineering Tests	233
10:2:1	Moisture Contents	233
10:2:2	Liquid and Plastic Limit Determinations	236
10:2:3	Particle Size Distribution	243
10:2:4	Soil pH	245
10:2:5	Strength	246
10:2:5:1	Overburden in the Blockley Area	246
10:2:5:2	In Situ Strength Tests	247
10:2:5:2:1	Shear Vane	249
10:2:5:3	Results	251
10:2:5:4	Strength Parameters for Unweathered Lower Lias Clay	251
10:2:5:5	Moisture Content and Torvane Tests	252
10:3	Discussion of Results	253
10:3:1	Strength: Water Content Relationship	253
10:3:1:1	Introduction	253
10:3:2	Strength: Depth Relationship	262
Chapter 11	Conclusions	265
11:1	Introduction	265
11:2	Structure	265
11:2:1	Macrostructural Changes	265
11:2:2	Microstructure	269
11:2:2:1	Fabric	270
11:2:2:2	Sedimentary Structures	271
11:2:2:3	Results of Weathering on Microstructure	271
11:3	Mineralogical and Chemical Changes	272

11:3:1	Mineralogy	273
11:3:2	Chemistry	273
11:4	Engineering Properties	275
11:5	Discussion	276
11:6	Further Work and the Value of Techniques Used	276
	References	282
	Appendices	302
Appendix A	Samples	302
A:1	Hand Samples	303
A:2	Borehole Samples	305
A:2:1	Borehole 1	305
A:2:2	Borehole 2	305
A:2:3	Borehole 3	306
A:3	Block Samples	306
Appendix B	A Method of Obtaining the Optimum Sample Size for a Truly Representative Fissure Fabric Proposed by Stauffer, M.R. (1966)	307
B:1	Simple Fabrics	307
B:2	Combined Fabrics	308
Appendix C	X-Ray Analysis	310
C:1	X-Ray Production	310
C:2	Recording Techniques	311
C:3	Types of Powder Specimen	312
C:3:1	Orientated Flat-Layer Specimens	312
C:3:2	Orientated and Non-Orientated Rod Type Specimens	312
C:3:3	Non-Orientated Plate Specimens	313
C:4	Sample Preparation and Size	313
C:5	Quantitative Analysis	314

Appendix D	Chemical Analysis	317
	D:1 Calcite Analysis	317
	D:2 Sample Preparation	317
	D:3 Procedure	317
	D:4 Calibration	320
	D:5 Calculation	320
Appendix E	Infra-Red Spectroscopy	321
	E:1 Introduction	321
	E:2 Sample Preparation	321
	E:3 Results	325
	E:4 Conclusions	333
Appendix F	Atomic Absorption	334
	F:1 Atomic Absorption Analysis	334
	F:2 Theory	334
	F:3 Method and Techniques	335
	F:4 Interferences	336
	F:5 Method of Analysis	337
Appendix G	Atomic Absorption Program	340
	G:1 Introduction	340
	G:2 Program Description	340
	G:2:1 Calculations	343
	G:3 Flow Diagram	344
	G:4 Programming Instructions	345
	G:5 Program Listing	348
	G:6 Store Registers Used	356
Appendix H		357
	H:1 Mossbauer Spectroscopy	357
	H:2 Theory	357
	H:2:1 Resonance and Resonant Absorption	357
	H:2:2 Emission of Gamma-Ray by Nuclei	358

Appendix I		363
I:1	Analysis of Mossbauer Spectra by Computer	363
I:2	Mossbauer Spectrum	368
I:3	Hardware Requirements	368
I:4	Input	370
I:5	Output	370
I:6	Example	371
I:7	Major Names used in the Program	373
I:8	Flow Diagram	374
I:9	Program Listing	383
Appendix J		
I	Mossbauer Spectra at Room Temperature	383
II	Mossbauer Spectra at 77°K	393

## LIST OF TABLES

Chapter 2		8
2:1	Jurassic System	8
2:2	Lias Stages and Zones	8
2:3	Main Iron Ores in the Lias	23
Chapter 4		
4:1	Weathering	47
4:2	Fundamental Weathering Processes	49
4:3	Weathering Scheme (Skempton & Davis 1966 for Keuper Marl)	62
4:4	Engineering Grade Classification of Weathered Rock (Fookes and Horswill 1969)	63
Chapter 5		
5:1	Fracture Development (Gramberg 1966)	85
5:2	Fracture Spacing Index ( $I_f$ )	87
Chapter 6		
6:1	Polyethylene Glycols	109
6:2	Properties of Araldite AY18	113
Chapter 7		
7:1	Mineralogy (Point Counting)	151
7:2	Clay Mineral Classification	154
7:3	Effect on the Basal Spacing of Various Pre-Treatments	160
7:4	Percentage of Major Clay Minerals	170
Chapter 8		
8:1	Variation of Carbonate Content	187
Chapter 9		
9:1	Isomer Shifts for Various Sources and Standards	215
9:2	Mossbauer Results of Previous Workers	218
9:3	Mossbauer Results of Blackley Clay Samples	221

9:4	Ionic Radii	224
9:5	Radius Ratio of an Octahedral Site	225
9:6	Mossbauer Results of Previous Workers	230
Chapter 10		
10:1	Liquid and Plastic Limits for Section One and Borehole Samples	237
10:2	Liquid and Plastic Limit Divisions	239
10:3	Particle Size Results	244
10:4	Soil pH Results	245
10:5	Strength Parameters for Unweathered Lower Lias Clay	250
10:6	Shear Strength at Failure, Section Two	250
10:7	Strength/Moisture Content Values for Block 2B	252
10:8	Forces between Clay Particles	258
Chapter 11		
11:1	Summary of Weathered Profile	266 & 267
Appendices		
C:1	X-Ray Wavelength Values	310
E:1	Carbonate Group Absorption Peaks	332
F:1	Elements and Detection Limits	339

## LIST OF FIGURES

Chapter 2		
2:1	Palaeogeography in Lower Jurassic Times	9
2:2	Lias Isopach Map of Western Europe	10
2:3	Lithofacies in Europe and Adjacent Areas during Lower Pliensbachian	10
2:4	Sketch Diagram of the Blockley Area	15
2:5	Section through the Basins of Sedimentation during the Lower Liassic period	21
2:6	Rhythmic Sedimentation (Klupfel 1917)	25
2:7	Rhythmic Sedimentation (Hallam 1964)	25
Chapter 3		
3:1	Outcrop of Jurassic Rocks in Britain	31
3:2	Geological Map of the Blockley Area	31
3:3	Geography of the Blockley Area	37
3:4	Geological Section, Blockley Clay Pit	39
Chapter 4		
4:1A)	Intensity of Chemical Weathering in Relation to Rainfall and Temperature	51
B)	Intensity of Frost Weathering in Relation to Rainfall and Temperature	51
4:2A)	Diagram of Climatic Boundaries of Morphogenetic Regions	52
B)	Weathering under various Rainfall and Temperatures	52
4:3	Weathering Processes	53 & 54
4:4	Correlation between Engineering and Pedological Classifications of Weathered Rock	65
4:5	Moisture Content/Depth Relationships, Blockley	72



4:6	Moisture Contents, Weathering Zones and Samples Section One	73
Chapter 5		
5:1A)	Hydrostatic Stress Conditions	83
B)	Tectonic Stress as Residual Stress	83
5:2	Joint Orientation Site II	103
5:3	Joint Orientation Site I	104
5:4	Joint Orientation Site I, II, III	105
5:5	Joint Orientation Block Sample 2B	106
Chapter 6		
6:1	Crystal Violet Structure	111
6:2	Slide Grinding Attachment	115
6:3	Apparatus for Epoxy Resin Impregnation	116
6:4	Birefringence Ratio/Depth Relationship	132
6:5	Types of Structure (Smart 1969)	135
6:6	Mechanisms between Adjacent Particles	136
6:7	Arrangements of Clay Particles (Burnham 1970)	137
6:8	Domains (Smart 1967)	136
6:9	Turbostratic Structure and Subdivisions	140
Chapter 7		
7:1	X-ray Diffraction Traces with Depth (Section One)	163
7:2	X-ray Diffraction Trace (Sample S17/1 - Normal, Heated and Glycolated)	164
7:3	X-ray Diffraction Trace (Sample S27/1 - Normal, HCl and Glycolated)	165
7:4A)	Percentage of Clay Minerals with Depth	166
B)	Peak Intensity with depth ( $14\text{\AA}$ , $10\text{\AA}$ , $7\text{\AA}$ )	167
7:5	Alterations of Clay Minerals	171
7:6	Spheroidal Mass of Pyrite Spheres	177

	7:7	A String of Pyrite Spheres	177
Chapter 8			
	8:1	HCl Extracted Iron with Depth (Section One and Two)	195
	8:2	Total Iron and Extracted Iron (Extraction Solution) with Depth, Section Two.	196
	8:3	Total Iron and HCl Extracted Iron with Depth, Section Two	197
	8:4	HCl Extracted Iron and Extracted Iron (Extraction Solution) with Depth, Section One	198
	8:5	Rate of Iron Extraction	199
Chapter 9			
	9:1	Decay Scheme for Co <sup>57</sup>	206
	9:2	Diagrammatic Layout of the Mossbauer System	207
	9:3	Typical Mossbauer Spectrum (Single peak)	206
	9:4	Ground and Excited States of Fe <sup>57</sup>	210
	9:5	Sample Holder	210
	9:6	Mossbauer Spectra of Natural-Iron and Stainless-Steel	216
Chapter 10:			
	10:1	Moisture Contents/Depth Relationships (Borehole Samples)	234
	10:2	Plasticity Index/Liquid Limit Relationships	238
	10:3	Plasticity Index/Clay Fraction Relationships	
		A) Various Clays (After Skempton 1953)	240
		B) Lias Clay	240
	10:4	Liquid Limit/Fe (HCl-Extracted) Correlation	242
	10:5	Strength/Water Content Relationship	254
	10:6	Strength/Water Content Relationship	255
	10:7	Strength/Depth Relationship	256
	10:8	Forces between Clay Particles	257

10:9	"Swelling Curves", Bjerrum 1967	
	A) Water Content/Effective Overburden Pressure	259
	B) Water/Strength	259
10:10	Strength/Weathering Zone Relationship	263
Chapter 11		
11:1	Blockley Profile Summary Chart	268
11:2	Birefringence Ratio Variations within Sample S11/1	274
Appendices		
Appendix D:1	Carbonate Analysis Apparatus	318
E:1	Crystal Structure of Kaolinite	323
E:2	Typical Infra-red Spectra of Clay Minerals	324
E:3	IR-Spectrum of Kaolinite	326
E:4	IR-Spectra of Blockley Clay Samples	327
E:5	Detail of 2.5-3.0 $\mu\text{m}$ Portion of Spectra in E:3 and E:4	328
E:6	Detail of 5.5 to 8.5 $\mu\text{m}$ Portion. Sample S40/1	330
E:7	IR Spectra of Blockley Clay Samples; Acetic Acid Treated	331
G:1	Atomic Absorption Plot	342
H:1	Optical Emission and Absorption Spectra	358
H:2	Optical and Gamma Ray Spectra	358
I:1	The Lorentzian Distribution	364
I:2	Typical Output	365
I:3	Computer Program Structure	364

LIST OF PLATES

Chapter 3		
3:1	Thin Sections of Tree Fragment (plane polarised light)	42
Chapter 4		
4:1	Blockley Clay Pit Section One(0.0m - 1.5m)	68
4:2	Blockley Clay Pit Section One(1.5m - 3.2m)	69
4:3	Blockley Clay Pit Section One(3.2m - 4.5m)	70
Chapter 5		
5:1	Block Technique for Fissure Analysis	90
5:2	" " " " "	90
5:3	" " " " "	91
5:4	" " " " "	91
5:5	" " " " "	92
5:6	" " " " "	92
5:7	" " " " "	93
5:8	" " " " "	93
Chapter 6		
6:1	Treated and Untreated Clay Surface (Electron Microscope)	119
6:2A)	Density Structures (Sample S39/1)	121
6:2B)	" " " "	122
6:3A)	Failure Zones (Sample S32/1)	126
B)	" " " "	127
6:4	Silt Bands showing Displacements Along Shear Plane (Sample S32/1)	128
6:5A)	Flame Structure and Shear Plane (Sample S32/1/A)	129
B)	Shear Plane (Sample S32/1/A)	129
6:6	Iron Stained Lithorelic and Remoulded Material	131

6:7	Turbostratic Fabric	143
6:8	Locked Turbostratic Fabric	143
6:9	Grain Turbostratic Fabric	144
6:10	Stereoscopic Pair (Parallel to Bedding)	145
6:11	Stereoscopic Pair (Parallel to Bedding)	146
6:12	Kaolinite Flakes	144
6:13	Kaolinite Flakes	147
6:14	Authigenic Magnetite	147
6:15	Selenite Crystals	148
6:16	Clay Growths	148
6:17	Clay Growths	149
6:18	Clay Growths	149

#### Chapter 7

7:1	Random Structure and Quartz Concentration (Sample S1/1)	173
7:2	Silt Horizons (Sample S32/1)	174
7:3A)	Pyrite Spheres in a Spheroidal Mass	178
B)	Pyrite Mass with Calcite Infilling	178
7:4	Pyrite Strings and Flame Structure	179
7:5	Feldspar Pseudomorphs (crossed nicols )	182
7:6	Feldspar Pseudomorphs (plane polarised light)	182

## CHAPTER 1

### INTRODUCTION

#### 1:1 OBJECT OF STUDY

Geological materials, when subjected to the processes of weathering undergo marked changes in both lithology and engineering properties. In virtually all civil engineering schemes such weathered materials are involved to some greater or lesser extent. The involvement may be in place either as a foundation or exposed in excavations and cuttings. Otherwise the material may be excavated and used as a fill in a variety of situations.

The rate of weathering is very variable ranging from a few days to thousands of years. In many cases the civil engineer is involved in assessing both the long term and the short term stability of foundations, side slopes etc. The accelerated degradation of buildings constructed of Magnesian Limestone and the part played by weathered material in the Malpasset (Report 1960) and Vaiont (Kiersch and Asce 1964) disasters highlights this importance.

Whilst the deterioration of strength as a result of weathering is greater in strong rocks than in weak, it is only rarely that the former is of consequence in civil engineering. In weak argillaceous rocks the unweathered strength may be barely sufficient to meet the civil engineering requirements and any reduction due to weathering will be critical.

Chandler (1969) when studying the effects of weathering on the Keuper marl indicated that the liquid limit and natural moisture content of the marl increased with increasing weathering whereas the bulk density, permeability,  $c'$ ,  $\phi'$  and  $\phi'_r$  (effective stress parameters describing strength) all decreased. The nature of the degradation will be dependent on the original material (mineralogy

and structure), the climate and time.

It is well known that slope failure occurs in very low angled slopes, often when it is not expected. Chandler (1971, 1972) has shown that slopes in Upper Lias clay have failed when the natural angle of slope was between  $7^{\circ}$  -  $16^{\circ}$  and yet cuttings in the Upper Lias in the same area, with similar slope angles and greater, are stable. Chandler therefore suggested that the failures have occurred at locations where the Upper Lias clay is less strong probably as a result of weathering or where there is a greater influence of ground water conditions.

Weathering leads to chemical and structural changes which in turn influence  $c'$ ,  $\phi'$  and  $\phi'_c$ . Therefore the use of strength parameters without reference to the state of the material may lead to the over-, or underdesign of slopes, even though the material has the same index properties.

The object of the present investigation was to obtain information on the degradation characteristics of Lower Lias clay due to weathering. It was intended to correlate weathering changes with engineering properties. Therefore a site was chosen where previous glacial and periglacial conditions had not seriously affected the normal weathering processes.

#### 1:2 ASPECTS TO BE INVESTIGATED

Observation of the degradation of Lower Lias clay due to weathering necessitates an intense study of the unweathered and weathered material in order that comparisons may be made. A program of sampling and examination was carried out with the view of inspecting all aspects that were likely to change with weathering.

All observations can be broadly grouped under three main

headings; Structure, Mineralogy and Chemistry, Engineering Properties.

### 1:2:1 STRUCTURE

Mesostructures can be defined as those structures visible to the naked eye, but excluding faults, folds etc., which have a large regional extent. Thus the nature of the material, its appearance, the orientation of discontinuities (primarily joints) can be treated in a single analysis. The data obtained here were often found to have important influences in later investigations.

Sedimentary structures would normally be treated as mesostructures, but due to the nature of the Lower Lias clay these are often only observable in thin section or acetate peels (staining with crystal violet or ferric chloride will often enhance any such structures). The smaller sedimentary structures and primary fabric (microstructure) can be investigated using the optical microscope.

As clays are often less than 2  $\mu\text{m}$  in size and therefore out of range of optical microscopes, (except when the clays form domains) the specialised techniques of scanning electron microscopy and texture determination by X-rays were necessary to determine the particle orientation.

Texture analysis by X-rays in the case of clays relies on the reflection of X-rays from the basal surfaces (001) of the clay minerals. Although it proved preferential orientation of the clay minerals in a quantitative manner it was felt that scanning electron microscopy enabled preferred orientation to be investigated in more detail since the particles can be observed directly.

Information obtained in this part of the investigation provided data on the physical changes in the material due to weathering.



### 1:2:2 MINERALOGY AND CHEMISTRY

Mineralogical and chemical changes are closely interrelated and the study of either has considerable bearing on the other. Mineralogy was investigated by both optical microscopy and X-ray diffraction techniques. Quantitative chemical analysis employed the use of Atomic Absorption, Infra-Red Spectrometry, Mossbauer Spectroscopy and Standard laboratory procedures. The information thus obtained enables the chemical changes due to weathering to be assessed.

### 1:2:3 ENGINEERING PROPERTIES

A detailed investigation of the engineering properties (index and strength parameters) was to be carried out at frequent intervals down the soil profile;  $c'$ ,  $\phi'$  and  $\phi'_r$  being obtained by further research students as part of a more extensive investigation of the Lower Lias clay. Due to unforeseen circumstances the only strength results available were those obtained by the Torvane (Chapter 10) and the  $c'$ ,  $\phi'$  and  $\phi'_r$  for the unweathered material.

### 1:3 CHOICE OF SITE

The project therefore required a reasonable thickness of Lower Lias clay, relatively uniform in nature with a well developed weathered zone. An investigation of the stratigraphy of the Liassic deposits (Chapter 2) indicated that the Midland basin was most uniform, with fewer limestone bands and greater thicknesses of clay. There was also the fact there this area had been exploited by the brick manufacturing industry and therefore excavations enabling direct examination would be available.

A survey of the area proved that apart from temporary exposures due to construction, brick pits were the only exposures of the Lias. The majority of these have now closed down and had become totally

overgrown. The Blockley Clay Pit was still working and therefore the profiles were fresh and easily examined. The site had good access and drilling was accomplished with minimum inconvenience to the Brick Company. The pit had previously been investigated on palaeontological grounds (Chapter 3) and therefore the stratigraphy of the section through the unweathered Lower Lias clay was known with reasonable accuracy.

#### 1:4 PREVIOUS WORK

Previous works on the weathering of hard rocks, the state of disintegration and the mechanisms of physical and chemical weathering have been numerous (Chapter 3). However, the effect of weathering of soft rock and particularly its influence on engineering properties has been neglected. Chandler (1969) in his study of Keuper marl, investigated the change of effective strength parameters with weathering; however, no work was carried out on the chemical and structural changes with a view to correlation. More recently, Chandler (1972) states that a detailed chemical and mineralogical examination of the Upper Lias clay was not attempted.

A literature search also revealed that very little had been done on the geochemistry of the Lias clay (Le Riche 1959, Hallam 1960, Catt et al. 1971). Similarly, it appears that no investigation of the mineralogy and structure of these clays has been attempted. Since only a few examinations had been carried out on the Lower Lias clay very little information could be used from previous workers to supplement this investigation. Such relevant work is referred to in the appropriate chapters.

## CHAPTER 2

### LIASSIC STRATIGRAPHY

#### 2:1 INTRODUCTION

The Liassic or Lias is the name given to the lowest of the three major divisions of the Jurassic which is also the most uniform in lithology, being usually argillaceous. The name Lias, stems from the Gaelic word "Leac", meaning a flat stone since at several horizons in the Lias, muddy and shelly limestones exist in thin beds.

The Jurassic system was defined as early as 1829 and takes its name from the development of strata of that age in the Jura Mountains. The relatively thick succession of strata in Britain which comprise the Jurassic system was initially subdivided on lithology and fauna by William Smith in the first half of the nineteenth century. However Oppel and Quenstedt working on the German Jurassic established a zonal system based on the ammonite fauna which redefined the lithological divisions on a faunal basis.

Eleven stages are now internationally recognised but in Britain it is still convenient to continue with the usage of a twelfth, the Purbeckian. These stages comprise a great number of Zones and Subzones due to the abundance of ammonites during the Jurassic times and their rapid and complex evolution. For example the Lower Jurassic or Lias is divided into twenty-two zones and forty-nine Subzones (Tables 2:1 and 2:2).

The base of the Jurassic system in Britain is now taken as the top of the Rhaetic, the Rhaetic being placed in the preceding Triassic system. In Britain early workers used lithology as the

main basis of division and since the Rhaetic was the first invasion of Keuper lake-flats by the shelf seas it was naturally placed in the Jurassic because of its marine nature. In the type area for the Rhaetic in the Eastern Swiss Alps, the ammonites found are similar to the marine Triassic of the Tethys environment. They differ considerably from the later Jurassic ammonite fauna and hence the Rhaetic is now placed in the Triassic system.

## 2:2 PALAEOGEOGRAPHY IN LOWER JURASSIC TIMES

The present day outcrop of the Jurassic in Britain, is arcuate in shape extending from Lyme Regis on the south coast in a north-easterly direction reaching the North Sea coast in Yorkshire. Outliers are found at Prees (Cheshire), Carlisle (Cumbria) and in the north-west Scotland notably Skye, Ardnamurchan, Mull, Raasay and Morvern.

From Yorkshire to the southern Midlands the Jurassic rocks have a gentle regional dip varying from east to south-east, the many minor divergences having little effect on the broad crescentic sweep of the main outcrop. In southern England the Alpine Orogeny of approximately early Miocene age has had a greater effect on the Jurassic strata with folds becoming more acute. In south Dorset the outcrop is complicated by the acuteness of the anticlines which have locally overturned northern limbs and are associated with reversed faulting. Furthermore intra-Cretaceous movements and the considerable overstep of the Upper Cretaceous also modify the outcrop considerably.

A general indication of the Lias palaeogeography which was inherited to some extent from the Triassic, is given in Figs 2:1, 2:2, 2:3.

TABLE 2:1

JURASSIC SYSTEM

Upper Jurassic	( Purbeckian
	( Portlandian
	( Kimmeridgian
	( Oxfordian
	( Callovian
Middle Jurassic	( Bathonian
	( Bajocian
	( Aalenian
Lower Jurassic or Lias	( Toarcian
	( Pliensbachian
	( Sinemurian
	( Hettangian

TABLE 2:2

LIAS STAGES AND ZONES

Toarcian or Upper Lias	( Pleydellia aalensi	) Yeovilian
	( Dumortieria levesquei	
	( Grammoceras thoursense	
	( Haugia variabilis	
Upper Pliensbachian or Middle Lias	( Hildoceras bifrons	) Whitbian
	( Harpoceras falcifer	
	( Dactylioceras tenuicostatum	
Lower Pliensbachian	( Pleuroceras spinatum	)
	( Amaltheus margaritatus	
	( Prodactylioceras davoei	
Sinemurian	( Tragophylloceras ibex	)
	( Uptonia jamesoni	
	( Echioceras raricostatum	
	( Oxynoticeras oxynotum	
	( Asterocheras obtusum	
Hettangian	( Caenisites turneri	)
	( Arnioceras semicostatum	
	( Arietites bucklandi	
	( Scholtheimia angulata	
	( Alsatites liasicus	)
	( Psiloceras planorbis	
	( Pre-Planorbis Beds	

FIG 2:1

PALAEOGEOGRAPHY IN LOWER JURASSIC TIMES

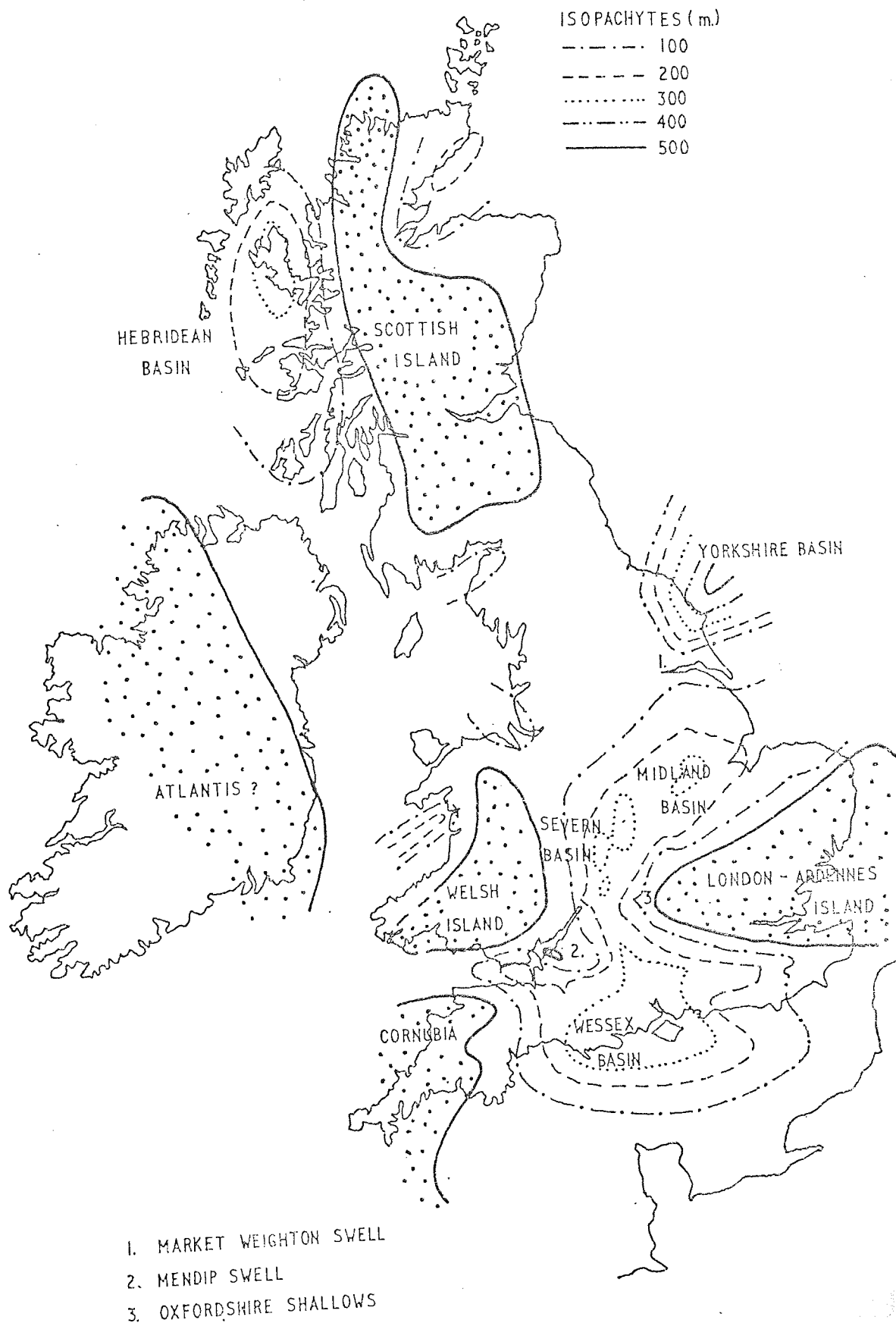
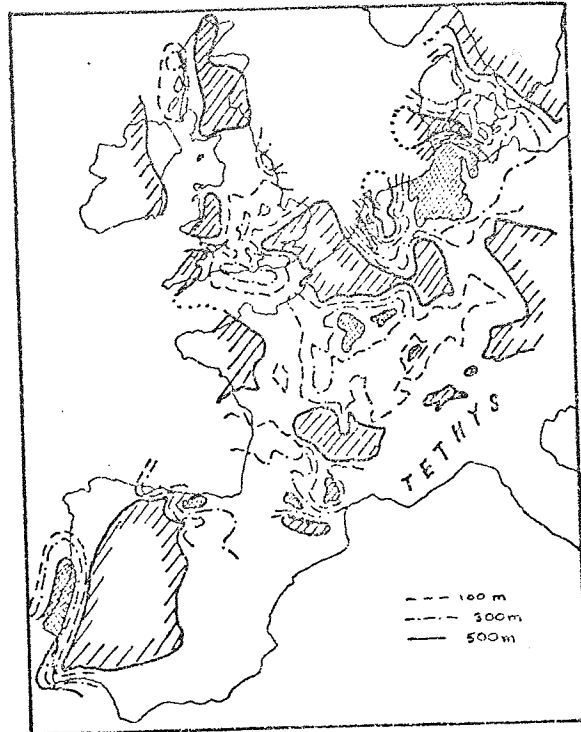
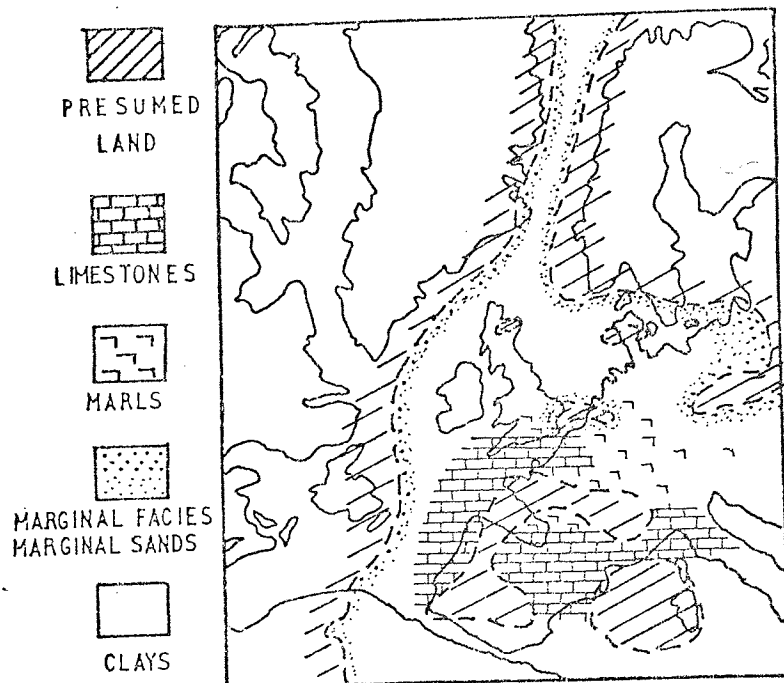


FIG 2:2



LIAS ISOPACH MAP OF W. EUROPE  
AFTER TOGT [1963]

FIG 2:3



LITHOFACIES IN EUROPE AND ADJACENT AREAS  
DURING LOWER PLIENSBACHIAN  
AFTER SELLWOOD [1972]

The major part of western Europe consisted of a shallow shelf sea with the deeper water of the Tethys geosyncline to the south. On the subdivision of basin types by Bitterli (1963), this shallow shelf sea would be classed as epicontinental;

"one which is generally of limited extent, covering temporarily or encroaching upon a previous continent, and in which the water is usually of shallow to moderate depth."

On the southern edge of this epicontinental sea bordering the Tethys deeps, a limestone facies developed whereas further north the sediment was mainly argillaceous in nature.

The area of deposition in the Lias of Europe consisted of basins, partially connected but separated by belts or areas of shallowing, or actual islands. In the west was the supposed land mass of Atlantis (covering the major part of Ireland) with its shores running parallel to the north-west of Scotland. In many palaeogeographical reconstructions Scotland is shown as one large landmass forming the Scottish-Pennine Island; there is however, no good evidence for this Pennine extension (Hallam 1964b, 1966). Initially Northern Scotland itself may have been a large land area in early Lower Lias times. However in the closing stages of the Lower Lias, when there is thought to have been a eustatic rise in sea level over the whole of Europe (Hallam 1961, 1964a) Scotland could have been reduced to a series of scattered islands. Hudson (1964) working on the petrology of the Great Estuarine Series of the Middle Jurassic concluded that the Scottish mainland was a major source of sediment. Therefore it is reasonable to suppose



that in Liassic times Scotland was in fact a large island or a series of small ones where little if any sediment was derived until after the earth movements of the Middle Jurassic.

Wales was originally thought to have been part of Atlantis. The discovery of 1304m of lias sediment in a borehole at Mochras, west of Llanbedr (Woodland 1971 ) has necessitated a reappraisal of the palaeogeography. A basin of deposition is postulated and Wales is now considered to have been similar to Scotland, either as one large island or an archipelago.

To the north east of Britain was Fenno-Scandia. This landmass had relatively sufficient relief to develop large river systems draining into the German basin and the North Sea area (Arkell 1956). An estuarine gulf existed in the area of present day east Germany and southern Sweden an area of seven hundred square kilometres. This suggests a large river system draining from northern Sweden and Russia across the low lying Russian Platform. It has been shown by recent work (Sellwood 1972) that the island of Bornholm Denmark was adjacent to this estuarine gulf. A section here of Sinemurian age was interpreted as a regressive tidal flat with a supra-tidal salt-marsh (coals and rootlet-beds) flaser- and wavy-bedded clays and sand, and subtidal sand bars. The quantity of sediment deposited in Jurassic times indicates that this was not the only major river, yet there is no good evidence for rivers from the north-west.

Information on the Jurassic climate is deduced from several disciplines although actual temperatures were first calculated by Urey et al. (1951). Colbert and Kay (1965) have calculated temperatures (based on a relative abundances of oxygen isotopes in carbonate

shells, mainly belemnites) for the Jurassic of western Australia. They indicate a mean annual temperature of  $25^{\circ}\text{C}$  with a seasonal range of  $\pm 5^{\circ}\text{C}$ . Temperature measurements of belemnoids of western Europe suggest a sea temperature of  $21^{\circ}\text{C}$  although Schwarzbach (1963) reports temperatures from the French Lias of  $24^{\circ} - 25^{\circ}\text{C}$  and from the Scottish Jurassic as  $17^{\circ} - 23^{\circ}\text{C}$ .

It is a known fact that temperatures in the Jurassic period were uniformly high, the difference between equatorial and polar temperatures were not as marked as at the present time. Although there was a cooler Boreal Province it is thought that temperatures were still high enough to prevent any glaciation taking place. A humid belt in Jurassic times existed crossing Scandis and northern Britain, the drier southern edge of this belt being marked by the northern limit of the coral reef. In the areas of more humid climate where coal formation sometimes resulted in extensive kaolinization as in Scandis, this, together with the characteristic clay mineral facies of the Lias, suggests intensive chemical weathering of the source area probably due to the development of red and yellow podzolic soils of subtropical woodlands. Fossil spore studies support this view. Strakhov (1962) reports that the flora of Europe consisted mainly of Cycadeans and Ginkgoaceous plants, conifers being reduced to a secondary importance. In Franz Josef land however in the Boreal region, the flora was mainly conifer.

### 2:3 BASINS OF SEDIMENTATION

Due to the nature of the ribbon like outcrop of the Jurassic in Britain, early workers Kendall (1905), Buckman (1901) and Arkell (1933a) postulated ridges or axes separating the basins of deposition, and since then it has been standard practice to relate all facies

changes and variations to these so called axes of uplift. Arkell (1933a) defined axes as;

"positive areas of little sedimentation and occasional unconformity separating basins one from another, linear in plan with a definite direction."

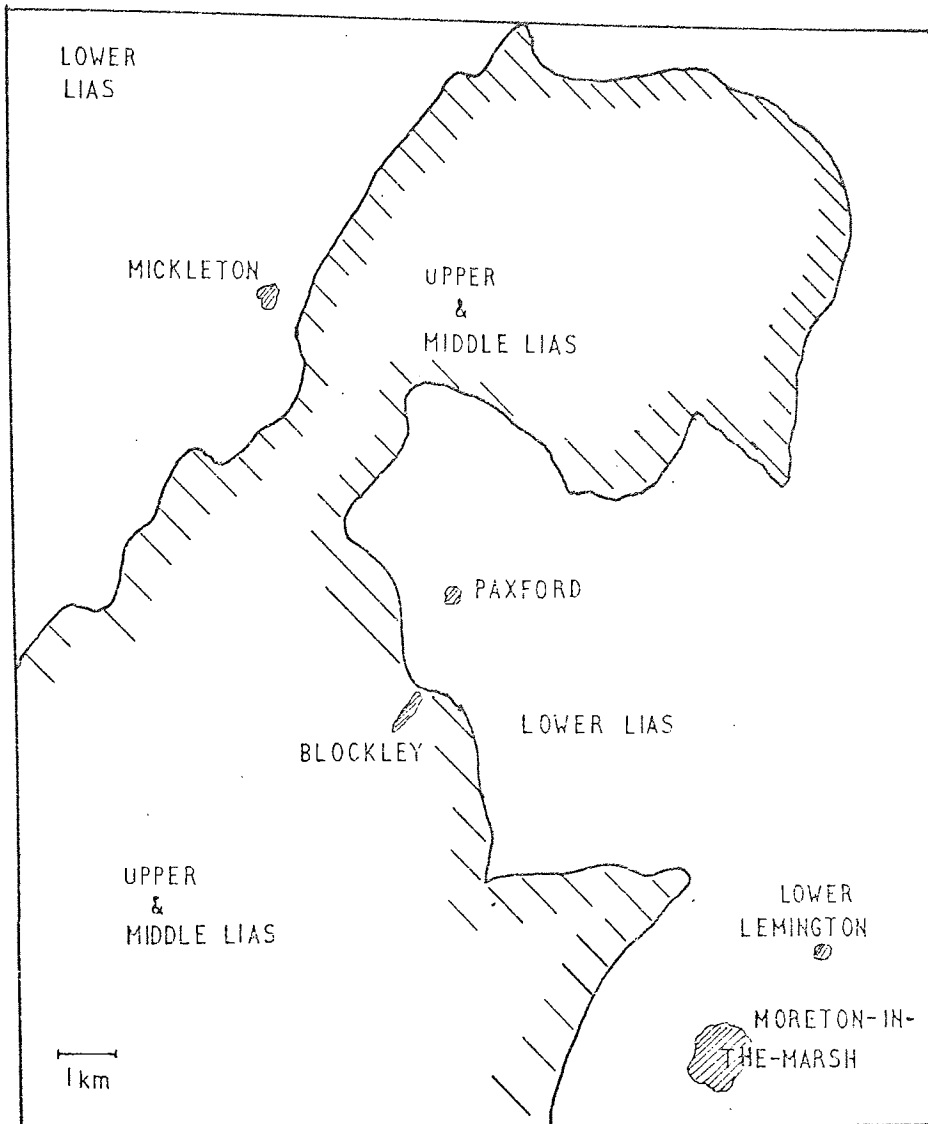
Godwin-Austin (1856) first put forward the theory of the Mendips acting as an axis in Jurassic times, soon after this many others were proposed: The Market Weighton, Melton Mowbray, Banbury Weedon Moreton-in-the-Marsh and several of minor importance. They were said to be related to ancient Palaeozoic structures and produced intra-Jurassic movements.

Arkell (1933a, b) in his works added several other minor axes but also wrote a critical review of all the axes suggested up to that time. Because of new evidence produced at this time Godwin-Austins Mendip axis was shortened in length since when originally proposed it extended through the Weald, and borings had now proved a thick sequence of Jurassic rocks in this area. Arkell (1933a) noted that the Vale of Moreton axis where Buckman (1901) had observed the Inferior Oolite to thin, could not be related to one line.

There was distinct evidence at the time for three Major axes, these being:

- 1) Mendip: trend east-west.
- 2) Market Weighton: trend east-west.
- 3) Oxfordshire or Moreton-in-the-Marsh: trend dominantly north-east south-west.

In the Moreton area the Lower Lias clays thin towards the south-east onto the Oxfordshire shallows, evidence coming from



SKETCH DIAGRAM OF THE BLOCKLEY AREA

FIG 2:4

boreholes. The Mickleton (SP162436) boring on the west side of Ebrington Hill proved the base of the Lias at 195m below O.D. giving the Lias a thickness of 292m. A second boring at Lower Lemington (SP219345) indicates the thickness of the Lias as 152m. This is a thinning in the region of 140m over a distance of 11km. (Sketch Diagram Fig. 2:4).

Hull (1855) and Buckman (1901) suggested an "anticline" in the lower rocks with the axis through the Vale of Moreton. Evidence comes from the beds of the Upper Lias and Inferior Oolite which thin over it and then thicken again. Such thinning across an axis has not been observed for the Lower Lias, the thinning in this case being interpreted by Arkell (1947) as due to a northward shelf like projection from the Oxfordshire shallows.

By 1947 when Arkell wrote his Geology of Oxford he was of the opinion that the Vale of Moreton axis was in fact a mythical entity and that the local thinnings and disappearance of Mesozoic sediments were better explained by the presence of the "Oxfordshire shallows", which were a broad extension of the London Platform. Kent (1949) examined the pre-Permian land surface in England by analysing borehole data and concluded that the Mesozoic basins did not arise from posthumous folding but were due to vertical movements on essentially different lines from those which controlled pre-Permian sedimentation. This suggests that the Mendip axis is in fact a shelf like projection from the Welsh Island.

Kent (1956) made a thorough investigation of the Market Weighton axis and concluded that the structure is in fact a stable "block" of limited extent, with a WNW - ESE orientation. There was evidence for troughs of deposition both to the east and west, and the facies changes in the Jurassic were gradual and not intimately related

to the structure.

He also concluded that the block could not have formed a barrier to faunal migration. This contradicts evidence of faunal variations put forward by Ager (1956) who postulated that to some extent these were barriers. Regional faunal differences in modern seas however are not always separated by any physical barriers and this could be the case in Liassic times.

In 1970 Audley-Charles produced a series of lithological-isopachous maps of the palaeogeography of the British Isles in Triassic times. He produced evidence to show that the grabens and most of the principal basins in which the Triassic sediments accumulated were structurally controlled. These fault controlled regions of deposition were formed before the beginning of the Triassic period and were probably initiated at the end of the Hercynian Orogeny.

The three major tectonic trends which appear to have influenced the orientation of the grabens are:

- 1) Caledonoid Trend in the : Irish Sea Graben,  
Cardigan Basin,  
Carlisle Basin and partly  
in the Cheshire Graben.
- 2) Charnoid Trend in the : Cheshire Graben,  
Needwood Basin,  
Bosworth Trough.
- 3) A North-South or Malvernian trend in the:  
Worcester Graben,  
Eccleshall Basin,  
Wessex basin and possibly in the  
St. Georges Graben.

Earth movements which produced these great thicknesses of Triassic sediment became inactive towards the Rhaetic which brought the Triassic to a close. In the Wessex basin there are great thicknesses of both Triassic and Liassic sediment. From the positions of the outliers, Carlisle, Prees (Cheshire) and Solihull, one can assume that the Lias at one time covered these areas also. These correspond to the basins of sedimentation in the Triassic period. Therefore it is probable that these Triassic basins were also the main basins of deposition for the Lias.

As already stated the Rhaetic (Division 6, Audley-Charles 1970) is regarded as a transition group between the Triassic and Jurassic marking the change from oxidizing conditions of the Triassic to a reducing, fully marine environment of the Jurassic. The flat plains of late Keuper times with the gypsiferous lakes were invaded by the sea which remained shallow with little lateral variation in facies. It has been suggested by Audley-Charles (1970) that the fault movements (which had been so influential in regards to sedimentation) during the earlier part of the Triassic period, now ceased to be important, this being shown by the way in which the Rhaetic passes unchanged over the Market Weighton axis.

It is probable that these graben and basins, although inactive in the Rhaetic became active again on a reduced scale during the Lower Jurassic, before dying out completely at the end of the Lias. The initial movements were relatively small, being more numerous in the Lower Lias, particularly in the Hettangian and Sinemurian stages deepening the basins rapidly but gradually.

Isopach maps compiled by Tegt (Bitterli 1963) Figs 2:1, 2:2 show the four main areas of deposition with thicknesses greater than three hundred metres. To obtain these thicknesses it is

probable that initial deepening was by epeirogenic movements, although as it will later be shown, eustatic movements did have some influence.

#### 2:4 LIASSIC SEDIMENTATION

A general lithofacies map of Europe (Sellwood 1972) Fig 2:3, shows limestones and dolomites in a broad band along the Tethys ocean border extending northwards to take in south-west England. These limestones pass laterally into marls, which in turn pass into clays which cover the major portion of this epicontinental shelf sea. Sandy marginal facies exist adjacent to the large continental land masses and islands, their lateral extent being rather limited.

In the area of Britain where deposition was limited to the basins, lateral facies variation is not as dramatic with only local marginal facies on the swells. These are however important, since the unconformities and non-sequences that are identifiable give a picture of the local disturbances as well as any eustatic movements of the sea level. An overall picture of the sedimentation in Britain can be obtained from Fig 2:5. The sediments, mainly clays and limestones give way to a thick sequence of clays, allowing the Lias to be subdivided on lithology into two distinct sections:

- a) intercalations of limestone and clay.
- b) clays (Fig 2:7)

Of the three Jurassic divisions the Lias shows best the marked variations in thicknesses in the different subsiding basins and across the intervening swells. In addition each major basin had its own variants in sedimentation and the way in which certain zones increase or decrease in thickness, cut out entirely, or change in facies from one basin to another is often complicated.



In the Midlands and south of England there is a tendency for the lowest Lias to be partly or entirely calcareous. In Lincolnshire for example the Pre-Planorbis beds are called the 'Hydraulic' limestones and consist of 6m - 9m of impure calcareous rocks.

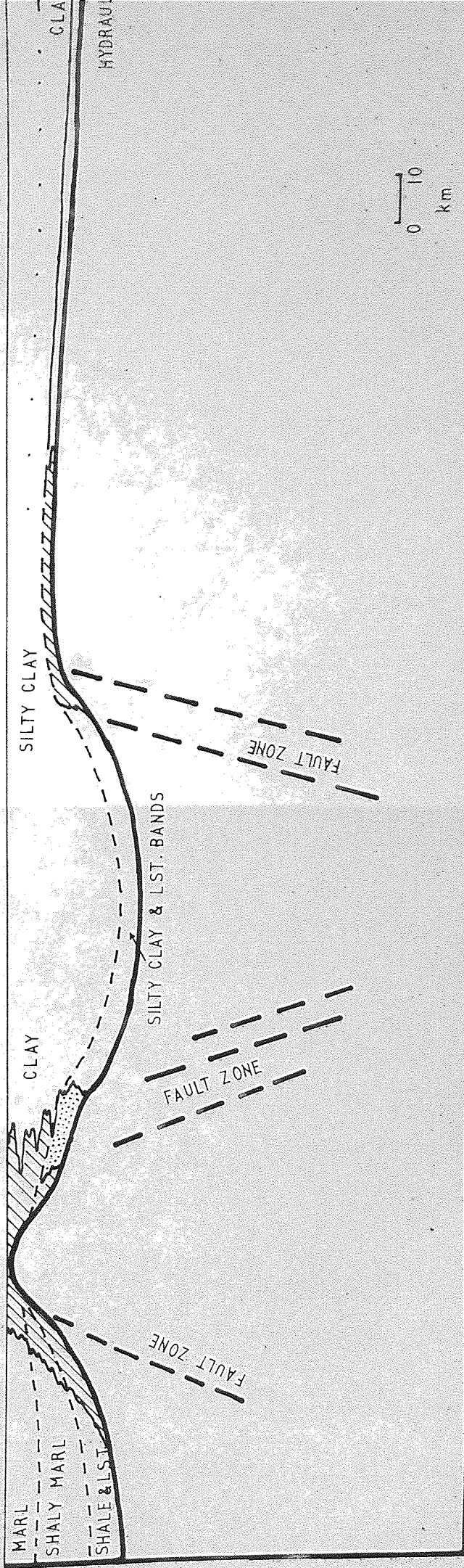
The Lias of the Wessex basin exposed in the Dorset cliffs, is of Lower and Middle Lias in age, much of the latter being sandy and standing out as beds of calcareous sandstone. The Blue Lias consists of marls, limestones (calclutites) fine laminated limestones and bituminous shales, the repetition of this unit producing cyclic sedimentation (Bitterli 1963). The marls and limestones are highly fossiliferous with both free swimming and bottom living fauna, ammonites and lamellibranchs being outstanding.

The Blue Lias in Glamorgan has an exceptional littoral facies in the most westerly outcrops (Wobber 1967), this facies butting up against the Carboniferous islands in the same manner as the underlying Rhaetic. The littoral beds consist of massive limestones with chert, sandy and conglomeratic beds, some of the limestones being rich in corals. In this nearshore facies, wave action is shown by the winnowing of shell debris on the upper surface of some limestones together with erosion surfaces when there is a relative lowering of the wave-base. Wobber (1967) has suggested that the bedding plane irregularities in the South Wales Lias are due to the instability of nearshore sediments compared with the deeper water deposits, this instability being due to three factors;

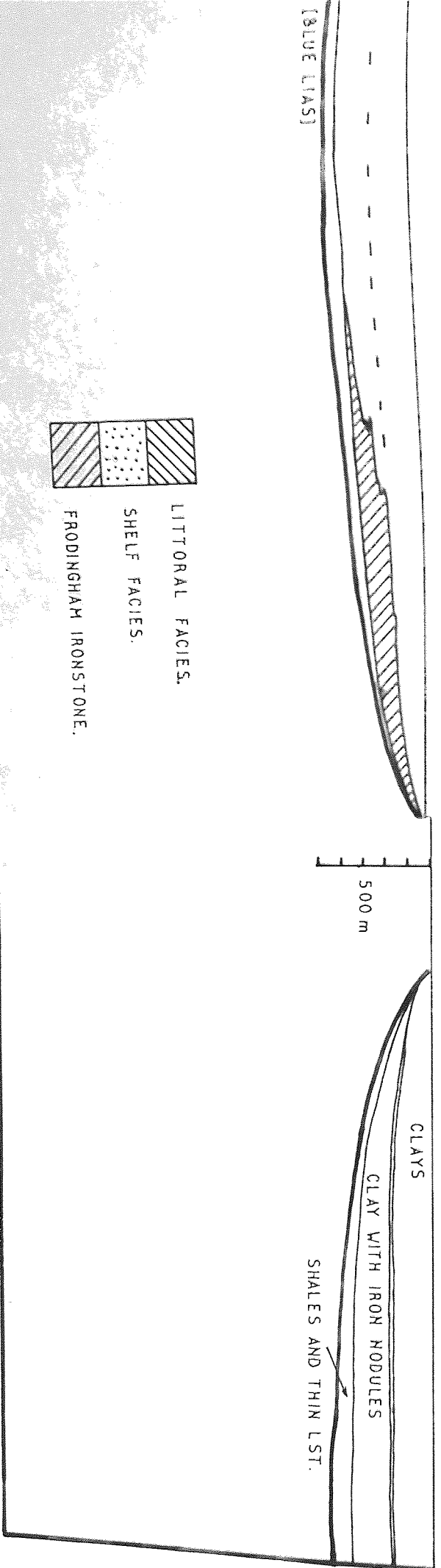
- 1) Dip at  $3^{\circ}$  -  $5^{\circ}$  away from the land therefore subject to gravity.
- 2) Subject to greater variations in density than offshore sediments because of a widely variable abundance of lithoclasts and fossil debris.

# MENDIPS

# OXFORDSHIRE SHALLOWS



# MARKET WEIGHTON



- 3) The shallow water Lias of South Wales contain trace fossils more than 20% of total rock volume, suggesting a high rate of sediment mixing by an infauna.

In Wales there are no beds above the semicostatum Zone. In fact there is no other Mesozoic or Tertiary material except that now known to exist at Mochras and Cardigan Bay (Wood and Woodland 1968, Woodland 1971).

The main outcrop of the Lias stretches northwards through the Mendips which formed islands and shallows of Carboniferous limestone beyond which lay the shallows of the Radstock shelf where sedimentation was slow and intermittent. This is well seen in the lowest zones of the Lower Lias which are locally thin and conglomeratic, and in places absent altogether Fig 2:5. The ibex and davoei Zones are however thicker and represented by the typical clay facies. Later there was further tectonic activity in this region resulting in the Upper Lias overstepping the Middle Lias.

North of Bristol is the Severn basin where the Lias is complete and thick, 505m of mainly clays and shales being found in the Stowell Park borehole. There is a general reduction over the Oxfordshire shallows, the effect being particularly marked in the Upper Lias which is reduced to approximately 1.5m in thickness.

The Severn basin and the Midland basin (Leicestershire, Northamptonshire and Lincolnshire) were partially connected and hence show similar sediments; the Midland basin however was much shallower the maximum thickness of the Lias being 335m. Deposition here was not continuous and the Upper Lias again shows local erosion and overlap within its zones, as if the basin had finally filled up.

All the Liassic divisions thin northwards through Lincolnshire.

The Lower Lias varies from 213m in Lincolnshire to 92m at the Humber and 30m at Market Weighton where it is the only division present. The full sequence reappears in the Yorkshire basin with a thickness of over 427m and is more argillaceous and less variable than in south-west England.

Workable iron ores are present in all divisions of the Lias but mainly in the northern part of the main outcrop (Table 2:3). The iron is present as siderite (ferrous carbonate), chamosite (hydrous iron aluminosilicate) and limonite (hydrous oxides of iron) with the non-ferrous components of calcite, quartz, and clay minerals

TABLE 2:3

Main Iron Ores in the Lias

- Upper Lias :- north-east Yorkshire.
- Middle Lias :- spinatum Zone of Cleveland, Yorkshire and the Marlstone Rock bed of the Midlands and Lincolnshire.
- Lower Lias :- Frodingham, north Lincolnshire (semicostatum and obtusum Zones).

The ironstone is generally oolitic with siderite, limonite, calcite and shell debris as the matrix. The ooliths originally of chamosite having been locally altered to siderite and limonite. The Frodingham ore is the most important among the Liassic ironstones. This bed is however limited since it passes southwards into 46m of clays that are locally ferruginous and thins northwards towards the Market Weighton axis. The formation of the ironstones and the origin of the iron has been discussed by Carroll (1958) and Hallam (1963, 1966). It is now considered that they were probably associated with a pro-delta. Where the rivers originated from is another problem and

as Hallam (1966), states there is little evidence for a Pennine land mass with a large river. Therefore the most likely area must lie to the north or north-east (i.e. Scandis).

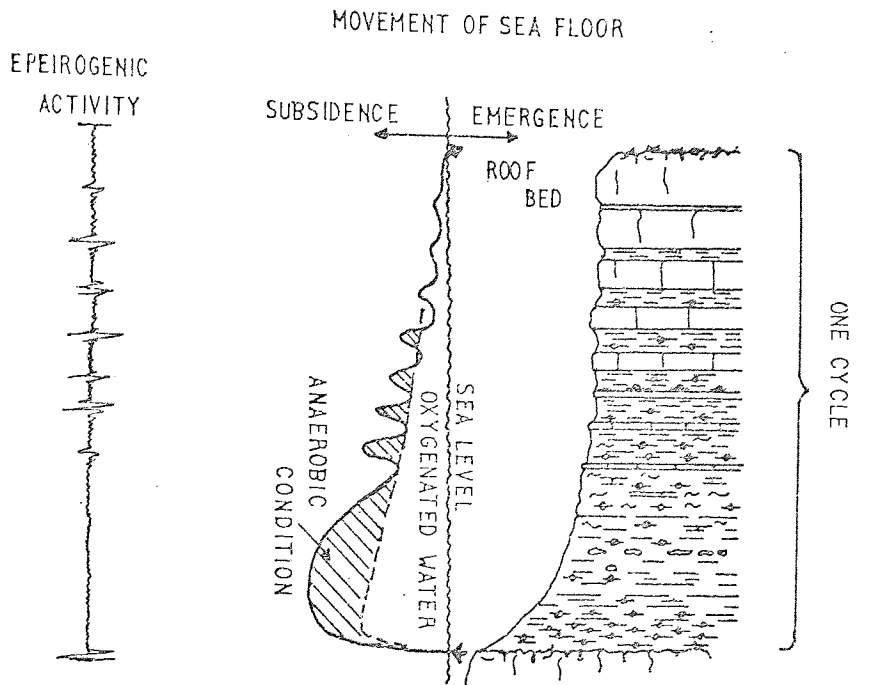
## 2:5 CYCLIC SEDIMENTATION OF THE LIAS

Bitterli (1963) in his examination of the Lower Lias of Pinhay Bay/Lyme Regis recognized a series of cycles extending from the planorbis to the lower part of the semicostatum Zone. Over this interval, eight main "cycles" can be distinguished, each comprising a strongly bituminous shale beds at the base followed by an alternation of about seven bands of limestone and (weakly bituminous) shale bed. In addition, a few incomplete cycles can also be recognized. Above this the Blue Lias (as it is known) merges into a more homogeneous but still fairly bituminous clay shale. This type of sequence can be recognised on many occasions throughout the whole of the Jurassic in Britain. This regular alternation of clay shales and argillaceous limestones of the Blue Lias facies is strong evidence of very quiet conditions especially during the formation of the limestones, these forming in conditions beyond wave action and outside current and coastal influences.

The rhythmic formation of clay/limestone alternations can be attributed to one or more of the following reasons:

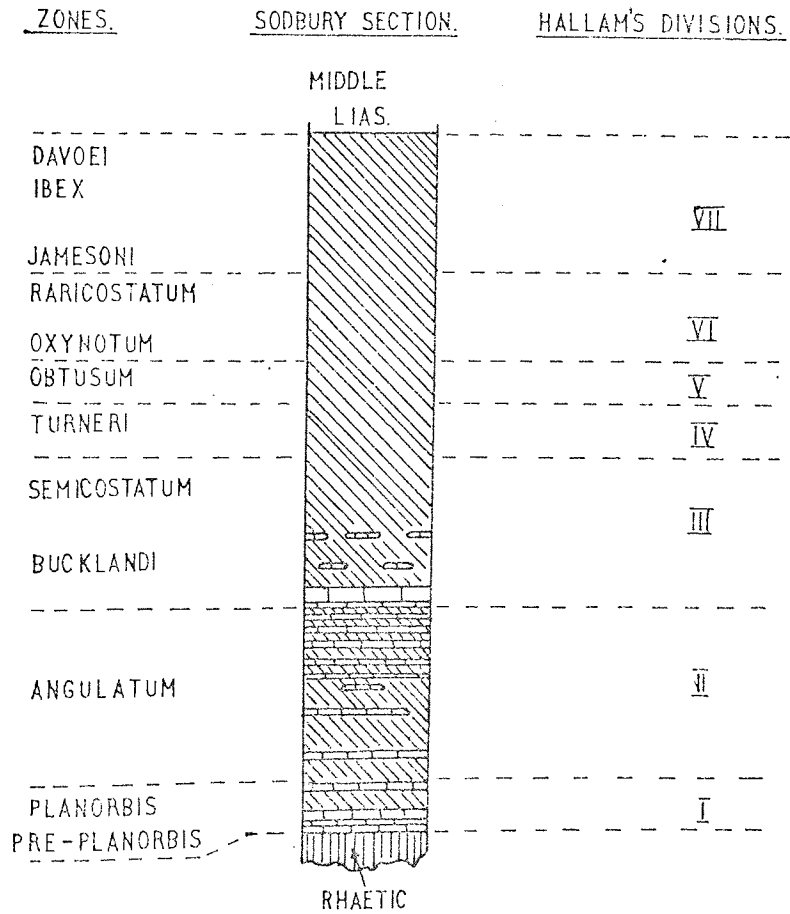
- 1) Intermittent fluvial influx of carbonate in solution and subsequent precipitation owing to climatic rhythms.
- 2) Periodic changes in the physical and chemical composition of the sea water.
- 3) Epeirogenic (or eustatic) movements.

FIG 2:6



RHYTHMIC SEDIMENTATION

FIG 2:7



Bitterli (1963) also noted that strongly reducing conditions recurred about a dozen times in the Lyme Regis area, due to intermittent anaerobic conditions probably restricted to the bottom water.

Hallam (1961) also recognized "an extraordinary lateral constancy of several distinct lithological horizons in north-west Europe". The eleven stratigraphical units he identified were related to faunal changes so giving an intimate relationship between ammonites and cyclothems.

Klupfel (1917) has shown in Germany that the rhythmic sedimentation which is asymmetrical, is due to rapid subsidences followed by gradual uplift and shallowing of the sea (Fig 2:6), followed by comparatively sudden deepening again. Klupfel interpreted this as due to regional epeirogenic movements of the sea floor, this being similar to the cycles described by Bitterli (1963) at Lyme Regis.

Hallam (1964a) put forward a different model in which regional facies variations were accommodated as well as cyclic variations in the vertical succession. Hallam showed that in areas of landlocked basins, which characterise the Lias, different environments of deposition existed. The environmental conditions and therefore the sediments deposited being determined by their positions relative to wave base and the level of the limit of oxygen availability. Using these environmental criteria he demonstrated that Klupfelian cycles in Britain, Germany and northern France were local expressions of extremely widespread and essentially synchronous variations in the depth of the sea which were independent of a complex pattern of basins and swells. He has suggested that the underlying control may have been the eustatic rise and fall of sea level rather than local epeirogenic movements.



Considering the Lias of Dorset only, it appears that approximately three of the cycles defined by Bitterli (1963) are equivalent to one of the cyclothems of Hallam (1964a). It is therefore reasonable to suppose that both epeirogenic movements as well as eustatic rise and fall of sea level, produced the conditions that existed during the Lower Lias, throughout Europe.

The Rhaetic is fairly uniform, being deposited in brackish water to almost marine. Its consistency of sediment type indicates that in fact there was very little difference in the depths of water between the two extremes. During the Lias, thicknesses in excess of 300m were deposited in the basins compared to a few metres on the swells. Since the land masses had been eroded to a virtual peneplain at this time, eustatic rises in sea level would have caused extensive transgressions across the land without developing major basins of sedimentation. Hallam (1961) admitted that deepening of the sea did not seem to be related to widespread transgressions or regressions over the neighbouring land masses. However, in a subsequent paper as already shown he suggested that sedimentary and faunal changes could be related to changes of sea level. If this is the case the formation of basins must have been due to local epeirogenic movements along lines of weaknesses that are similar to the Triassic grabens. These would produce the cycles recognised by Bitterli (1963) in the Blue Lias with eustatic rises of sea level giving a widespread lithological boundary thus explaining the cycles within the major cyclothems of Hallam (1964a). In Britain towards the end of the Sinemurian (a eustatic boundary), the cycles within the cyclothems then become difficult to recognise and non-existent in most localities. The small epeirogenic movements must therefore have ceased at the end of the Blue Lias, the basins having finally reached their maximum depths. These then began to fill up

with argillaceous material producing large thicknesses in excess of three hundred metres in the deepest parts. The eustatic changes of sea level however, still caused non-sequences and lithological changes on the shoals and shallows, and edges of land masses.

One final point to be considered here, is the question as to why there should have existed such a large expanse of sea which had uniform conditions with basins in which stagnant conditions formed with apparent ease. At the present day there is no area of equivalent size where conditions of this type exist. However, Kaare Munster Strom (1939) put forward the suggestion that under suitable natural conditions seas and even oceans can become stagnant. He demonstrates that the Atlantic ocean deeps are well ventilated (5ml of oxygen/litre) yet at depths of 50 to 1,200 metres in areas north and south of the equator, the oxygen content is low (1ml/litre at a depth of 500 metres). If there was a more globally equable climate the bottom waters would also become stagnant since at the present time the deeps are being ventilated by cold aerated waters from the Arctic and Antarctic oceans. In the Jurassic, as already shown, the temperatures were uniform with the difference between polar and equatorial temperatures being small. There were also major land masses lying between the Liassic seas and both the north and south poles. Thus both climate and physical barrier conditions existed during the Liassic to facilitate the development of stagnant conditions by reducing circulation in the seas.

## CHAPTER 3

### AREA OF STUDY

#### 3:1 INTRODUCTION

The selection of an area for study had several restraints imposed upon it, these being:

- a) Lithology
- b) Availability and accessibility of outcrop
- c) Size of outcrop

the major restraint being lithology. This was important since material was needed which was fairly homogenous (or appeared to be so). It was therefore necessary to have a large thickness of clay with as few limestone bands as possible. The Midland basin and Wessex basin were ruled out on lithological grounds since there are many limestone horizons within the clay, some even being used in the manufacture of cement. The largest thicknesses of suitably exposed clays are found in the Severn basin and since this was relatively close it was decided to examine this area for exposure. As expected, the clays occupy low lying, well cultivated ground with little or no exposure. Brickworks and recent excavations for building were the only source of sizeable outcrops extending into the unweathered clay. Recent excavations reaching this depth were very limited (and of a temporary nature) and to take samples and notes on the exposure would have hindered work and these had to be ruled out. At the beginning of the century brickworks were quite numerous. This is no longer the case and many are now overgrown, and without extensive excavation few, if any, intact unweathered samples could be obtained. The brickworks selected is located in the northern Cotswolds half a

kilometre south of the village of Paxford (SP 185378), and belongs to the North Cot Brick and Tile Company Limited (SP 181372). Of the other brick pits in the area, none provided the necessary profile.

### 3:2 DESCRIPTION OF THE AREA

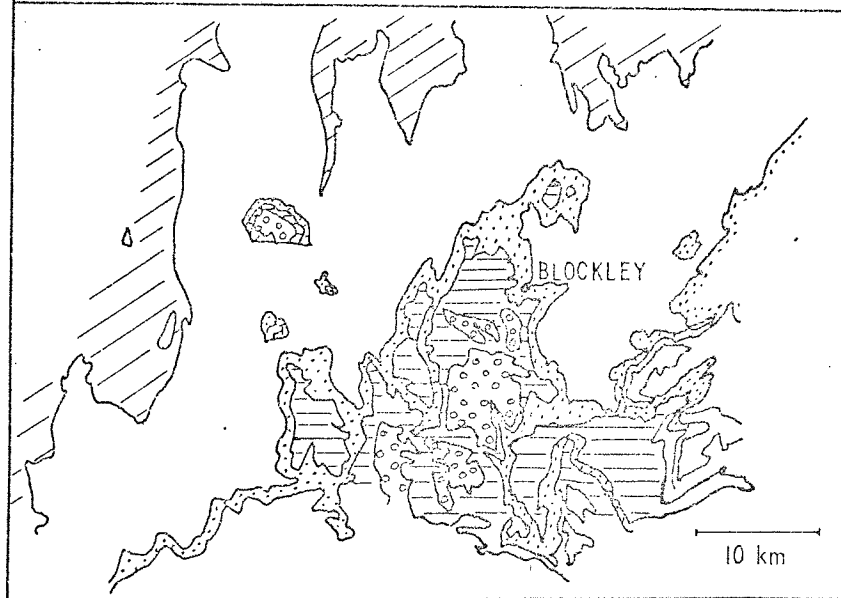
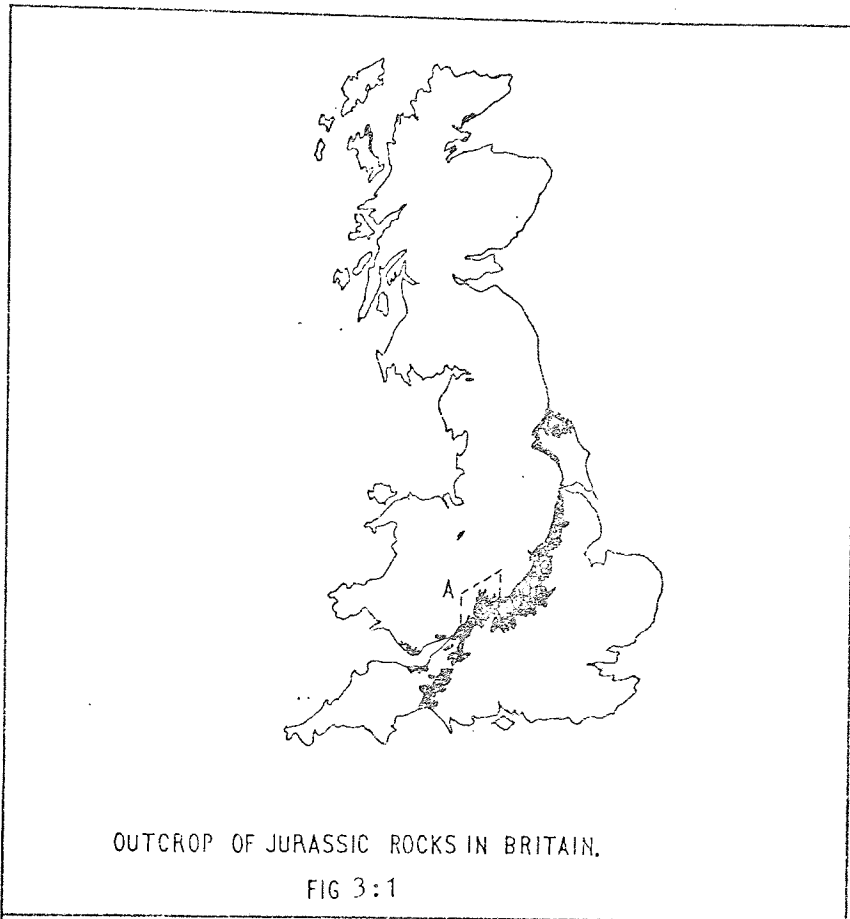
The following region to be discussed is the outcrop of Lias (Fig 3:1) which lies north of the line running from Evesham in the west, through Broadway (SP 095374) to Moreton-in-the-Marsh (SP205325) in the east and bounded northwards by the Keuper Marl (I.G.S. 1" to 1 mile sheet 217). A large percentage of the area is the flat alluvium covered Vale of Evesham (its rich soil ideal for market gardeners) with the River Avon draining down this vale to the south-west. The only high ground is the Cotswolds in the south. The majority of the smaller streams drain northwards into the Avon or eastwards into the River Stour which eventually joins the Avon south of Stratford-upon-Avon.

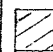

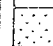
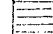

The Cotswolds themselves form a ridge with an axis running N.E. - S.W. with its highest point in the area being 283m O.D. The geology of the area has affected the landscape and this will be described in more detail later. It is sufficient to say that the lower ground is made up of the Lower Lias clay, with the higher ground being Keuper in the north, and the Middle Jurassic capping the Cotswold Hills.

The site of the brickworks in relation to the outcrop of the Jurassic is shown in Fig 3:1 and Fig 3:2, being 20km due south of Stratford-upon-Avon and known locally as the Blockley Clay Pit. The pit is situated alongside Blockley railway station (now closed) and the labour for its operation is drawn from the villages of Blockley (SP 164348), Paxford, Draycott and Aston Magna.

#### 3:2:1 GEOLOGY

The geological succession in the area is given in Fig 3:2 and



-  KEUPER MARL
-  LOWER LIAS
-  MIDDLE LIAS
-  UPPER LIAS
-  INFERIOR OOLITE

GEOLOGICAL MAP OF AREA A, BLOCKLEY

FIG 3:2

the following is a brief description of the deposits in the area.

#### Keuper Marl

This is a series of red-brown mudstones and silty mudstones of Triassic age. Interspersed in the series are a number of sandstones and frequent siltstones with occasional pebble beds. Vast quantities of the fine grained material were transported and deposited both by wind and water from the surrounding higher ground. In this arid environment flash floods must have been common, as these give rise to pebble beds, with halite and anhydrite deposits forming when the lakes and pools dried up. The Keuper Marl outcrops to the north (Stratford-upon-Avon) and to the west (Tewkesbury) forming higher ground overlooking the flatter outcrop of the Lower Lias.

#### Rhaetic

There are no outcrops of Rhaetic in this area. However, its presence is known from the boreholes put down at Mickleton and Lower Lemington (Chapter 2). The Rhaetic is 22.5m thick at Mickleton thinning to 14.7m at Lower Lemington. This indicates that a "barrier" existed at the end of the Triassic period, giving further evidence that the basins of deposition during the Lower Lias are identical to those of the Triass.

#### Lower Lias.

As already stated these form the low lying ground with very little exposure, the majority of exposures recorded being old brick workings and railway cuttings. These are now overgrown and weathered and are of little value. These exposures were produced when the railways in this area were first built and were of great use in mapping the Lias.

As already shown (Chapter 2) the Lias thins to the south-east. Arkell (1946) has suggested that there may be a fault in the Lias

unobservable from the outcrop, to explain in part this thinning. The evidence for fault controlled basins in the Triassic is considerable (Chapter 2) and further movement during Lower Lias times on such faults could have resulted in the thinning in this area.

The variation in sediment type and thickness apparent through the Jurassic period in the Moreton region suggests a boundary to a basin of deposition along which epeirogenic movements have occurred from time to time.

The clays of the Blockley area are almost entirely above the jamesoni Zone. At Aston Magna (SP 200357) the small brick pit is in the davoei Zone, the top of the pit being in the Middle Lias almost up to the ironstone. The Lower Lias/Middle Lias junction can still be seen but is rapidly becoming overgrown and destroyed by landslips. The Blockley Clay Pit (North Cot Brick Works) exposes the lower section of the davoei Zone and the ibex Zone (Fig 3:4). Other exposures in the area consist of old railway cuttings which are now overgrown although fossils from the davoei Zone were reported when a cutting near the village of Dorn (SP 294340) was excavated.

#### Middle Lias

This consists of micaceous silts and clays in the lower beds, increasing in sand content up the sequence, the upper layers forming a harder marlstone band. The marlstone contains a high proportion of iron. Some workers refer to it as an ironstone although the iron is not in economically workable quantities in this locality. This ironstone forms the first noticeable escarpment especially in the area around Chipping Campden (SP 150390). The escarpment becomes even more pronounced towards the east where at Edge Hill it is worked as an iron ore.

## Upper Lias

This is a variable formation consisting of sands and clays, the sand forming the diachronous Cotswold Sands. They are fine grained, yellow in colour, often loose and friable, although sometimes they are rendered coherent by a calcareous cement.

## Inferior Oolite

This oolite attains its greatest thickness (106.68m) in the Severn basin to the north of Gloucester and in the Blockley region it reaches a thickness of 90m. It is almost entirely calcareous, including sandy and rubbly limestones, pisolites and oolitic freestones. It is cream in colour, shell banks and shells are abundant, echinoderms and corals being common in certain beds. The oolite forms the indented scarp of the Cotswolds and is quarried extensively as a building stone and for road construction.

The oolite being a relatively competent rock rests on a weak foundation the Upper Lias clays. The clay has a low shear strength and will under certain conditions flow laterally into the valleys so causing fracturing of the rocks above. These fractures (approximately at right angles to the bedding planes) eventually become filled with debris and are often cemented by percolating water rich in calcium carbonate. These are then termed gulls. In some cases these gulls can become more resistant than the surrounding oolite and are finally weathered out as pillars. As the foundered masses of oolite slide down the hillside the bedding planes become rotated and dip towards the valley or plains, (cambering).

This cambering is a slow process of erosion, a more rapid one being the slips (rotational and slab) that also occur along this escarpment (good examples can be seen at Dover Hill SP 140399). In valleys that are steeply cut down into the Lower Lias clay, valley



bulging also occurs hence it is not only the Upper Lias clay that deforms by plastic flow.

### Pleistocene and Recent

Glacial drift covers a relatively large area of the Midlands. Around Moreton-in-the-Marsh it is virtually continuous yet at Blockley the drift is patchy. It has been shown (Tomlinson 1963, Shotton 1953) that the Cotswold region has been affected by at least two glaciations, an older Elsterian (Anglian) glaciation (equivalent to the Lowestoft glaciation) and a younger one of Saalian (Wolstonian) age. At the height of the Elsterian glaciation the areas now occupied by the Severn valley and the upper part of the Thames valley must have been buried beneath thick ice. Hawkins and Kellaway (1971) have shown that at least two glaciations affected the higher parts of the Mendips possibly carrying Welsh erratics to Salisbury Plain.

Kellaway, Horton and Poole (1971) suggest that these ice-sheets from Wales were then joined by ice pushing southwards from the Midlands onto the Cotswolds. At the maximum of the Elsterian Glaciation the great Northern Drift ice-sheets extended across Oxfordshire towards the Chilterns and to the south-west across Berkshire as far as the Chalk escarpment.

This was the first glaciation in which the Welsh ice had maximum influence and the drift that formed around Oxford is a red boulder clay with Triassic pebbles. Its character mainly influenced by the large expanse of Triassic deposits which the ice had crossed.

An interglacial (Holstein) period then followed with the formation of interglacial deposits (Nechells, Birmingham). During the second major glaciation the Welsh ice was initially the more influential, over running the Severn and on towards the Cotswolds.

The Eastern ice proceeded along the Avon valley blocking the drainage northwards and eventually allowed Lake Harrison to form covering the Midlands with its associated deposits. The Eastern ice pushed further south destroying Lake Harrison, yet when this ice retreated a lake again formed on the same site but its extent was not as great.

The deposits in the Vale of Moreton are associated with both these glaciations, the boulder clay being a plastic red-purple clay containing scattered Bunter quartzite pebbles. In the Blockley area the drift is patchy, the gap between Ebrington Hill and Dovers Hill is covered by drift containing gravel with both Bunter pebbles and Welsh igneous rocks, with well-bedded sands. The Paxford Gravel found to the east of Paxford and at the village of Stretton-on-Fosse consists of pebbles of local oolitic limestone and ironstone with Jurassic fossils and pebbles of Triassic origin. Both the Paxford Gravel and the Lower Stretton Sands are fluvial in origin and thought to have accumulated during the interglacial period. Above the Paxford Gravel at the Stretton sand pits are the lake-clays deposited when Lake Harrison formed. These clays finally being capped with boulder clay when the Eastern ice moved further south.

The area surrounding the Blockley Clay Pit was examined and no boulder clay or fluvial gravels were found in the close proximity. There was thus no problem in confusing drift with a fully weathered zone. A fully weathered zone of Keuper marl however, can be confused with a boulder clay mainly due to the similarity in colour (Chandler 1969) which was the reason why the drift was examined locally to ensure no confusion with the weathering profile.

Melt water from the ice sheets led to the development and deepening of the Avon Valley and the Evenlode but it has had little effect on the broad Vale of Moreton. In fact the main features of

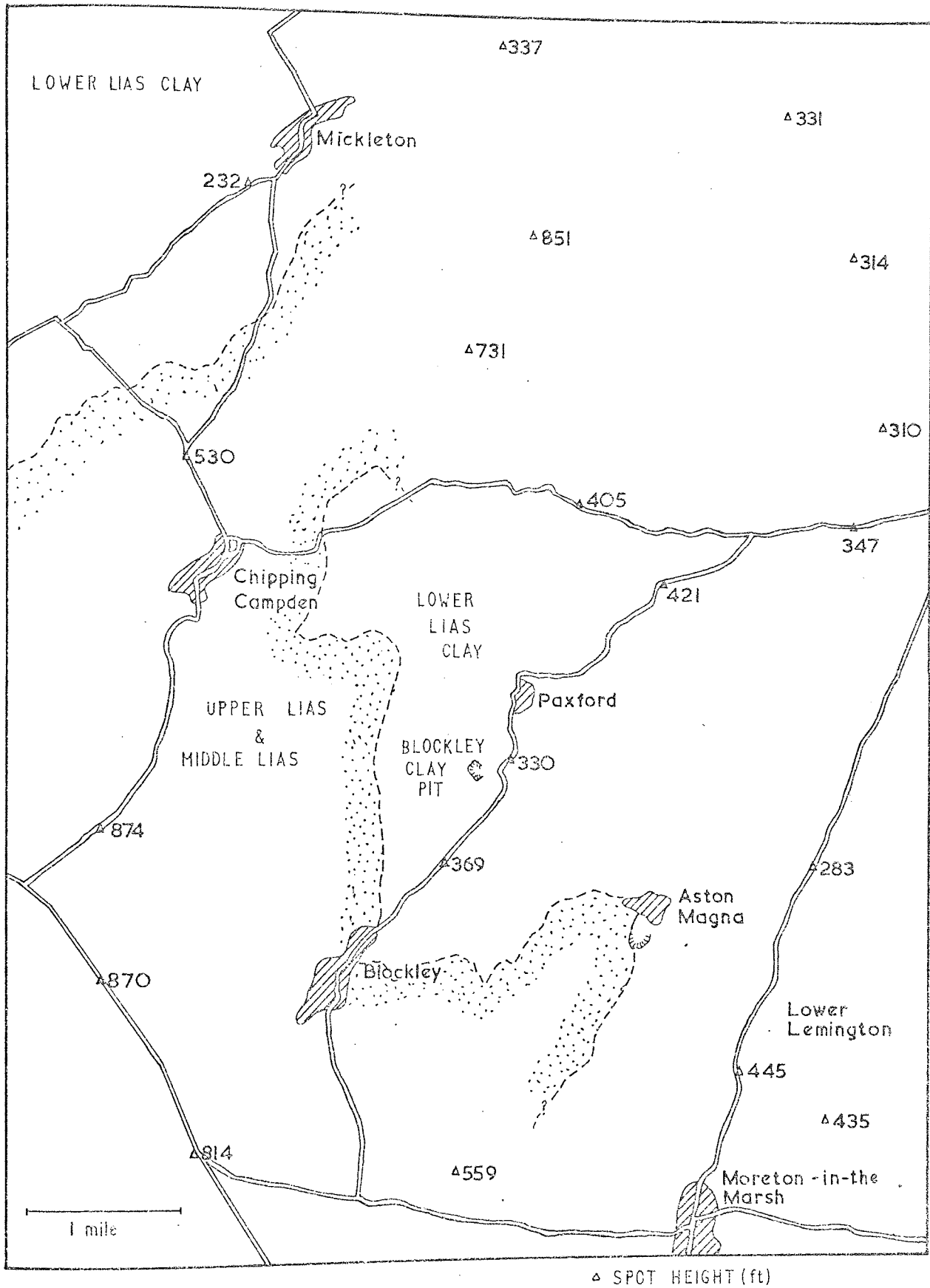


FIG 3:3

drainage and relief of the Cotswolds were formed soon after the retreat of the ice (Shotton 1953, Tomlinson 1963).

In the deeply dissected valleys, cambering is widespread and the occurrence of landslips today is not uncommon. In the Midlands many of the old slips are in a state of metastable equilibrium, this relative stability being due to the existing low relief (Chandler 1971). There is no slipped material in the vicinity of the clay pit and no bulging.

### 3:2:2 North Cot Brick and Tile Works (Blockley Clay Pit).

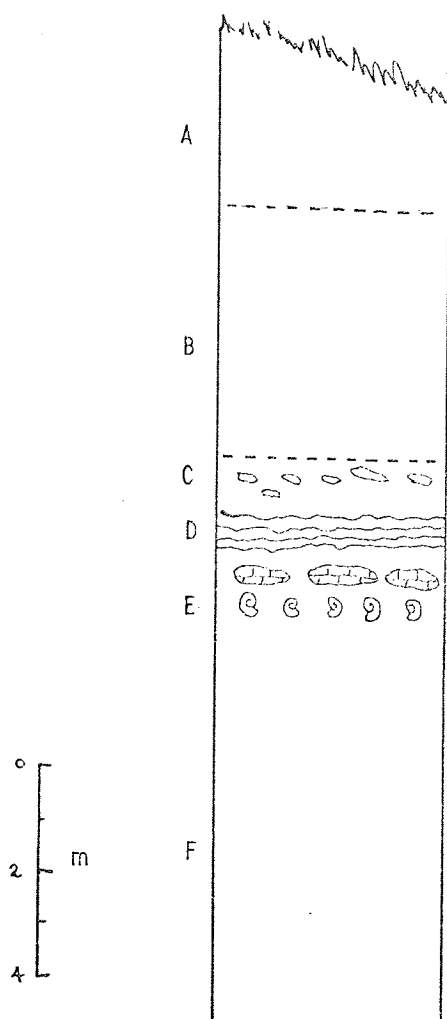
This is an open excavation covering  $0.5\text{km}^2$  to a depth of 9-12m approximately 0.8km from the Middle Lias. Bedding is not easily discerned except where the harder argillaceous calcilutite beds occur and these show an almost horizontal bedding. The pit exposes the upper part of the Lower Lias clays as a thickened sequence of the ibex Zone. This zone in Dorset is limited to a single bed less than 0.3m thick. However by careful collecting of the ammonite at Blockley, Callamon (1969) was able to further subdivide the ibex Zone and to define the luridum Subzone.

A section through the pit is shown in Fig 3:4 and the upper weathered and lower unweathered portions of the section are considered separately.

#### Unweathered

- A. Weathered clay to be described later.
- B. Dark grey clay, highly fissured (Fracture spacing,  $I_f$  medium; Fookes, Dearman, Franklin 1971), with iron staining along the joints close to the base of the weathered zone, occasional nodules, very few crushed fossils and fossil fragments these increasing toward the mudstone beneath. The clay close to the mudstone is finely bedded with thin bands (1-2mm) of quartz rich material.

GEOLOGICAL SECTION, BLOCKLEY CLAY PIT



- A WEATHERED CLAY : YELLOW WITH OCCASIONAL IRON NODULES.
- B BLUE-GREY CLAY : OCCASIONAL NODULES AND FOSSILS.
- C MUDSTONE VERY LIMY IN PLACES.
- D CLAY WITH SILTY HORIZONS.
- E PECTEN BED : LIMY MUDSTONE WITH GREY MASSES OF FOSSILS.
- F BLUE-GREY CLAY WITH CRUSHED FOSSILS.

FIG 3:4

Thickness varies due to the varying depth of the weathered zone but is the range 2.7m - 2.9m.

Fauna: Lytoceras frimbratum

- C. Thin inconsistent, calcareous mudstone; carbonate concretions are common both in the mudstone and replacing it. No bedding is visible so it is not possible to say if the concretions are syngenetic or diagenetic. The inconsistent nature of the bed appears due to vertical loading at a time when the bed was still in a plastic state.

Thickness: 0-0.15m.

Fauna: Liparoceras sp. Aegoceras sp. Gryphaea arcuata

- D. Silty clay, very fossiliferous with lamellibranches, ammonites and gastropods.

Thickness: 0.3m.

Fauna: Tragophylloceras loscombi

Astarte guexi

- E. Pecten Bed: Grey calcareous mudstone becoming an argillaceous limestone in places; fauna abundant with nodular ironstone locally or fossil breccia in the clay immediately below the mudstone. Banks of shells were occasionally unearthed as the pit overburden was removed. These banks were in localized concentrations and appear to have been formed by current action. The fossils found include lamellibranches, gastropods and ammonites, one ammonite Psiloceras sp. measured 0.3m in diameter and fragments indicated ammonites larger than this with whorls 0.12m thick. As will be shown this sediment was deposited in shallow water. It is unlikely that such large ammonites could survive in this environment and they probably

floated into this area when they died and then sank to the sea bed.

Thickness: 0.3-0.5m.

Fauna: Liparoceras pseudostriatum, Aegoceras luridum,  
Astarte guexi, Gryphaea arcuata,  
Pleuromya costata, Mactromya cardioides,  
Pecten sp

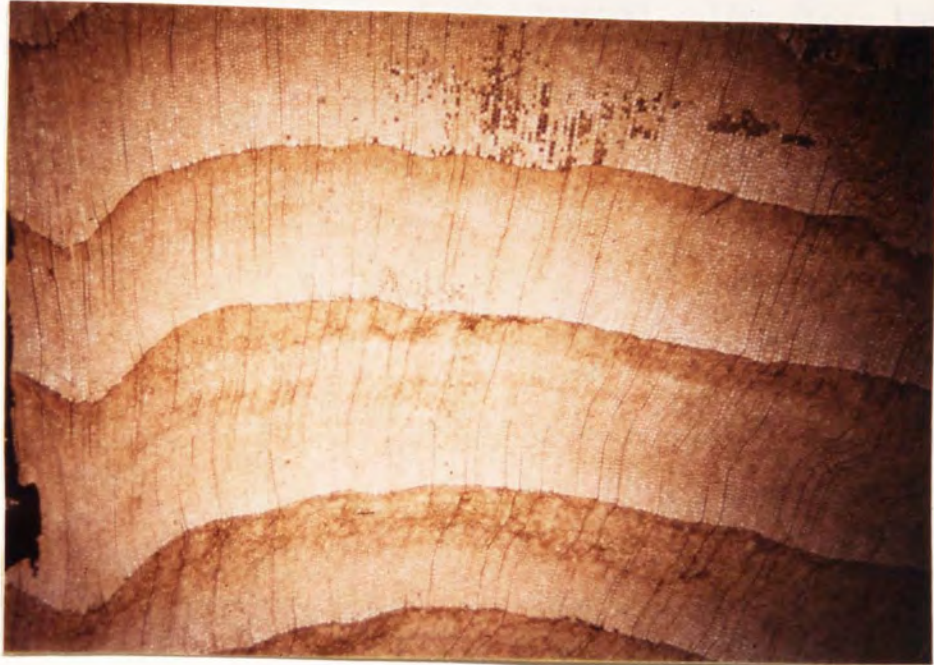
Below the Pecten Bed is the blue-grey clay which is used for the manufacture of bricks. The top few metres still contain an abundance of fossils and fossil debris, Liparoceras pseudostriatum being very common. The quantity of fossils decreases with depth but local pockets of fossils are not uncommon. The clay is a fine micaceous clay, blue-grey in colour with thin silty horizons of limited lateral extent.

Fauna: Liparoceras pseudostriatum, Liparoceras cheltiense  
Astarte guexi.

Apart from the hard mudstone bands it is impossible to determine the bedding. The mudstone indicates a horizontal bedding and on close examination a definite lineation could be seen in the clay itself almost paralleling the mudstones above.

#### Interpretation of the Section.

The clays at the base of the section which are very dark blue-grey to almost black were deposited in an almost euxinic environment. It is not necessary for the bottom waters to be euxinic for euxinic conditions can exist immediately below a normally oxygenated water/sediment interface. The bottom water contained a varied amount of benthonic fauna and their remains together with bacterial action could give rise to the anaerobic environment just below the water/sediment interface. The possibility that anaerobic conditions existed in the bottom water is ruled out by the considerable benthonic fauna. Iron pyrite is associated with



X13



X20.7

PLATES 3:1

THIN SECTION OF TREE FRAGMENT  
(PLANE POLARISED LIGHT)



fossil remains but is also found in irregular string like masses, these possibly being produced by bacterial action (Love 1957). Higher up the section fossils become more numerous, indicating a shallowing with an increased food supply. The shallowing was probably due to the filling up of the region by sediment. Conditions finally enabled calcium carbonate to be precipitated to form a calcareous mudstone (Pecten Bed). The formation of the Pecten Bed was close to wave base and in part fossil debris has been concentrated into shell banks.

Several fragments of wood (Plate 3:1) many larger than 150mm in length were found indicating that the source area supported forests. The wood was well preserved allowing the cells and structure to be examined. Examination of a thin section of the wood suggests a gymnosperm. The fragment has thirteen distinct annual rings indicating that the climate at this time was seasonal with definite temperature changes.

Soon after deposition of the Pecten Bed there was a slight deepening of the sea. Clay and silt were laid down in thin layers with some reworking of the upper surfaces showing that there was some increase in turbulence.

The subsidence was not too marked and the area again filled up and the second calcareous mudstone formed. Kent (1937) and Simpson (1956) have suggested that these inconsistent mudstones occurring in nodular masses were formed by the segregation of calcium carbonate from the surrounding sediment into the nodules where it has crystallized between the clay particles without causing any increase in the original volume of sediment. Simpson (1956) based his theory on the state of the fossil Chondrites found in the nodular limestones near Bristol. In the Blockley section there did not appear to be any Chondrites

in the nodules exposed.

There was then a second subsidence, greater than the first with mud and silt being deposited in thin layers, these passing vertically into blue-grey clay.

WEATHERING AND SOILS

4:1 INTRODUCTION

In the description of a weathered section there are two weathering schemes that can be used to define the weathered horizons. Each classification is designed for a specific purpose for use in different disciplines;

a) The Engineering Weathering Scheme; a scheme based on morphology, being dependent on in situ observational examination. The grade of weathering defined in this scheme is often accompanied by information assessing the mechanical nature of the material to help the Engineer.

b) The Pedological Scheme; a scheme whereby the chemical and to some extent the physical nature of the weathered horizons are described.

Both schemes cover the range of weathering of rocks in a profile thus each scheme will be described to allow their useability to be examined in a later section.

There are various definitions of weathering emanating from the differing viewpoints of pedologists, geomorphologists, geologists and engineers. The most widely accepted definition is that of Reiche (1950);

"Weathering is the response of materials which were in equilibrium within the lithosphere to conditions at or near its contact with the atmosphere, the hydrosphere, and perhaps still more important, the biosphere".

Keller (1957) was of the opinion that this definition could be improved if the words "which were in equilibrium" were removed since rocks are only in equilibrium momentarily while the environment in which they were formed persists. An early definition by Polynov (1937) defined weathering as;

"the change of rocks from the massive to the clastic state",

this however does not take into account extensive chemical weathering. The definition by Ollier (1969) covers the main criticisms that have been levelled at previous definitions;

"Weathering is the breakdown and alteration of materials near or on the earths surface to products that are more in equilibrium with newly imposed physico-chemical conditions".

Engineers tend to use a more simplified definition such as that used by Saunders and Fookes (1970) which is based on that of Weinert (1965);

"Weathering is that process of alteration of rocks occurring under the direct influence of the hydrosphere and atmosphere". \*

This definition ignores the deep weathering which can penetrate to depths of several hundred metres, engineers applying the general term "rotting" for weathering at this depth. This can be very important in engineering projects and can cause severe problems as occurred at the Keiwa hydro-electric project, Victoria, Australia

---

\* In both definitions the term rock has been used in the geological sense to include both soft rock or engineering soils and hard rocks.

where weathered mylonite, was found at a depth of 122m on the Keiwa river. During the excavation of the head race tunnel an oxidized copper lode was also found at a depth of 320m with partially weathered feldspars and open iron stained joints at depths of 350m.

An engineer is not only concerned with the results of weathering that have taken place over long periods of geological time. He is also interested in the shorter term effects which are concerned with the durability of rocks which may continue to weather in a slope, tunnel or during use as a construction material. Weatherability was defined by Fookes, Dearman and Franklin (1971) as "the susceptibility of rock to short weathering" implying that the rock is forming some part of an engineering structure e.g. dam abutment, road base or sub-base.

#### 4:2 WEATHERING

In any consideration of weathering, it is possible to visualise it as a combination of processes and products, a suggested subdivision is given in Table 4:1.

TABLE 4:1

WEATHERING

- 1) Fundamental Weathering processes.
  - a) Mechanical.
  - b) Chemical.
- 2) Weathering Controls.
  - a) Climate
  - b) Topography
  - c) Hydrological Conditions
  - d) Properties of the Material
  - e) Biotic
  - f) Time

TABLE 4:1 (continued)

- g) Depth of Burial
- 3) Results of Weathering.
  - a) Soil and Soil Formation
  - b) Landform Evolution
  - c) Deep Weathering
- 4) Rates of Weathering
  - Dependent on.
    - a) Environmental Factors:-  
climate, parent material,  
hydrological and biological  
conditions, topography.
    - b) The properties of the  
material forming the rock:-  
mineral composition, clay size  
percentage, permeability.
    - c) The properties of the Rock  
Mass:- jointing and fracture  
spacing.

A rock can weather either by physical breakdown without considerable change of its minerals (disintegration) or by chemical alteration of the minerals (decomposition). These are the two fundamental processes of weathering. Several workers place organic weathering as a fundamental process but since this is a combination of physical and chemical effects it is best referred to as a controlling factor of weathering. A summary of the fundamental processes based on Krumbein and Sloss (1958) is shown in Table 4:2.

TABLE 4:2

Type of Weathering	Examples	Summary
Physical- disintegration	<p>Sheeting, unloading and spalling of rock (during erosion)</p> <p>Thermally induced volume changes. Frost Action (ice wedges).</p> <p>Colloid plucking (pulling effect of gels)</p> <p>Wetting and drying.</p>	<p>Generally of secondary importance in warm climates.</p> <p>Net effect is particle size reduction; increased surface area; no change in chemical composition.</p>
Chemical- decomposition	<p>Solution</p> <p>Hydration, hydrolysis</p> <p>Oxidation (with or without valence increase).</p> <p>Reduction.</p> <p>Carbonation.</p>	<p>Changes of chemical and physical properties</p>

Climate affects rock directly and also acts through vegetation and the hydrological situation, and is therefore the most important controlling factor of weathering. Certain climates tend to give rise to particular soils, for example loose soils with a carbonate accumulation may develop in dry areas and whilst in warm humid areas red earths with iron accumulations tend to dominate.

Certain climatic factors have singular significance more or less independently. Temperature itself is important since high temperatures speed up the majority of chemical reactions and, therefore, in warm climates chemical weathering more significant. In cold areas there is little chemical action, organic action is reduced therefore soil formation is limited. Rainfall is clearly important for leaching.

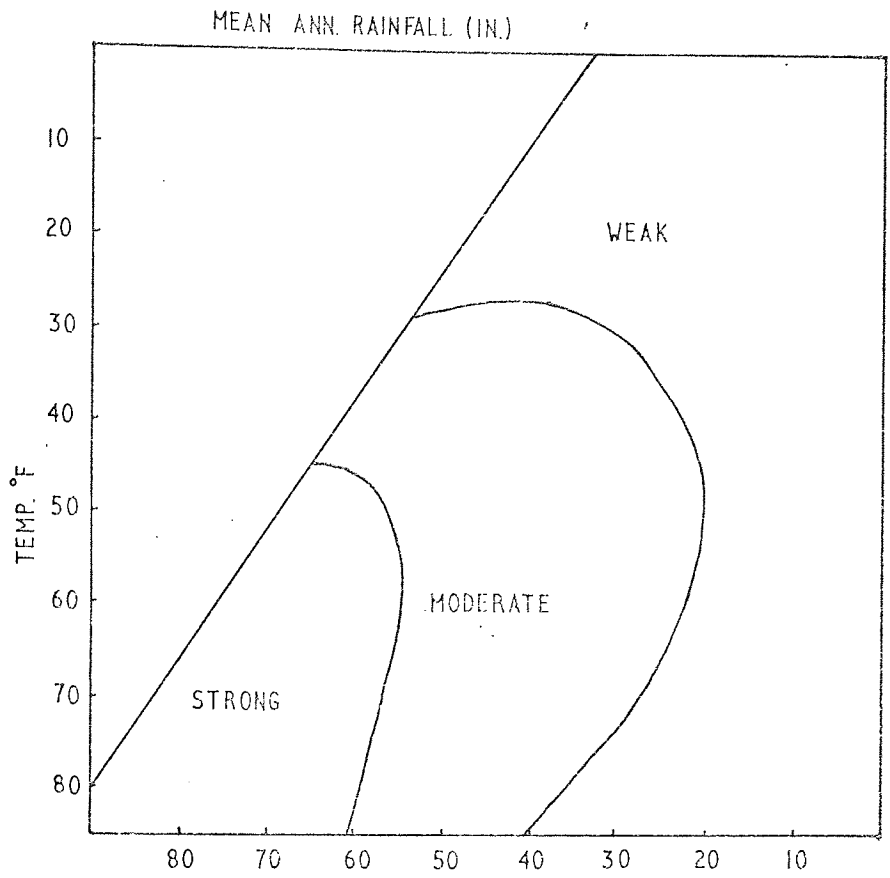
The precipitation/evaporation ratio is also of great importance. If evaporation exceeds precipitation there is usually an accumulation of salts at the surface to form saline soils. If precipitation exceeds evaporation there is a loss of ions due to leaching and the formation of podzolic type soils. (See Ollier 1969, Rieche 1950).

On a broad scale it can be seen that there is a correlation of type and intensity of weathering with different climatic regions. Peltier (1950) recognised a series of morphogenic regions within which the intensity and relative significance of the various geomorphic processes are thought to be essentially uniform. This relation between climate and weathering can be represented in diagrammatic form Figs 4:1, 4:2, 4:3 and provides a summary of climate control on weathering.

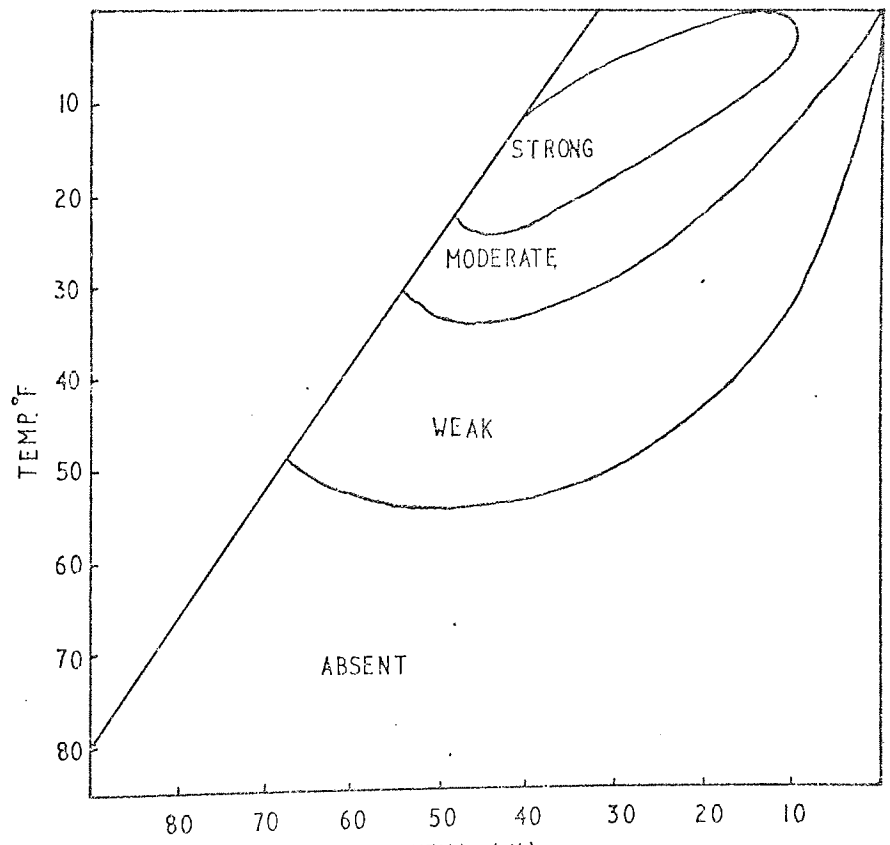
#### 4:3 SOILS

There is no agreed distinction between weathering and soil formation





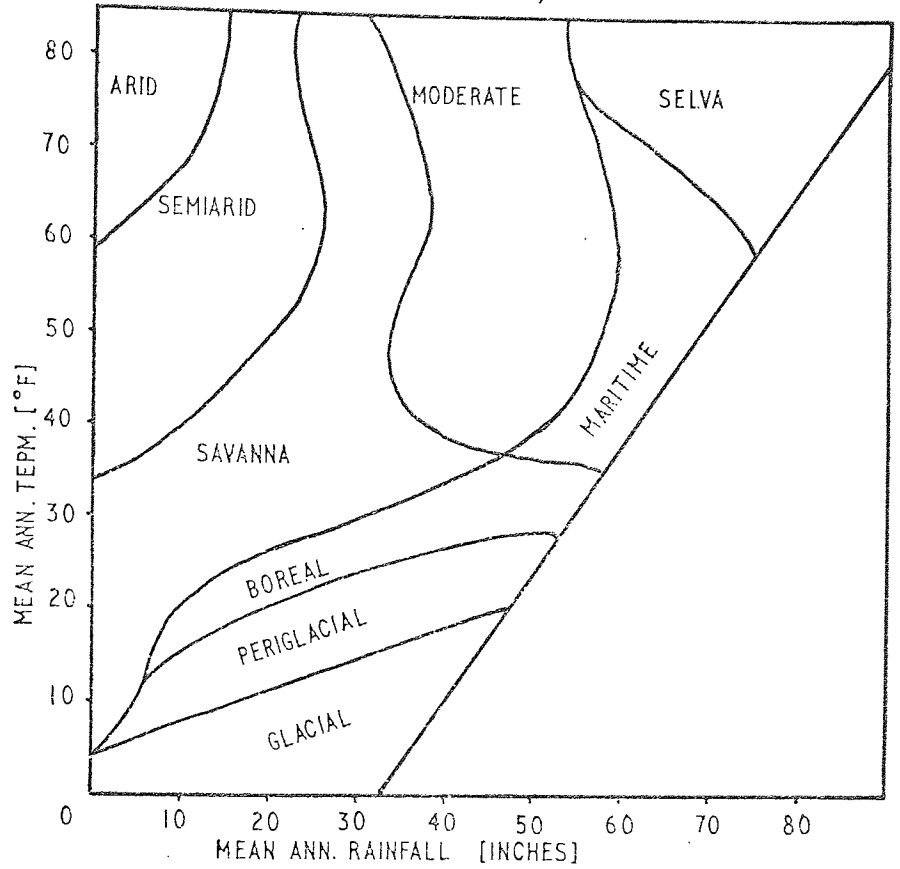
A) INTENSITY OF CHEMICAL WEATHERING IN RELATION TO RAINFALL AND TEMPERATURE



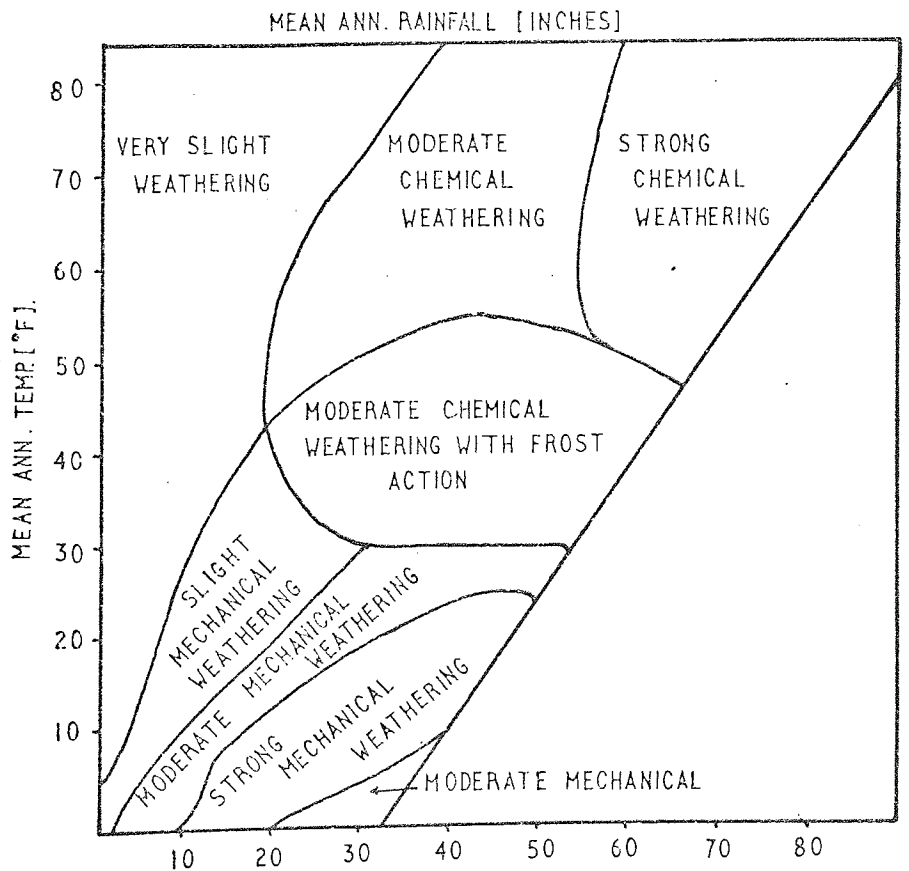
B) INTENSITY OF FROST WEATHERING IN RELATION TO RAINFALL AND TEMPERATURE

(PELTIER 1950)

FIG 4:2



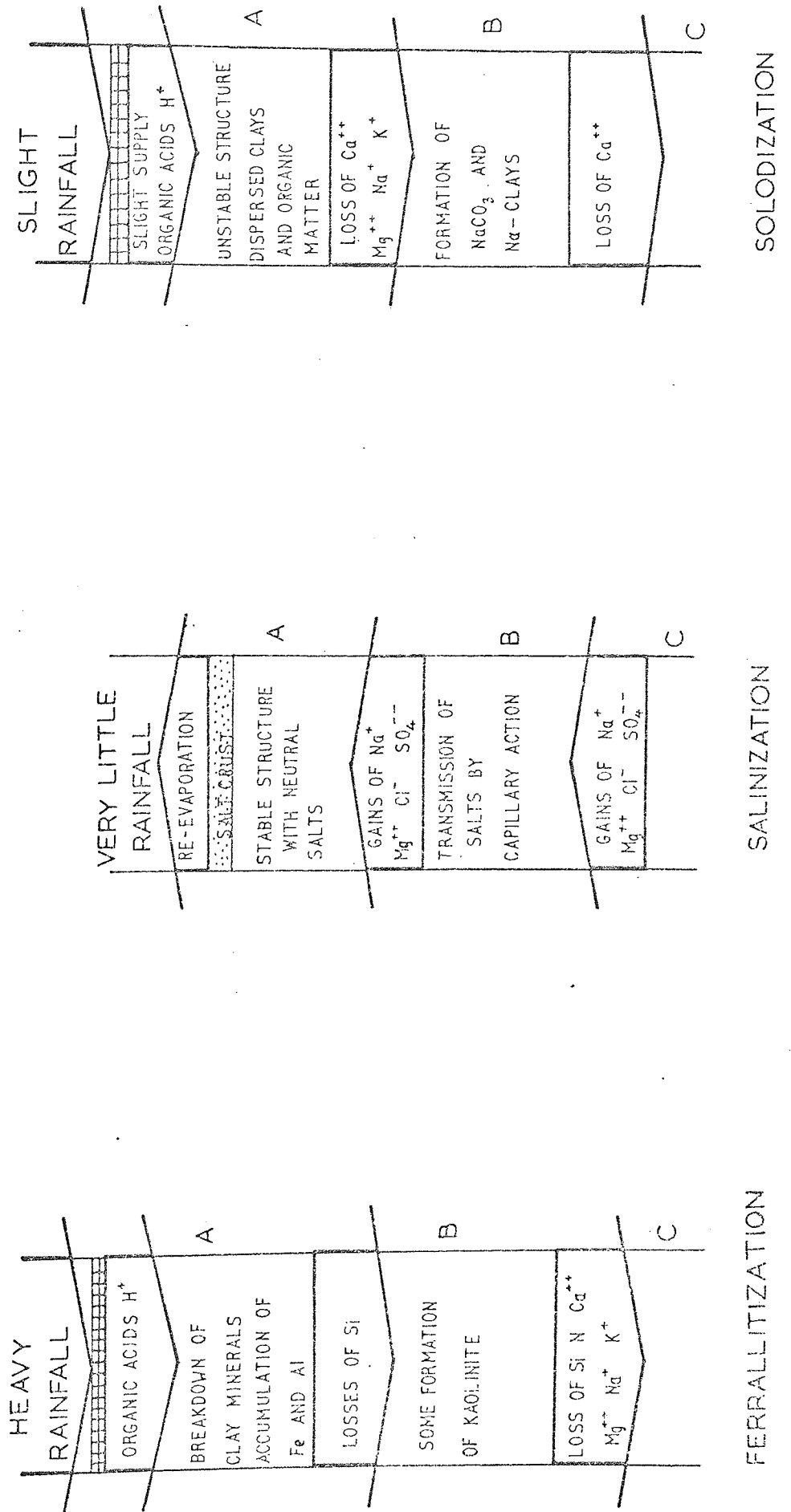
(A) DIAGRAM OF CLIMATIC BOUNDARIES OF MORPHOGENETIC REGIONS



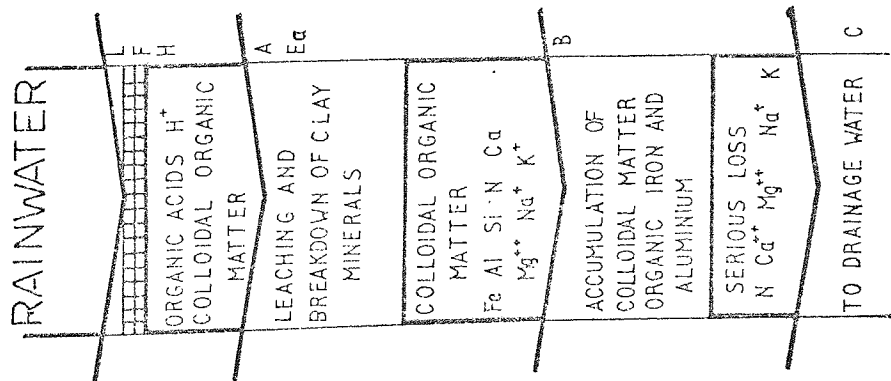
(B) WEATHERING UNDER VARIOUS RAINFALL AND TEMPERATURE.

AFTER PELTIER [1950]

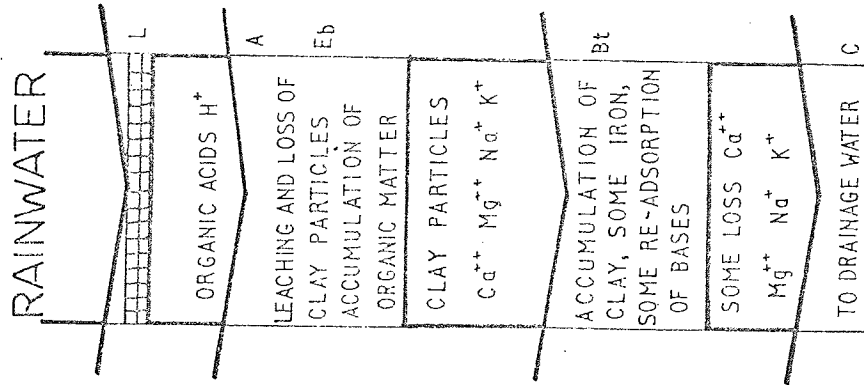
FIG 4:3  
WEATHERING PROCESSES



### PODZOLIZATION



### LEACHING



### CALCIFICATION

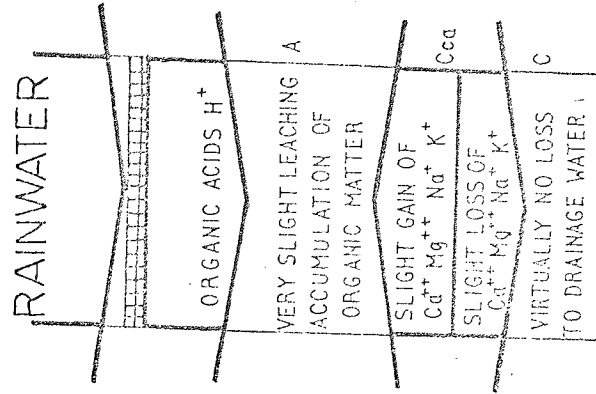


FIG 4:3(cont)

Rieche (1950) states that there is no useful purpose in making such a distinction. However, one can regard soil formation as one end of the weathering processes as in Table 4:1.

The controls for soil formation are also the controls for weathering and one should refer to Ollier (1969), Rieche, (1950), Saunders and Fookes (1970) for a comprehensive account of the soil types, classifications and formation.

Millar, Turk and Foth (1966) regard soil formation as a result of gains and losses, transformations and translocations, i.e. the top soil gains; water (by precipitation, condensation and flow), oxygen, carbon dioxide, organic matter, mineral matter (washed down) and energy from the sun, and losses; water (by evaporation, transpiration, seepage), nitrogen (by denitrification), carbon dioxide and mineral matter.

There are several major soil-forming processes that can occur during soil formation and are taken into account when the horizons are described and classified. These are defined below:

1. **ORGANIC ACCUMULATION:** Takes place at the ground surface due to accumulation of decaying vegetable matter although in Podzols there may be a secondary accumulation lower down the profile. (B horizon).
2. **ELUVIATION:** The mechanical translocation of clay or other fine particles down the profile.
3. **LEACHING:** Removal of material from a horizon in solution, and its movement down the profile.
4. **ILLUVIATION:** Accumulation in the lower part of the profile, of material washed down (eluviated) from above.

5. PRECIPITATION: Formation of solid matter in the subsoil from solutions washed down.
6. CHELUVIATION: Downward movement of material, similar to leaching but under the influence of organic chelating agents.
7. ORGANIC SORTING: The separation of material, usually into different grain sizes by organic activity (worms, termites, etc.).

#### 4:3:1 SOIL HORIZON NOMENCLATURE

An assemblage of soil layers or horizons is known as a soil profile, the soil profile concept being developed by the Russian Dokuchaiev (Glinka 1928) who also provided a system for labelling the component horizons.

Dokuchaiev originally used the letters A, B, and C for the layering in a chernozem soil formed on loess in Russia; A was the eluviated horizon, the eluviated material being deposited in the B horizon, the parent material beneath being termed C. Since then there have been many difficulties with the definition of the C horizon which in many cases was found not to be the parent rock. This can be shown if one considers a granite which is deeply weathered with a podzolic soil on the upper part of the regolith. The A and B will be the eluviated and illuviated horizons, the weathered granite being the parent material for the soil and therefore the C horizon, and the parent rock would then be labelled the D horizon.

The initial horizons were developed for freely drained soils, the waterlogged soils producing conditions (anaerobic) which enable different features to develop. These grey, often mottled horizons are called gley or glei, the horizons having complex relationships

to other horizons. The gleys can be either ground water gleys due to waterlogging at depth or surface water gleys produced by perched water over deeper soil or, seasonal waterlogging.

The main difficulty arises from assumptions regarding genesis of horizons, i.e. by using the A, B, C nomenclature one is assuming that the layering was developed from the parent material. How does one know from direct observation that the layers have been formed by eluviation and illuviation since one or more of the layers could have been due to a depositional origin (i.e. wind, hillwash or creep) which are unrelated to the C horizon?

This recognition and distinction between soil horizons and depositional strata is a major problem in many studies of soil genesis. Layering due to geological conditions was often overlooked in the early work and everything attributed to pedological processes. Many recent descriptions of soil profiles from Australia recognise geological events for most of the horizons and very little pedological layering (Churchward 1963 , Butler 1967 ).

In the majority of instances profile nomenclature is becoming standardized although there is still a great amount of variation. The A, B, C horizon is now accepted for the main horizons, with a variety of suffixes to imply specific conditions or subdivisions.

The nomenclature and definitions below are to some extent those currently in use.

#### 4:3:1:1 ORGANIC AND ORGANO - MINERAL SURFACE HORIZONS

L Undecomposed litter

F Decomposed litter

H Well-decomposed humus layer, low in mineral matter

- A An horizon, which, though mainly inorganic, consists of an intimate mixture of organic and inorganic materials resulting from the activity of soil animals and the decay of roots in situ. It is generally dark-coloured.
- Ap Ploughed layer of cultivated soils.
- (A) An incipient A horizon in raw soils.

#### 4:3:1:2 SUB-SURFACE HORIZONS

- Ea Bleached or pale coloured subsurface horizon in podzolized soils more or less depleted of sesquioxides and clay.
- Eb A layer, paler in colour than overlying or underlying horizons (especially when dry) slightly depleted of clay and/or sesquioxides.
- (B) Horizon without appreciable depletion of, or enrichment in colloidal material, distinguished from the overlying A horizon and from underlying horizons of less altered material by colour and structure.
- Bt Horizon containing illuviated clay.
- Bh Black or very dark brown horizon enriched in illuviated organic material.
- Bfe An orange-brown or brown horizon enriched in illuviated iron (and often aluminium).
- C Little altered substratum apparently similar in constitution to the material from which the overlying horizons have developed. Can be subdivided into distinct subhorizons.



- D If parent material is known then this is labelled D indicating that the profile developed from unweathered material of this composition and form.
- g Used as a prefix with other horizon symbols (except D) when morphological features resulting from gleying are superimposed.
- (g) This is used when gleying is only weakly expressed.
- ca Used with symbols C and D when there is an appreciable amount of deposited (secondary) calcium carbonate.

A/(B)

or Transitional horizons of intermediate character

(B)/C

As one would expect, the influence of the different weathering factors, principally those contributed by climate, results in substantially different profiles. For a comprehensive account of the soil types and their classifications one is referred to the works of Ollier (1969), Saunders and Fookes (1970), Bridges (1970)

#### 4:4 ENGINEERING CLASSIFICATION

It has been apparent for some time that the engineering properties of weak argillaceous rocks especially, vary throughout the weathered profile, The assessment of rock weathering is therefore necessary to the understanding of the behaviour of the materials.

Engineering classifications are based on the concept of weathering zones (grades). In certain rocks the junction between the weathered and fresh rock is sharp this being termed the "basal platform" by Linton (1955), "basal surface of weathering" by Ruxton and Berry (1957)

or the now commonly accepted "Weathering front" proposed by Mabbutt (1961).

Between the fresh rock at some depth and the topsoil at the surface, the regolith is not even and may be divided into a number of zones that occur in fairly constant arrangement. These according to Ollier (1969) are not the soil horizons, though soil layering may add to or overlap zones.

The first classification was devised by Moye (1955) from the work on the Snowy Mountain Scheme and covered from the completely altered state at the surface down through zones of decreasing weathering to fresh rock at depth.

Ruxton and Berry (1957) working on granite in Hong Kong produced a similar scheme but excluded the soil.

Soil (not counted by Ruxton and Berry as a weathering zone)

Zone I - residual debris of structureless sandy clay or clayed sand

Zone II - Residual debris with rounded free corestone

Zone III - Angular, locked corestones with residual debris

Zone IV - Partially weathered rock with minor residual debris along structural planes.

A sharp junction separated Zone IV from the unweathered rock.

Knill and Jones (1965) used a fourfold classification to describe the stages of weathering of igneous rocks. In the

geotechnical assessment of a site at Mundford, Norfolk for the proton accelerator, Ward et al. (1968) used a five fold grading scheme for the chalk.

Grade V :- Structureless melange. Unweathered and partially - weathered angular chalk blocks and fragments set in a matrix of deeply - weathered remoulded chalk. Bedding and jointing are absent.

Grade IV :- Friable to rubbly chalk. Unweathered or partially - weathered chalk with bedding or jointing present. Joints and small fractures closely spaced, ranging from 1cm apart to about 6cm apart. Joints commonly open up to 2cm and infilled with weathered debris and small unweathered chalk fragments.

Grade III :- Rubbly to blocky chalk. Unweathered medium to hard chalk with joints 6cm to 20cm apart. Joints open up to  $\frac{1}{3}$ cm, sometimes with secondary staining and fragmentary infilling.

Grade II :- Medium hard chalk with widely-spaced closed joints. Joints more than 20cm apart.

Grade I :- Hard brittle chalk with widely-spaced closed joints.

The grades I, II and III describing unweathered chalk of different hardness.

TABLE 4:3

Skempton & Davis 1966 for Keuper Marl

	Zone	Description	Notes
Fully Weathered	IVb	Matrix only	Can be confused with solifluction or drift deposits, but contains no pebbles. Plastic, slightly silty clay. May be fissured.
Partially Weathered	IVa	Matrix with occasional clay stone pellets, to 1/8" dia. but usually coarse sand size	Little or no trace of zone I structure, although clay may be fissured. Lower permeability than underlying layers.
	III	Matrix with frequent lithorelicts up to 1 in. As weathering progresses lithorelicts became less angular	Water content of matrix > than that of lithorelicts.
	II	Angular blocks of unweathered marl, virtually no matrix	Spheroidal weathering Matrix starting to encroach along joints first indications of chemical weathering.
Unweathered	I	Mudstone (often fissured.)	Water content varies due to depositional variations.

TABLE 4:4  
ENGINEERING GRADE CLASSIFICATION OF WEATHERED ROCK  
(Fookes & Horswill 1969)

<u>GRADE</u>	<u>DEGREE OF DECOMPOSITION</u>	<u>FIELD RECOGNITION SOIL (SOFT ROCKS)</u>
VI	Soil	The original soil is completely changed to one of new structure and composition in harmony with existing ground surface conditions.
V	Completely Weathered.	The soil is discoloured and altered with no trace of original structures.
IV	Highly Weathered.	The soil is mainly altered with occasional small lithorelicts of original soil. Little or no trace of original structure.
III	Moderately Weathered	The soil is composed of large discoloured lithorelicts of original soil separated by altered material. Alteration penetrates inwards from the surfaces of discontinuities.
II	Slightly Weathered.	The material is composed of angular blocks of fresh soil, which may or may not be discoloured. Some altered material starting to penetrate inwards from discontinuities separating blocks.
I	Fresh rock.	The parent soil shows no discolouration, loss of strength or other effects due to weathering.

A scheme for soft rock was adopted by Skempton and Davis (see Davis (1966)) when investigating the engineering behaviour of the Keuper Marl in the Midlands (Table III). Chandler (1969) using this scheme has quoted permeabilities (from triaxial test specimens) of  $5 \times 10^{-6}$  to  $5 \times 10^{-7}$  mm/s for Zone IV marl compared to  $1 \times 10^{-5}$  to  $1 \times 10^{-6}$  mm/s for Zone III marl. He has accounted for this lower permeability of the more weathered Zone IV marl as due to the increasing proportion of free or disaggregated clay particles. This increasing proportion of free clay particles could also be due to the process of illuviation which would in pedological nomenclature be part of the B horizon.

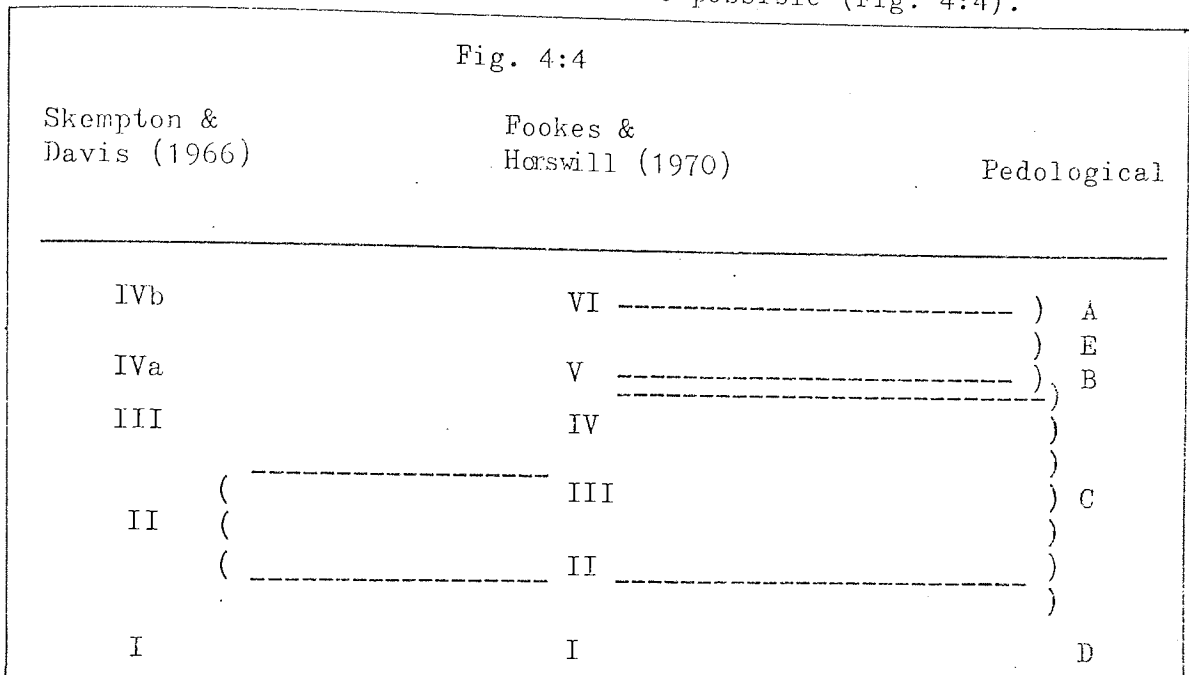
A more versatile scheme of weathering zones is that of Fookes and Horswill (1969) (Table 4:4) and is the one used in this project. It should be noted that this weathering scheme was adopted by the Engineering Group Working Party (1972) in their report on "The Preparation of Maps and Plans in Terms of Engineering Geology".

#### 4:5 SUMMARY OF CLASSIFICATIONS

Saunders and Fookes (1970) have stated that in all the classifications the prime object is the subdivision of the weathered rock and that the true residual "soils" (approximating to the A and B pedological horizons) are generally contained within the engineering Zone VI (zones based on Fookes and Horswill 1969).

It can be seen from the descriptions and the development of the weathering schemes, that both the full pedological profile and the engineering zones cover the same ground, yet each is emphasising specific data. The engineer is considering the state of the rock material whereas the pedologist is concerned with the nature and state of the upper horizons (chemical and physical).

Since the engineering scheme is based primarily on the degree of disintegration it gives no indication of what is occurring chemically. The use of both schemes is therefore required to cover both the character and the origin of the weathered profile, but only a general correlation between the two schemes is possible (Fig. 4:4).



#### 4:6 WEATHERED PROFILE AT BLOCKLEY CLAY PIT

The weathered material appears to have formed directly from the underlying clay and has had something in the order of 11000 years in which to form. This assumes that the clay was left exposed to the elements after the last ice sheet had retreated. This is unlikely as some glacial material must have been deposited and this would first have to be removed before an equilibrium profile based on the parentage of the Lias clay could evolve. Both the pedological nomenclature and the engineering classification of Fookes and Horswill (1969) are used to describe the weathering.

#### BLOCKLEY SERIES.

Location:- North Cot Brick and Tile Works (SP 164348)

Parent Material:- Lower Lias clay. (ibex Zone)

<u>Pedological</u>	<u>Scheme</u>	<u>Depth</u>	<u>Description</u>
	<u>Fookes &amp; Horswill 1969</u>		
Ap	VI	0-0.2m	Dark brown earth, very firm when moist. Reddish ochre material in lenses and streaks. Material is a silty clay loam. Microscope examination shows 60-80% of quartz of silt size this being easily felt between the fingers; no stones coarse blocky structure (4-6cm.), extremely hard when dry. Pierced by roots and small animal burrows.
Ebg	VI	0.2-0.46m	Paler in colour than overlying ploughed layer, grey brown with reddish brown mottling although pale grey clay is noticeable on the surfaces of fissures. This indicates that these surfaces are continually wetted by a reducing vadose water. Coarse (<6cm) sub-angular to prismatic structure. Open fissures (5-8mm) with smooth undulating grey surfaces extending through this section (from the surface) into the material below. Only very strong roots penetrate to this depth. Mica flakes become noticeable. Non calcareous.
Btg(fe)	V	0.46-0.92m	Layer of pale grey clay, soft, plastic when wet with extensive reddish brown to yellow brown mottling. Roots do not penetrate far into this material. Coarse (4-6cm) prismatic structure, open fissures (3-4mm) extending down to a depth of 1.4m. Limonitic nodules are present in horizontal layers these being the remains of clay ironstone nodules that have now



<u>Pedological</u>	<u>Scheme</u>	<u>Depth</u>	<u>Description</u>
	<u>Fookes &amp; Horswill 1969</u>		
Btg(fe)	V	0.46-0.92m	(cont.) weathered indicating the parent material to be Lias Clay. The soil matrix near the nodules is redder indicating that iron oxides are moving away from the nodules, (usually spheroidally). It was ensured that no nodules were near when sampling the soil for testing. Lithorelicts (Brewer 1964) are less than 2cm in size. Non-calcareous.
C <sub>1</sub> (g)	IV	0.92-2.28	Olive grey clay with ochreous iron mottling (yellowish brown to reddish brown) firm when moist. The grey becomes more intense with depth (towards the blue-grey of the parent material) Coarse prismatic structure (4-6cm), slightly fissured at the base of the zone. Lithorelicts frequently up to 3cm and larger at the base. Non-calcareous.
C <sub>2</sub>	II	2.28-2.70	Blue grey clay, highly fissured (If. low to medium) amount of fissuring decreasing to an If. of medium with depth. Weathering is chemical along joint surfaces and is mainly a ferric oxide coating although on rare occasions there are then coatings of pale clay. Calcareous although fossil fragments are rare.
D	I	2.7 →	Unweathered blue-grey clay, fissured, no signs of weathering although along open joints (<1mm) at depths of 8 to 9m superficial clay coatings were found. Calcareous.



PLATE 4:1

BLOCKLEY CLAY PIT SECTION ONE  
(0.0m - 1.5m)



PLATE 4:2

BLOCKLEY CLAY PIT SECTION ONE  
(1.5m - 3.2m)



PLATE 4:3

BLOCKLEY CLAY PIT SECTION ONE  
(3.2m - 4.5m)

This profile appears to be typical of the weathering profile that has formed on, and from, the Lower Lias clays. Its extent and development has been dependant on such factors as climate, water table, time etc. The clays are poorly drained and are sesonally waterlogged near the surface to produce the surface water gley soils. The anaerobic conditions produced by waterlogging and the chemical reactions which occur include changes in the form of the iron compounds. In well aerated parts of the soild the brown and red colours of ferric oxides predominate, whereas in waterlogged anaerobic parts (i.e. surfaces of fissures) grey or blue-grey colours are present. In many instances the excess of water is self-evident when water seeps from the soil profile at specific horizons and from the increase of water contents in the samples. This is very noticeable in the Sections at Blockley (Fig 4:5) where water contents increased and seepage occurred near the Btg(fe)/C<sub>1</sub>(g) junction.

The samples take in relation to the profile for Section One and Two are shown in Fig 4:5 together with their moisture contents. The Sections were taken at different times, hence the difference in shape of the water content curves.

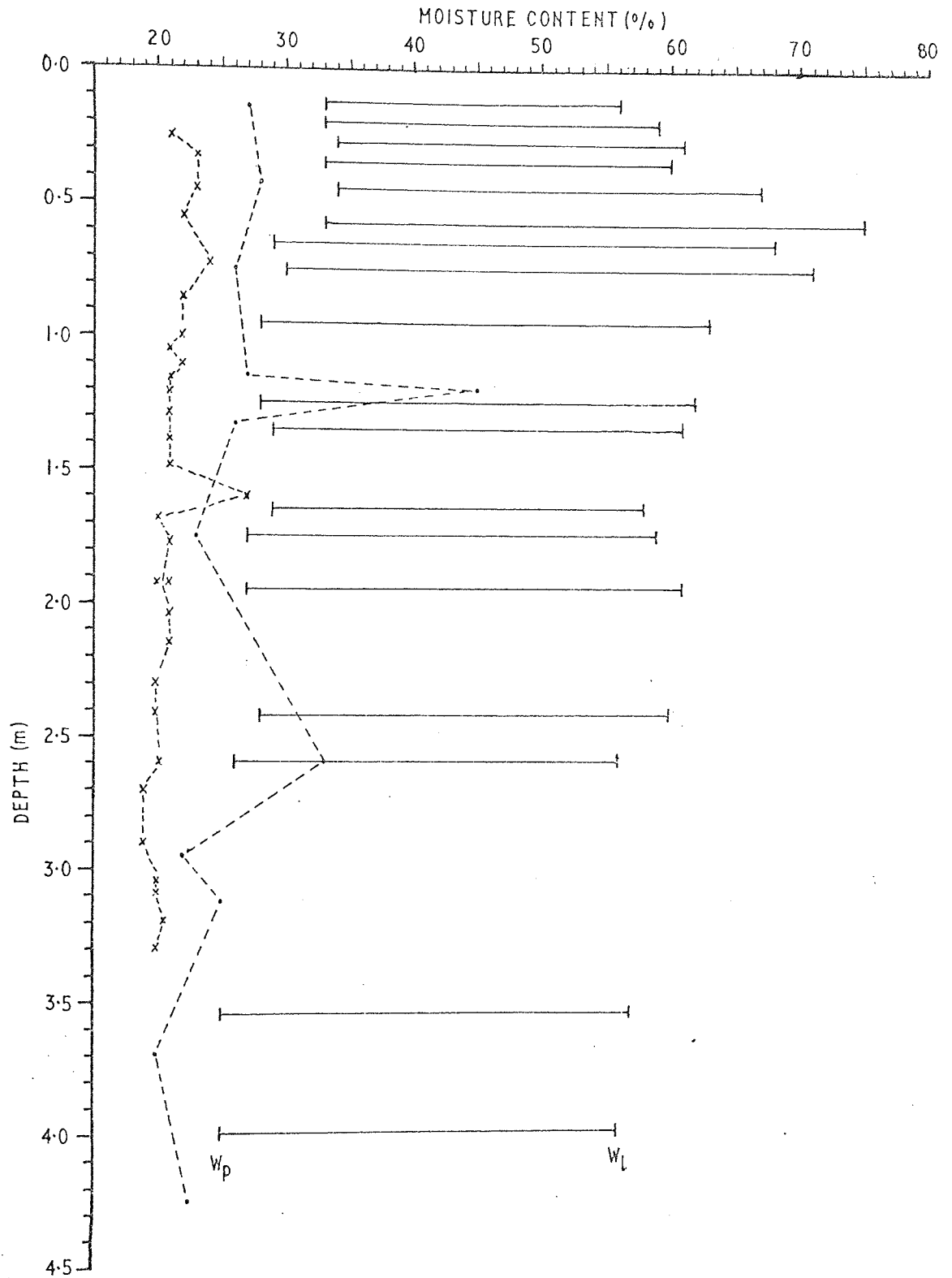
Section One: one day after rain showers

Section Two: after a relatively dry period

#### 4:7 HONEYBOURNE CLAY PIT

For comparison a profile at the Honeybourne clay pit is briefly described. The pit is located approximately 0.4 km north of Church Honeybourne in the Vale of Evesham, and is one of the pits examined during the search for a suitable profile. The pit is very small in comparison with the Blockley pit being no greater than

MOISTURE CONTENT/DEPTH RELATIONSHIPS,  
BLOCKLEY



SECTION ONE - - - - -  
 SECTION TWO - - - x - - -  
 $W_p$  = Plastic Limit  
 $W_l$  = Liquid Limit

FIG 4:5

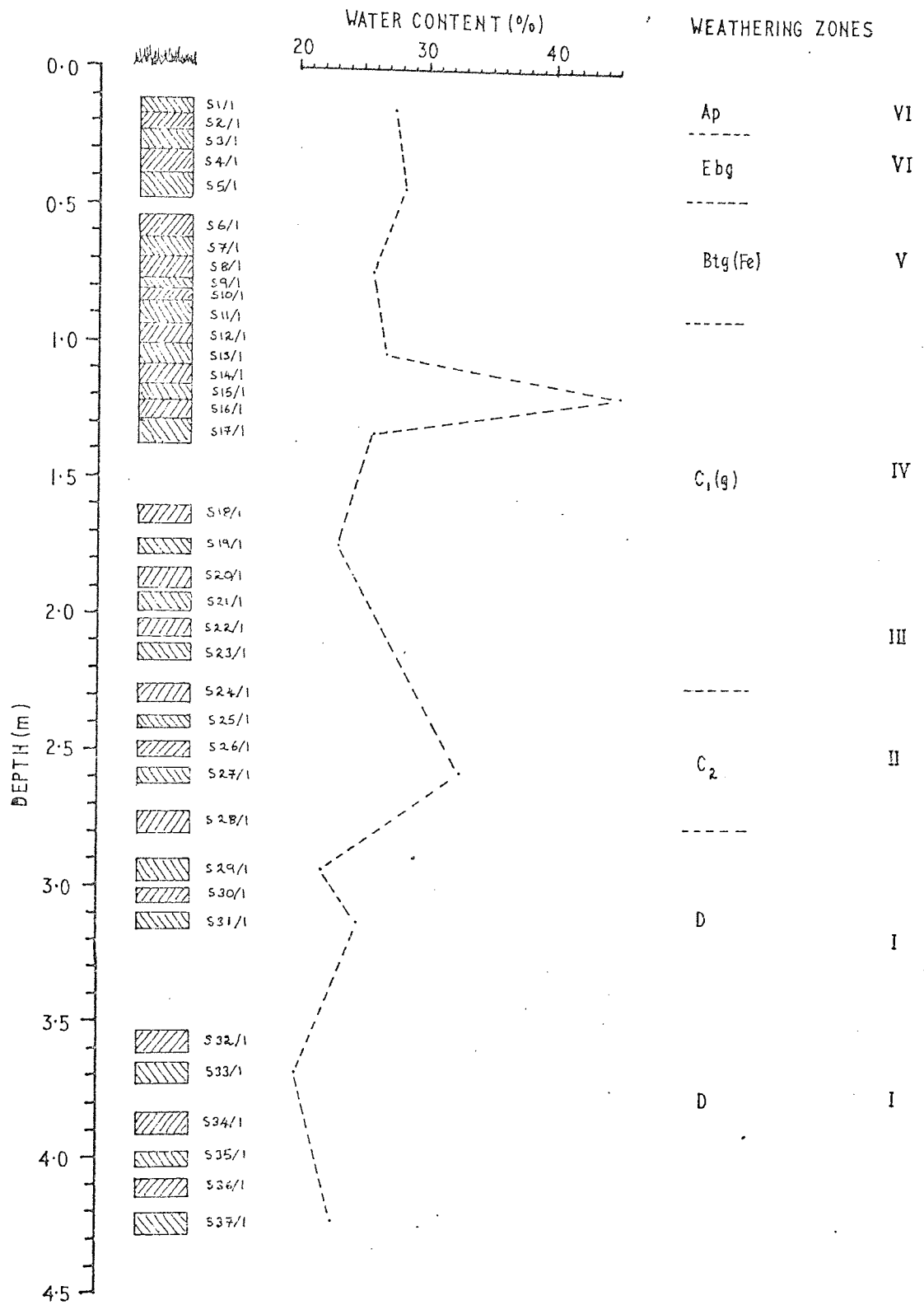


FIG 4:6

MOISTURE CONTENTS, WEATHERING ZONES AND SAMPLES, SECTION ONE

3.6m deep with mainly weathered material exposed. The clay belongs to the semicostatum Zone of the Sinemurian stage just above the Blue Lias. Remains of these ammonites being fragmental but numerous in the southern half of the excavation. The weathered clay is used to manufacture tiles and pipes (no bricks are manufactured). The water table is relatively close to the surface in the vale so the weathered profile is somewhat attenuated.

Location: Church Honeybourne SP 115454

Parent Material:- Lower Lias clay (semicostatum Zone).

<u>Pedological</u>	<u>Scheme</u>	<u>Depth</u>	<u>Description</u>
	<u>Fookes &amp; Horswill 1969</u>		
Ap	VI	0-0.2	Dark brown, rich in humus, silt material blocky structure, firm when moist.
Eb/Bt(g)	V	0.2-0.6	Difficult to distinguish any definite boundary to either of these zones. Olive grey with a small amount of gleying, pale grey on the ped surfaces. Coarse (4-6cm) blocky structures becoming highly fissured at the base.
C	IV	0.6-	Very highly fissured (I <sub>f</sub> . medium to low) brownish grey with little or no mottling, fissured blocks (2-20 cubic cm) have unaltered lithorelicts inside having a lower water content and are much firmer. These lithorelicts increasing in size with depth. Fissure surfaces are often pale grey in colour, brownish



(continued)

grey beneath the surface  
covering, with the  
unweathered blue-grey  
within the lithorelict.

## CHAPTER 5

### MESOSTRUCTURES

#### 5:1 INTRODUCTION

Structure in rock is an extremely complex concept to quantify, since structure can exist at a number of levels from micro to macro. Mesostructures include such features as horizontal layering, laminations, varves; vertical root channels and tension cracks; and random fissuring and jointing. In other words the majority of mesostructures can be termed discontinuities.

These discontinuities can exert a dominant influence on the strength of the material. Terzaghi (1936) described a stiff fissured clay as

"When it is dropped a big chunk of such clay breaks into polyhedric, angular or subangular fragments with dull or shiny surfaces. The diameter of the fragments may range between less than one centimetre and more than twenty centimetres. In some cases the jointing has been produced or intensified by preceding natural slides".

In the same paper he also pointed out that the overall strength of these "stiff fissured clays" could be as low as one fifth to one tenth of the strength as measured on small intact samples.

It was after the publication of Terzaghi's paper that work was carried out on long-term stability problems. Skempton (1948) showed that the strength of the London Clay continued to decrease after a cutting had been excavated. Direct evidence was produced to show that at least a part of the loss in strength could be attributed

to softening of the clay along fissures which as Terzaghi (1936) had suggested, became open as a result of small movements occurring after the removal of lateral support when the excavation was made.

Further work by Skempton (1964) suggested that in addition to allowing the clay to soften, the joints and fissures cause concentrations of shear stress which locally exceed the peak strength of the clay and lead to progressive failure. Skempton and La Rochelle (1965) at the site of the nuclear power reactor, Bradwell, gave a ratio of short-term overall strength to the strength measured in conventional laboratory tests of 55% and yet a ratio of 75% was obtained for large-scale loading tests at depths of 15m by Whitaker and Cooke (1966). Rowe (1972) reported an incident when a trench dug in the Lower Lias clay failed within half an hour of completion. The undrained strength had been given as  $200 \text{ kN/m}^2$  with an associated factor of safety exceeding 5, but the high permeability at this site allowed rapid softening and the approach of the long term condition within half an hour. With an excavation the loss of suction on the open face decreases the effective stress and as the fabric opens up the permeability is increased causing rapid softening with the result that slips occur, working inwards from the face.

It can be seen therefore that discontinuities are of great importance to the engineer.

## 5:2 DISCONTINUITIES

### 5:2:1 DEFINITIONS AND OBSERVATIONS

Skempton, Schuster and Petley (1969) in their work on joints and fissures in the London Clay distinguished five types of discontinuities. They stated that there was some degree of overlap between the categories and it was not always possible to assign

a given feature unambiguously to one particular class. Their five discontinuities were

- (a) Bedding
- (b) Joints
- (c) Sheeting
- (d) Fissures
- (e) Faults

These discontinuities cover a range of stress conditions from zero to brittle fracture.

Pettijohn (1957) was only concerned with discontinuities of sedimentary origin which are mainly associated with bedding yet this leads to a classification in which the terms are defined with some genetic implications.

Braybrooke (1966) suggested a classification based on genesis on the grounds that different origins produce features with different physical properties. Three major types of discontinuity were proposed.

- 1) Discontinuities of sedimentary origin.
- 2) Discontinuities associated with brittle fracture.
  - (a) Tectonic
  - (b) Intrusive
- 3) Discontinuities associated with plastic deformation.

Unfortunately joints were not defined in this context and the existing definitions could be applied to any of the three groups. If this classification were applied to clays then group (3) would have to be either omitted or redefined, as in the existing context, it applies only to terms defined by Turner and Verhoogen (1960) for igneous and metamorphic rocks.

It seems that of the five discontinuities defined by Skempton et al. (1969) only two, bedding and faults have a good definition;

"Bedding planes record the termination of one episode of sedimentation and the beginning of another". Pettijohn (1957).

"A Fault is a plane of fracture which exhibits obvious signs of differential movement of the rock mass on either side of the plane". Price (1966).

Krynine and Judd (1957) defined a fracture as any break in a mass of rock regardless of size and then subdivided this into:

(a) Joint: a fracture along which no visible differential movement has occurred in the plane of discontinuity.

(b) Fault: a fracture along which visible movement has occurred in the plane of fracture.

Skempton et al. (1969) when talking about joint, fissure and sheeting described them as;

(a) Joint: predominantly vertical (normal to the bedding at the site they investigated).

(b) Sheeting: surfaces of moderate size, more than 323 cm<sup>2</sup> in area dipping at angles between 5° and 25° with a smooth surface, slightly undulating.

They can be differentiated from bedding by the dip and topography of their surfaces and classed as low angle joints or sheeting.

(c) Fissures: in the London Clay are planar or conchoidal fractures, rarely more than 150.0 mm in size with a matt surface texture.

There is no comparable definition for the term joint as used by geologists and engineers.

The American Geological Institute (1962) regard small scale discontinuities and closed large discontinuities as joints and open large discontinuities as fissures. Engineers on the other hand use the British Standards Institute (1957) definition and regard large discontinuities open or closed, as cracks and joints respectively and small discontinuities.

Fookes and Denness (1969) when working on the Cretaceous rocks of south-east England used the term fissure regardless of size or closure and described them on their morphological properties; size, shape, geometry and surface marking.

In this way the old definitions of joints, fissures and sheeting are combined and they are all classed as discontinuities but separate features. In this study the same concept will be followed and the same size, surface and geometry descriptions are used (Fookes & Denness 1969). One change was made in the geometry descriptions. It was found very difficult to distinguish curved, semicurved and planar on the definition by Fookes and Denness since the radius of curvature was impossible to determine with accuracy. The geometry was therefore simplified and the fissures recognised on profile.

#### 5:2:2 ORIGIN

Joints and fissures are of interest since they give a general expression of the stress field to which the rocks have been subjected,

and by careful mapping, the orientations of the joints may reveal a geometrical relationship to other elements, i.e. fold, faults, bedding etc.

Berger and Gnaedinger (1949) worked on thixotropic clays and found that a system of fine fissures developed during a period of long storage at constant water content and suggested that syneresis may be the cause. Skempton and Northey (1952) and Skempton (1953) define syneresis as:

"a colloidal process whereby the particles draw themselves together, under the action of attractive forces and expel some of the pore water".

They demonstrated this fissure development with London Clay, remoulded at the liquid limit and stored under water. It eventually became "chunky" in nature this they attributed to syneresis. They found that the water content in the immediate vicinity of the fissures was slightly lower than in the bulk of the clay. Rosenqvist (1955) was also convinced that syneresis is a prime factor involved in the development of fissures and slickensides in fine grained sediments.

The majority of joint and fissure patterns are related to some tectonic event such as folding, faulting or uplifting. This has led to classifications and theories of origin based on the stress system that the rocks have undergone.

Griggs (1935) noted that shear fractures in the laboratory are inclined to the direction of maximum compression, at angles somewhat less than  $45^{\circ}$  and that these were commonly slickensided. Tension fractures (according to Griggs) were characterised by clean,

granular breaks, with Nadai (1950) noting plumose markings on such surfaces produced under tension in the laboratory. Parker (1942) associated plumose patterns with shearing, while Hodgson (1961), Muehlberger (1961) and Badgley (1965) all favour a tensional association.

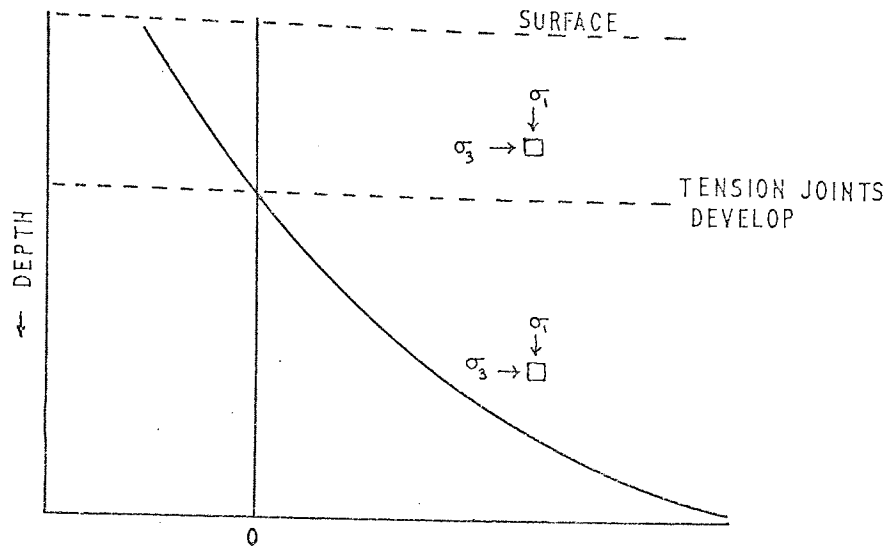
Roberts (1961) considered that feather-fracture itself was not indicative of either shearing or tensile stress, but demonstrated that feathering was produced by rapid separation of the medium. This was supported by Gramberg (1966) on laboratory tests on rocks.

Muehlberger (1961) analyzed diagonal fractures with small dihedral angles and concluded that there is a continuous spectrum between tensional and shear failure, this means that extension fractures should be a near surface phenomenon.

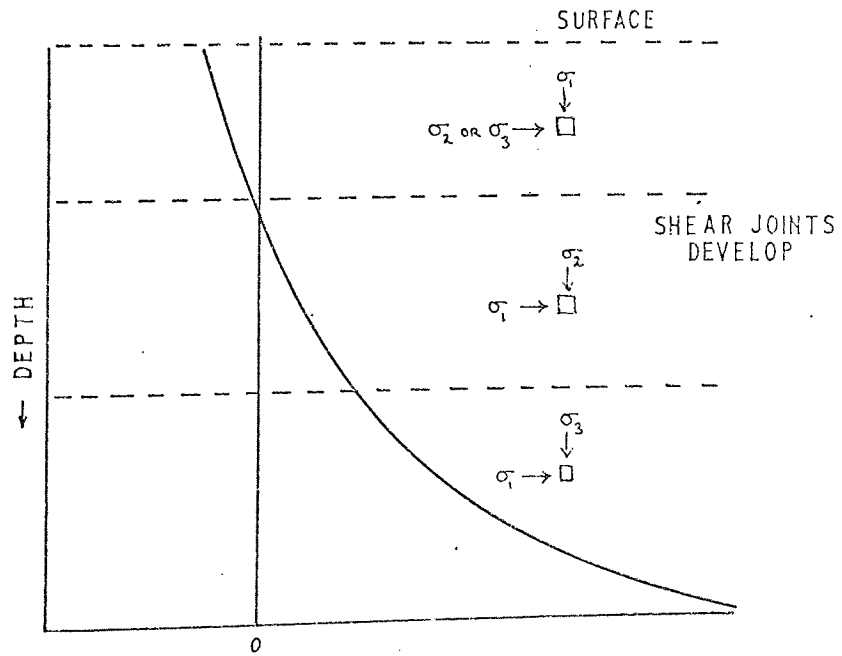
Price (1966) has shown that fractures which could form in a rock are dependant on the stresses set up in the rock. A rock initially under approximately hydrostatic stress when uplifted towards the surface will form tension joints or fractures at a specific level due to the decay of stress. If it is assumed that tectonic stresses which develop during a compressive phase, remain as residual stresses then the stresses on uplift will not only decay but also change in orientation (Fig 5:1).

The greatest principal stress initially acts horizontally and as uplift proceeds, stress changes until  $\sigma_2$  replaces  $\sigma_3$  in a vertical direction. The ratio of greatest to least principal stress at this stage may be too small to cause fractures to develop yet with continued uplift the ratio will increase until the conditions necessary for the development of shear fracture is fulfilled.





STRESS LEVEL  
A) HYDROSTATIC CONDITIONS



STRESS LEVEL  
B) TECTONIC STRESS AS RESIDUAL STRESS

FIG 5:1

The development of shear fractures will release an unknown proportion of residual stress and at this point vertical load will become the maximum principal stress direction. Further uplift will cause the rock to pass into tension with possible subsequent development of a system of tension joints.

Price in the same discussion also suggested that sheeting was due to strain energy release parallel to the surface due to erosion and uplift.

Gramberg (1966) also advanced similar ideas in that most vertical fractures in the crust without shearing movement in the fracture plane, are caused by tensile stresses; the best explanation is that they begin as a "Griffith Crack". He recognised two types of external loading;

1. Direct tensile loading in which the crack forms normal to the tensile load; a single crack is formed leaving an open gap with rough walls;
  2. Indirect or induced tensile loading in which the fracture plane extends in the direction of the major load axis and is normal to the minor load
- (Table 5:1).

According to Gramberg's model most regional fracture patterns particularly those in basement rocks, form as a result of ductile flow in Zone 1 which causes destressing in horizontal directions within Zones 2 and 1. Two vertical fracture systems may also form at right angles if both the least and the intermediate stress directions are horizontal and multiple vertical fracture directions may arise from several periods of destressing.

TABLE 5:1  
AFTER GRAMBERG 1966

Zone	Confining Pressure - Horizontal Stress	Cause of Fracturing	Fracture Type
	SURFACE		
3	destressed ensile	Direct tensile stress	Vertical open, non-planar, extensive direct tensile fractures at regular distances
	TENSION POINT		
2'	$\sigma_3$ low transition zone	Indirect tensile stress at low confining pressure	Vertical closed planar extensive a) single b) or multiple
2	$\sigma_3$ high	Indirect tensile stress at high confining pressure	Vertical closed planar short cleavage - fractures evenly distributed
1	$\sigma_1 \rightarrow \sigma_2 \rightarrow \sigma_3$	no fracturing pure plastic flow	

Fookes (1965) summarised the origin of fissures and joints prior to his orientation studies and these he used as a working hypothesis. He assumed that fissures in general could be formed and modified by one or more of the following processes:

1. Formed at the time of deposition or soon after by syneresis and/or changes in the salt chemistry of the environment of deposition.

2. Formed or modified some time later than (1) by insitu physicochemical changes brought about by such agencies as groundwater, weathering or ion exchange.
3. Formed or modified by tectonic (or quake) stresses during folding, faulting or shearing of the beds.
4. Formed or modified by non-diastraphic processes, eg. drying, hill creep, rebound on unloading or stress release during erosion.

### 5:2:3 CLASSIFICATIONS

As stated previously joints and fissures can be related to some stress distribution to which the rock has been subjected or it may be random. The classification of joints and fissures is dependant to some extent on the area examined.

The main factor that is of interest is the fissuring intensity. Fookes and Wilson (1966) in the Siwalik clay defined a classification for assessing the degree of fissuring, based on the distance between the fissures. Denness (1969) modified this and used the area of fissures per unit volume ( $m^2/m^3$ ) and the average size of intact blocks ( $m^3$  or  $cm^3$ ).

Area and volume classifications are ideal but they are cumbersome to use in the field and Fookes et al. (1971) have returned to the fracture spacing index which is the average distance between fissures (Table 5:2).

### 5:3 OBSERVATION OF DATA

For joint and fissure analysis there are two main methods, the cavity and the block technique. In this study both cavity and

block technique were employed and compared.

TABLE 5:2

FRACTURE SPACING INDEX ( $I_f$ )

	$I_f$ in metres
Extremely High	> 2
Very High	0.6 - 2
High	0.2 - 0.6
Medium	0.06 - 0.2
Low	0.02 - 0.06
Very Low	0.006 - 0.02
Extremely Low	< 0.006

5:3:1 BLOCK TECHNIQUE

In this technique the site area is selected and a one foot square column of clay is exposed by careful excavation. The final trimming of the block is done by palette knife to avoid mechanical disturbance. In most cases the block sample is cut and trimmed to a 200 mm cube, covered in waxed hessian, further waxed and a biscuit tin placed on top. It is then severed at the base, inverted and the base treated similarly. The space between the block and tin is filled in with wax. The tin is then sealed and suitable for transport.

The samples at Blockley were taken 10.35 m. below the surface in the side of the excavation, the weathered material and the unwanted overburden being removed by scraper and bulldozer to a depth of 7.5m - 8.8m. The remainder was removed by hand to produce a ledge in the side of the pit from which the samples were taken. All blocks were taken 0.91 - 1.22m from the edge to reduce sample disturbance and any moisture loss due to drying from the face.

Initial experiments were carried out on the use of a chain saw for extracting block samples. The chain saw used was an "Oregon Super Tronic", petrol driven, two stroke. It was found difficult to handle and there was considerable vibration.

Although the saw provided clean cuts when used, especially when cutting a block to size, a spade was used for trimming and final trimming done by hand using stiff spring steel spatulas.

A 30cm square column of clay was carefully exposed and the top was planed flat using a small "surform". The magnetic north was indicated on the surface by an arrow carved in the material to facilitate the reorientation of the block in the laboratory.

The faces and top are then immediately covered with wax to prevent moisture loss, the wax being a mixture of paraffin wax and petroleum jelly (ratio of 1:1). The molten wax was kept a degree or two above melting point and brushed on in a thick even coat. By keeping the wax close to its freezing point application of the wax by brush causes the wax to solidify almost immediately. This technique avoids wax penetrating any fissures or pores in the clay. The block was then severed from the rest of the column and placed on heavy duty aluminium foil on a timber stretcher. The base was then trimmed and coated with wax and then the whole block wrapped in foil. The foil was pressed close against the block to exclude all air and then waxed again with several coats. An external coat of pure wax is recommended for easy handling and the block should be transported on the wooden stretcher and never removed. This method can take from about an hour if the column is already almost exposed to about a working day if the block is to be taken from a few metres below an exposed surface.

PLATES 5:1-- 5:8  
Sequence Illustrating Block Technique for  
Fissure Analysis



PLATE 5:1

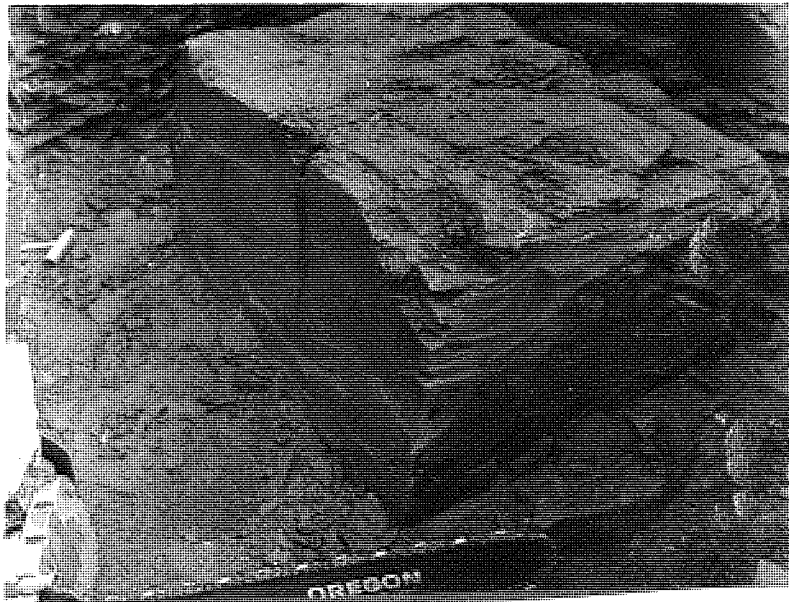


PLATE 5:2



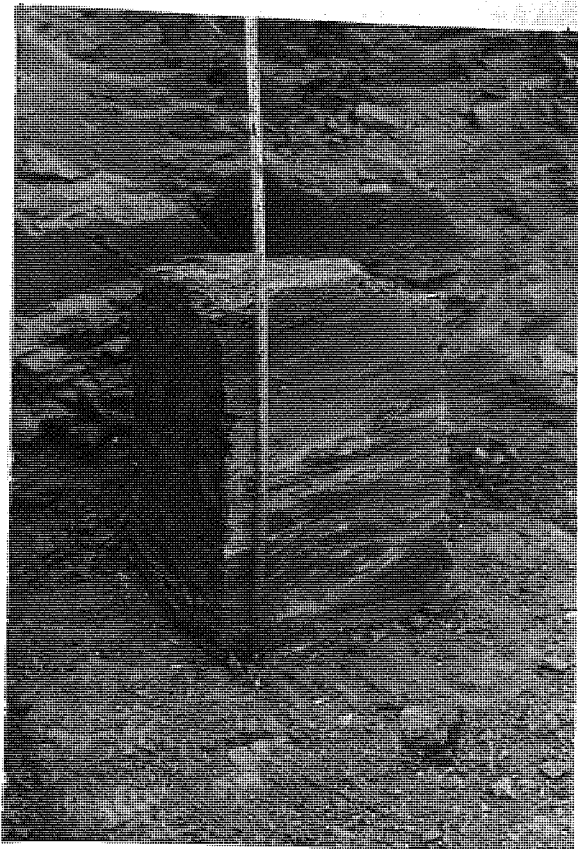


PLATE 5:3

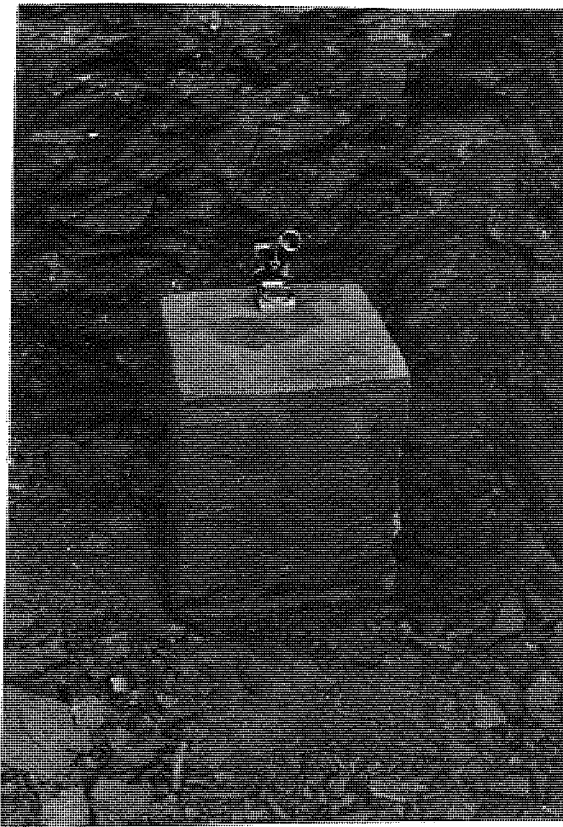


PLATE 5:4



PLATE 5:5



PLATE 5:6

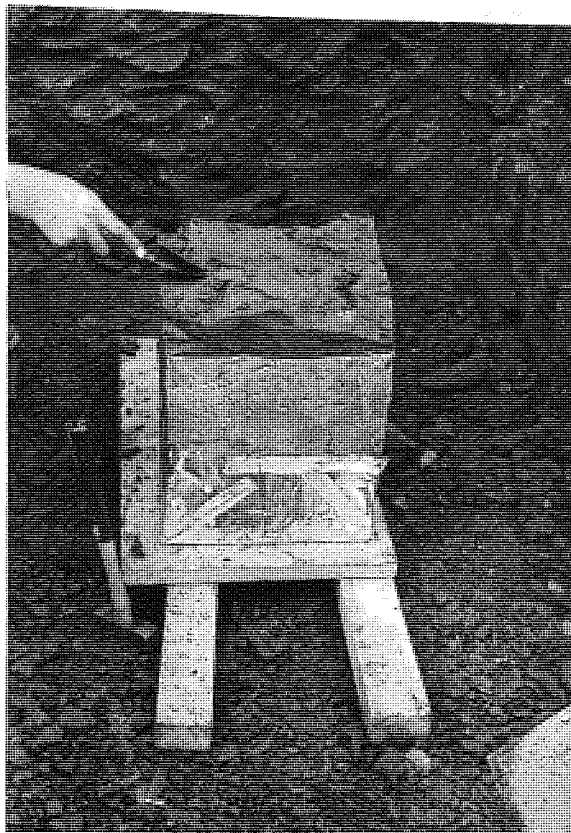


PLATE 5:7



PLATE 5:8

To make the measurements the block is orientated in exactly the same position as it was in the field, this is done in the same way as orientating a map. To record the required data about individual fissures the block is carefully dissected using a palette knife and gentle manual persuasion. The orientation of the fissures is recorded as a dip and strike measurement directly, using the compass and clinometer.

The method of wrapping the block is very efficient, moisture contents before wrapping gave 17.5% and one year later an average value of 16.2%.

#### 5:3:2 CAVITY TECHNIQUE

Measurement problems can be overcome to a certain extent by measuring the fissures in the field in the usual geological way. The major difference between the field technique and the laboratory one is that, instead of exposing and removing a block, recording of data is done in place by careful excavation (by hand) of a small recess in the material having similar dimensions to the size of a block that has also been examined.

The major problems of mechanical disturbance do not exist with the cavity technique although there are other inherent problems.

Suitable weather conditions are necessary for the block technique only when the block is being removed and in fact this can be eliminated by using a suitable shelter. Weather is critical for the cavity technique since clay will shrink on drying so it is essential to avoid direct sunlight and drying winds. Rain will not cause any volume change to saturated materials but will tend to disguise minor features such as roughness. Therefore, examinations should not be made in the rain unless an adequate shelter is provided. The cavity technique can take from one to three days so

the cavity must be protected at night.

The method is good for highly fissured clay or soil which is not too highly overconsolidated. At Blockley the Lias clay is very firm. The majority of fissures are closed and manual dissection is difficult.

Due to inherent problems in both techniques it was decided that the fissures would be examined using both methods. Five block samples were taken of which two were used in the fissure analysis.

#### 5:4 PRESENTATION OF DATA AND VALIDITY

In order to evaluate the relative frequencies of the joint orientations observed and to clarify the geometrical relationships between the various joint sets, the joints are represented as points on the projection of a reference sphere. One is referred to Phillips (1960), Turner and Weiss (1963) and Terzaghi (1965) for a detailed description of the mathematics involved. There are two different varieties of projection that are in common use in geology and engineering.

In many instances it is desirable to use a projection in which angular measurements are not distorted, in these circumstances the Wulff projection is used. This enables one to reorientate joint sets without distorting the angle between them.

The other projection, the Lambert or Schmidt equal area projection is important since it preserves areas correctly this being necessary when any statistical appraisal of the density of structural elements in different orientations is required.

Once the poles of the joint surface are plotted, the projection can be contoured. This can be done only with an equal area projection. It is not valid to contour a Wulff stereographic projection.

Contours are usually based on the number of data points within each one per cent unit area of the projection. Since standard Schmidt nets have a 200mm diameter, a circular counter of 20 mm in diameter has one-hundredth the projection area. A 1 cm square grid can then be used beneath the projection and the counter moved systematically to each grid intersection. The number of data points within each area being classed as a percentage.

Several other counting methods have been produced, in particular Denness (1969).

The validity of the trends obtained depend on the extent to which the data is a representative sample of the parent population. The optimum sample size as defined by Stauffer (1966) is; "the minimum sample size required to give good representation", and this will vary with the complexity of fabric and strength of concentration. A double standard exists in this definition of optimum sample size, depending on the use being made of the fabric interpretation. If one is interested only in the approximate orientation of the symmetry elements, then fewer points are required than if a study is being made that involves variations in the development of preferred orientation.

For the purpose of structural analysis the statistical correlation coefficient is a more critical test of preferred orientation. However, in the case of a strong fabric it need only be supplementary to visual determinations of symmetry and grouping.

Since the fabric under examination was quite strong it was felt unnecessary to carry out a correlation coefficient analysis.

The number of points needed to obtain a representative sample was based on the method developed by Stauffer (1966).

(Appendix B).

## 5:5 JOINT ANALYSIS AT BLOCKLEY

Three cavities were excavated by hand and are referred to as sites I, II, III. They were excavated at different positions along the working face during weekends and holidays.

A total of five block samples were taken, two of which were for joint and fissure analysis, the other blocks were for shear failure, consolidation and residual strength tests. Both the block and cavity technique were undertaken to ensure that any of the problems outlined earlier in taking the measurements did not result in a radically different picture.

To elucidate the relationships of the fissures, the measurements are shown as stereographic projections.

As soon as data became available it was plotted and contoured and Stauffers method (1966) (Appendix B) was used to determine the optimum sample size. Initial plots of 100 points gave a point maximum of between 8% to 12%. This indicated that at least 300 points would be necessary to obtain a representative sample. In the region of 100 to 150 data points were obtained from each site.

The majority of fissures were planar and although a method of plotting non planar fissures was attempted no relationship could be obtained. Denness (1969) showed that there is a relationship between the proportion of planar to non planar fissures and the period of time an exposure had been uncovered. The non planar fissures increased in number. He accounted for the formation of extra non-planar fissures by either being present in previously intact material or from the extension of a planar fissure. Denness (1969) suggested that the stress conditions during unloading at the

extremities of a planar crack are such as to propagate it in a curved or semicurved manner, this being analogous to the propagation of cracks in metal. Although non planar fissures exist before excavating the exposure, he concluded that stress release tended to generate more non planar than planar therefore the latter were earlier in origin.

He has made no suggestion that once the exposure is excavated it immediately begins to dry out and stresses are set up at the extremities of the fissures, and this could be the cause of the increase in the number of non planar fissures rather than unloading since unloading in many cases would be relatively small.

No statistical analysis was undertaken in respect to size of the fissures or surface markings (details were recorded). The majority of fissures were in the size range of 0.01 to  $1\text{m}^2$  (Fookes and Denness 1969) with the surface texture varying from smooth to rough. It was noticeable that the fissures that were pock marked all had an orientation paralleling the main orientation as deduced from the stereographic projections.

#### 5:5:1 CAVITY TECHNIQUE RESULTS

As one can see from Figs 5:2, 5:3 there is a medium to strong uniplanar set of fissures with a dip of  $11^\circ$  N.E. on a strike of  $45^\circ$  at Site I to a horizontal set at Site II. According to Stauffer (1966) three hundred data points were necessary to obtain a representative result, so three hundred points taken at random from the results from Site I, II and III were plotted to produce Fig 5:4. Again this shows an almost axial symmetry with a medium strong uniplanar set of fissures dipping at  $11^\circ$  N.E.,  $45^\circ$  ( $J_1$ ).

A second set of vertical conjugate fissures ( $J_2$  and  $J_3$ ) with



strikes of  $042^{\circ}$  ( $J_2$ ) and  $127^{\circ}$  ( $J_3$ ) are present. These are weak concentrations. The  $J_2$  set of fissures are stronger in number than the  $J_3$  set. This set of fissures encloses a mean dihedral angle of  $85^{\circ}$  about their E. - W. bisectrix.

Another very weak concentration is observed with a strike of  $173^{\circ}$ . There are two uniplanar sets  $J_4$  dip  $84^{\circ} - 90^{\circ}$  E strike  $164^{\circ}$ ,  $J_5$  dip  $50^{\circ}$  W. strike  $164^{\circ}$  and this may be a conjugate set with an acute bisectrix of  $46^{\circ}$ .

A very weak concentration of a uniplanar set with a strike  $148^{\circ}$  and dip  $84^{\circ} - 90^{\circ}$  E is observable but its existence is doubtful.

#### 5:5:2 BLOCK TECHNIQUE RESULTS

One block sample (number 2B) was taken from a depth of 10.349m below ground level and corresponds to the approximate depths at which the cavities themselves were excavated. Only 100 data points were plotted to allow a comparison with the cavity data (Fig 5:5). It can be seen that around 300 points will be needed to be absolutely valid, but an approximate comparison can be made.

A 7% concentration of a uniplanar set of fissures occurs with a dip  $0 - 5^{\circ}$  E strike  $132^{\circ}$ . This is almost the same as the  $J_1$  set found with the cavity technique and a closer examination indicates the presence in weak concentrations of  $J_2$ ;  $J_3$ ;  $J_4$ ;  $J_5$  although  $J_5$  is rather doubtful, and it would be impossible to infer a  $J_6$ .

As one can see there is very little difference between the stereographic projections for the block sample and those of the cavity samples.

In all stereographic projections the poles of the planes are plotted in the southern hemisphere and the black line is the trace

of the excavation face. The excavation face has a strike of  $133^{\circ}$  and a dip  $55^{\circ}$  E.

#### 5:6 DISCUSSION

The fissures fall into three groups; a weak major girdle and two uniplanar sets. The probability of the uniplanar set concentration of 9% being found in a randomly orientated set of fissures is many millions to one against, therefore the uniplanar set orientated at strike  $132^{\circ}$ , dip  $10^{\circ}$  E is very significant. ( $J_1$ ).

The major girdle is rather weak with concentrations of 2% or 3% and not fully developed. The two major concentrations in this girdle are  $J_2$ ,  $J_3$  with a very weak  $J_4$ .

Set  $J_2$  and  $J_3$  are probably one set with an acute bisectrix of approximately  $85^{\circ}$ .

The uniplanar set  $J_5$  could be associated with  $J_4$  forming a conjugate set.

Since the fissure analysis was carried out below the depth of weathering in the same horizon (i.e. The ibex Zone of the Lias clay), lithology and weathering should have little effect. Data from the borehole cores taken on the same site give a very small variation in both clay content and the plasticity index; clay content 38 - 47%, plasticity index 28 - 36%. These are insignificant variations and should have no effect on the types and intensity of the fissures.

The other factors as defined by Fookes and Denness (1969) that could have some affect are as follows:-

- (a) Bedding,
- (b) Stress release parallel to exposure surface,

- (c) Stress release parallel to ground surface,
- (d) Tectonism,
- (e) Age of Exposure.

The uniplanar set  $J_1$  is almost paralleling the ground surface and the bedding. The set  $J_4, J_5$  could be related to the stress release parallel to the exposure surface. Tectonism is limited to earth movements during the Jurassic period and gentle warping during the Alpine earth movements and probably had very little effect. The age of the exposure has negligible effect since no exposure was more than one day old and all measurements were completed within two days.

Hancock (1968) working on the Middle Jurassic limestone in the same area found six uniplanar sets of joints, four cozenal and statistically normal to the bedding surfaces and two inclined to the bedding of moderate angles. The oldest (which he termed  $J_1$  and  $J_2$ ) appeared to form a complementary system of wrench shear fractures enclosing an acute dihedral angle ( $85^\circ$ ) about an E. - W. bisectrix. This is the only set of joints found by Hancock which shows similarities to that found in the Lower Lias clay in this study. Hancock (1968) follows the opinion of Price (1966) who postulated that in horizontal rocks which have been compressed but not folded, two sets of shear joints develop and these may be subsequently followed by two sets of tension joints. The occurrence in the Cotswolds of a conjugate pair of wrench shear joint sets led Hancock to suggest that the region was subjected to a single cycle of subsidence, compression and uplift as Price proposed for the general case. There was remarkable similarity between the geometry

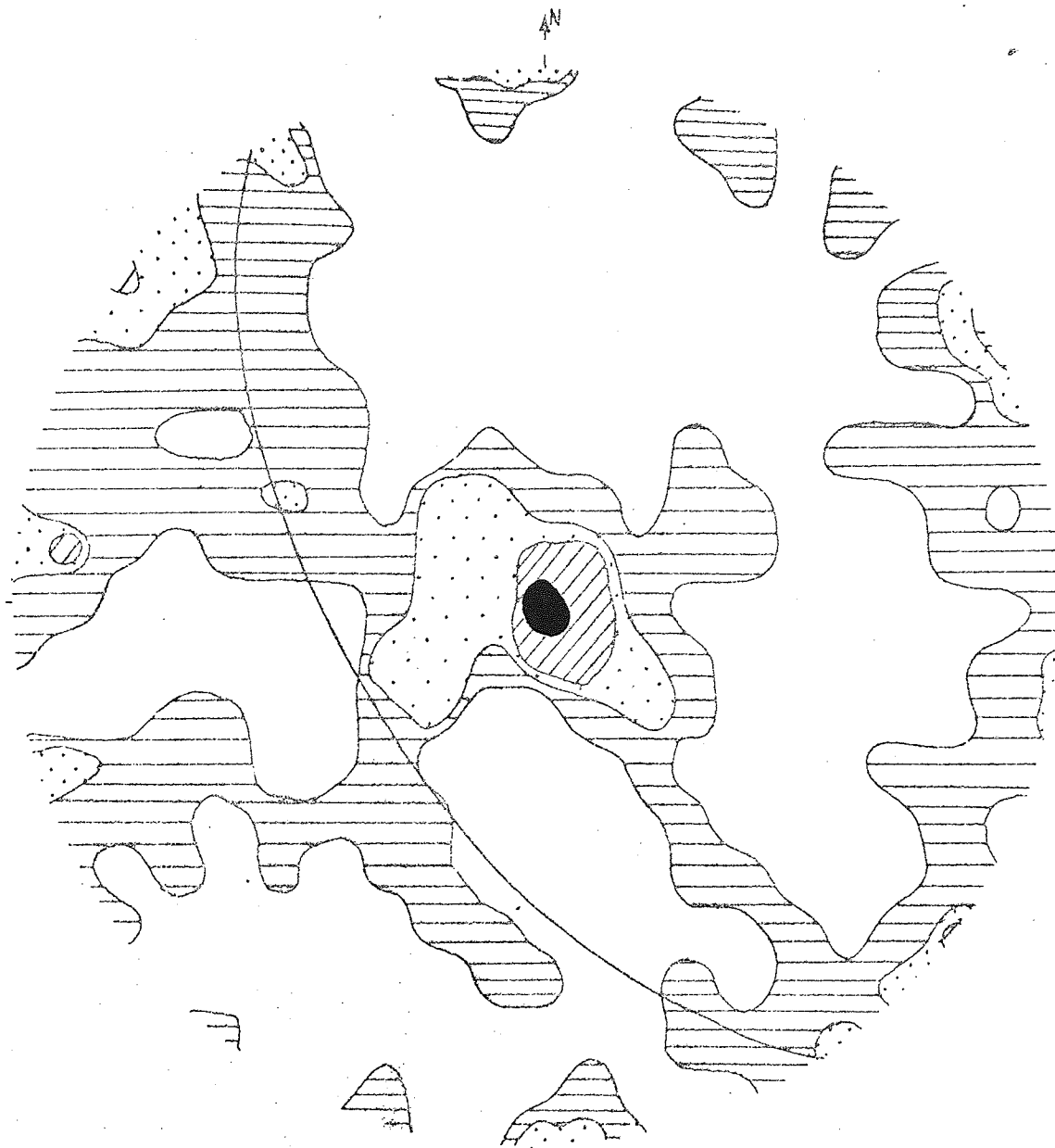
proposed by Price (1966) and that found by Hancock in the oolitic limestones.

There is no way in which the fissures at Blockley can be identified as shear as no slickensided fissures were observed. It is therefore almost impossible to indicate the stress system under which they developed.

There is good evidence to suggest that the factors which produced the uniplanar set ( $J_1$ ) were a combination of bedding foliation of the clay minerals and stress release parallel to the ground surface. The set  $J_4$  and  $J_5$  that are probably associated with the exposure face could develop in time and pose a problem for any long term slope stability.

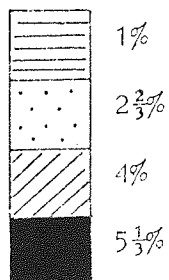
The intensity of fissuring increases in a narrow zone just below the weathering profile and just above in the weathered zone the true fissures change into apparent. Fissuring had no effect on excavation stability in the weathered and unweathered except for the deep desiccation cracks (2 - 3m) that occurred during dry spells.

SITE II



Contoured equal-area projection  
for 150 joint orientation in the  
Lower Lias, Blockley (Site II).

CONTOURS





SITE I

CONTOURED EQUAL-AREA PROJECTION FOR  
100 JOINT ORIENTATIONS IN THE LOWER  
LIAS AT BLOCKLEY

CONTOURS

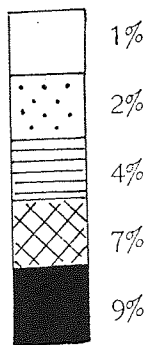
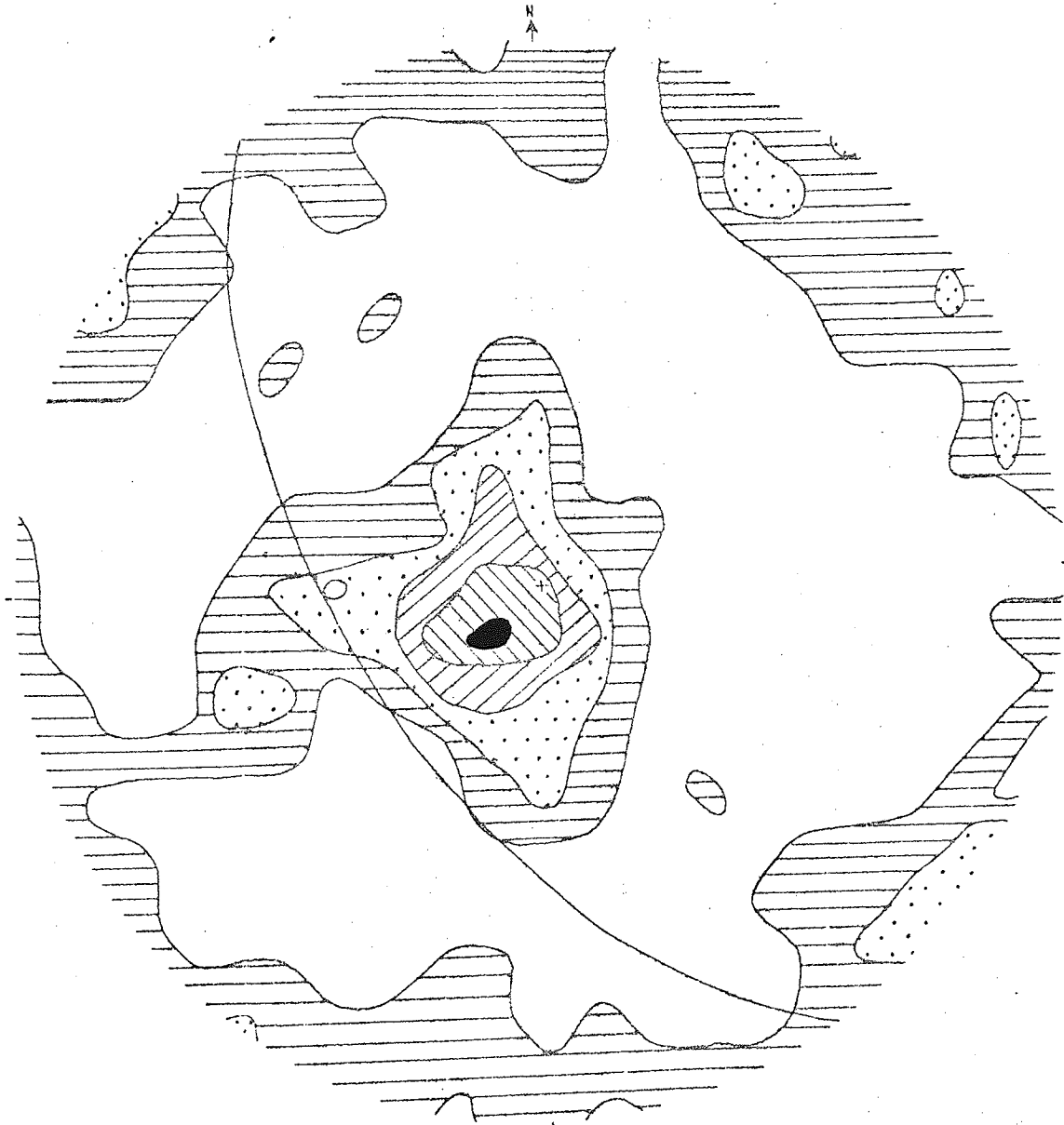


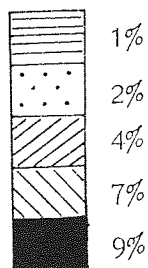
FIG 5:4

SITE I, II, III

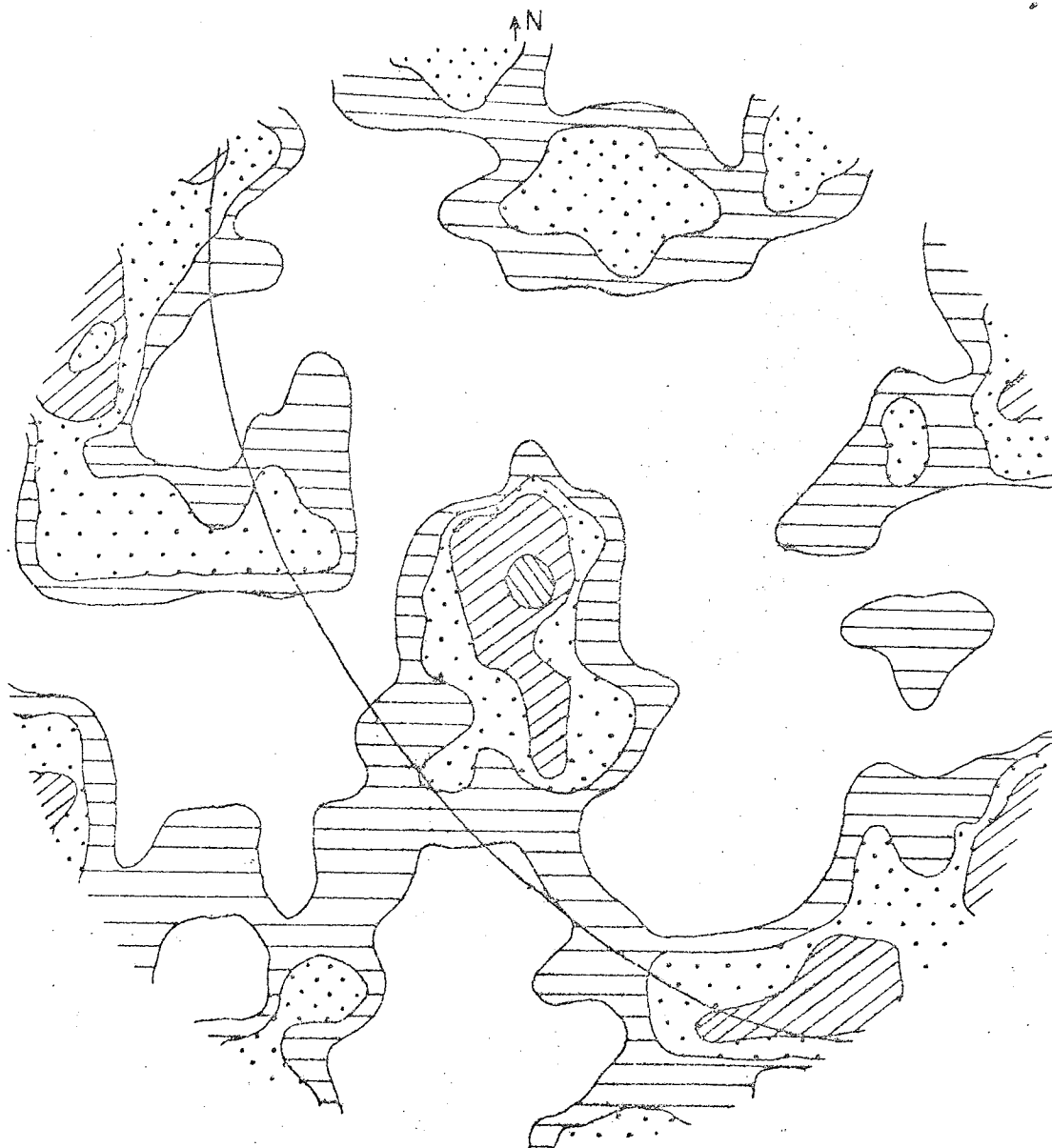


Contoured equal-area projection for 300 joint orientations  
in the Lower Lias at Blockley

CONTOURS

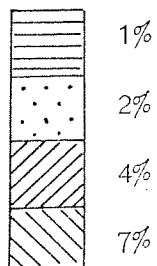


BLOCK SAMPLE 2B



Contoured equal-area projection  
for 100 joint orientations in the  
Lower Lias from Block 2B

CONTOURS





MICROSTRUCTURES6:1 INTRODUCTION

Much of the engineering behaviour of a soil can be attributed to its structure or fabric which in turn is a result of the geological conditions governing the deposition, and subsequent stress history and weathering of the soil.

In the previous chapter joint analysis was described under the heading of Mesostructures these being defined as those structures visible to the naked eye, but excluding faults, folds etc., which have a large regional extent. Microstructures are therefore those structures that can be observed by magnification of some kind although as will be seen later some of these structures can be quite large but due to the nature of the Lias clay, they can only be seen in thin sections.

Microstructures can be studied by a polarising microscope, a scanning electron microscope or an X-ray diffractometer. The scanning electron microscope has a high resolution and will therefore give detailed information at the scale of individual clay particles. The X-ray diffractometer and the polarising microscope have a lower resolution, in the case of the polarizing microscope not less than two microns and they therefore use a larger area to gain information. This information can however be on a quantitative basis whereas the electron microscope at the present time is only be qualitative. Only the polarising microscope and the scanning electron microscope were used with success, the X-ray diffractometer giving limited results. All methods required

specimen preparation and these will be described first.

## 6:2 PREPARATION OF THIN SECTIONS

It is well known that clays will absorb water (especially when in direct contact) and expand, causing an increase in volume hence the preparation of thin sections of a soil or rock with a high percentage of clay in the normal geological way is out of the question. There are two basic methods for the preparation of thin sections of soils and clays dependant on the initial state of the specimen in each case;

(a) Wet

(b) Dry

each method having its advantages and disadvantages, but both are impregnations. The wet method involves the replacement of water by a wax that is miscible with water in most cases Carbowax 6000 (a polyethylene glycol fraction of average molecular weight 6000). The dry method requires the sample to be thoroughly dried before impregnating with a media such as epoxy resins (Araldites).

### 6:2:1 CARBOWAX 6000

Mitchell (1956) first successfully used Carbowax 6000 to produce 40  $\mu\text{m}$  sections of moist clays. He immersed small samples in molten Carbowax 6000 for several days and found that impregnation was complete and therefore permits the use of procedures similar to those used in preparing rock sections. The only modifications necessary were the use of paraffin (Kerosene) instead of water for all grinding and cleaning operations, and a cement that did not require heat treatment for securing the specimen to the slide.

Polyethylene glycols (PEG) have the general formula

$\text{HO}(\text{CH}_2\text{CH}_2\text{O})_n\text{CH}_2\text{CH}_2\text{OH}$  and are known by various names such as polyoxyethylenes, polyglycols, carbowaxes, aquawaxes and oxydwacks. The lower members of the series are obtainable in the pure state. However, commercial products are fractions consisting of mixtures of glycols i.e. in PEG 6000,  $n$  might range between 130 to 170. At room temperature the fractions of molecular weights less than 600 are colourless liquids but those between 1000 - 20000 are white, soft to hard, waxy crystalline solids. The latter being soluble in solvents such as water, alcohols, ketones, ethers and esters, but are relatively insoluble in saturated hydrocarbons (for properties of PEG 6000 see Table 6:1).

TABLE 6:1

Fraction No. Carbowaxes.	Av. Mol. Wt.	m.p. range °C	Solubility in H <sub>2</sub> O at 20°C (% w/w)
1000	950 - 1050	38 - 41	≈ 70
1549	1300 - 1600	43 - 46	70
4000	3000 - 3700	53 - 56	62
6000	6000 - 7500	60 - 63	50
20M	15000 - 20000	≈ 70	-

The technique has been developed by a succession of workers Morgenstern and Tchalenko (1967c), Quigley and Thompson (1966) and Greene-Kelly et al. (1970). The samples are immersed for varying times in a succession of aqueous Carbowax mixtures of various strengths. Cohesive clays that have a high water content often require only 5 minutes immersion in a 10% solution, followed by 2 hours in 25% and 4 hours in a 50% solution and then overnight in molten Carbowax.

The moisture content of a sample can be raised as employed by Davis (1966). However, in many cases this is unnecessary as the sample

can be immersed in a higher strength aqueous Carbowax mixture. The strength of the mixture must be carefully chosen as too dilute a mixture may cause disturbance with the interaction of the clays. Too strong a mixture can set up an osmotic pressure difference which could produce artifacts in some clays because of rapid dehydration.

When impregnation is complete, the sample is removed and either cast as a block or the excess wax is drained away and allowed to solidify. Greene-Kelly et al. (1970) suggests slow cooling to avoid cavitation in the centre of the sample however this has the disadvantage of allowing the wax to crystallize in large crystals and spherulites. Carbowax is not isotropic and it can produce second order interference colours. Birefringence is thought to vary with the differing amounts of water absorbed in the wax. This can cause problems with the identification of argillaceous cutans. Mitchell (1956), Morgenstern and Tchalenko (1967 a,b) recommend rapid cooling, primarily to reduce the crystal size of the Carbowax, immersion in liquid nitrogen being recommended.

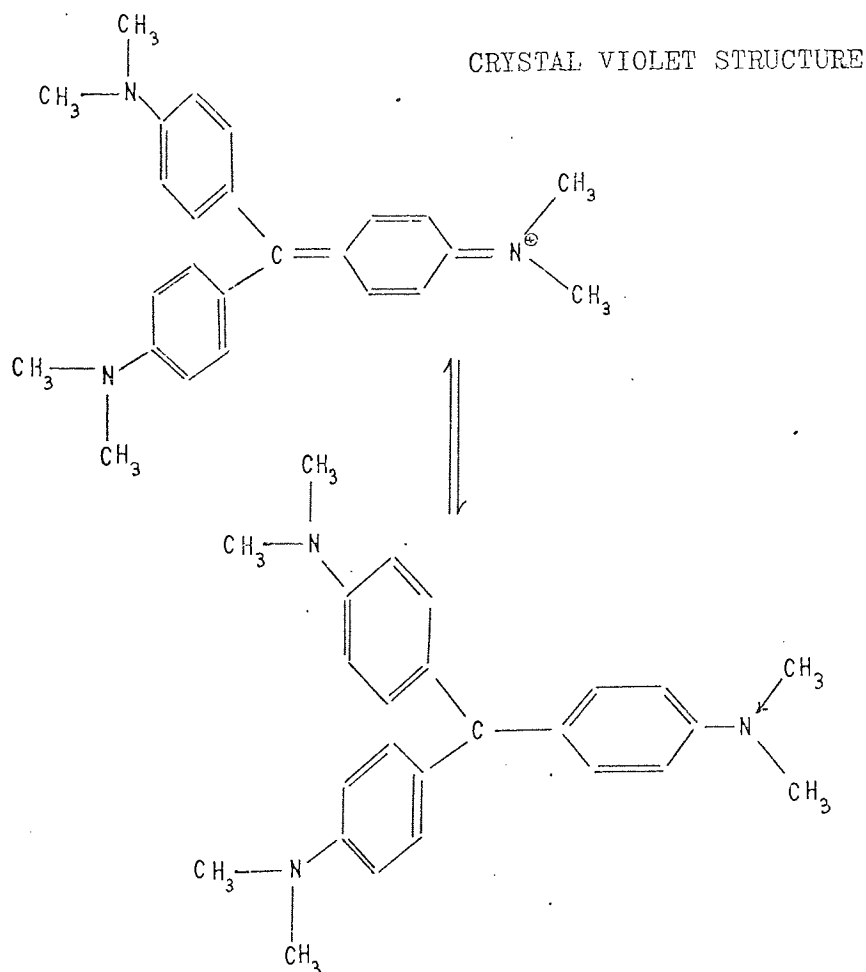
The cutting of thin slices are then carried out normally using a lubricant such as Kerosene, Shell Fusus A or Castrol Honilo. The surface then being ground flat in the usual way using 200, 400 and 600 Carborundum powder.

Dyes can be incorporated within the impregnating solution and can be used to identify voids and structures in fine grained material. Adsorption of dyes by mutually orientated clay particles often greatly changes the optical properties of the stained area. The clay may become pleochroic and the refractive indices change in

such a way that the birefringence may increase or decrease, and the optical sign may change. Greene-Kelly (1963) described the kind of optical effects observed when expanding or partially-expanding clay minerals are immersed in simple aromatic liquids.

Crystal violet dye stains intensely without distorting the clays optical properties. The staining may be carried out either during impregnation or after grinding and before mounting the cover slip. Crystal violet in aqueous solution will turn from violet to blue, to green, to yellow depending on the acidity of the solution. (Fig 6:1). The water molecules held strongly to the surface of the clays can therefore react with the crystal violet dye with resultant colour changes.

(Fig 6:1)



Carbowax 6000 having a low melting point ( $60^{\circ}\text{C}$ ) means that the section must be cemented to the slide by a cold setting Araldite rather than the usual Lakeside which has a melting point of  $80^{\circ}\text{C}$ .

#### 6:2:2 EPOXY RESINS

It was found that the Carbowax 6000 was ideal for samples with a relatively high permeability such as the weathered Lias clay. Unweathered clay however, has a very low permeability in the order of  $10^{-6}$  mm/s . This low permeability causes impregnation with Carbowax 6000 to be difficult and in fact almost impossible. Impregnation was no more than a few millimetres after several days immersion in Carbowax 6000. Thus, only very small samples could be impregnated. Any attempt to cut the clay without impregnation resulted in the clay fracturing along the bedding planes. herefore, it was necessary to use an epoxy resin that could penetrate much more easily. Carbowax has a viscosity of 6 to 9 poise which is high compared to water (0.01 poise).

The majority of the araldite epoxy resins have quite high viscosities compared with water. The most common Araldite used is AY103 Resin and Hardner HY951, this is a cold setting resin although it can be cured at elevated temperatures to speed up the process. The viscosity of this resin is 18 poise though this can be reduced by using acetone as a solvent. This causes the impregnation to become rather lengthy since the acetone must be allowed to evaporate off before the resin is cured.

A hot setting Araldite that until now has not been used for impregnation is the Resin AY 18 with the Hardner HZ 18 the properties of which are given in Table 6:2.

TABLE 6:2

<u>Mixture</u>	<u>Parts by Weight</u>	<u>Parts by volume</u>
Araldite AY 18	100	100
Hardner HZ 18	75	96

Useable Life:- The useable life of the mixture is about  
5 - 7 days at 21°C (70°F)

Drying times:-

45 - 50 hours at 15°C (59°F)  
or  
40 hours at 22°C (72°F)  
or  
1 hour at 80°C (176°F)  
or  
30 mins at 100°C (212°F)  
or  
12 mins at 120°C (248°F)

Curing times:- Cure adhesive for at least

2 hours at 80°C (176°F)  
or  
30 mins at 100°C (212°F)  
or  
20 mins at 140°C (284°F)  
or  
15 mins at 180°C (356°F)

Initial Viscosity at 21°C 0.2 poise.

This viscosity can be reduced using acetone.

The maximum temperature to which clays can be raised without too much distortion is 100°C therefore this resin can be used with great success with any type of material especially the fine grained clays with low permeability. Using this Araldite, impregnation of 50 mm cubes of Lias clay has been achieved successfully.

### 6:3 PROCEDURE FOR IMPREGNATION AND CUTTING

#### 6:3:1 CARBOWAX

1. The appropriate aqueous carbowax mixtures are determined and made up.

2. Sample is wrapped in either gauze or placed in a wire mesh cage. This is to prevent the sample from being damaged when being transferred from solution to solution and for easy removal.
3. A dye can be incorporated with the final immersion in the carbowax.
4. The sample is drained and allowed to harden for several hours.
5. Slices approximately  $\frac{1}{8}$ th inch thick can be cut with the appropriate lubricant. A WHI cutting and grinding machine, manufactured by Cutrock Ltd., London was found to be ideal for the job.
6. The slice was ground flat and mounted using cold setting araldite, this being ground down to 0.2 mm on the grinding wheel using the device that was specially designed for this purpose. (Fig 6:2).
7. This can then be ground to thickness using 200, 400 and 600 Carborundum powder.

At this stage the clays can be dyed by immersing the slide in a Kerosene solution of crystal violet.

8. A cover slip is attached in the normal manner using Canada Balsam.

#### 6:3:2 EPOXY RESINS

1. Air dry the sample at room temperature for two days.
2. Place the sample in the vacuum desiccator in the apparatus as shown in (Fig 6:3). The resin mixture being placed in the funnel above.
3. The desiccator is evacuated. With fine grained material that is very friable this should be done slowly over a period of half an hour and should be kept at this for an hour.



# SLIDE GRINDING ATTACHMENT

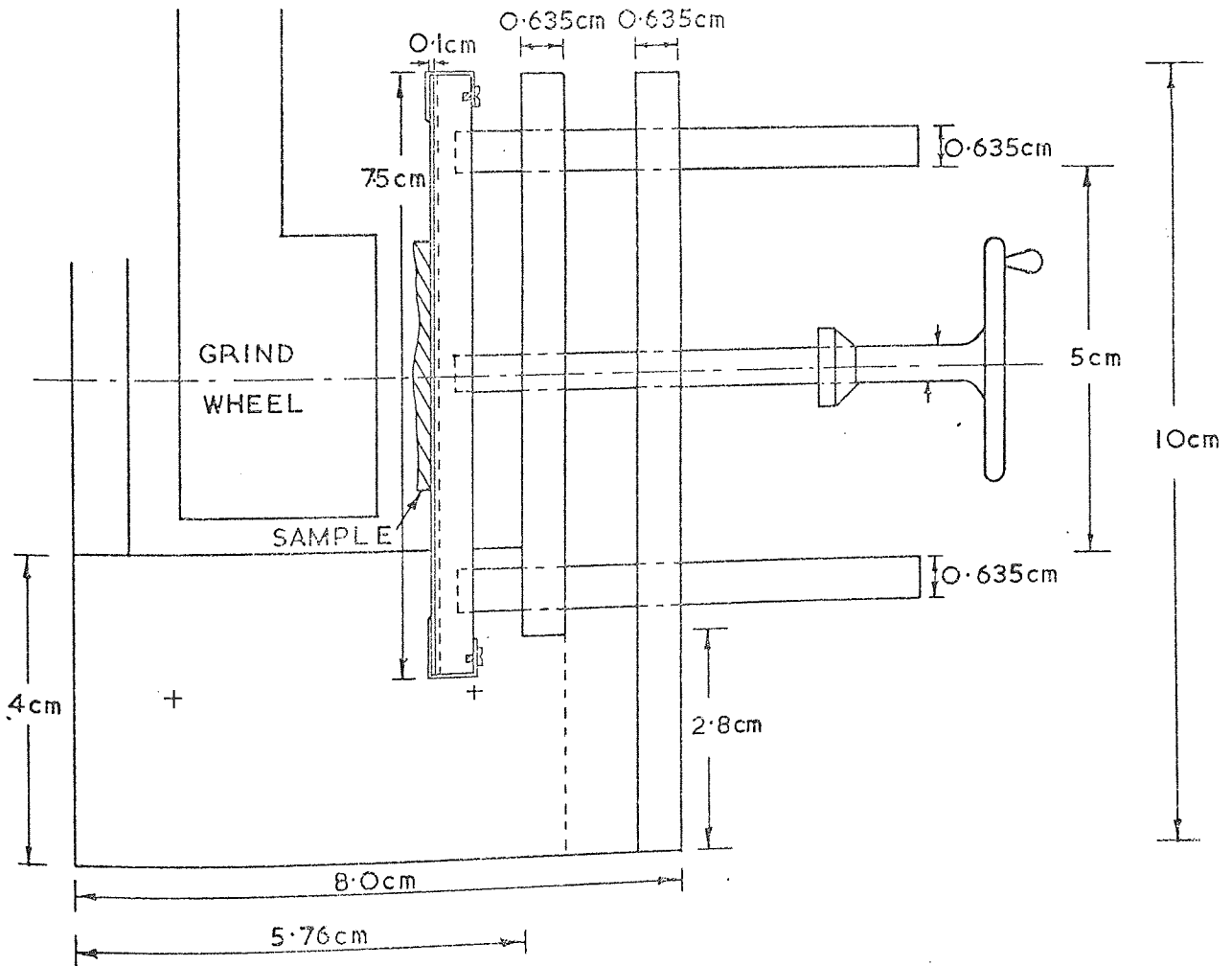
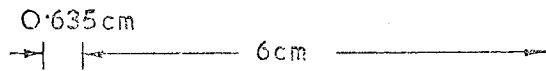
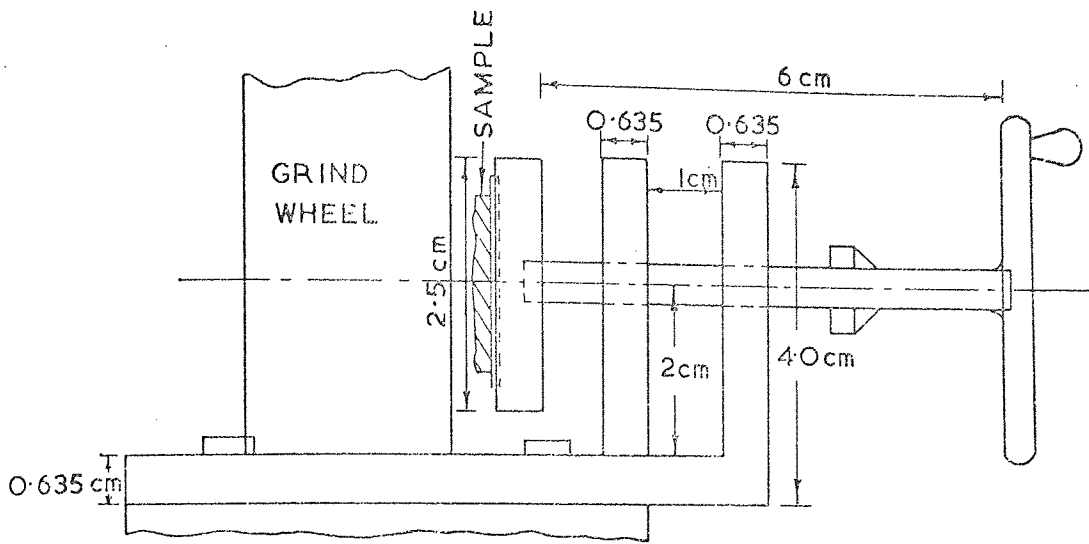


FIG 6:2

APPARATUS FOR EPOXY RESIN IMPREGNATION

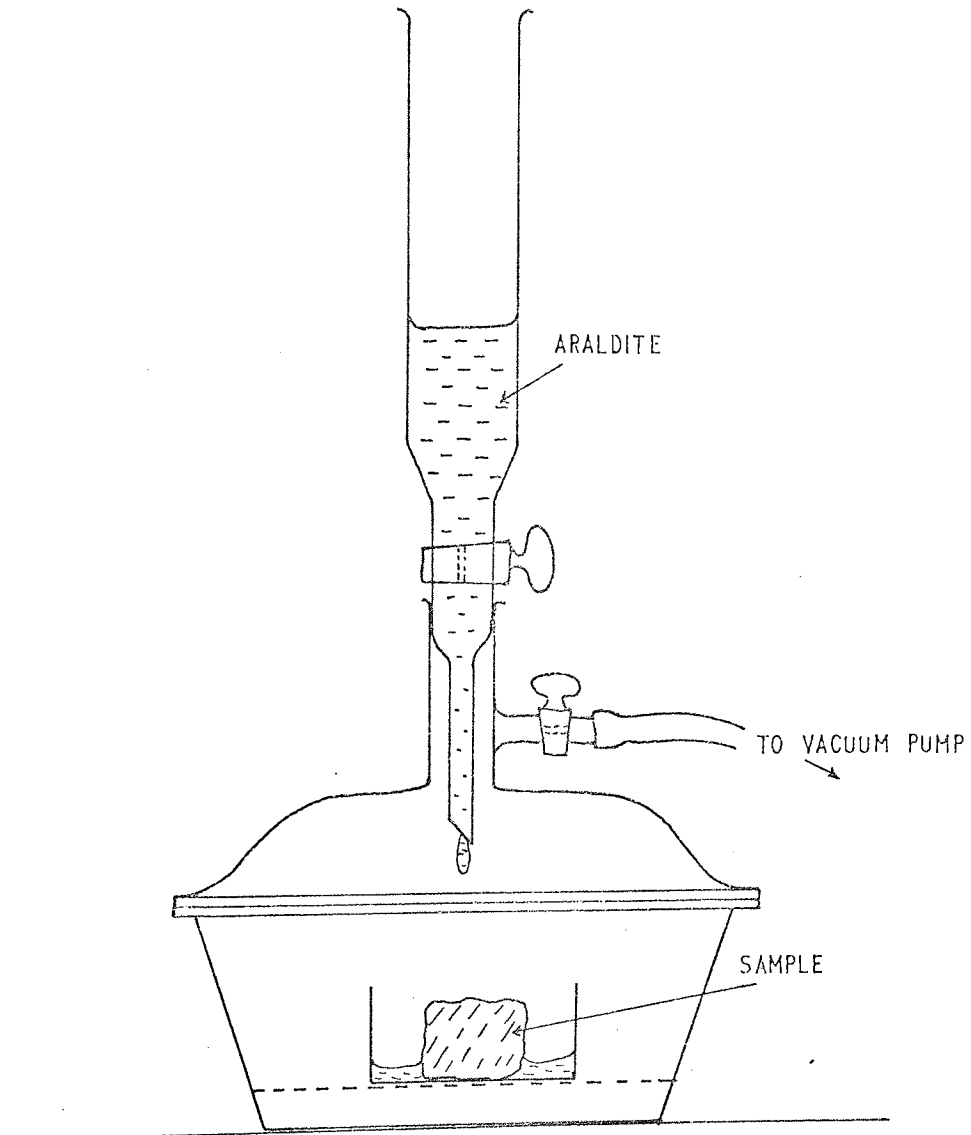


FIG 6:3

4. After this period the necessary amount of resin mixture is run in ensuring no air enters the vacuum desiccator.
5. The specimen is then left under vacuum for 1 to 2 hours or less if it has a high permeability. The sample is either removed and drained of excess Araldite or it is cast in a block in the container.
6. Cutting and grinding is as before.

N.B. Before fixing the slip to the glass slide, the excess grinding powder and the orientated clay flakes should be removed using the peel technique (as described in the next section) and the surface is flooded with Araldite before fixing to the glass slide.

#### 6:4 PREPARATION OF ELECTRON MICROSCOPE SAMPLES

As with most analytical methods sample preparation is very important. There are two main types of electron microscopy in current use, based on transmission and reflection, respectively.

For the transmission microscope the most common procedure is to use replicas of fracture surfaces of air dry samples, or alternatively freeze drying may be used and one is referred to Smart (1969) and Silva et al. (1965). Other methods reported in soil structure investigations are the impregnate - section -etch - replica of Silva et al. (1965); and the impregnated ultra thin section method of Pusch (1966).

The scanning electron microscope uses the reflection of a beam of electrons from the surface of the object rather than transmission through a thin section. The instrument was first used in soil structure by Roscoe at Cambridge University (Roscoe 1967), and this led other workers to investigate the method. The main advantages of this method are that the actual surfaces can be examined with

magnifications up to 50,000X and the instrument has a high depth of focus thus providing a strongly three dimensional (almost stereoscopic) picture. Actual stereoscopic pictures can be obtained by tilting the specimens through  $3^{\circ}$  and a quantitative analysis of the fabric can be obtained.

When the sample is placed in the scanning electron microscope it is subject to a high vacuum, therefore it must contain no water or loose particles. The sample should therefore be dry or impregnated. Work by Barden and Sides (1971) have shown that impregnation is unsatisfactory and air dried samples are much better. Gillot (1969) gave details of the freeze drying method however, efforts by other workers (Smart 1967, Barden and Sides 1971) have shown that this process is difficult to control. Gillot (1969) also proposed the method of "critical point drying" but again this is rather a complex procedure and has not been used by many researchers.

These methods of Gillot were proposed mainly because it was thought that drying of samples would produce internal changes. For most materials this is not so unless the water content is very high and thus the amount of shrinkage large. The Lias clay in this investigation had a water content between 17% and 19% which is very close to its shrinkage limit of 17%.

The simplest and most effective procedure is air drying followed by mechanical fracture to expose a surface for viewing. The mechanical fracture may however not be typical since the fracture may form along preferred orientations and microfeatures. There is also the chance of loose debris on the surface which if not removed can cause severe overcharging during examination.

Barden and Sides (1971, 1970) used a fractured surface



PLATE 6:1  
TREATED AND UNTREATED CLAY SURFACE  
(UNTREATED SURFACE, INTENSE CHARGING  
PRODUCING NO DETAIL) X53.

and removed the debris by a series of applications and removals of Sellotape, they recommended 50 - 100 peels with Sellotape,

To remove the probability of the fracture surface being non typical an air-dried sample was cut very slowly by a diamond wheel saw using a lubricant or an air blast. The flat surfaces were carefully ground with 200 and 400 Carborundum to remove the disturbance caused by the cutting wheel. The orientation of the surface particles due to grinding and the loose grinding powder was removed by several applications of cellulose acetate. Two coats are applied and allowed to dry and then peeled away to remove the surface material. Three to four successive applications are sufficient and this would be equivalent to 50 peels with Sellotape. The difference between the treated and untreated surface is shown in Plate 6:1. Both the fracture surface and the cut surface methods were used.

The samples are then fixed to the support stub with Durofix and earthed to the stub with colloidal silver. The sample and stub is then shadowed first by carbon and then by silver at a higher angle. The conducting coat which is only a few Angstroms thick is necessary to prevent charging of the sample under the electron beam and improves the quality of the pictures.

For detailed descriptions of the equipment and mode of operation one is referred to Birks (1964), Zussman (1967).

#### 6:5 RESULTS OF THIN SECTION ANALYSIS

Thin sections of the Lias clays can be used:

(a) to obtain a picture of the structures present



PLATE 6:2A  
DENSITY STRUCTURES (SAMPLE S39/1)  
PERPENDICULAR TO BEDDING

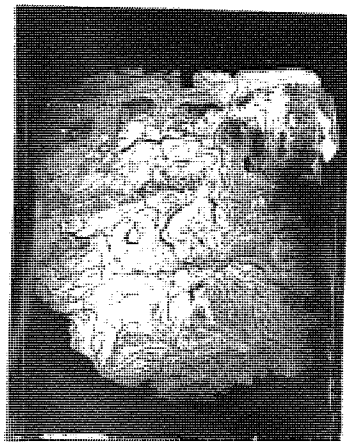


PLATE 6:2B  
DENSITY STRUCTURES (SAMPLE S39/1)  
PERPENDICULAR TO BEDDING



in the weathered or unweathered material.

(b) to obtain a quantitative measure of orientation using the method initiated by Mitchell (1956) and developed by Morgenstern and Tchalenko (1967 a,b).

In hand specimens one observes a lineation of the clay particles parallel to bedding which is confirmed in thin section. The profile examined is over 15m in depth and samples for sectioning were taken mainly in the weathered zone, though some were cut from the unweathered clay for comparison.

In the unweathered clay, certain horizons show alternate layers of clay and silt. In most cases this shows up as a coarser texture in the hand specimen but these horizons cannot be seen clearly by the naked eye. The only horizon where the interlayering is observable, is just above the Pecten Beds. Here the horizons are 2 - 3 mm thick, slightly contorted in places and broken as if reworked after deposition.

The layering observed in thin section are no greater than 1 mm in thickness and are usually much smaller than this. Reworking, producing ruptured and very slightly contorted bedding is common. (Plate 6:2).

Convolute bedding on a fairly large scale was also found at one horizon, there could however, be others, since the convolutions were only found after the examination of thin sections. The convolutions were large rounded folds, large slides being necessary to examine them. The deformations were highlighted by using the dye crystal violet for easier observation. Convolute bedding is a name

coined by Keunen (1953) to apply to peculiarly deformed laminations which have the following characteristics:

1. Crumpling of the laminations increases in intensity upward and then gradually dies out again so that the upper laminae of the bed are flat.
2. No rupture of laminae has occurred. The lamination planes can be traced across several undulations showing rounded distortions.
3. Only one bed is affected at a time, but the disturbance can be traced laterally in all directions within that bed.
4. Affected bed shows no external irregularities in thickness.
5. The degree of distortion is of almost equal intensity in two planes, the other at right angles to the original slope.

Keunen (1953) suggested that deformation was caused by turbidity currents soon after deposition. At the present time there are a variety of views for the explanation of convolute bedding. The most satisfactory one in the case of Lias clays is plastic flow induced by gravity, and is demonstrated well by the experimental work of Dzulynski et al. (1969). The experiments were designed to investigate the effect of density controlled deformation on the character of the sediment water interface. They produced unstable, water-saturated, layered sequences in sedimentation tanks by alternate deposition of clayey silts and fine sands from dilute suspension. Each suspension

was introduced after the preceding one had settled, at time intervals short enough to ensure a loose packing and high water content throughout the system. Deformation usually started spontaneously with the deposition of a "critical layer" which raised the total weight of the column beyond the limits of its bearing capacity. The deformation can also be triggered off by a slight shock. The deformation, once initiated, proceeded in the known pattern for density controlled deformation. They found very complex structures forming when sequences of clay laminae were topped by very fine cohesionless sand.

Conditions during Lias sedimentation were just perfect for this to take place. Quiet conditions existed for the clays to be deposited in laminae with porosities in the range of 70 - 80%. Further clay laminae would initiate compaction, however, any silt horizons deposited on clay of this porosity would have an above average chance of producing density structures.

The convolute bedding found at a depth of 4 m has almost unaltered silty clay horizons above which suggests a density controlled deformation (Plate 6:2).

This type of deformation took place before lithification; another type of deformation must also have occurred when the sediment was lithified. Shear planes are found in specific thin sections, cutting across silt horizons and offsetting them by several millimetres. Large mica flakes that extend into the shear zones do become bent. However, these shear zones are no more than 12 - 24  $\mu\text{m}$  thick occasionally reaching 100  $\mu\text{m}$  thick, (Plates 6:3, 6:4, 6:5) and consist of orientated clays.



PLATE 6:3A  
SAMPLE S32/1 PERPENDICULAR TO BEDDING

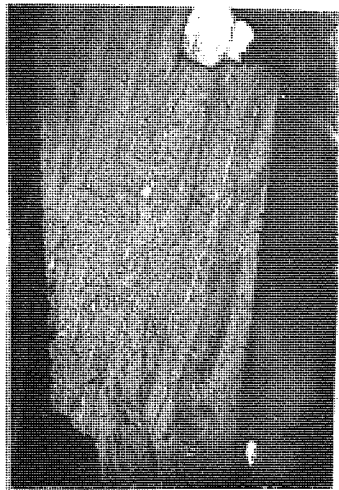


PLATE 6:3B  
SAMPLE S32/1 PERPENDICULAR TO BEDDING



X13.2

PLATE 6:4  
SILT BANDS SHOWING DISPLACEMENT  
ALONG SHEAR PLANE (PERPENDICULAR TO BEDDING)  
SAMPLE S32/1



X13.2

PLATE 6:5A  
FLAME STRUCTURE AND SHEAR PLANE (SAMPLE S32/1/A)  
PERPENDICULAR TO BEDDING



X41.25

PLATE 6:5B  
SHEAR PLANE (SAMPLE S32/1/A)  
PERPENDICULAR TO BEDDING

Some shear planes arise from what appear to be flame structures (Plate 6:4) indicating that there was a density control in some cases. The majority of the shear planes have well defined boundaries. However, none of the orientated bands reported by Tchalenko (1968) for the London Clay were found in the Lias clay examined. A few minor secondary shears were found associated with a major shear plane at angles of up to  $45^{\circ}$  to bedding.

When one examines the weathered material there is a gradation in the proportion of lithorelicts and remoulded material. The original clay material and its structure is preserved in the lithorelicts, these also have concentrations of iron oxide in the form of  $Fe_2O_3$ . The lithorelicts are separated by remoulded material either in narrow zones or broad bands, the type dependant on depth. The narrower zones are confined to the deeper less weathered material of Zone III (Fookes & Horswill 1969), and have a strong orientation. The wider bands nearer the surface show increased weathering and remoulding of material. Eventually at depths of 0.5 - 1.0m below the surface these zones have coalesced and the majority of the soil is remoulded and has a random structure, although remnants of the orientated bands are still seen. These remoulded zones are lighter in colour and are more easily reduced under reducing conditions (i.e. waterlogging).

Most clay crystals are birefringent and if they are orientated within aggregates, the aggregates themselves will exhibit a birefringence. Increasing parallelism of platy clay crystals will correspond with increasing aggregate birefringence.

Fry (1933) pointed out that clay aggregates may exhibit optical properties similar to those of single crystals, and Grim



(1934) suggested that aggregate birefringence is enhanced by a uniformity in particle orientation. Individual clay particles are submicroscopic and therefore not discernable but aggregates of clay particles will exhibit optical birefringence in transmitted light. Thus this property provides a measure of the preferred orientation or structural anisotropy. The thin sections were examined with a polarising microscope set up for quantitative fabric analysis using the method initiated by Mitchell (1956) and developed by Morgenstern and Tchalenko. (1967 a,b).

In this method the ratio of the minimum to the maximum light intensity transmitted through crossed polars as the thin section is rotated, is measured photometrically. This ratio is termed the birefringence ratio,  $\beta$ , and it is used to interpret the degree of preferred orientation in an aggregate of particles. For random orientation  $\beta = 1$  and for perfect orientation  $\beta = 0$ . At intermediate orientations the magnitude of  $\beta$  indicates the degree of orientation. In monomineralic aggregates the orientation can also be expressed in terms of an orientation ratio, R, which is uniquely related to a particle distribution model. The relationship between  $\beta$  and R is dependant upon the model used; in this case it is the two dimensional model. The intensity readings were taken on an area of 0.25mm diameter or less on sections cut perpendicular to the bedding.

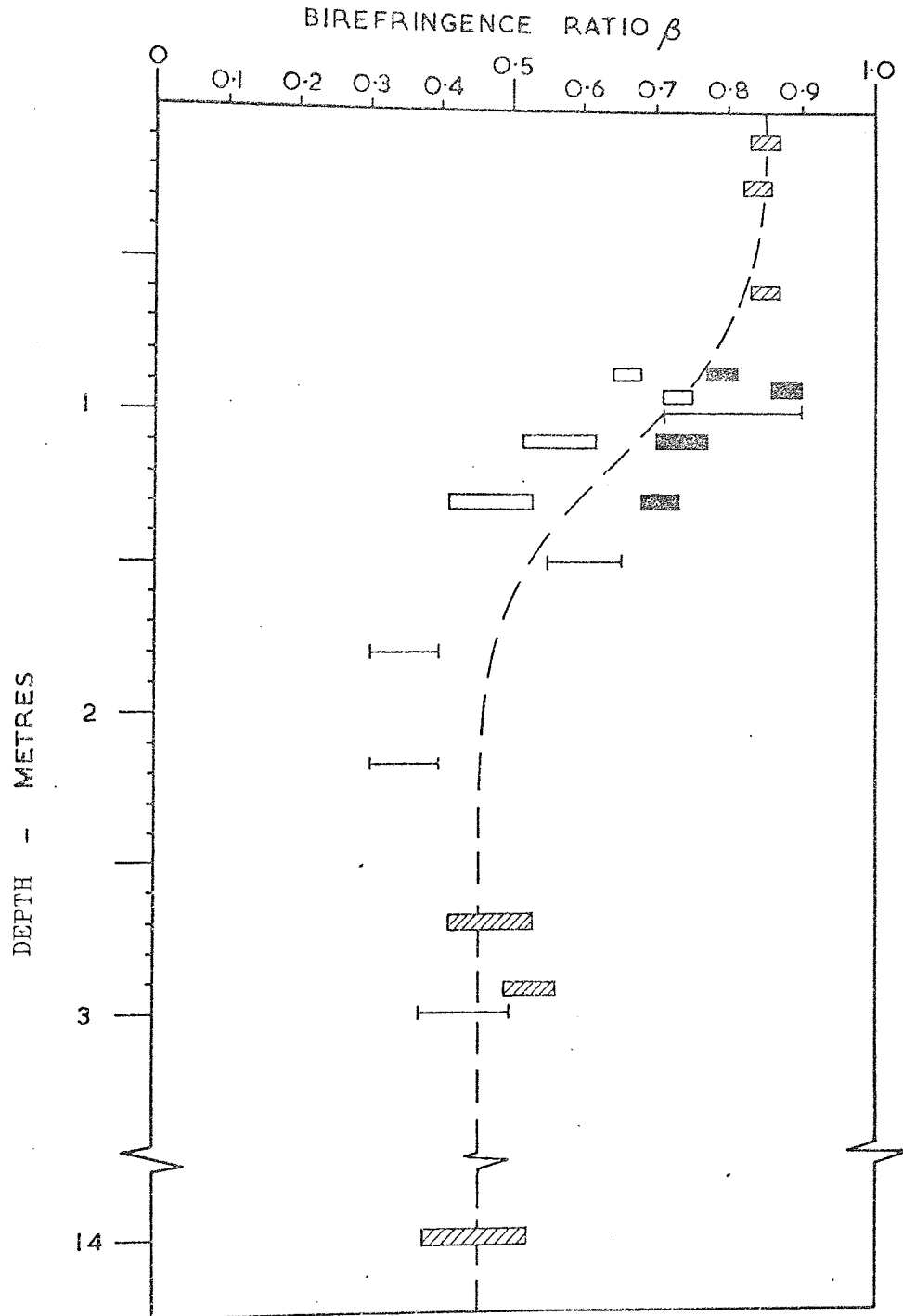
A measure of the birefringence ratio will therefore give an indication of the amount of remoulding and the change in any particle orientation.

The unweathered material has a birefringence ratio of 0.38 to 0.52 this being steady up to a depth of 1.4 to 1.8m. At this

BIREFRINGENCE RATIO/DEPTH RELATIONSHIP

PERFECT  
STRUCTURE


RANDOM  
STRUCTURE



KEY

 AVERAGE TEXTURE

 LITHORELICT

 REMOULDED

 UPPER LIAS FROM GRETTON  
AFTER CHANDLER [1972]

BIREFRINGENCE RATIO MEASURED PERPENDICULAR TO BEDDING

FIG 6:4

point remoulding becomes dominant and the  $\beta$  ratio of the lithorelicts changes slightly. The remoulded material has a ratio of 0.7 - 0.8 and increases towards 1.0 nearer the surface.

The change of the  $\beta$  ratio with weathering is shown in (Fig 6:4), with an average curve. An almost identically shaped curve was obtained by Chandler (1972) for the Upper Liassic clay of Northamptonshire.

It was noticed that the fabric structure of the lithorelicts is identical to that of the parent material and the majority of the lithorelicts were yellowish brown to dark red-brown in colour due to iron staining (Plate 6:6). These kept their colour until they became remoulded, and at this point the iron was probably leached out to a large extent by the percolating water. The remoulded material then became more easily invaded by water and therefore becomes reduced in waterlogged conditions whereas the lithorelicts remain in an oxidised state.

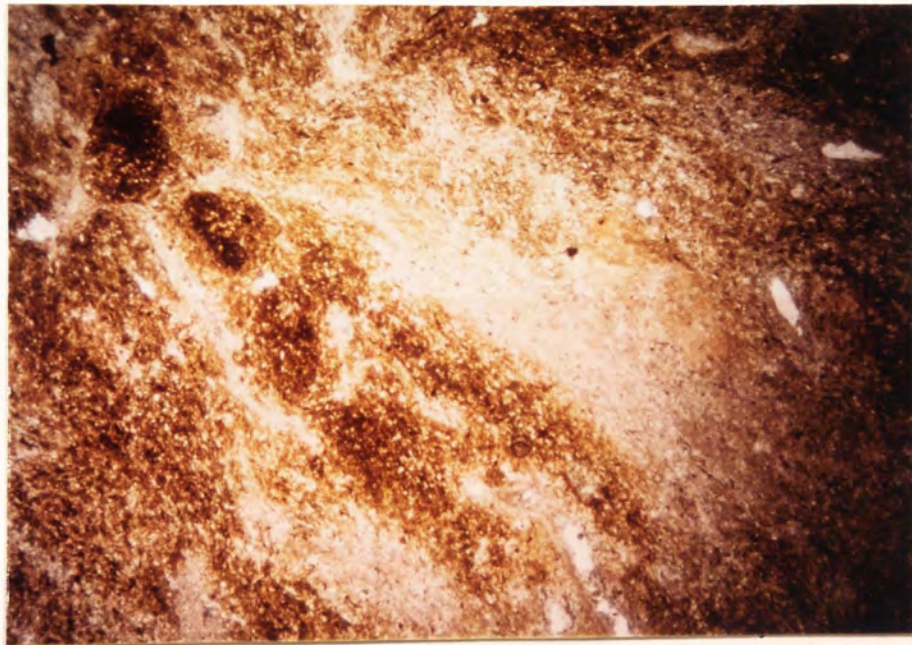
#### 6:6 RESULTS OF THE SCANNING ELECTRON MICROSCOPE (SEM)

As stated previously the SEM can examine structure down to clay particle size, the resolution on such instruments being in the order of  $100\text{\AA}$  and less on the larger machines.

Since the initiation of SEM studies, a terminology has been built up regarding the fabric and structure at this level. Smart (1969) has defined the following terms (Fig 6:5).

Domains:- Aggregates of platy particles, laths or tubes, large in comparison with the particles, in which almost all the particles are approximately parallel to a smooth surface, plane or curved. (Fig 6:5)

Packets:- Aggregates in which platy particles are almost parallel,

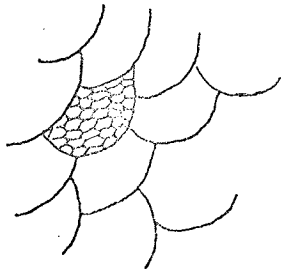


X13.2

PLATE 6:6

IRON STAINED LITHORELICIT AND REMOULDED MATERIAL  
(VERTICAL SECTION)  
SAMPLE S16/1

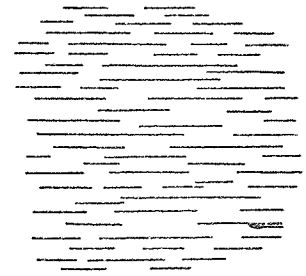
# TYPES OF STRUCTURES



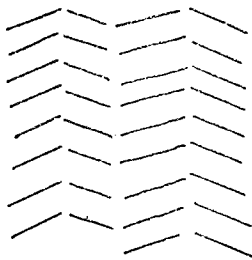
A.



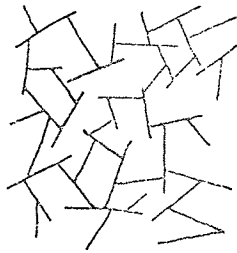
B.



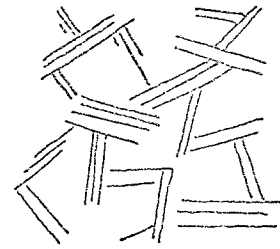
C.



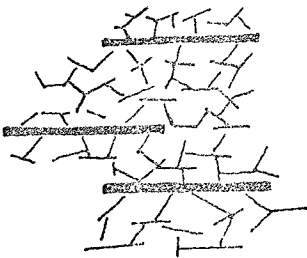
D.



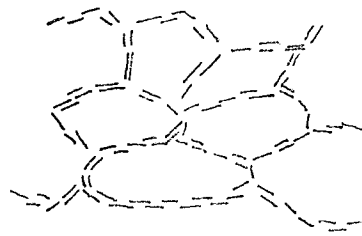
E.



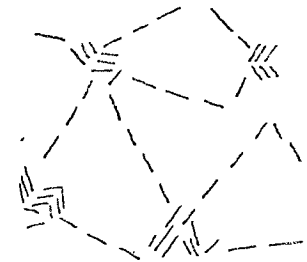
F.



G.



H.



I.

A: KIDNEY STRUCTURE.

B: PACKET.

C: DOMAIN.

D: HERRING BONE.

E: CARDHOUSE.

F: SALT FLOCCULATED.

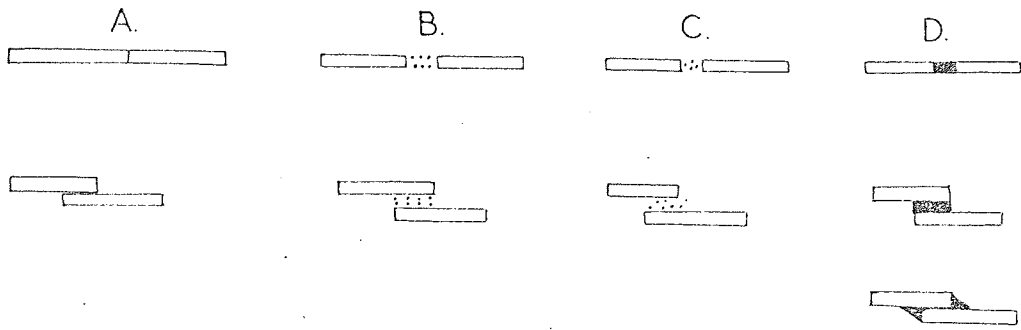
G: BROWNIAN.

H: FLOCCULENT.

I: PUSCH'S STRUCTURE.

AFTER SMART [1969]

FIG 6:5



MECHANISMS BETWEEN ADJACENT PARTICLES.

A: CONTACT.      B: ORDERED WATER.      C: DISORDERED WATER.      D: CEMENT.

FIG 6:6

DOMAIN TRACE DIAGRAM OF AN ELECTRON MICROGRAPH OF A THIN SECTION OF CONSOLIDATED KAOLIN [SMART 1967]

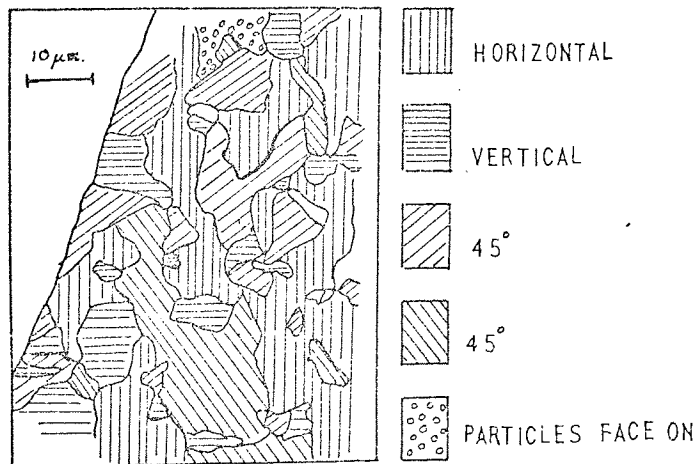
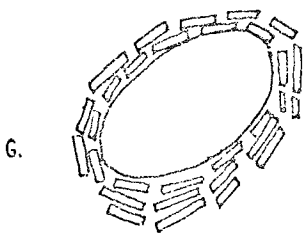
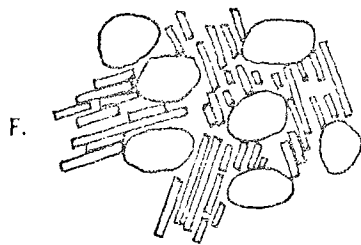
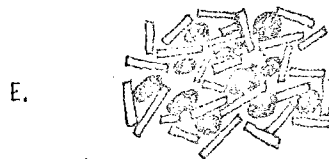
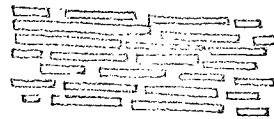
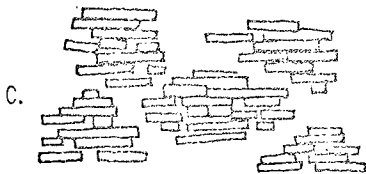
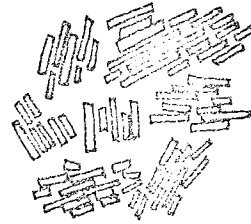
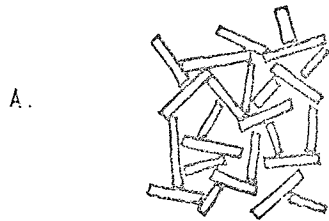


FIG 6:8

ARRANGEMENTS OF CLAY PARTICLES.



A: RANDOMLY ORIENTATED FLAKES

B: RANDOMLY ORIENTATED DOMAINS

C: DOMAINS IN PARALLEL ALINGMENT

D: PARALLEL ORIENTATED FLAKES.

E: GRANULAR PARTICLES OF FERRIC OXIDE,

ORGANIC MATTER OR FINE SILT INTERFERE WITH  
THE PARALLEL ORIENTATION OF CLAY FLAKES.

F: RANDOMLY ORIENTATED DOMAINS BETWEEN GRAINS  
OF COARSE SILT.

G: LARGER SAND PARTICLES ALLOW THE ALINGMENT  
OF CLAY PARALLEL TO THEIR MARGIN.

FIG 6:7

extend across the packet and are capable of admitting water between themselves.

Stacks:- Aggregates of platy subparticles, almost parallel, and in permanent contact; thus stacks are a form of granule. (However, being difficult to distinguish from packets, they are often classified as such).

Bundles:- Aggregates of laths or tubes approximately parallel to a line, straight or curved.

Cement:- Material which bonds particles together.

Mortar:- Material in which particles are embedded and does not bind the particles together.

The mechanism of joining between adjacent particles is summarised in Fig 6:6 .

Clay structure is the arrangement of the clay particles or aggregates of clays and they vary according to age, environment of deposition and stress history but basically they can be divided into two groups:

(a) Open Structures.

(b) Denser Structures.

#### 6:6:1 OPEN STRUCTURES

These usually have a high porosity and permeability, the different structures being dependant on environment and charge effects on the clays. Edge to face (EF), edge to edge (EE) attraction with face to face (FF) repulsion resulting in a cardhouse structure. A salt flocculated or bookhouse structure is a modified cardhouse structure with FF attraction in the packets (Fig 6:5F and Fig 6:7B). Evidence by Rosenqvist (1959) supports the existence of these types of structure. The honeycombe structure (Fig 6:5H) proposed by Casagrande (1932) and confirmed by Pusch (1966) is an open flocculated



structure with EE and FF attractions. Sand and/or silt sized particles and organic matter are important in this structure.

#### 6:6:2 DENSER STRUCTURES

A dispersed structure implies a rather closely packed structure involving essentially FF arrangements (Fig 6:7D). Aylmore and Quirk (1966) proposed a more realistic representation of a dispersed structure (Fig 6:9) which they called turbostratic. In this case domains are closely packed and their overall orientation has two extremes, the random and the almost perfectly orientated.

It is now the practise of many workers to use the simpler terminology taken from Brewer (1964) one of the most common terms being a ped. A 'ped' is a compound particle separated from adjoining peds by surfaces of discontinuity, including fissures, voids or skins of different composition known as cutans. Thus a large ped can contain smaller peds and so on down to the scale of domains.

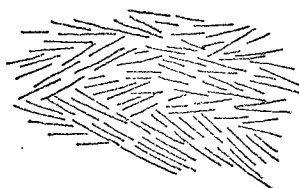
Other types of structures both dense and open are shown in Fig 6:7, 6:8 .

Examination of the unweathered Lias has shown the majority of the material to be turbostratic with a high degree of overall orientation. In the coarser material there are larger muscovitic flakes (silt size) between which is the turbostratic structure (Plates 6:7, 6:8, 6:9).

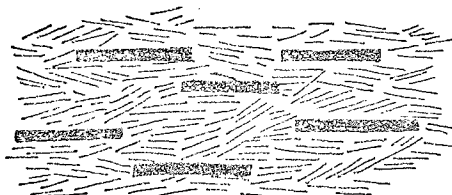
Again the highly orientated nature of the clay is easily seen in the photographs, the larger silt size flakes emphasising the parallelism. Plates 6:7, 6:8, 6:9 are sections at right angles to the bedding, Plate 6:10 is a stereoscopic pair parallel to the bedding.

A slightly more random structure, although still with some

TURBOSTRATIC STRUCTURE



LOCKED TURBOSTRATIC



GRAIN TURBOSTRATIC

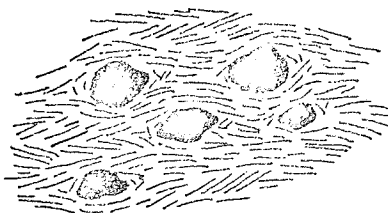


FIG 6:9

degree of orientation can be seen in certain specimens (Plate 6:11 stereoscopic pair). In this structure it appears that the domains wrap round silt sized particles of randomly orientated clay flocules. This type of structure does not appear to be very common.

The larger clay particles with irregular shape and ragged outlines are possibly illitic in nature. Smaller particles are present that appear to be relatively well crystallized (Plates 6:12, 6:13). These small crystals with an almost hexagonal outline are probably kaolinite, these types of crystals being characteristic of kaolinite.

Authigenic magnetite crystals (Plate 6:14) can be found but they are rare; the importance of these and the conditions under which they formed will be discussed later.

Crystals (Plate 6:15) which appear to be similar to the selenite crystals reported by Barden (1972) in the Ardleigh Clay are also found. In the Ardleigh Clay the oxidation of iron pyrite had led to the formation of selenite crystals in layers. The sample of Lias clay in which these were found appeared to be unweathered with pyrite still present. However, only a small amount of pyrite need weather for these to form. Another possibility is that they formed when the sample was being air dried. It has been noticed that larger samples when they dry out do form selenite crystals in the form of spherulites on the joint surfaces or just beneath.

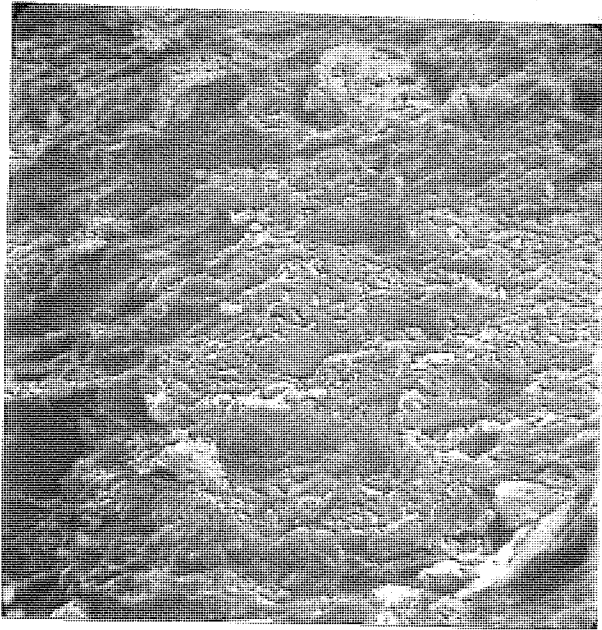
Further growths were noted on the surfaces of the larger irregular shaped clay particles (Plates 6:16, 6:17, 6:18). They were irregular raised portions of the clay particles with a dendritic pattern on their surface. They occurred in a random fashion both

---

\* Kaolinite often exhibits pseudo-hexagonal crystals.

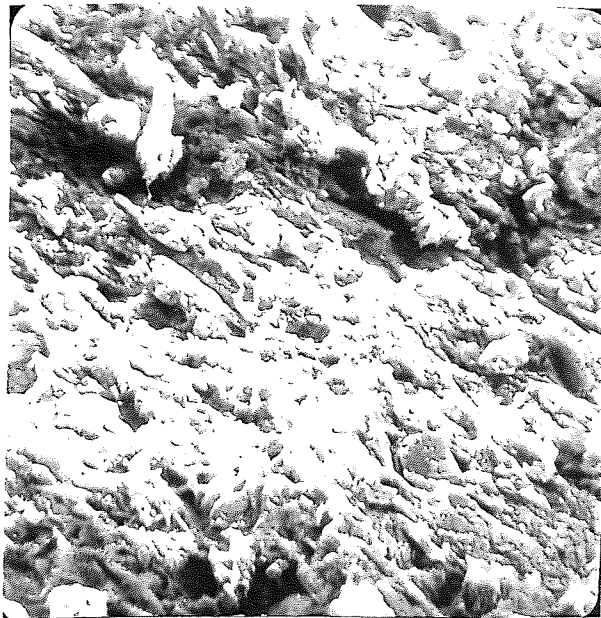
in numbers and shape, and their size is in the region  $1 - 10 \mu\text{m}$ . Using an energy dispersive X-ray system connected up to a Cambridge Stereoscan 600 a qualitative analysis of the whole sample was obtained. The main elements were Al, Si, Fe, Ca P, Ti with a trace of scandium, using a beam with a diameter of  $120\text{A}^0$  the individual growths themselves were analysed and they gave almost identical results. The only major difference was the lower amount of Ca in the growths than the overall sample. This analysis was one of the main reasons for assuming these to be growths, the deficiency of calcium is explained if the majority of calcium is contained in calcite which is present mainly as micrite or in the shell remains.

These new growths of clay on the surfaces of the clay flakes probably formed soon after deposition in early diagenesis, this will be discussed in more detail in the section on geochemistry.



—  
20 $\mu$ m

PLATE 6:7  
TURBOSTRATIC FABRIC  
SAMPLE S40/1



—  
10 $\mu$ m

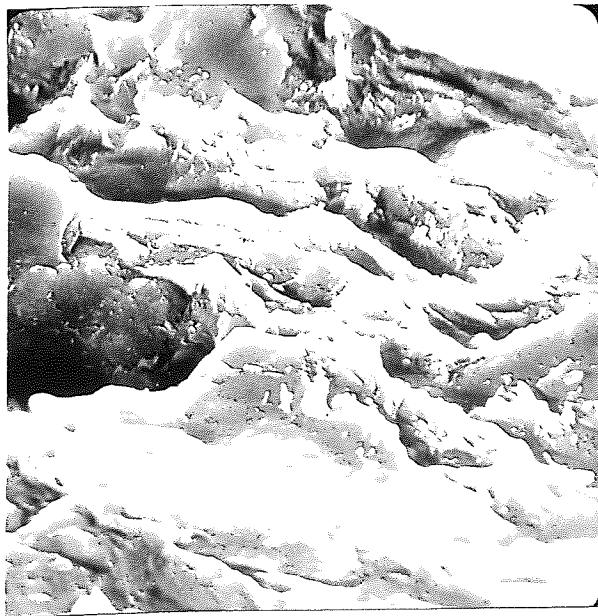
PLATE 6:8  
LOCKED TURBOSTRATIC FABRIC  
SAMPLE S40/1



I  
5 $\mu$ m

PLATE 6:9

GRAIN TURBOSTRATIC FABRIC  
BOREHOLE DAMPLE, DEPTH 13.3m



I  
5 $\mu$ m

PLATE 6:12

KAOLINITE FLAKES  
BOREHOLE SAMPLE, DEPTH 11.7m

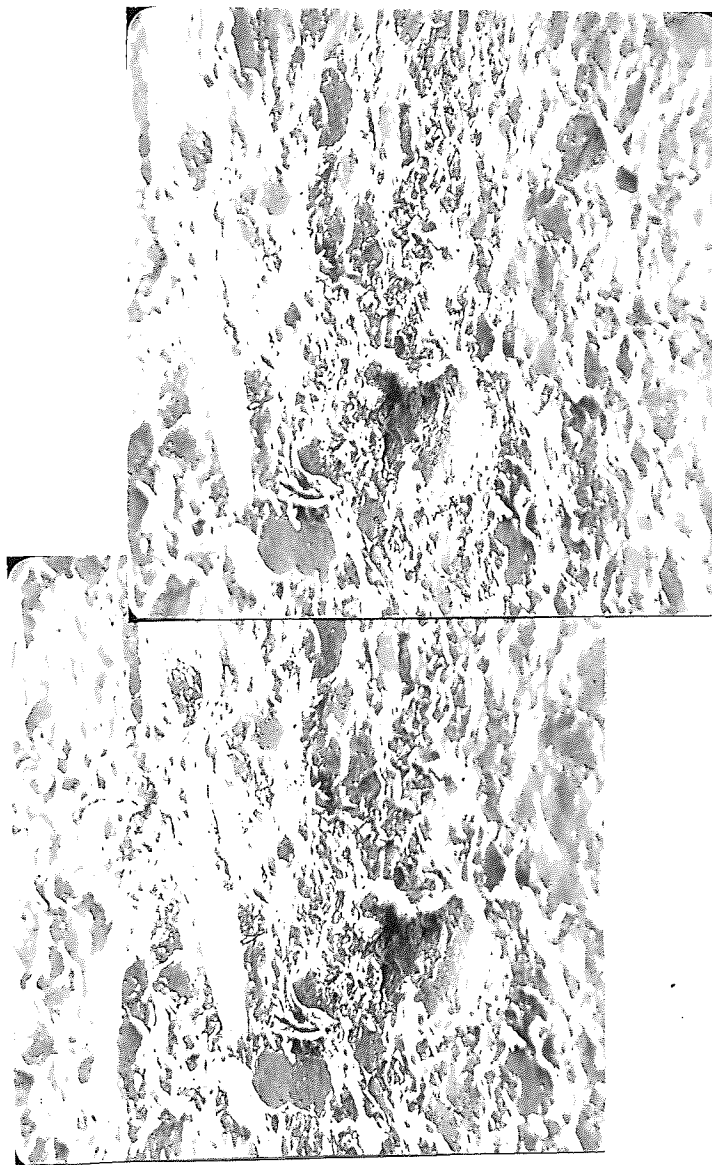


PLATE 6:10  
STEREOSCOPIC PAIR, PARALLEL TO BEDDING ( X220 )  
BOREHOLE SAMPLE, DEPTH 13.3m

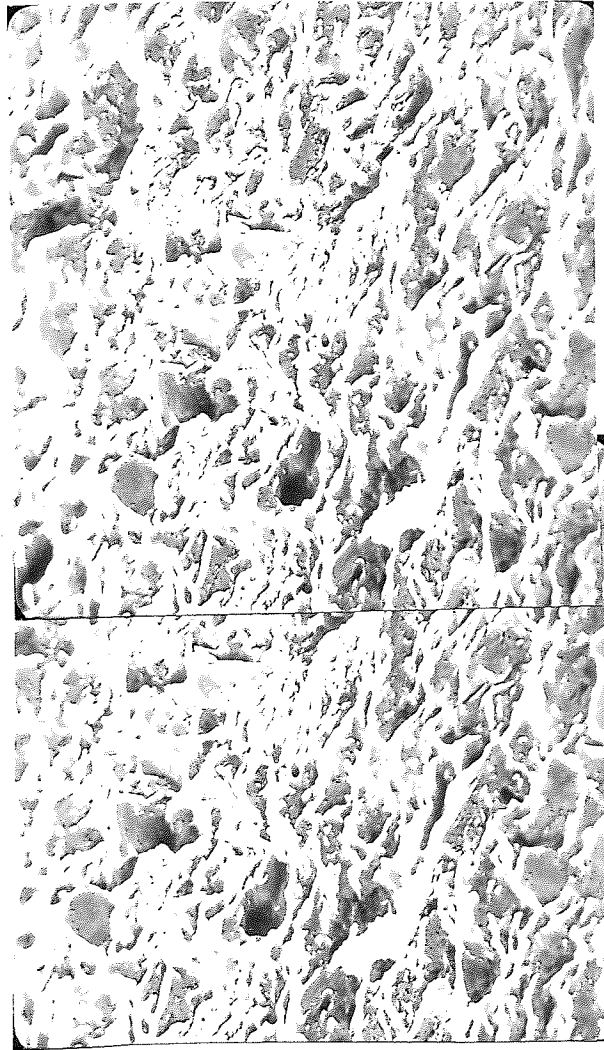
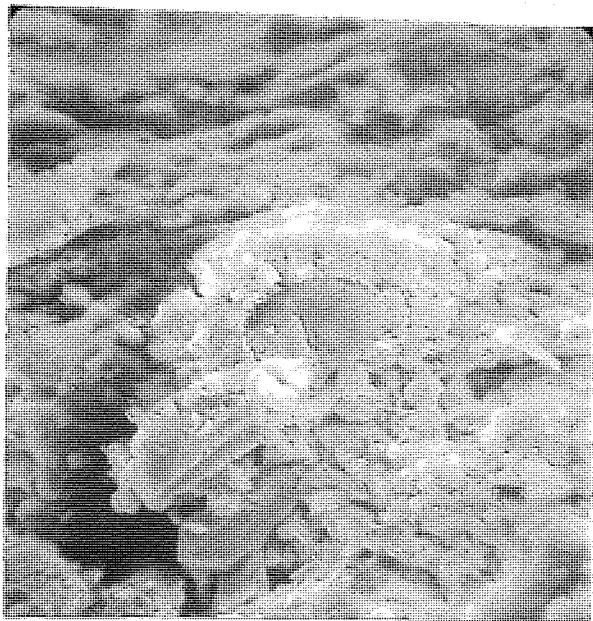


PLATE 6:11

STEREOSCOPIC PAIR PARALLEL TO BEDDING ( X500 )  
BOREHOLE SAMPLE, DEPTH 13.3m





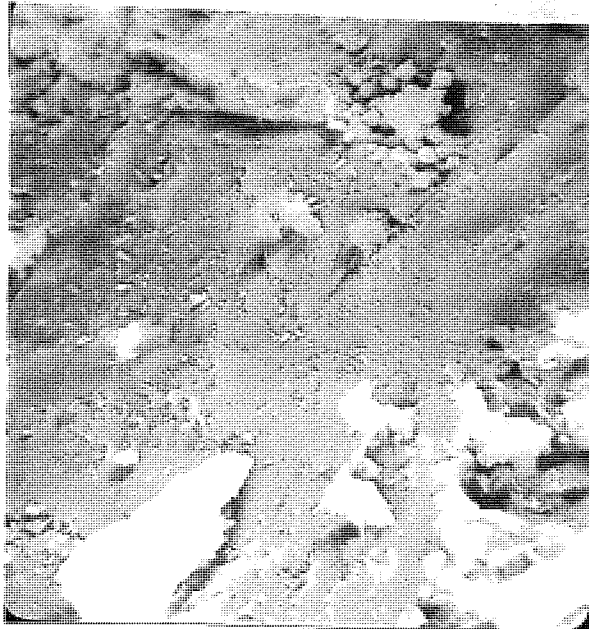
5 $\mu$ m

PLATE 6:13  
KAOLINITE FLAKES  
SAMPLE S16/1



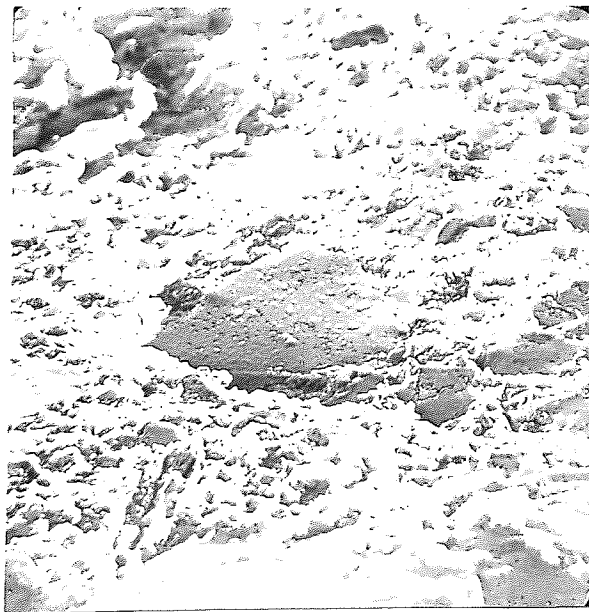
1 $\mu$ m

PLATE 6:14  
AUTHIGENIC MAGNETITE  
BOREHOLE SAMPLE, DEPTH 11.7m



1  $\mu$ m

PLATE 6:15  
SELENITE CRYSTALS  
SAMPLE S40/1



50  $\mu$ m

PLATE 6:16  
CLAY GROWTHS  
BOREHOLE SAMPLE, DEPTH 13.3m

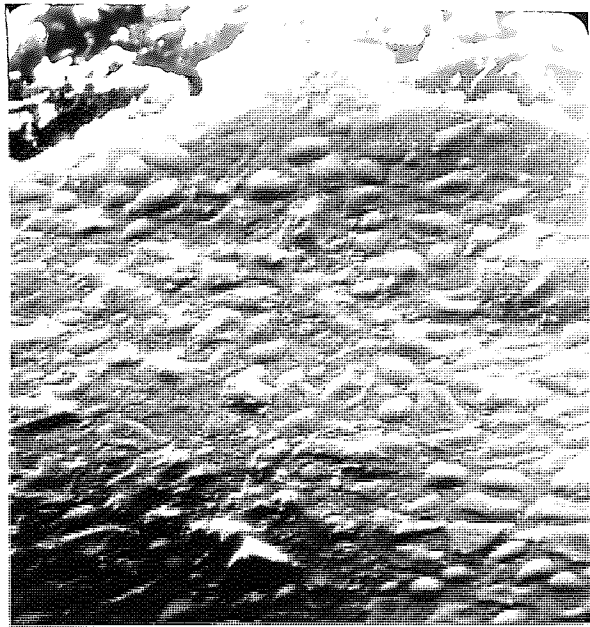


PLATE 6:17  
CLAY GROWTHS  
BOREHOLE SAMPLE, DEPTH 13.3m

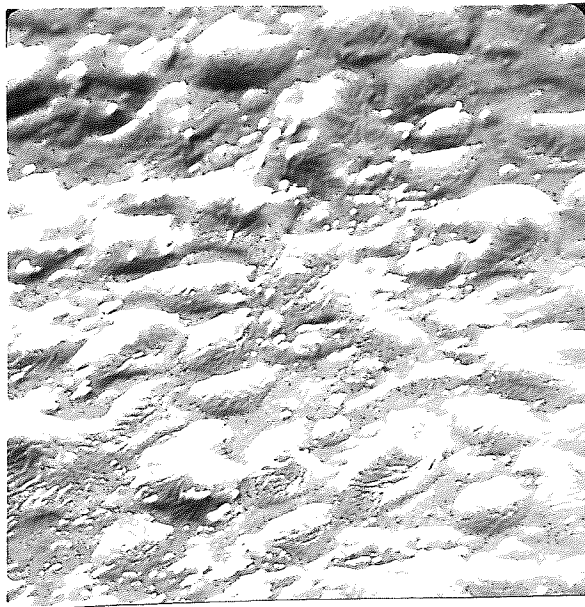


PLATE 6:18  
CLAY GROWTHS  
BOREHOLE SAMPLE, DEPTH 13.3m

## CHAPTER 7

### MINERALOGY

#### 7:1 INTRODUCTION

It has already been shown in the previous chapter that the Lower Lias clay consists of domains of clay minerals forming a turbostratic structure. The non clay minerals of quartz, calcite and pyrite can be studied by the petrological microscope, the clay minerals however must be identified by X-ray diffraction. Although the turbostratic domains and the large silt sized mica particles can be seen by the petrological microscope it is however almost impossible to identify the clay minerals.

The main constituents observed in thin sections are:

- a) Clay Minerals:- including the large muscovite flakes
- b) Quartz
- c) Iron Pyrites
- d) Calcite
- e) Organic Material

A quantitative analysis (using the Glagolev-Chayes 1933 point counting method) was carried out on the thin sections. The whole area of the thin section was used and the step movement on the point counter adjusted for the grain size. In the case of the unweathered clay sections the results are the average from ten thin sections.

It can be seen from Table 7:1 that clays are the major constituent in both the unweathered and weathered material and as shown in Chapter 4 the mineralogy of the weathered profile is

Table 7:1

Sample	Depth (m)	Clay %	Quartz %	Calcite %	Pyrite %	Voids %	Organic %
S1/1	0.15	78	11.8	-	-	1.82	8.2
		+ -0.6	+ - 2.0	-	-	+ -1.0	+ -0.6
S3/1	0.27	86.4	2.7	-	-	6.0	4.9
		+ -0.6	+ - 1.0	-	-	+ -1.0	+ -0.6
S6/1	0.6	91.2	4.18	-	-	3.12	1.57
		+ -1.0	+ - 0.8	-	-	+ -0.5	+ -0.5
S11/1	0.9	86.5	2.32	-	-	6.5	4.65
		+ -1.0	+ -0.8	-	-	+ -0.5	+ -0.5
S16/1	1.25	91.0	3.18	-	-	1.59	4.23
		+ -1.0	+ -0.8	-	-	+ -0.5	+ -0.5
S28/1	2.75	86.0	4.25	< 1	7.5	< 1	2.7
		+ -1.0	+ -0.8	-	+ -1.0	-	+ -0.5

TABLE 7:1 (continued)

Sample	Depth (m)	Clay %	Quartz %	Calcite %	Pyrite %	Voids %	Organic %
S32/1*	3.56	82.36	9.0	< 1	5.5	-	1.34
		+ -2.0	+ -2.3		+ -1.2	-	+ -0.8
Average Unwea- thered	-	83.8	6.74	1.82	6.64	-	1.09

\* Sample S32/1 was taken at an horizon where layering of silt and clay was pronounced, the silt layers containing a higher proportion of quartz. This results in wider confidence limits for both clay and quartz fractions.

Below 2.75m in depth material unweathered.

dependant on the parent material, climate, time and biological factors. Therefore, it is necessary to examine the unweathered material in detail in order to determine the exact changes.

## 7:2 CLAY MINERALS

### 7:2:1 CLASSIFICATION

Clay minerals are extremely difficult to classify due to their variability. Clays have a fine particle size and this fraction may contain tiny fragments of non clay minerals but in the main, consists of distinctive clay minerals with some amorphous colloidal material.


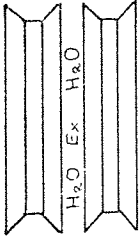
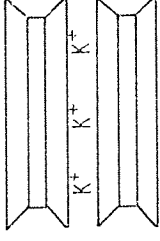
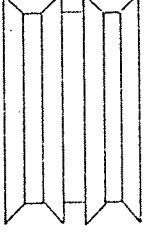
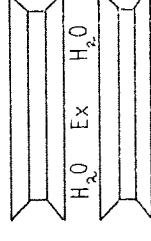


The common sedimentary clay minerals can be subdivided into five groups; the kaolinite group, the montmorillonoids or smectites, the micas, the chlorites, and the vermiculites. A detailed discussion of crystal structure and variental species is not given here and one is referred to the works of Grim (1968), Brown (1961), Deer, Howie and Zussman (1966). The present discussion is concerned mainly with identifying the chief compositional and structural differences between each group.

One feature that the five classes have in common is that they are all layer-type aluminosilicates and each unit cell consists of layers of aluminium ions octahedrally co-ordinated by  $\text{OH}^-$  or  $\text{O}^{2-}$  (octahedral layer) and layers of silica tetrahedra (tetrahedral layer), combined in various proportions with some separated by cations (hydrated or otherwise). Ionic substitution occurs in both the octahedral and tetrahedral layers. A summary of the structure from Grim (1968) is shown in Table 7:2.

#### Kaolinite Group (Kandites).

These are essentially the 1:1 clay minerals consisting of one

TABLE 7:2

Mineral	Structure	Composition (idealized)	Cation Exchange Capacity
Kaolinite		$Al_2Si_2O_5(OH)_4$	1 - 10
Montmorillonite		$Ex [Al_{2-x}Mg_x] < Si_4 > O_{10} (OH)_2$	80 - 140
Micas (Illite)		$K_{1-x} [Al_x] < Al_{1-x} Si_{3+x} > O_{10} (OH)_2$	10 - 40
Chlorite		$[Mg,Al]_3 (OH)_6 [Mg,Al]_3 < Si,Al >_4 O_{10} (OH)_2$	5 - 30
Vermiculite		$Ex_x [Mg_x] < Al_x Si_{4-x} > O_{10} (OH)_2$	100 - 180
	Tetrahedral layer		∧
	Octahedral layer		┌ ┐



octahedral layer and one tetrahedral layer forming a unit cell. These individual sheets are firmly linked by H bonding of the  $\text{OH}^-$  ions in the octahedral layer to the  $\text{O}^{2-}$  ions of the tetrahedral layer. This basic unit cell has a thickness of approximately  $7\text{\AA}$  and hence a characteristic basal spacing. Kaolinite is the most important and commonest mineral of this group, although dickite and nacrite are chemically identical, they are monoclinic in form and rare compared to the triclinic kaolinite.

Halloysite has a single layer of water molecules between the basic units, consequently stacking is disordered and the inter layer distance is increased to  $10\text{\AA}$ . The inter layer water of halloysite may be replaced by glycol causing the spacing to increase to about  $11\text{\AA}$  other kandites show no swelling properties. There is little ionic substitution for Al or Si resulting in a low ion-exchange capacity.

Electron micrographs show halloysite to be tubular, kaolinite when well crystalline has a hexagonal sheet appearance. Halloysite however, is very rare in rocks of sedimentary origin and it is usually associated with hydrothermal deposits (Millot 1964).

### Smectites

In this group the basic unit consists of one aluminous octahedral layer sandwiched between two tetrahedral layers. There is limited substitution of  $\text{Al}^{3+}$  for  $\text{Si}^{4+}$  in the tetrahedral layers and extensive substitution of  $\text{Mg}^{2+}$  (and to a lesser extent  $\text{Fe}^{3+}$  and  $\text{Fe}^{2+}$ ) for  $\text{Al}^{3+}$  in the octahedral layers. This gives rise to a large net negative charge. To balance this, exchangeable cations accumulate in the interlayer positions between each unit cell and hence the minerals have a high ion exchange capacity (Table 7:2). The cations

are hydrated and as a result variable quantities of water accumulate in the interlayer positions. Variable hydration gives rise to an expandable structure and a variable thickness for the unit cell. This variable amount of water between the unit layers causes the stacking periodicity to vary although in many cases it is close to  $14\text{\AA}$ . With glycolation the basal spacing reaches  $17.8\text{\AA}$  and collapses to  $10\text{\AA}$  with heat treatment. Hence the permutation of exchangeable ions, heat treatment and the action of polyalcohols can cause this periodicity to vary between  $10\text{\AA} - 20\text{\AA}$ .

Due to ionic substitution the number of species known is large, montmorillonite being one of these with a set composition (Ross and Hendricks (1945)).

#### Micas

This term covers a broad class of 2:1 minerals, having a similar structure to montmorillonite, i.e. the basic unit consists of one aluminous layer sandwiched between two tetrahedral layers. Two of these units are then held together by  $K^+$  cations so giving a repeat basal spacing of  $10\text{\AA}$ . Mica can vary from detrital muscovite to well crystallized sericite and neoformed micas. Biotite mica can be recognised from muscovite in the XRD trace. However, it is usually weathered to some other clay mineral and therefore the majority of micas in sediments are of the muscovite variety.

In "ideal" muscovite there is no substitution in the octahedral layer and in the tetrahedral layer one out of four silicons is replaced by an aluminium. The resulting net negative charge is balanced by non-hydrated, non-exchangeable  $K^+$  ions in the interlayer position and because the  $K^+$  ions are firmly bound and not hydrated, muscovite is non-expandable.

For several years the term illite was used to cover this group. Illite was proposed and defined by Grim, Bray and Bradley (1937) and used to designate the whole group of clay minerals with a structure similar to that of micas. Illites on analysis have a deficit of potassium ions and are replaced by water molecules, therefore illite is basically a compositional variant of the mineral muscovite and usually very fine grained.

In muscovites and to a slightly greater extent in illites there is some octahedral substitution, a lesser amount of aluminium substitution in the tetrahedral layer (consequently lower  $K^+$  in the interlayer), and some replacement of  $K^+$  by exchangeable cations.

The micas, muscovite and illite are the commonest in sediments yet pyrophyllite, talc and glauconite also belonging to the mica group can be found in sediments formed under specific conditions.

#### Chlorite Group

Chlorite, an aluminosilicate of magnesium and iron has a unit cell consisting of a 2-tetrahedral-plus-1-octahedral unit combined with an additional octahedral layer which is often termed the brucite layer. The principal ion of both octahedral layers is magnesium. Substitution of  $Al^{3+}$  for  $Si^{4+}$  in the tetrahedral layers is balanced by substitution of  $Al^{3+}$  for  $Mg^{2+}$  in the octahedral layers; thus there are no interlayer ions.  $Fe^{2+}$  iron does substitute for  $Mg^{2+}$ , and it is due to this characteristic that Werner originally used the term chlorite to designate green foliated minerals rich in ferrous ions.

Chlorite has a basal spacing of  $14\overset{\circ}{\text{Å}}$  that does not collapse on heating or expand with polyalcohols.

A swelling chlorite with a basal spacing of  $14.2\overset{\circ}{\text{Å}}$  that expands to  $17.8\overset{\circ}{\text{Å}}$  with glycerol and yet is stable on heating has been

\* Deer et al. 1966

described from the English Keuper Marls by Honeyborne (1951) and Davis (1968). This chlorite only forms under certain conditions and is not common in many sedimentary rocks.

### Vermiculites

Vermiculite could be placed in the chlorite group on the basis of its  $14\text{\AA}$  basal spacing; however, it does have several different properties.

Macroscopic crystals have been known for many years and are probably of secondary origin, i.e. the alteration of mica, pyroxene, chlorite or other similar minerals by natural weathering. Weaver (1958) with regard to clay minerals considers that vermiculites can form from mica, chlorite, serpentine, talc, volcanic ash, hornblende and feldspar.

Vermiculites have a basal reflection of  $14\text{\AA}$  which collapses to  $10\text{\AA}$  when heated to  $200^{\circ}\text{C}$ ; however, care must be taken to ensure rehydration does not occur. For this reason all samples after heating should be kept in a desiccator prior to being examined on the X-ray diffractometer.

Although it appears straightforward to identify the clay minerals, only basal spacings were mentioned in the preceding section. Kaolinite for example has a basal spacing of  $7\text{\AA}$ , but non-expanding chlorite has a strong  $7\text{\AA}$  second order peak. Montmorillonite and sometimes vermiculite can interfere with the  $10\text{\AA}$  peak of the micas, as well as the  $14\text{\AA}$  peak of the chlorites and so far no mention has been made of the Mixed layer clays. Weaver (1956) showed that randomly interstratified 2:1 clays are abundant in sedimentary rocks and demonstrated that their ratios could be estimated from the X-ray diffraction pattern. One

must use not only the first order peaks but also the second, third, etc. With multicomponent mixtures this can become extremely complex in some cases, and this is best done with clay minerals only after some careful separation process.

The main criteria used in the identification of the clay minerals is summarised in Table 7:3, and this together with further information from Brown (1961), Millot (1964) and the A.S.T.M. powder files was used for the final determinations.

#### 7:2:2 SAMPLE PREPARATION

The identification of clays by X-ray diffraction is almost a standard technique, although it is still very specialised with many difficulties. The difficulties arise mainly from the size of the clay minerals themselves and their variability in both mineralogy and chemistry. The methods of sample preparation and equipment used are described in Appendix C.

Samples from both the detailed profiles were examined in the air dried state at a scan rate of 2,20/min thus enabling a rough identification and comparison. Comparison of the diffractometer traces revealed that there was little or no difference between the profiles and so fifteen specimens from Section One were taken for detailed analysis, both qualitative (air dried, glycolation, heated, acid treatment) and semi-quantitative (Appendix C).

#### 7:2:3 PREVIOUS WORK

Prior to analysing the results obtained a short time should be devoted to examining previous work. In actual fact there is scant data on the mineralogy or geochemistry of the Lias, since the majority of the work has been on the fauna in respect to the ammonite zones and subzones.

TABLE 7:3

## EFFECT ON THE BASAL SPACING OF VARIOUS PRE-TREATMENTS

Mineral	Air dry basal spacing	Moistened with glycerol	Heated to 200°C	50% HCl	Notes
Kaolinite	7Å	Unaffected	Unaffected may sharpen	Unaffected	
"Mica"	10Å	Unaffected	Unaffected may sharpen	Unaffected	
Smectites	12Å - 15Å	Shifts to 17.8Å	Shifts to 10Å	Glycolated material unaffected	Some may dissolve in HCl
Chlorites	14Å with strong second order 7Å	Unaffected	14Å & 7Å can be enhanced	All lines should vanish	Will dissolve in HCl
Vermiculite	14Å	Unaffected	Shifts to 10Å	Will vanish	rapidly re-hydrates after heat treatment

Hallam (1961) when working on the Blue Lias of Dorset and Glamorgan did publish a chemical analysis and the results of an X-ray analysis of the insoluble residues of the calcareous mudstones. He reported that the residue consisted of 90 - 100% illite and up to 10% kaolinite with traces of vermiculite. The major criticism concerning these results is that the clays were treated with HCl to remove the carbonates which may also destroy any chlorite and vermiculite present. This can be seen in Fig 7:3 when samples from Blockley were treated with acid, thus causing the 14Å<sup>0</sup> peak to be reduced and could in cases disappear altogether.

Wobber (1967) working on the Lower Lias of South Wales concentrated on the limestones and carbonate geochemistry. Le Riche (1959) produced detailed geochemical analyses from the Stowell Park Borehole, Northleach and the Dorset coast but again the mineralogy was not investigated since trace elements were his major concern.

The recent publication by R.M. Perrin (1972) on the Clay Minerals of British Sediments gives further results which up to the present time have not been published. He quotes results by Holdrige and Keeling (1953) of the British Ceramics Research Association (Stoke-on-Trent). Their results produced by plastic limit analysis and ignition loss/moisture absorption method only indicates a high mica material for the clay minerals, but they do state that quartz, pyrite, calcium and siderite are the non-clay minerals. Perrin also quotes results by Brown and Du Feu (1956) of Rothamsted Experimental Station (Harpenden) who worked at Robin Wood Hill near Gloucester in the davoei Zone where they found:

Kaolin	Mi	Sm
15%	30%	55% with feldspars, quartz and goethite

It was also noticeable that Freeman (1964) left out the Lias clay when he examined the mineralogy of certain British brick clays, since the Lias has been used and still is, extensively used for the manufacture of bricks, this fact is surprising.

Chandler (1972) on his engineering work on the Lias clay did produce some chemical data which will be discussed in another chapter, but here again no attempt was made to define the mineralogy.

#### 7:2:4 CLAY MINERALOGY OF THE LIAS AT BLOCKLEY

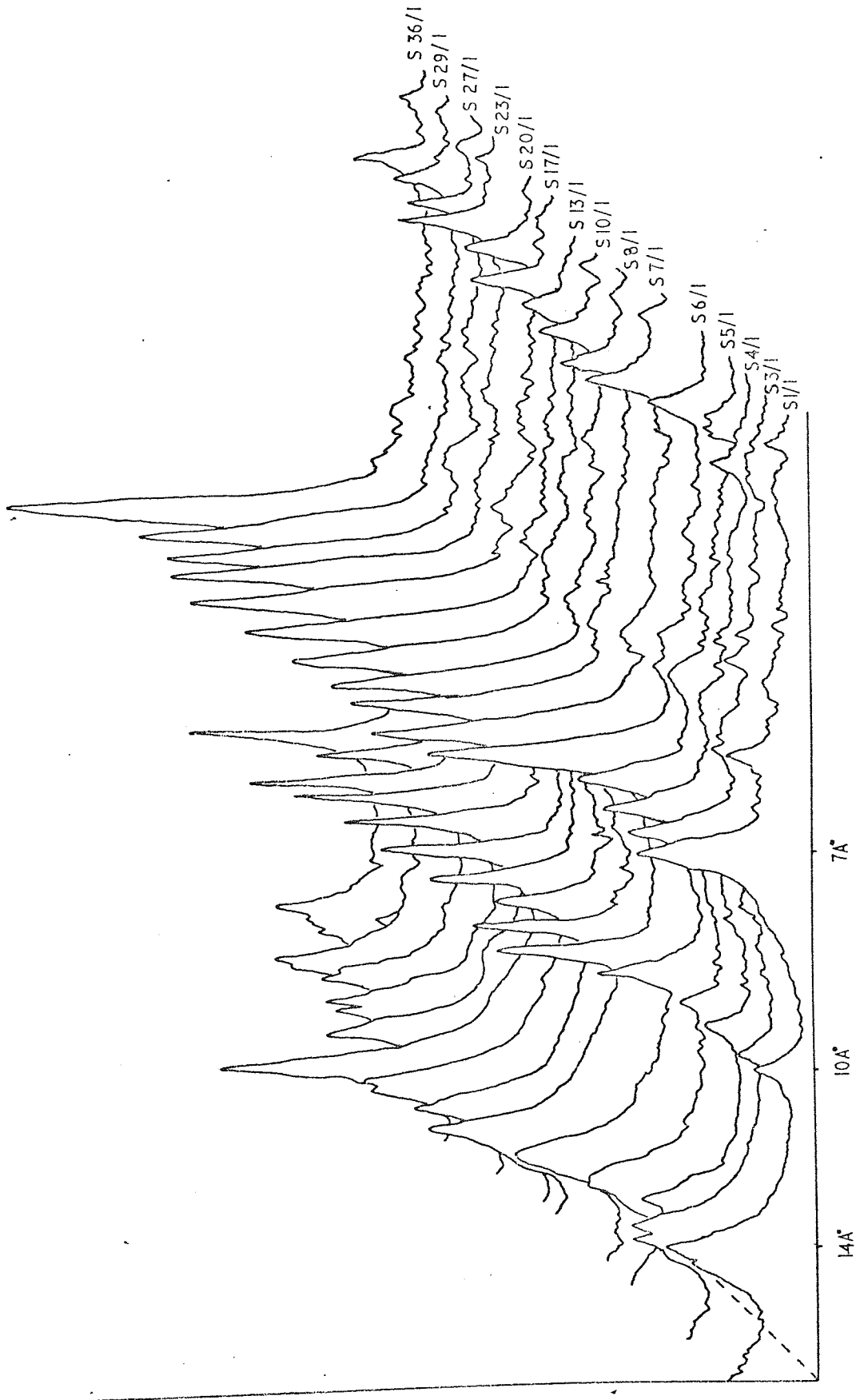
As already stated in Chapter 2 the Blockley site is close to the London-Ardennes Island therefore one would expect a clay containing a relatively high percentage of kaolinite, though there has been no detailed study of the Lias mineralogy with respect to shore lines at the present time.

The results from Blockley are shown in Figs 7:1, 7:2, 7:3 and Table 7:4 (representing a summary of the work).

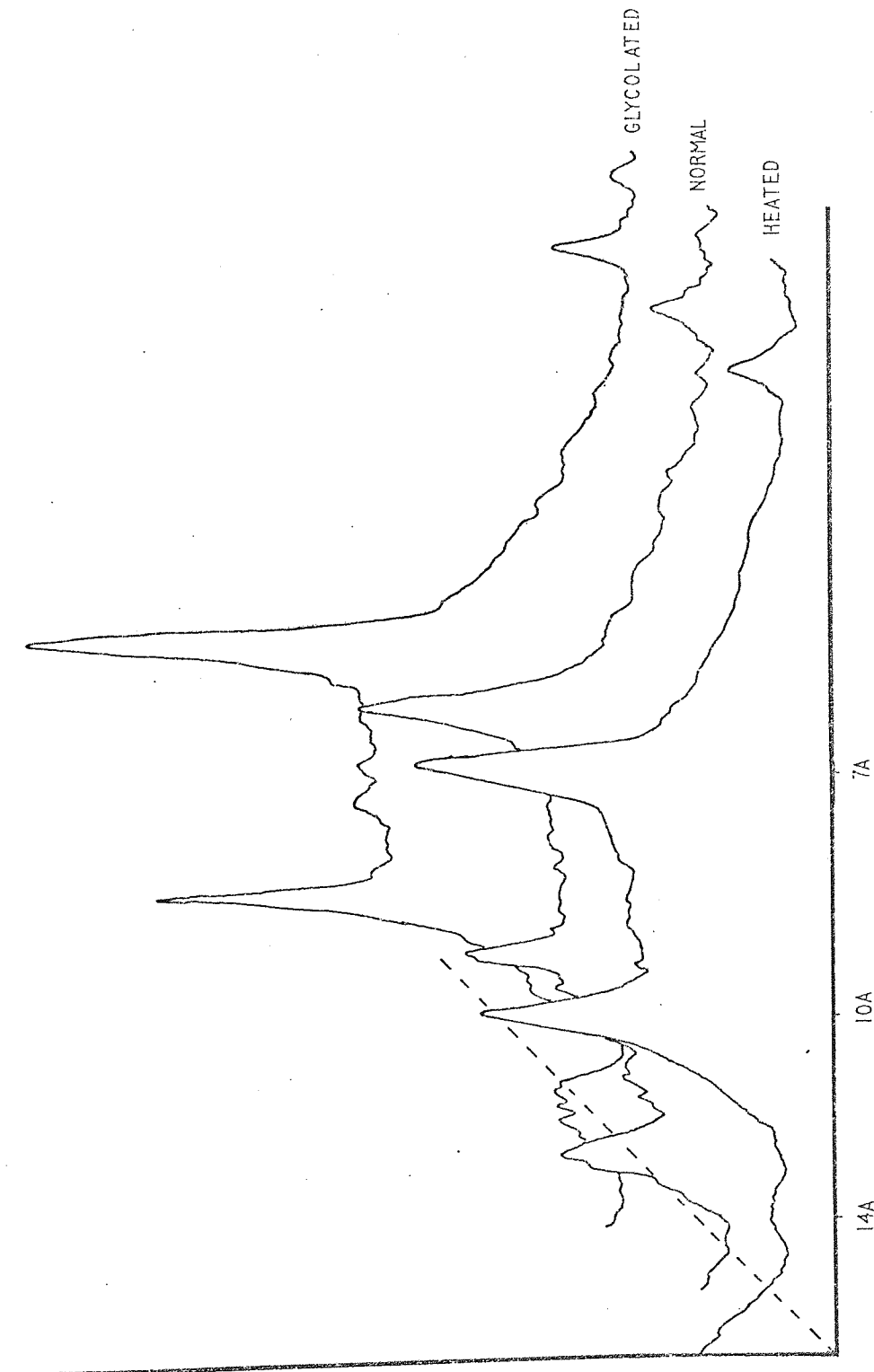
Kaolinite and the micas were relatively easy to identify from the XRD-diffraction trace. Minerals in the  $14\text{\AA}$  region were however more difficult. The peak could have been due to either; chlorite, vermiculite or a smectite. Glycolation caused some broadening of the  $14\text{\AA}$  peak in many samples but not to any great extent, therefore there is the possibility that there is a trace of a smectite present in most of the samples. On treatment with 50% HCl, in unweathered samples the  $14\text{\AA}$  peaks were reduced by almost half and the very weathered samples they were removed altogether, chlorites/vermiculites are soluble in acid. The use of acid treatment in the identification of chlorite when a kaolin and chlorite are present in the same



FIG 7:1

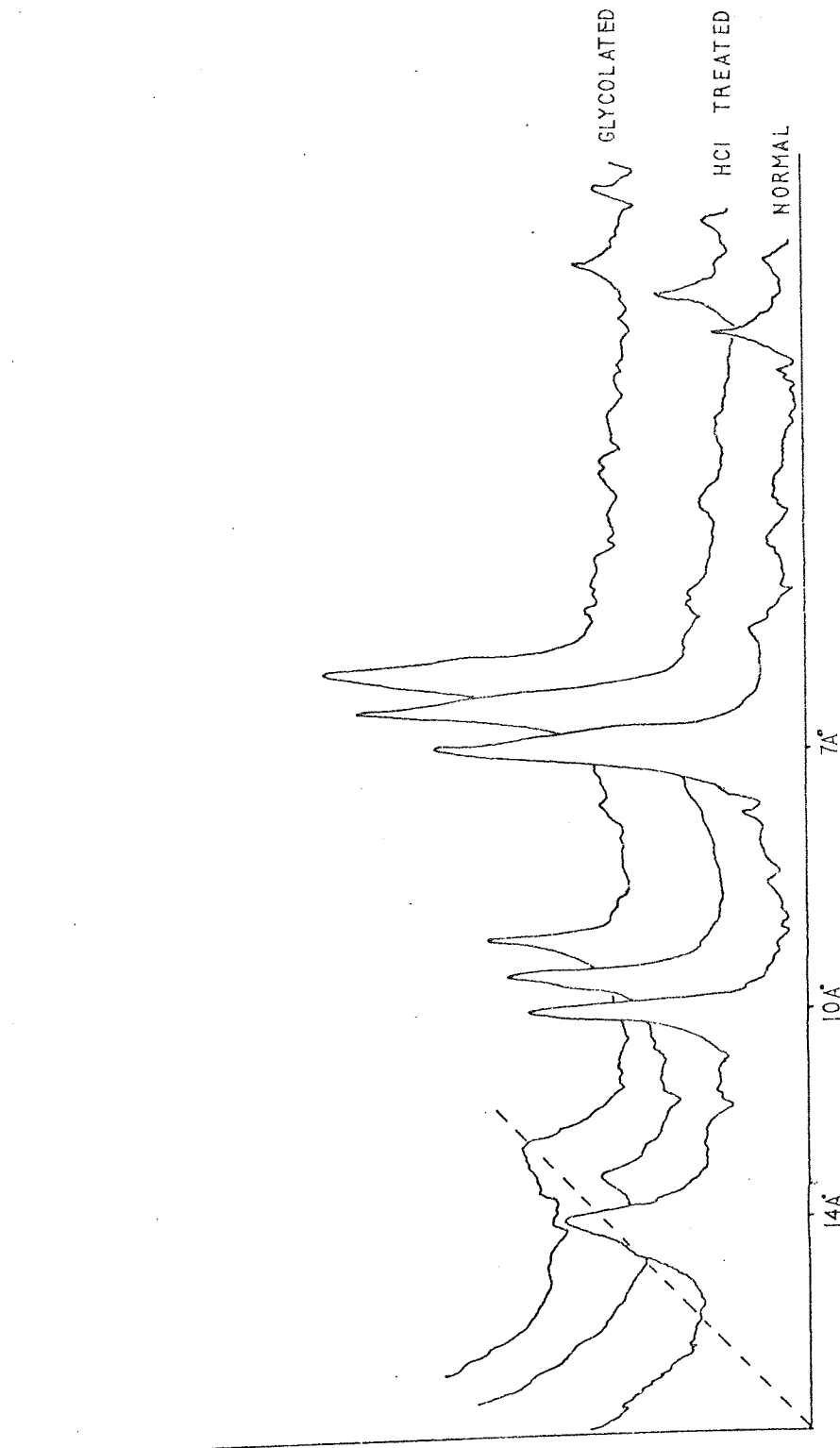


X-RAY DIFFRACTION TRACES WITH DEPTH (SECTION ONE)



SAMPLE S17/1 X-RAY DIFFRACTION TRACE

FIG 7:2



SAMPLE S27/1 X-RAY DIFFRACTION TRACE

FIG 7:3

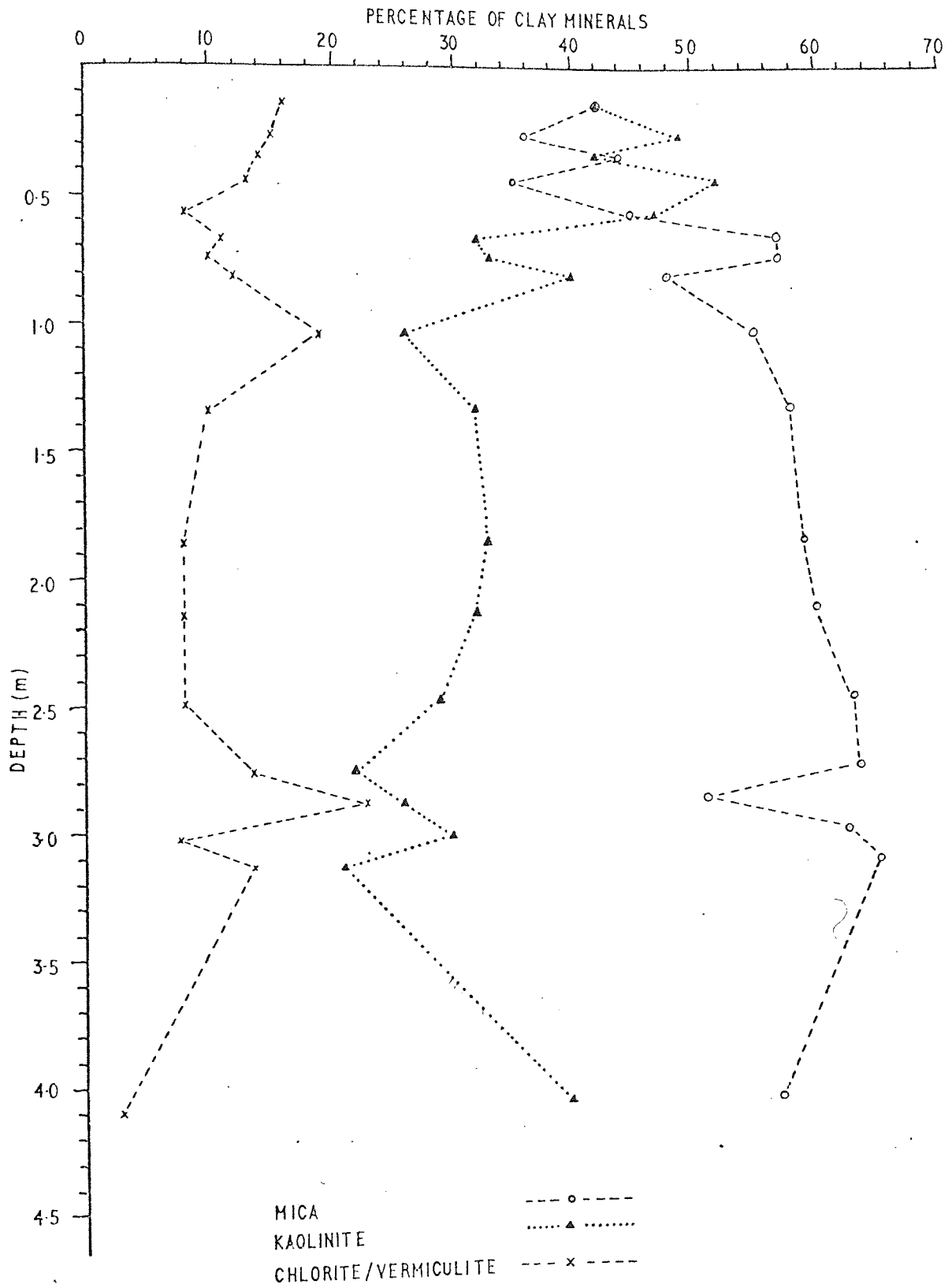


FIG 7:4A  
 PERCENTAGE OF CLAY MINERALS WITH DEPTH

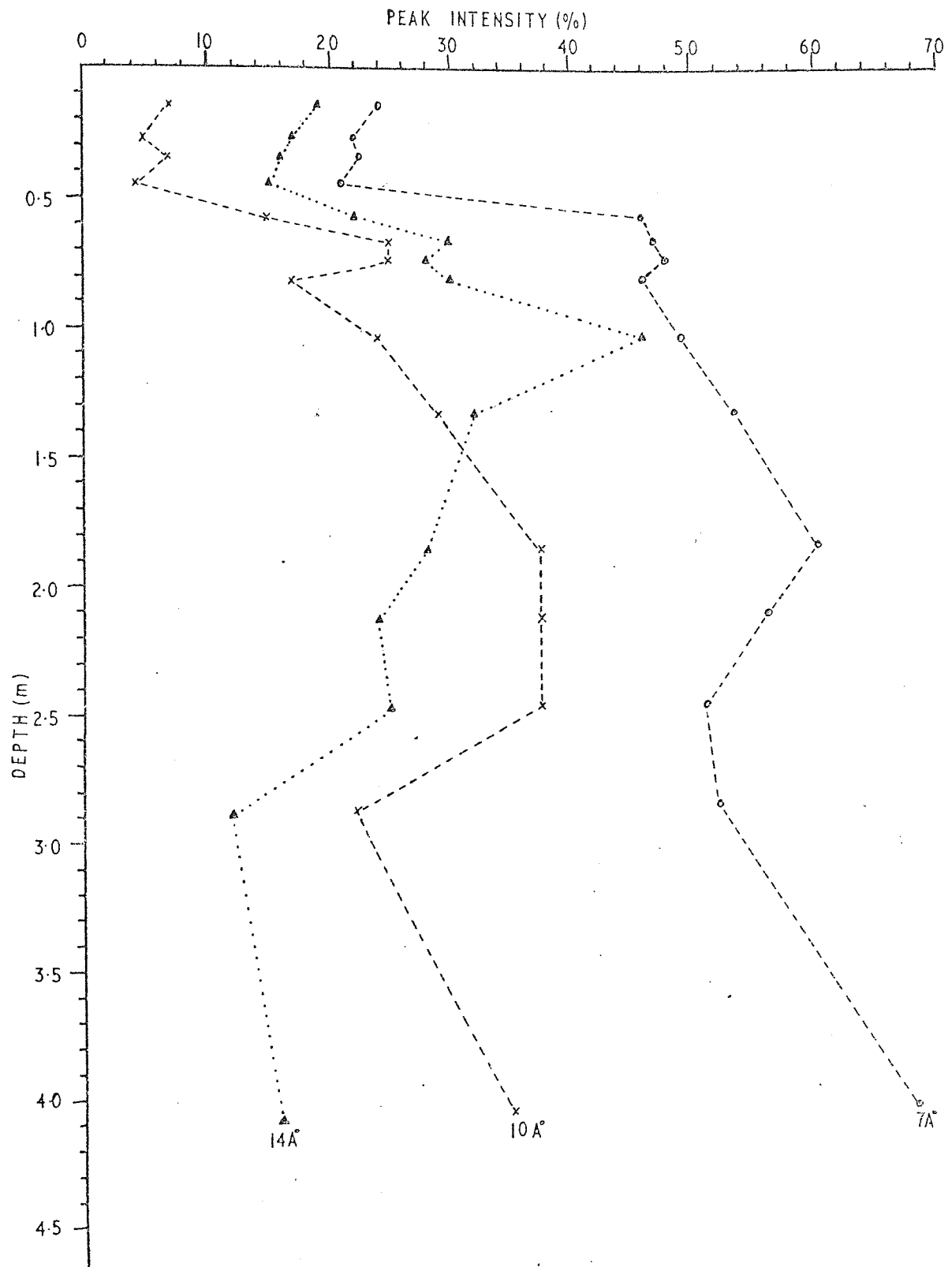


FIG 7:4B

PEAK INTENSITY WITH DEPTH ( $14\text{\AA}$ ,  $10\text{\AA}$ ,  $7\text{\AA}$ )

sample was examined in detail by Vivaldi and Gallego (1961). Their work proved that although thermal treatment is useful in confirming the presence of chlorite, it could not give definite information on the presence of kaolinite, acid treatment however is conclusive in this respect.

On heating to 200°C the 14Å peak in all but the unweathered samples was displaced to the 10Å position. It was on this fact that the 14Å mineral was identified as vermiculite, although in the unweathered material chlorite is also present but in smaller quantities (Fig 7:2, 7:3).

The results show that there is a change of mineralogy with weathering. The chlorite:vermiculite ratio tends to decrease generally with increase in weathering, although the increase is very small. The actual percentages of chlorite and vermiculite are impossible to estimate but relative proportions could be judged from the intensity of the 3.54Å peak of chlorite. This is almost unobservable on the traces produced from weathered material, but could clearly be seen in traces from the unweathered clay.

Bradley (1953) described and demonstrated that expandable layers in the mica structure result in asymmetry of the 001 peaks toward the low-angle side, broadening of the 002 peak, and asymmetry of the 003 peak towards the high angled side. Harrison & Murray (1959) when examining clay mineral stability during weathering confirmed this view.

This effect is also noticeable in the highly weathered Lias indicating the presence of some mixed layerclays probably mica/smectite.

The broadening of the  $14\text{\AA}^0$  peak in the weathered material could also indicate a vermiculite/chlorite mixed layer clay although evidence for this is scanty.

As can be seen from Fig 7:1 samples down to a depth of 0.6 - 0.7 (S6/1 - S7/1) metres have very small  $10\text{\AA}^0$  peaks. This zone represents the most intense zone of weathering. The mica loses its potassium both to the plants and the percolating water thus reducing its basal spacing. This together with the oxidation of iron (Murray & Leininger 1956) are the main mechanisms for the disintegration and degradation of the micas and the chlorites. This zone of weathering is generally acidic in nature and therefore an unlimited supply of hydronium ions is available. The radii of hydronium ( $1.4 - 1.5\text{\AA}^0$ ) and potassium ( $1.33\text{\AA}^0$ ) ions are similar and so once the oxidation of the iron has begun the net negative charge is reduced and so an exchange of hydronium and potassium ions often occurs. The mechanism of the iron oxidation will be examined in detail in the discussion on the ferrous/ferric ratio.

This reduction in the amount of mica with weathering is also seen in the quantitative analysis (Table 7:4). The percentage of kaolinite appears to be constant through the profile with a very small increase towards the upper soil layers. The higher content of kaolinite in sample S5/1 is probably due to the preferential elluviation of this mineral from higher horizons but the profile is relatively young and therefore the increase is not excessive. The micas on the other hand decrease noticeably and there is a definite decrease in the chlorite/vermiculite ratio as the surface is approached.

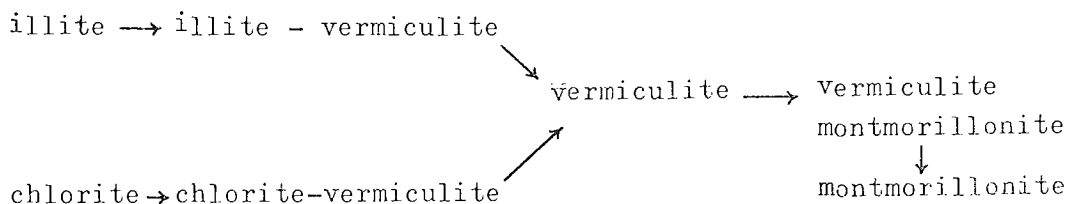
TABLE 7:4

## PERCENTAGES OF MAJOR CLAY MINERALS

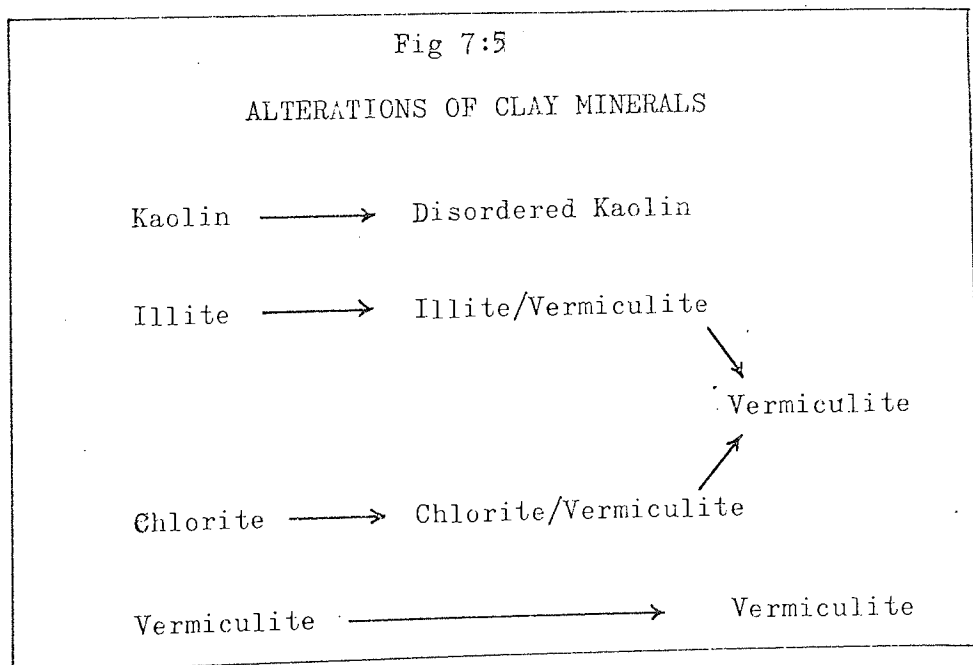
Sample No. Section One	Depth (m)	Percentage $\pm$ 4%			
		Mica	Kaolinite	Chlorite/Vermiculite	Dominant mineral
S1/1	0.14	42	42	16	v
S3/1	0.27	36	49	15	v
S4/1	0.35	44	42	14	v
S5/1	0.44	35	52	13	v
S6/1	0.57	45	47	8	v
S7/1	0.66	57	32	11	v
S8/1	0.74	57	33	10	v
S10/1	0.83	48	40	12	v
S13/1	1.05	55	26	19	v
S17/1	1.34	58	32	10	v
S20/1	1.87	59	33	8	v
S23/1	2.15	60	32	8	v/c
S27/1	2.5	63	29	8	v/c
S28/1	2.77	63.5	22	13.7	v/c
S29/1	2.9	51	26	23	c
S30/1	3.04	62.4	30	7.6	v/c
S31/1	3.14	65.0	21	13.7	v/c
S36/1	4.1	57	40	3	c



Brown (1953) and Millot (1964) have outlined the degradation transformation of micas and chlorites under acidic (especially in podzolic soils) weathering (see below)



The degradation of the two-layered kaolin is less well known. Millot (1964) suggests that this alters to halloysite or disordered kaolinites and gibbsite. The transition of illite → kaolin could also take place and this necessitates a restructuring, and, in the terms used by Millot, this would be a neoformation.



As a summary, the possible alterations that take place are shown in Fig 7:5. Only a small percentage of the clays have undergone any transformation in the short time available, since there is no correlation between increases in chlorite and reductions in micas.

### 7:3 NON CLAY MINERALS

Quartz, pyrite and calcite constitute the major non-clay minerals. At one horizon euhedral feldspar pseudomorphs were associated with a higher quartz content and coarser grain size. A small amount of organic matter is ubiquitous.

#### 7:3:1 QUARTZ

The quartz fragments on the whole are of coarse silt size to very fine sand in size (0.02 mm - 0.10 mm), although coarse sand size fragments were noticeable in the surface material S1/1 (Plate 7:1).

Although the sand appears to be randomly distributed in the more homogenous clay, it tends to be concentrated in layers and lenses in silty horizons, which aid the definition of any shear zones present (Plate 7:2) and their displacement (Chapter 6). The percentage of quartz increases towards the surface due to the processes of weathering.

#### 7:3:2 CALCITE

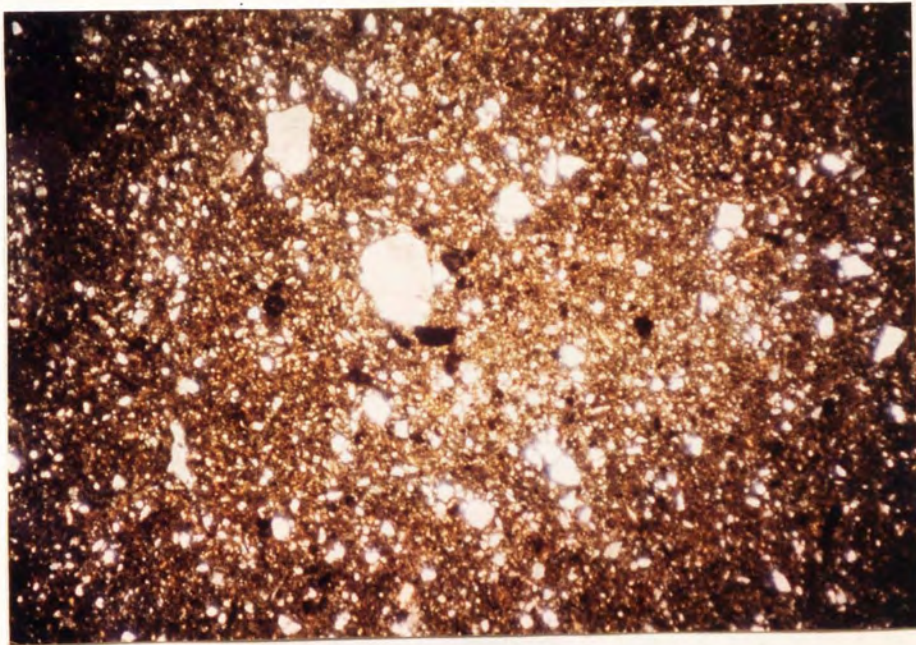
The calcite content on average was low, in the region of 2% (point counting) and carbonate analysis of sub-samples weighing 1 gm (taken from a larger 10 gm sample) gave a carbonate percentage of 3% - 10% .

The calcite is only present in samples below the C2 or Zone II of weathering (Chapter 3). Above this the calcite has been leached out by the acidic percolating water.

Calcite is present principally in three forms, each form having a specific association:

##### (i) Micrite

Tends to be rare but can be seen round the edges of larger clusters of sparry calcite and within the clay matrix remote from



X33

RANDOM STRUCTURE AND QUARTZ  
CONCENTRATION (SAMPLE S1/1)  
VERTICAL SECTION

PLATE 7:1



PLATE 7:2  
SILT HORIZONS (SAMPLE S32/1)

such aggregates.

(ii) Sparry Calcite

This is closely associated with pyrite when the pyrite is in its spheroidal form (see below). The sparry calcite rarely reaches 1mm in size and it is almost impossible to determine whether the sparry calcite is recrystallized micrite or otherwise since pre-existing textures and structures have been obliterated.

(iii) Skeletal Calcite

Well crystallized calcite of shells and shell fragments with the complicated structural layering of molluscan shells are still evident. Only the foram tests appear to be infilled with calcite, the molluscs being infilled with clay and occasional pyrite.

7:3:3 IRON MINERALS

Examination of the slides of the unweathered material indicates that iron is present in several phases. The major phase appearing to be that of iron sulphide (pyrite) although one must also remember that the iron oxide hematite, is also present, attached to clay minerals. This iron oxide is in a finely disseminated form and can only be seen by its colour. It is probably safe to assume that the iron attached to the clays is in fact the major phase, the iron in the pyrite being concentrations due to local conditions.

Both in thin sections and the hand specimen, iron pyrites is easily recognisable in one of two forms.

7:3:3:1 SPHERES

Only visible in thin section and found in various associations and overall form. The pyrite is opaque and the individual spheres vary in size up to 0.01mm. The pyrite does not appear to surround a centre of formation (Plate 7:3).

These spheres can be clustered together to give one of three forms.

(i) Spheroidal Masses

Pyrite spheres, aggregated, with many contacts to form a spheroidal mass, in some cases almost perfectly spherical.

In the majority of cases calcite is the main mineral associated with the pyrite. The calcite fills the pore space between the individual spheres and in two cases examined, calcite also surrounded the spheroidal mass. The calcite in both these cases had crystallised radially thus producing a stationary polarization cross under crossed nicols.

On Slide BM/1 (borehole sample) a spheroidal mass was found with the foliations (bedding) of the clay material being pushed round the mass (Fig 7:6), there are two possible explanations for its formation.

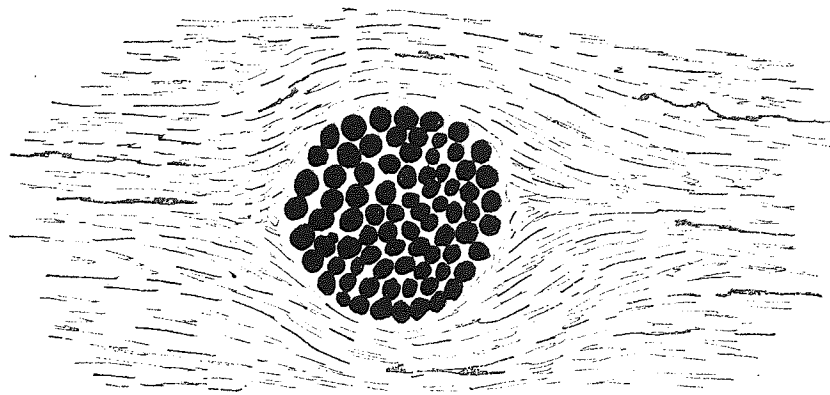
(i) Pyrite precipitated at centres and pushed the sediment layer apart.

(ii) The Pyrite spheres formed when the void ratio was in the order of 70 to 80% and during the consolidation phase, the clay was moulded round the spheroidal mass of pyrite which was more resistant to compression.

(ii) Strings

Pyrite spheres occur in a string usually parallel to the bedding, never more than two layers of spheres in thickness but up to several mm in length.

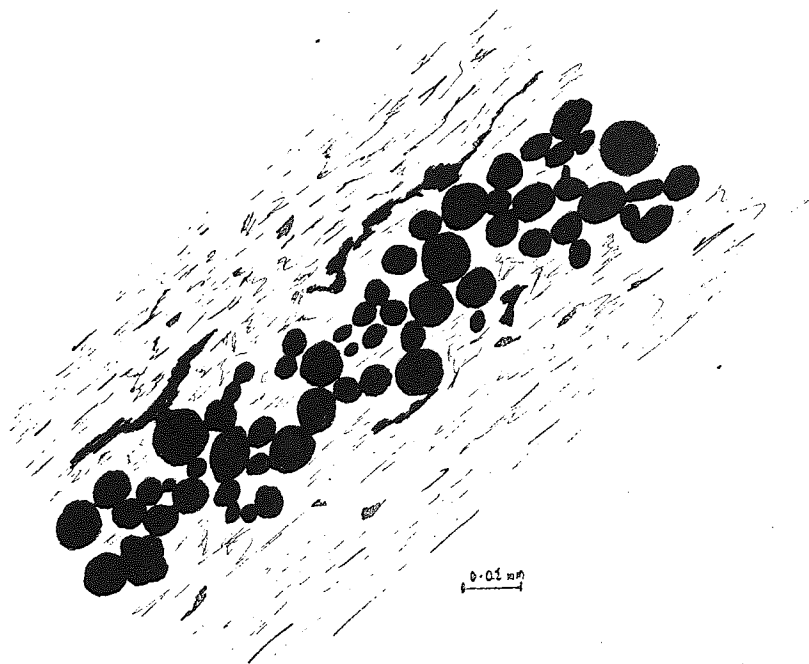
In certain slides e.g. BH/2 a peculiar parallel arrangement of the strings can be observed in close association with calcite.



0.01 mm  
|

SPHEROIDAL MASS OF PYRITE SPHERES

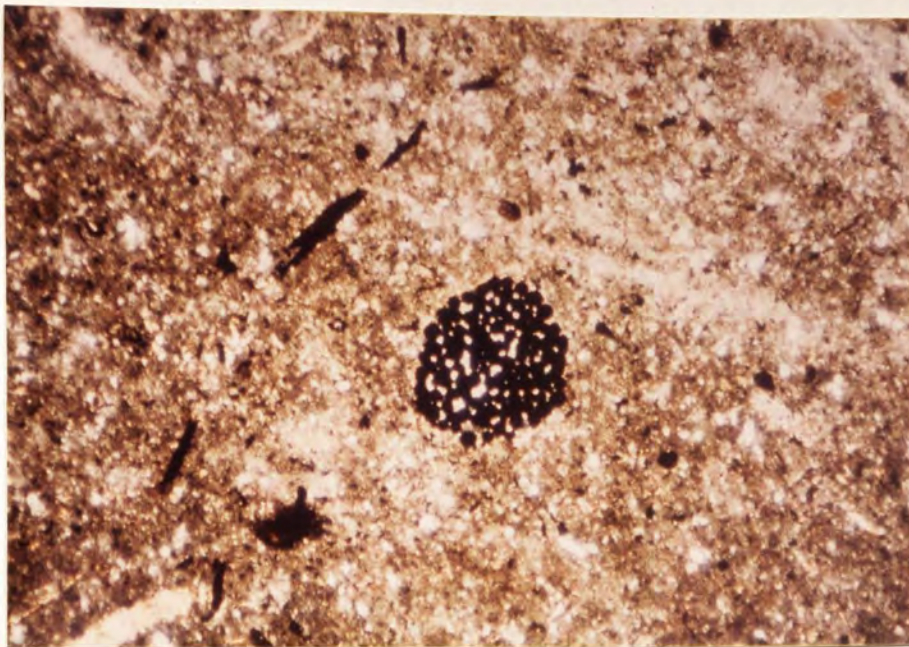
FIG 7:6



0.01 mm  
|

A STRING OF PYRITE SPHERES.

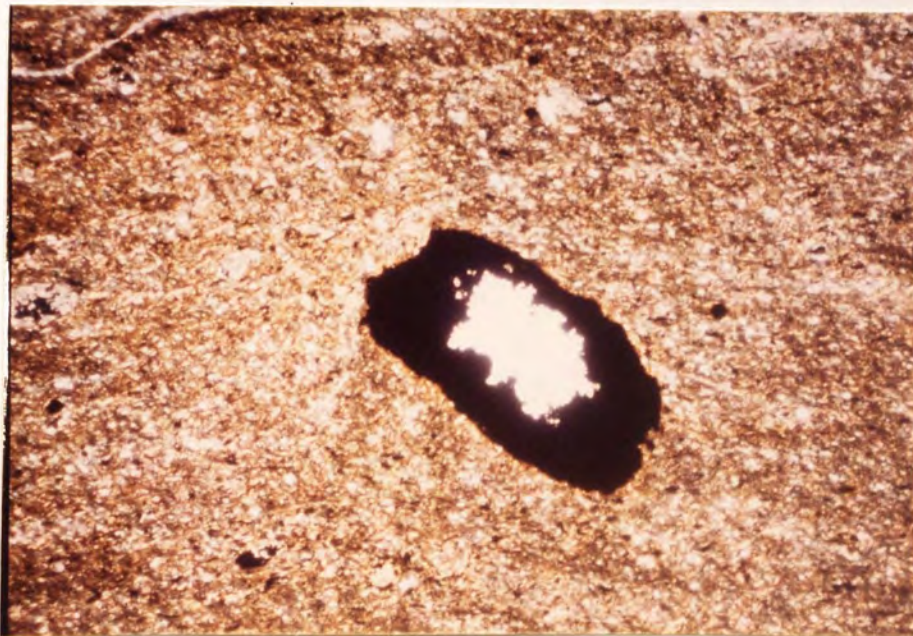
FIG 7:7



X41.25

PYRITE SPHERES IN A SPHEROIDAL MASS  
BOREHOLE SAMPLE, DEPTH 11.7m (HORIZONTAL SECTION)

PLATE 7:3A

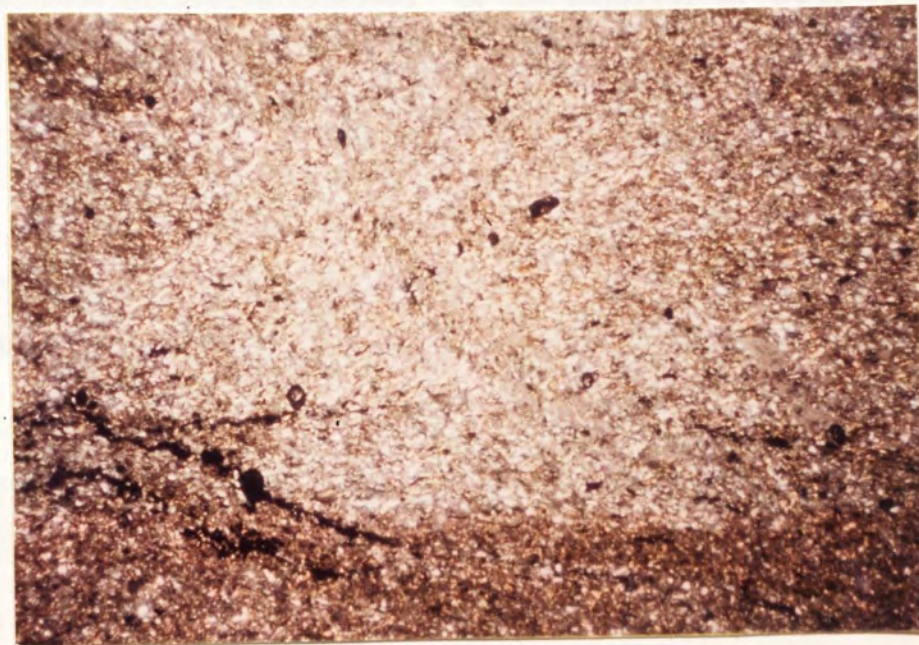


X33

PYRITE MASS WITH CALCITE INFILLING  
BOREHOLE SAMPLE, DEPTH 13.3m (VERTICAL SECTION)

PLATE 7:3B





PYRITE STRINGS AND FLAME STRUCTURE  
SAMPLE S32/1 (VERTICAL SECTION)  
PLATE 7:4

The strings are often in parallel rows consisting of 5 to 10 spheres in each string, each string being separated by a distance of 0.02 to 0.04mm. This arrangement may be associated with some organic material. However, no conclusions could be reached from the slides examined.

(iii) Irregular Masses

A mass of pyrite that shows no structure but could be a coalesced mass of pyrite spheres. In the majority of these cases the pyrite is surrounded by sparry calcite.

7:3:3:2 IRREGULAR VEINS

Seen in hand specimens of unweathered Lias clay as an Irregular vein varying in length from 20 to 60mm (1mm and less in thickness). They are found with no apparent relationship to bedding or discontinuities which suggests they formed some time after deposition.

The percentage of pyrite by the point counting method is rather high. This may be due to the fact that the pyrite spheres are in fact hollow, thus giving an error in counting.

Magnetite is also thought to be present from the evidence shown in (Plate 6:14). This crystal is assumed to be a magnetite crystal which formed soon after deposition of the sediment just below the sediment/fluid interface when there was sufficient room for the crystal to form without any restrictions.

7:3:4 ORGANIC MATERIAL

Dark brown, reddish brown material constituting roughly 1%

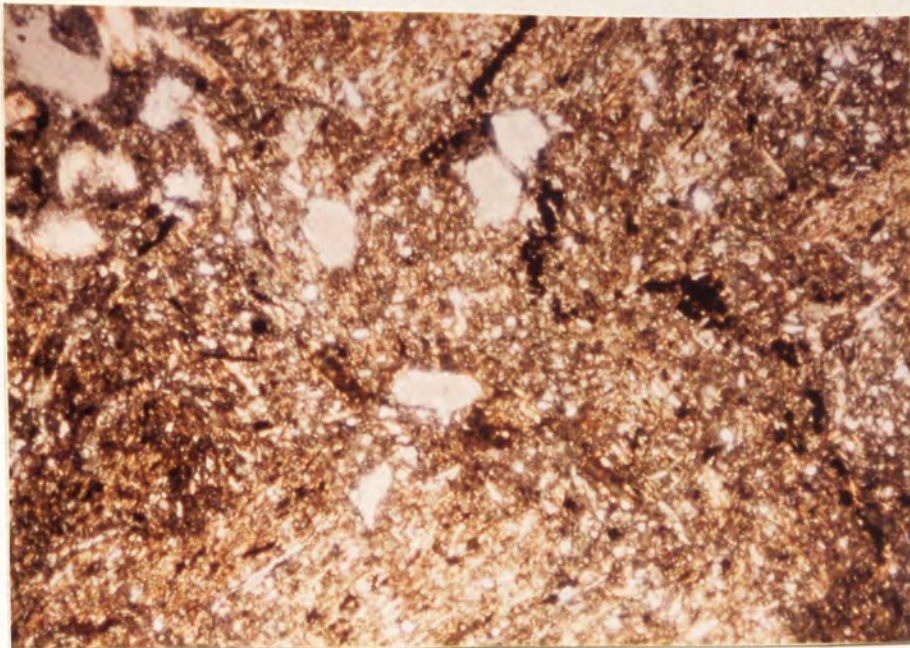
of the Lias clay. A separation process was carried out but on examination nothing definitely could be identified since the material consisted of an assortment of spore fragments and organic debris.

#### 7:3:5 FELDSPARS

In Samples S39/1 and S29/1 what appear to be feldspars have been found in the thin sections from these samples. (Plates 7:5 , 7:6). Hand specimens show the clay to be highly contorted, more so in sample S39/1 than S29/1 (Chapter 6).

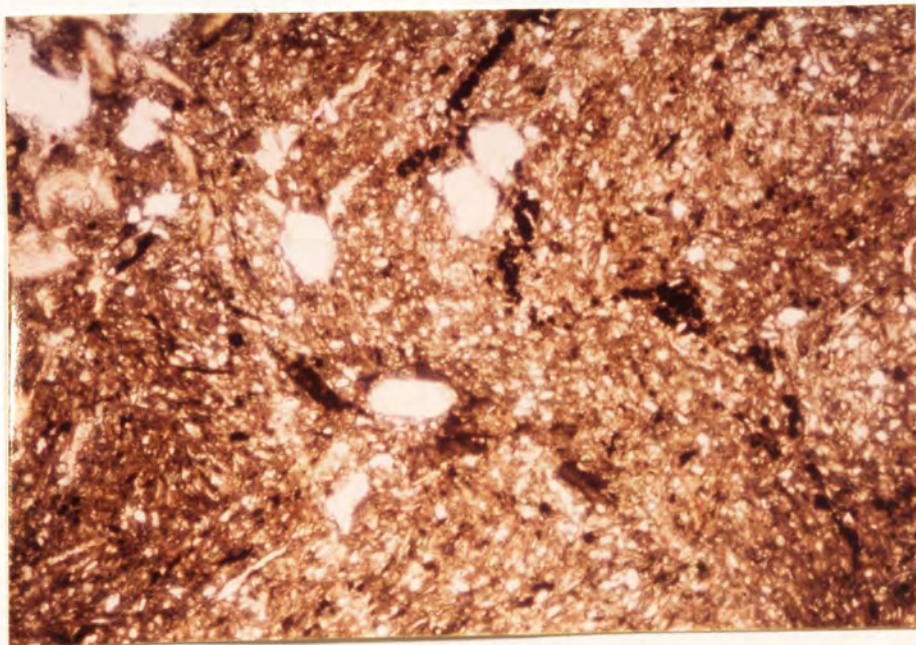
They are euhedral, the form similar in several cases to that of a 001 cross section of plagioclase. They occur in narrow defined bands across the thin section, the bands being parallel to the bedding. The identification of the type of feldspar is impossible since they are now pseudomorphed by a fibrous mineral. The fibrous mineral has low order colours, birefringence 0.008 to 0.015, straight extinction and length slow, suggesting kaolinitic material.

Their origin is a problem, it seems unlikely that the feldspar formed in situ and therefore they must be transported from the adjacent landmass. Transportation and deposition must have been relatively fast allowing little time for weathering (flood material). These samples also show a higher quartz content compared to material above and below. This sudden local influx of large quantities of coarser material would then be sufficient to act as the trigger mechanism for spontaneous density deformation (Chapter 6). Did the feldspars originate from an igneous body, or from deposits of the previous age (Triassic) is a matter for speculation. However, it can safely be assumed that they were pseudomorphed in situ.



X52.8

FELDSPAR PSEUDOMORPHS (xnic), SAMPLE S39/1  
(VERTICAL SECTION)  
PLATE 7:5



X52.8

FELDSPAR PSEUDOMORPHS (pp), SAMPLE S39/1  
(VERTICAL SECTION)  
PLATE 7:6

It should be pointed out that of all the investigations of the Lias only one, that of Brown and Du Feu (1956) reported feldspars present in the Lias. These workers were examining the Lias of the davoei Zone (Rotum Hills Brick Pit, 50km south-west of Blockley).

At the Blockley Clay Pit the division between the davoei and the ibex Zone has not been identified. Without further evidence a suggestion that these feldspars could mark a boundary would be unjustified.

GEOCHEMICAL ANALYSIS8:1 INTRODUCTION

The visual examination of most materials which have been subjected to weathering reveals that a colour change has taken place. Strength tests also show that in general the material has suffered an overall reduction in strength. Since weathering is the result of a number of mechanical and chemical processes then in particulate systems it is to be expected that the system will undergo both mechanical and chemical changes.

It has already been shown (Chapter 6) that the structure of the Lias clay undergoes marked changes during weathering, and it was thus decided to investigate the nature of the geochemical changes which had also occurred. No attempt was made to establish in full, the geochemical variation throughout the weathered profile but an examination was carried out of those aspects which were anticipated as being of value in the correlation of the structure, chemistry and physical (engineering) properties of the Lias clay.

The mineralogy of the clays provides an insight into the basic chemistry of the system from which it can be suggested that the following parameters contribute to the bonding of the clay particles and hence the engineering properties of the material:-

- (a) Physical attraction of the clay particles  
(ionic forces) dependant in part on overburden  
pressure.
- (b) Growth of new clay minerals (see p.142) during  
diagenesis that tend to bind the clay particles.
- (c) Interstitial cementing agents bonding the

particles of, which two cements are

dominant.

(i) Carbonates

(ii) Iron oxides.

The overall ionic attraction will be reduced as the ground surface is approached due mainly to the influx of water as overburden becomes less. This influx of water will alter the chemical environment within the pores and hence chemical interaction between pore water and soil constituents can take place. This will result in the degradation of the clays ( Chapter 7) and exchange of clay cations, However, changes in clay cation concentration throughout the profile were not investigated.

The growth of new clay minerals was seen in the unweathered clay and as they appear absent in the weathered profile it is assumed that such growths are rapidly destroyed by weathering. It would in any event be extremely difficult to assess the importance of the new clay minerals on a chemical basis.

Any interstitial cementing agents are expected to play an important role in the strength of the clay and their breakdown under weathering deserves attention. The proportion of carbonate present can be estimated by chemical techniques and the colour changes seen in the weathered profile are obviously associated with chemical changes involving the iron minerals. The distribution of carbonate and iron in the profile were therefore investigated and the oxidation state of the iron was also investigated using Mossbauer Spectroscopy and this aspect is considered in the following chapter.

## 8:2 CARBONATE ANALYSIS

Since the mineralogical investigation was restricted to a

specific number of thin sections, it was decided to carry out a more rigorous analysis to cover the majority of the samples. The method used was based on a rapid method by Bush (1970), modified to a more standard method of analysis (Appendix D). Although soda asbestos was used to trap the carbon dioxide, barium hydroxide  $\text{Ba}(\text{OH})_2$  0.1N can also be used and after titration with 0.2N HCl (Bush 1970) the percentage carbon dioxide by weight of the sample can be found. Both barium hydroxide and soda asbestos were used but as the former can absorb carbon dioxide from the air it was decided to utilize soda asbestos as a means of measuring the carbon dioxide.

Two types of carbonate occur in the Lias clay; calcite,  $\text{CaCO}_3$  and siderite,  $\text{FeCO}_3$ , the siderite occurring mainly in the nodules. It was therefore assumed that the carbon dioxide was evolved from calcite and calculations are based on this assumption.

#### 8:2:1 RESULTS AND DISCUSSION

A representative selection of samples taken from Section One were used for carbonate determination, the samples being taken as characteristic of the weathering zones encountered. At the same time as the initial carbonate determinations another set of samples were subjected to qualitative analysis by Infra-Red Spectroscopy (Appendix E). These results together with the selected samples showed that calcite was contained primarily in the unweathered material. The weathered clay gave no indication of calcite being present, thus all samples from S25/1 - S40/1 were analysed (Fig 11:1, Chapter 11).

Sample preparation (Appendix D) was designed to provide a



homogenous dried specimen. Whilst the majority of samples gave reproduceable results ( $\pm 2\%$ ), the mean  $\text{CaCO}_3$  content for the unweathered material was less than six percent. However the specimen of unweathered clay S40/1 showed considerable variation in calcium carbonate content between sub-samples which could not be attributed to experimental error. (Table 8:1).

TABLE 8:1

SECTION ONE (BLOCKLEY)

SAMPLE S40/1		SAMPLE S38/1	
RUN NUMBER	% $\text{CaCO}_3$	RUN NUMBER	% $\text{CaCO}_3$
* 1	0.68	1	3.32
2	7.4	2	3.3
3	9.5		
4	6.4		
5	10.5		
6	9.5		
7	12.7		

\* suspected leakage in apparatus.

It is thought in this case that the calcite derived from fossil shell fragments has remained as a distinctly coarser fraction within the sub 120  $\mu\text{m}$  particle size sample (Appendix D): Splitting the sample using the Glen Creston Rotary Splitter (Model P.T.) demands the uniform flow of a homogenous sample with respect to size distribution. In a sample such as this composed dominantly of clay aggregates (10 - 20  $\mu\text{m}$  in size) plus calcite fragments which may well be of the order of 100  $\mu\text{m}$ ; it is unlikely that such a splitter will perform satisfactorily thus a large variation between samples is possible.

Field sampling could also affect the amount of calcite

present since the fossil remains themselves were in pockets separated by areas relatively free of fossil remains. This was most noticeable when dissecting the block samples during the fissure analysis, thus reproducibility between specimens of the same horizon will inevitably be poor.

An average result for the calcite content in the unweathered material is in the range 3% - 10%; which agrees well with the results obtained by Le Riche (1959). Although he was working on the Stowell Park Bore hole, figures for the ibex Zone range from 3.9% near the upper boundary, to 53.7%, 16m below the previous specimen. The majority of the samples taken in this study were close to the upper boundary of the ibex Zone, this upper boundary at Blockley being undefined although it is thought to be close to the limit of weathering or within the weathered profile. It should be pointed out that carbonate percentages obtained for the davoie Zone (zone above the ibex) are quite low Le Riche (1959) quoting values of 1.7% and less.

Close to the weathering boundary the calcite averaged 3%. However, there was only one sample (S26/1) of weathered clay that gave any indication of calcite (<1%). The sample S26/1 came from Zone II (Fookes & Horswill 1969) where weathering is restricted to the surfaces of fissures and therefore some shell remains could still be present within the lithorelicts.

The calcite in the weathered clay will have been removed by the action of oxygen rich groundwater on pyrite. The groundwater will react with pyrite producing ferrous sulphate and sulphuric acid. The latter can react with calcite and,

under certain conditions produce gypsum which crystallizes out as selenite. Selenite was not observed in the profiles examined.

It is considered that calcite is present as shell fragments preserved as fossils and that no general redistribution of the carbonate has occurred during diagenesis. The possibility of calcite cementation contributing to the strength of the clay is thus unlikely and as the mineral is absent in the weathered zone such cementation cannot account for the gradual strength reduction with increased weathering.

### 8:3 IRON ANALYSIS

Iron analyses were carried out to determine not only the percentage of iron present in the samples, but also the oxidation state of the iron and the position of the iron within the minerals.

The iron content can readily be determined by a chemical analysis, the only problem in this respect is the treatment of the samples in order to obtain accurate results. An Atomic Absorption spectrometer was available and this was used for iron determinations in preference to titration or colorimetric methods. (Appendix F).

The oxidation state and position of the iron is rather more difficult since chemical pretreatment can alter both, prior to any quantitative determinations being carried out. Chemical determinations of the state and position of the iron have been successful but the pretreatments are complex and tedious. It was therefore decided to use Mossbauer Spectroscopy for the oxidation state and position of iron (Chapter 9).

#### 8:3:1 IRON CONTENT DETERMINATION AND SAMPLE PREPARATION

It has already been shown that iron (Fe) is present in the

clay in several phases (Chapter 7).

- (a) Iron pyrite
- (b) Iron oxides (attached to the clays or as discrete particles).
- (c) Within the clay mineral lattice.

The percentage in each phase being dependant on the state of weathering.

#### 8:3:2 REMOVAL OF FREE IRON OXIDES

In general iron can be regarded as being fixed in a crystal lattice (iron pyrite , clay minerals, magnetite etc.) or it can be in the form of an oxide coating the clay minerals. This coating can be either held strongly by the unsatisfied broken bonds on the planes parallel to the c-axis of the layer clay minerals or as weak attachment by electrostatic forces (Van der Waal's forces).

Appreciable amounts of free iron oxides during X-ray diffraction can (due to fluorescence) raise the level of background radiation, and their presence may even prevent complete identification of the clay minerals present by the submergence of weak peaks below the level of background radiation. The removal of this free iron oxide is only necessary for detailed examination of subtle variations of clay species. It is however useful to determine the quantity of free iron oxides.

A technique for the removal of the free iron oxide without any damage to the clay minerals was demonstrated by Mehra and Jackson (1958). The use of a citrate chelating agent helps in the removal of amorphous coatings and crystals of free iron oxides particularly haematite and goethite (Anderson & Jenne 1970). Mehra and Jackson (1958) clearly demonstrated that clay minerals are

unaffected by this technique. A comparison of several methods was made to measure their destructive effect on other iron silicates in the soils, and they showed by means of cation exchange capacity studies on the soil before and after treatment that the citrate method provided the cleanest clay surface with least structural damage.

A series of samples were treated with both the citrate system and an extraction solution of the following preparation: 50 ml of 1N HCl + 25 ml of 1N  $\text{H}_2\text{SO}_4$  made up to 1 litre with  $\text{H}_2\text{O}$ . The solutions were then analysed for iron content, the results showing that both systems extracted similar amounts of iron. Sodium citrate may cause interference with the absorption. Pawluk (1967) showed for his extractions that for the detection of iron only, sulphur and dithionate gave no apparent interference with atomic absorption analysis.

It was felt that since the normal extraction solution gave similar results and an analyses for copper and nickel were also to be carried out then this solution would be satisfactory.

A sample size of approximately 2 - 3 gm was taken for all analyses therefore the sample has to be representative and all material was ground down to at least fine silt size ( $< 20 \mu\text{m}$ ). Normally this is relatively easy by using a Tema mill, but Fitton and Gill (1970) have shown that during mechanical grinding ferrous iron is oxidised to ferric. The samples prepared at this time were also used to provide sub-samples for X-ray, Mossbauer, chemical etc., analysis and were therefore carefully ground by hand in a pestle and mortar ensuring minimum destruction of the clay

mineral. This was considered to provide a homogenous and representative sample for each of the various analyses to be undertaken.

#### 8:3:2:1 PROCEDURE

The sample was placed in a polypropylene bottle and 12ml of extraction solution added and shaken for 15 minutes. The reaction was stopped by centrifuging in a high speed centrifuge. The liquid was then poured into a grade A, 100ml volumetric flask and the sample was washed with double distilled water and centrifuged, the washings being placed in the volumetric flask and the volume being made up to 100ml with water.

This extraction was analysed for iron content using the Atomic Absorption technique.

#### 8:3:3 TOTAL IRON DETERMINATIONS

Since the majority of iron will be strongly attached to the clays and within the clay mineral lattice, total iron determinations necessitate the total dissolution of the samples.

Clays are some of the most resistant materials to chemical attack and therefore complete dissolution requires extreme measures. To obtain a solution the simplest solvent is the best as this will eliminate interferences, thus the order of preference is as follows:-

- (a) Fusion.
- (b) Concentrated acids or acid mixtures with prolonged digestion under pressure if necessary.

#### 8:3:3:1 FUSION

This requires that the clay sample is fused with sodium

carbonate in a platinum crucible at temperature of the order of 1,000°C - 1,200°C. Platinum is used because of its high melting point 1,770°C and its resistance to chemical attack. Platinum crucibles are very expensive and should be treated with care since the heating of platinum in unburned gas or sooty flames leads to the formation of a carbide of platinum rendering the metal brittle (Easton 1972). There is also the problem of violent reactions and loss by boiling over. Once fusion is complete the fusion cake has to be removed and then dissolved. Although this was tried with Lias clay the time required, and the problems involved were greater than the method employing concentrated acids, and this method was abandoned.

#### 8:3:3:2 CONCENTRATED ACIDS

The initial problem with clays and shales is the presence of organic material. This can be difficult to digest using the normal acids and carbon is often left after digestion. The undissolved carbon should be avoided if possible since metal ions can attach themselves to the carbon, and if it is just filtered off erroneous results can occur (especially in the case of trace elements). This carbon problem is most common in metamorphosed shales and clays where the organic material has already been changed to carbon.

Organic material can be removed by either ignition or hydrogen peroxide ( $H_2O_2$ ). Due to the small size of sample being used for total iron determination (0.5g) it was decided that the Hydrogen peroxide method would be more suitable.

An investigation was then carried out to determine the optimum digestion time using a concentrated acid. For this investigation a sample weight of 0.5 gm was weighed into a polypropylene bottle.

To this was added 5 ml of concentrated (Analar) hydrochloric acid, the bottle then being mechanically shaken. The sample used for the investigation was S40/1 which had a percentage of iron in the range 2.3 - 2.8 percent. The extraction was terminated by centrifuging and decanting the extraction and washings into a 100 ml volumetric flask (Grade A) and making up to volume. This was then sampled by an auto-diluter and iron content determined by Atomic Absorption, the whole extraction being carried out at room temperature (25°C). This procedure was repeated at a temperature of 100°C, the bottles being heated in a water bath instead of being shaken mechanically. The results are shown in (Fig 8:5).

It can be seen from the graph that at room temperature it would take almost 24 hours to reach complete extraction, whereas at the elevated temperature of 100°C the operation could be carried out in two hours thus speeding up the analyses.

It should be pointed out that the removal of iron (Fe) by HCl is not 100% complete since the clays themselves will not be entirely broken down. Only surface coatings of iron oxide disseminated iron pyrite together with iron from partially broken down illites and chlorites will be removed. However, this initial attack on the clays and on any carbonates or sulphates present will ensure an easier digestion using hydrofluoric acid (HF).

The remaining residue was then treated with HF to obtain complete dissolution and determination of total iron.

#### 8:3:3:3 PROCEDURE FOR TOTAL IRON DETERMINATION

- 1) Weigh out 0.5 gm of material into a 25 ml polypropylene bottle.
- 2) Add 5 ml of concentrated Analar hydrochloric acid and shake.



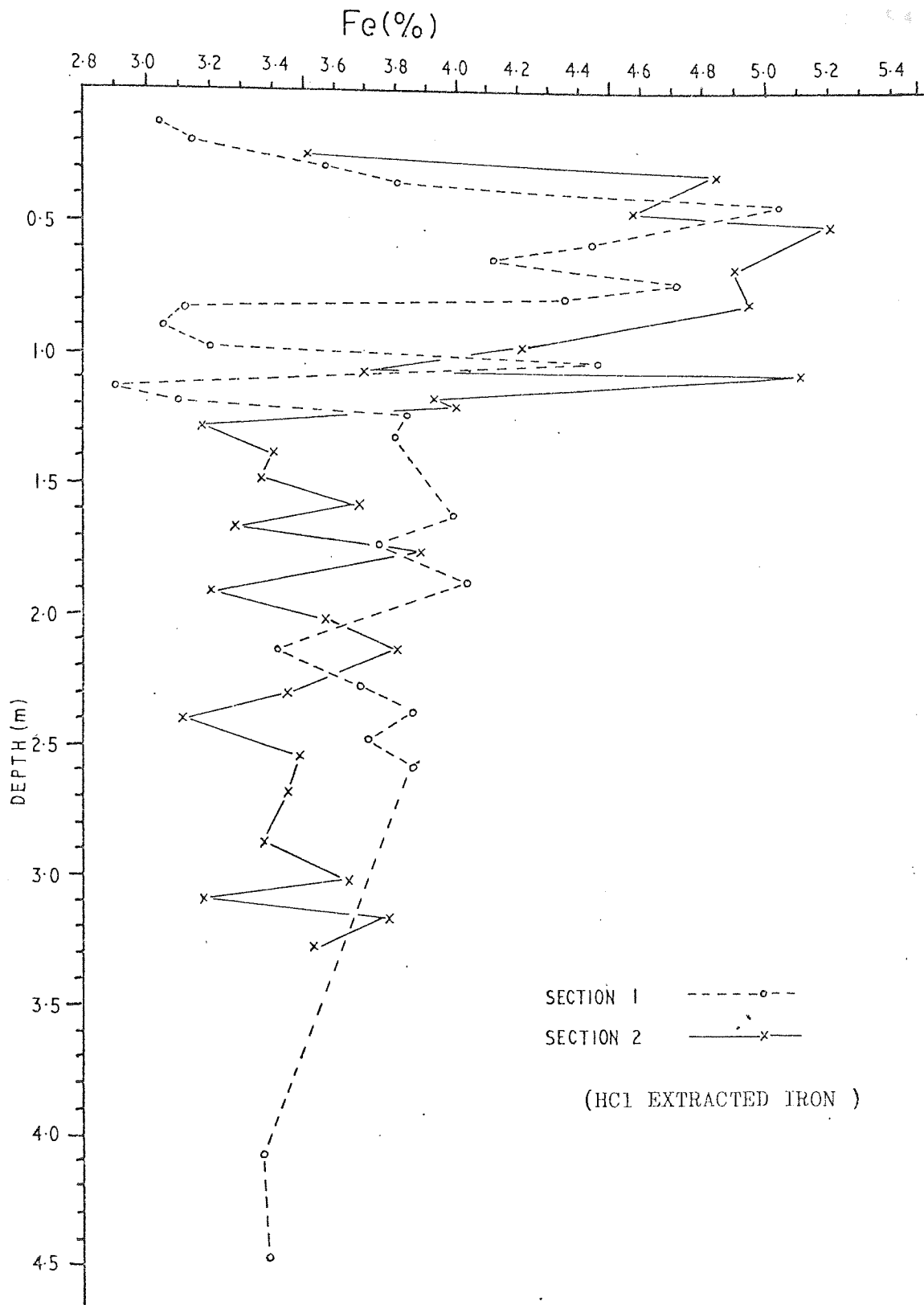


FIG 8:1

HCl EXTRACTED IRON WITH DEPTH  
(SECTION ONE AND TWO)

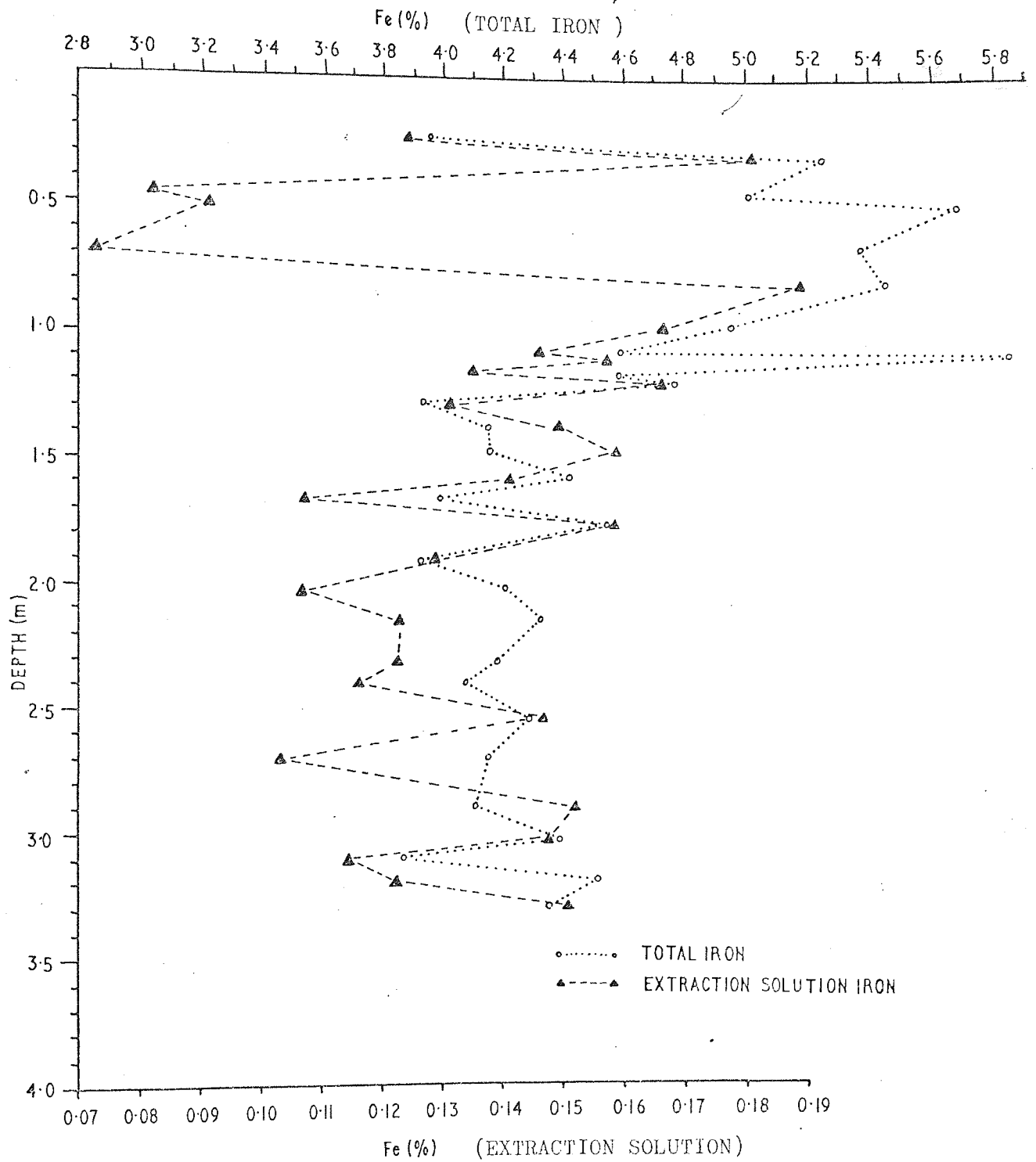


FIG 8:2

TOTAL IRON AND EXTRACTED IRON (EXTRACTION SOLUTION) WITH DEPTH, SECTION TWO

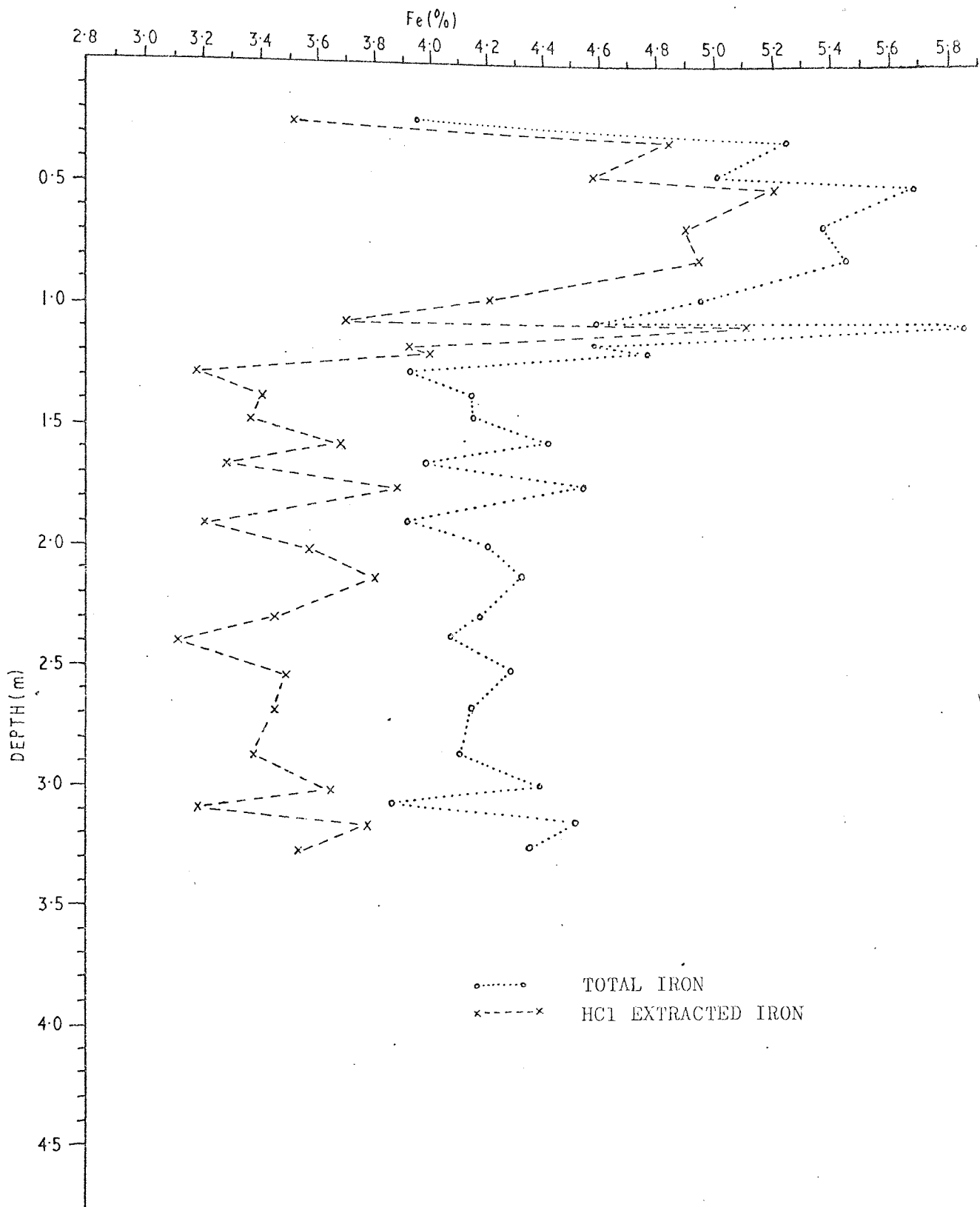


FIG 8:3

TOTAL IRON AND HCl EXTRACTED IRON WITH  
DEPTH, SECTION TWO

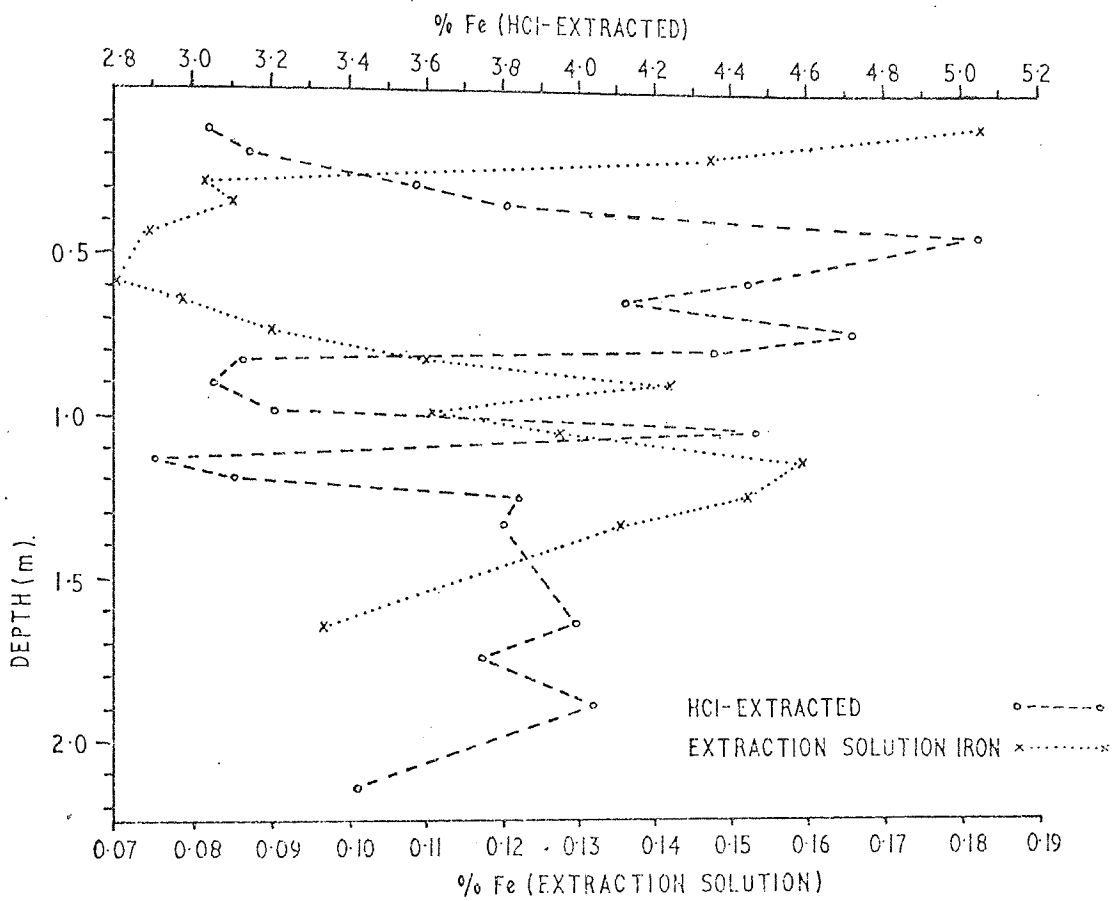
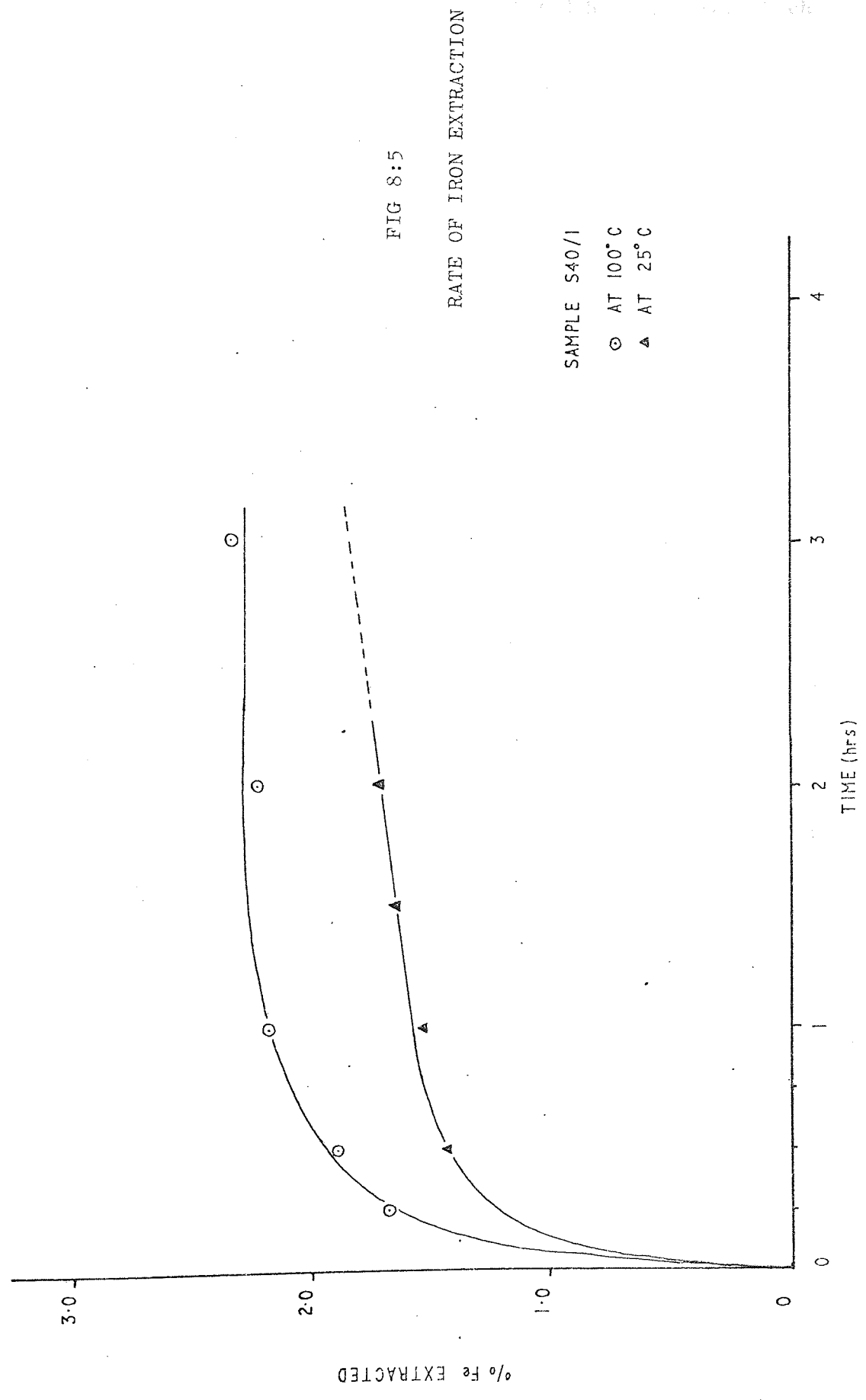


FIG 8:4

HCl EXTRACTED IRON AND EXTRACTED IRON  
(EXTRACTION SOLUTION) WITH DEPTH.



- 3) Heat the bottle in an oven of 100°C for 2 hours, after which remove and allow to cool for half an hour.
- 4) Wash the sample into a centrifuge and terminate the reaction by centrifuging. Decant off the liquid into a 100 ml (Grade A) volumetric flask. The sample should then be washed twice with approximately 20 ml of double distilled water, the washings being placed in the volumetric flask.
- 5) The volume is then made up to 100 ml and the solution sampled by an auto-diluter for atomic absorption analysis.
- 6) The residue is washed into a Teflon crucible and heated to almost dryness. To this is added 10 ml of concentrated hydrochloric acid and 10 ml of hydrofluoric acid and evaporated to almost dryness.

(Hydrofluoric acid is extremely dangerous and this evaporation should be carried out in an efficient fume cupboard)

This procedure should be repeated twice.

- 7) The residue is taken up into solution using either concentrated hydrochloric acid or aqua regia.
- 8) The solution is then centrifuged to ensure that it is particle free, and the solution is then decanted into a 250 ml volumetric flask. Ideally there should be no particles present. If a residue is found it should be thoroughly washed and the process continued or the analysis should be abandoned and started again.
- 9) The volume is made up to 250 ml and analysed for iron by Atomic Absorption.

10) Total iron is therefore the sum of procedures 5 and 9.

#### 8:3:4 RESULTS AND DISCUSSION

##### 8:3:4:1 TOTAL IRON \*

A plot of total iron against depth is given in Figs 8:1 8:2

---

\* see p.201

and 8:3 . It can clearly be seen that the percentage of iron increases sharply to 5.7% at a depth of 0.4 m with an equally sharp drop to 4.6% at a depth of 1 m. This depth interval corresponds to the Zone V (Weathering Scheme - Chapter 4) or Btg(fe) layer (0.46m - 0.92m).

A similar peak can be observed between depths of 1.0 - 1.2m in both sections, below which there is a general reduction to a value of approximately 4.2%. There is a general trend showing a small decrease until the unweathered material is reached which has an average iron content of 4.0%.

In both Sections examined a subsidiary peak indicating an increase in iron content was observed at a depth of 1.0m to 1.2m. This increase in iron content exceeds the previous maximum to 5.9% and was restricted to a very narrow zone 0.1m to 0.15m in depth. It has been noted in Chapter 3 that open fissures were seen to extend to a depth of 1.2m to 1.4m. It is therefore possible that this peak may define the base of a fissured zone caused by wetting and drying of the clay.

---

\*

When determining total iron content of the clay, the analysis is carried out in two parts.

- (a) HCl extraction (concentrated acid).
- (b) HF digestion.

The first process was found to be quite efficient since it was possible to extract 85%  $\pm$  8% of the total iron present.

#### 8:3:4:2 EXTRACTABLE IRON

A plot of percentage iron extracted by the extraction solution against depth is given in Fig 8:2, 8:4 . In both Sections there is a decrease in the percentage of iron in the region of Zone V, the very region which shows the highest iron concentration present in the soil profile. Why should this be so; is the iron in a different state or a different environment?

It is most probable that the iron deposited in this zone as a result of leaching forms a larger percentage of discrete iron oxide particles in comparison to the surface coating of iron oxide on the clays. It is also possible that at this level the majority of clays already have an extensive coating of oxides and therefore further input of iron will accumulate in small voids to form discrete iron oxide particles. Anderson and Jenne (1970) have shown that two such phases have distinct dissolution rates, and Coffin (1963) when he investigated free iron oxides in soils and clays demonstrated a similar result. The rapid dissolution rate reflects the more easily dissolved material i.e. the microcrystalline oxide coatings, the less soluble material being the macrocrystalline coatings and discrete particles. In Zone V, due to the conditions existing, there is a greater possibility of the macrocrystalline coating and discrete particles forming due to the excess iron.

How the iron is brought down is still problematical, and there are several opinions as to the reasons for deposition in Zone V. The iron is probably brought down by chelation with humus and organic acids thus rendering it mobile, yet once mobile why should it stop at a specific level? It is probable that deposition is due to physical reasons, i.e. the low permeability of the clay. Closer to the surface the weathered material will have a higher permeability



due to wetting and drying cycles causing the formation of a fissured material. It will only be during very dry periods that fissures will open to a depth of 1.4m. The lower permeability will therefore increase the time for the water to flow through the clay thus allowing the iron-humus bonds to break down by either bacterial attack or ageing. This in turn would result in a pH change as is observed at this level (Fig 11:1, Chapter 11) and the formation of the oxides. Once formed the oxides would be only rendered mobile if the groundwater became very acidic.

The subsidiary peak signifying the base of the fissures open to a depth of 1.4m, would only develop after several dry periods where water would then be able to reach this level. It was noticed that the water content increased at this level even after a dry period. In normal or wet conditions the water flow appeared to be more horizontal than vertical, indicating a greater horizontal than vertical permeability at this level (due to interconnecting fissures).

OXIDATION STATE AND POSITION OF IRON9:1 MOSSBAUER SPECTROSCOPY ANALYSIS

Mossbauer Spectroscopy is a technique which utilises gamma-ray nuclear fluorescence to obtain structural information on chemical compounds. It has primarily been used by physicists and chemists although its application in other fields is becoming more common.

Nuclear resonance fluorescence depends on the phenomenon known as the Mossbauer effect (Appendix H). Gamma-radiation from a radioactive source falls on a sample (the absorber) and the resultant absorption measured.

9:2 SOURCE

Since iron (Fe) is the element under investigation the source chosen is cobalt 57 ( $\text{Co}^{57}$ ). Radioactive  $\text{Co}^{57}$  has a half life of 270 days and decays by electron capture to an excited state of  $\text{Fe}^{57}$  with a spin of  $\pm 5/2$ . From this state there are three possible transitions (Fig 9:1), each with the emission of a gamma-ray.

It is the decay from the  $\pm 3/2$  state ( $\gamma_m$ ) that emits the gamma-ray having an energy of 14.39 eV above the ground state, that leads to a very sharp resonance absorption peak that can be used for Mossbauer Spectroscopy.

The radioactive nucleid  $\text{Co}^{57}$  is diffused into a suitable metal base such as steel, platinum, copper or palladium to increase the Mossbauer fraction of recoilless emissions.

The source used during the experiments was  $\text{Co}^{57}$  in palladium with an initial activity of 25 mC (obtained from the

Radiochemical Centre, Amersham).

### 9:3 APPARATUS

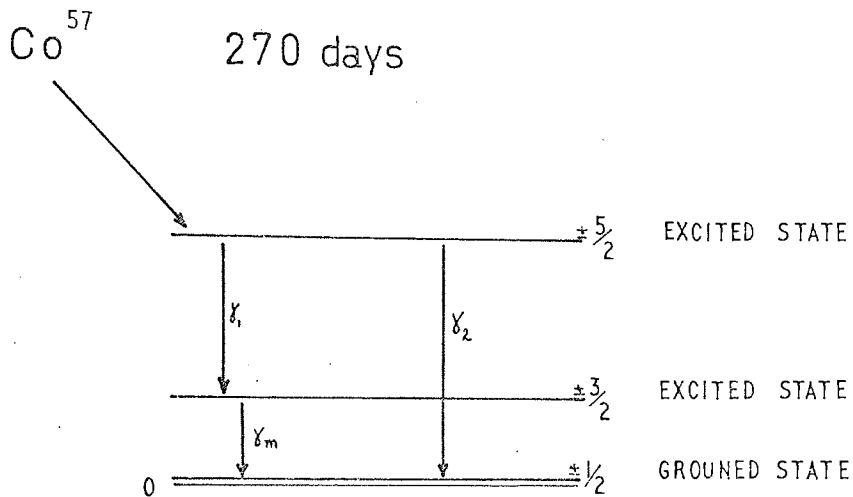
The arrangement of the apparatus is shown diagrammatically in Fig 9:2.

The source is mounted on a dual-voice coil loudspeaker, which is driven by the waveform generator. The waveform provides constant acceleration and therefore a varying velocity for the Doppler Shift. One voice coil carries the drive signal, the other coil being used as a motion sensor. The absorber is stationary, and the radiation passes through the absorber to the detector.

The source radiation energy lies between 10 - 100 keV. For iron detection only the lower end of this range is used and a xenon filled proportional counter is used as a detector, a high tension supply being necessary. This signal is then amplified by the head amplifier and then passed on to the single-channel analyser.

Since we are only interested in the 14.4 keV radiation then all other radiation (including the 7 keV X-ray) must be excluded by a single-channel analyser that delimits the pulse height window. Information from this is then stored in the multichannel analyser which is synchronized with the signal emitted from the waveform generator. Thus the velocity range is scanned and placed over 400 channels so that the absorption is shown as a plot of intensity of the gamma-rays transmitted by the sample at each instant as the relative velocity varies.

The spectrum can be displayed on the oscilloscope of the multichannel analyser and a photograph taken, or the information can be extracted in the form of counts by a typewriter. This



Fe<sup>57</sup>

$\gamma_1 = 122.0 \text{ keV}$        $\gamma_2 = 136.4 \text{ keV}$   
 $\gamma_m = 14.39 \text{ keV}$        $t_{1/2}(\gamma_m) = 1.0 \times 10^{-7} \text{ s.}$

FIG 9:1  
 DECAY SCHEME FOR Co<sup>57</sup>

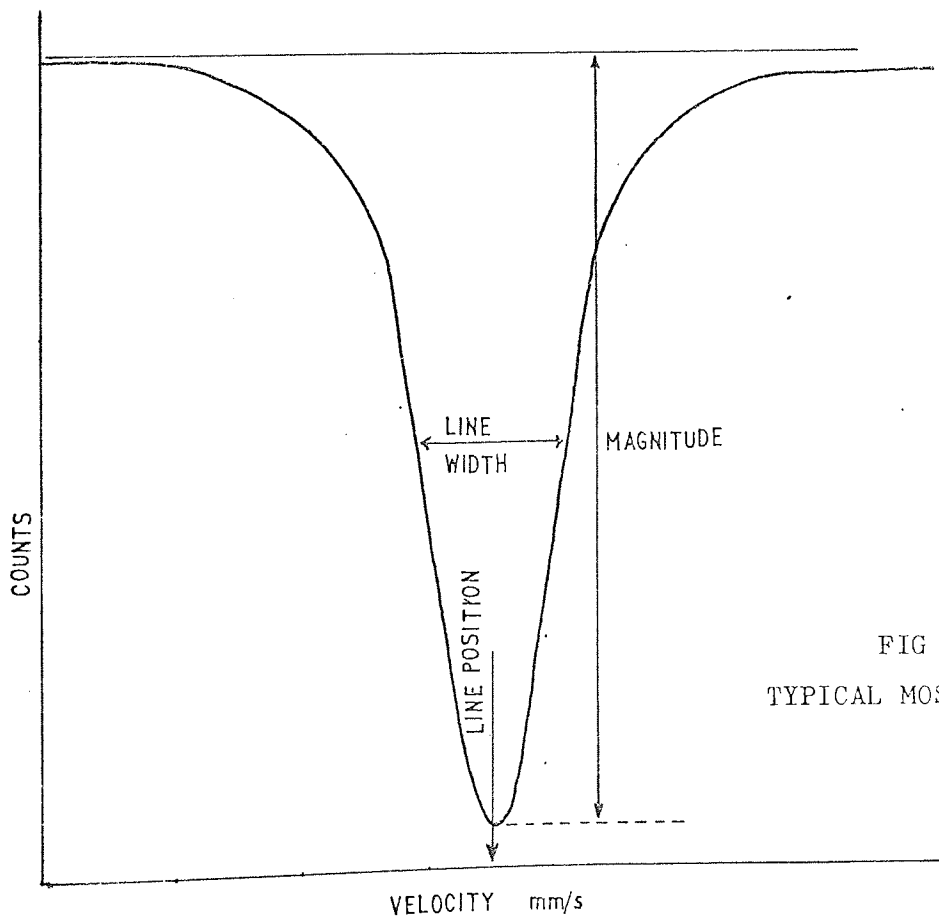


FIG 9:3  
 TYPICAL MOSSBAUER SPECTRUM

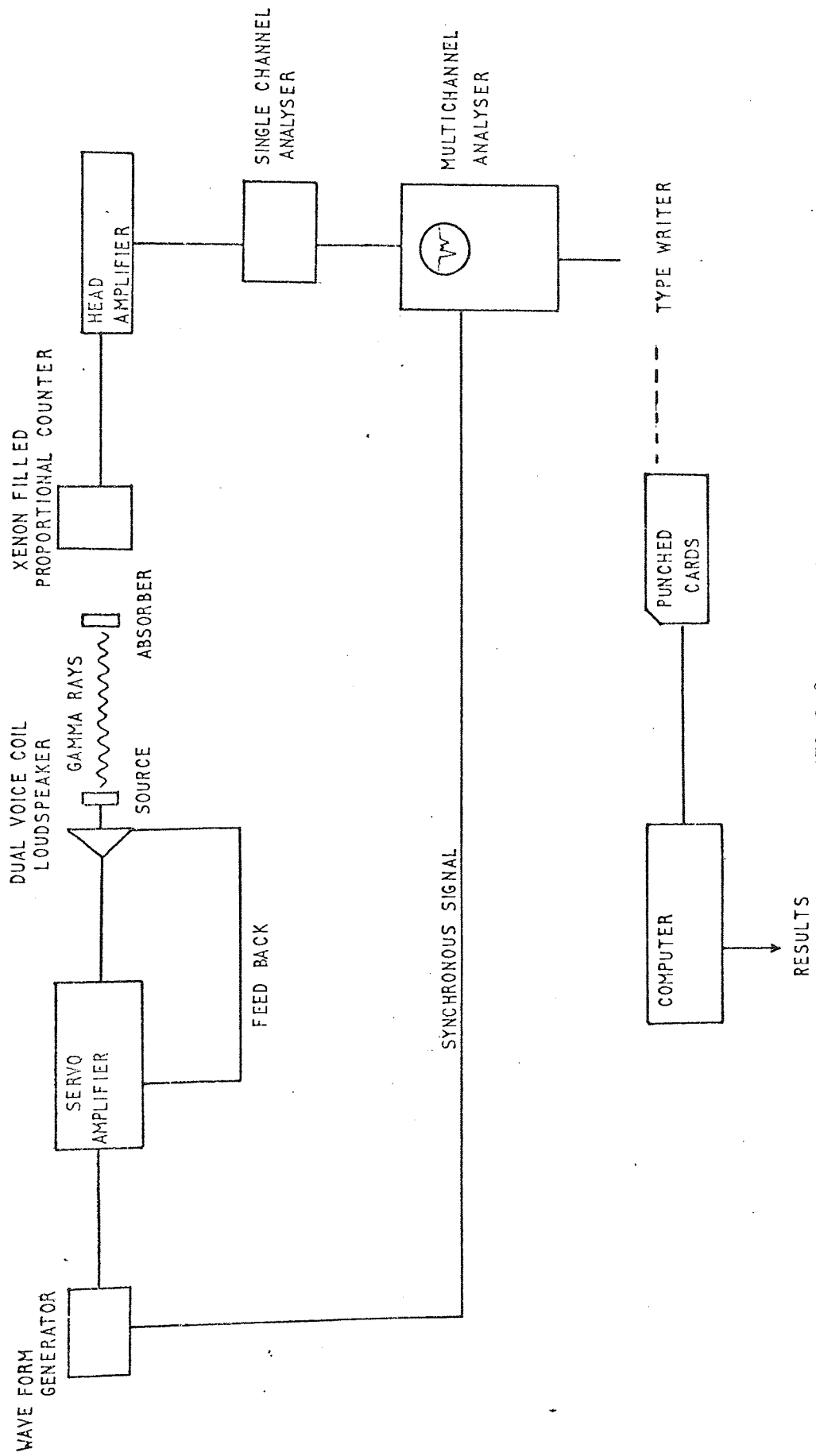


FIG 9:2  
 DIAGRAMMATIC LAYOUT OF THE MOSSBAUER SYSTEM

information was used for the computer program (Appendix I) that was developed during this research to analyse the spectrum. A paper tape punch device was not available, therefore the data had to be punched onto computer cards from the typewriter printout.

A typical Mossbauer spectrum consisting of a single peak is shown in Fig 9:3. Each peak is characterised by a magnitude, a line position and a line width (the line width shown is normally twice the natural line width). The shape of a single peak is assumed to be Lorentzian (Appendix I), the computer program thus iterates to find the values of magnitude, position and line width that best fits the data. The number of peaks however, must be assumed and constraints such as paired peaks may be imposed.

#### 9:4 APPLICATION OF SPECTRAL DATA

The spectrum produced may provide information on the isomer shift, quadrupole splitting and hyperfine magnetic interactions. These are discussed below. Other characteristics, mainly of interest to chemists and physicists will only be mentioned briefly.

##### 9:4:1 ISOMER SHIFT (I.S.)

The isomer shift or chemical shift arises from the fact that a nucleus has a finite radius, i.e. it is not a point source, and can therefore interact as a region of charged space within electrostatic environment. If the radii of the nuclear excited state and the ground state are different, the extent of interaction with the environment will be different. The isomer shift is actually related to the difference in the square of the excited state radius and the ground state radius (Wertheim 1964) (equation 1).

$$I.S. = (\langle r_{ex}^2 \rangle - \langle r_{gr}^2 \rangle) \dots\dots\dots 1$$

where  $r_{ex}$  = radius in the excited state

and  $r_{gr}$  = radius in the ground state

$\langle \rangle$  = mean value.

Equation 1 can be rewritten in the following form (equation 2).

$$I.S. = C \frac{dr}{r} \delta |\psi_s(0)|^2 \dots\dots\dots 2$$

C = constant

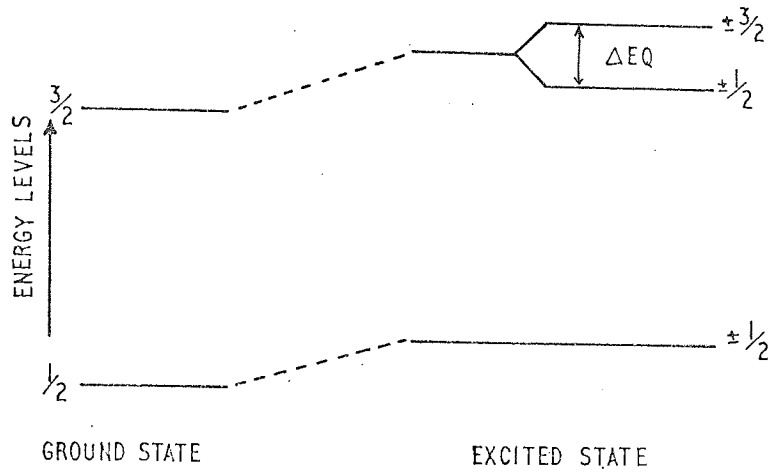
Equation 2 which defines the isomer shift has a nuclear term ( $dr/r$ ) that is always non zero hence the isomer shift will always have some finite value. The second term is an atomic term that indicates changes in the s electron density ( $\delta |\psi_s(0)|^2$ ). Changes in s electron density at the nucleus will result in differing values of isomer shift, and depending on whether the excited state radius is larger or smaller than the ground state, the isomer shift will have either a negative or positive value. The s electron density will be affected by the chemical environment, thus by the use of isomer shift the co-ordination and site can be elucidated for the element under investigation on an empirical basis.

#### 9:4:2 QUADRUPOLE SPLITTING (Q.S.)

All nuclei are characterised not only by their energy but also by a spin quantum number. For nuclei with an even number of nucleons (protons and neutrons) the spin quantum number is either zero or some integral number ( $\pm 1, \pm 2, \pm 3, \dots$ ). Nuclei with an odd number the spin quantum number is an integral multiple of  $\frac{1}{2}$  ( $\pm \frac{1}{2}, \pm \frac{3}{2}, \dots$ ).

$Fe^{57}$  has an odd number of nucleons and a nuclear ground state with a spin of  $\pm \frac{1}{2}$ . The first excited state has a spin

GROUND AND EXCITED STATES OF Fe<sup>57</sup>



Fe<sup>57</sup>

FIG 9:4

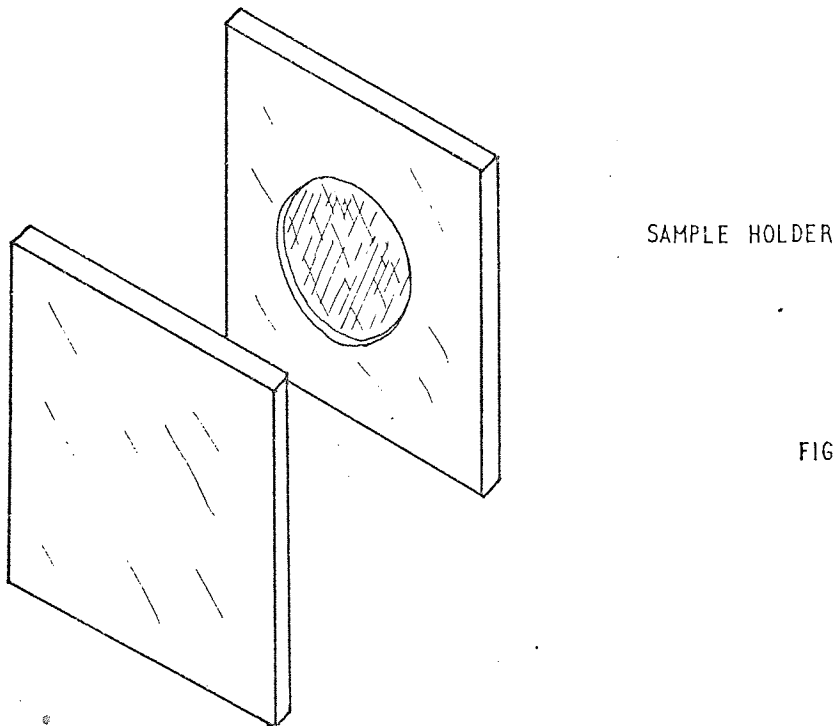


FIG 9:5



of  $\pm 3/2$ , can be split into two sub-levels, identified as  $\pm 1/2$  and  $\pm 3/2$  (Fig 9:4) when the nucleus is in a non-spherical charge field. (i.e. octahedral or tetrahedral sites). Distortion of the site from true octahedral or tetrahedral symmetry by adjacent nuclei will modify the value of the quadrupole splitting.

The difference in energy between these two sub-levels is known as the quadrupole splitting, and the Mossbauer spectrum will show two resonance lines rather than one. The quadrupole splitting energy ( $\Delta E$  or Q.S.) is dependant on oxidation state and co-ordination number (i.e. symmetry of environment). Burns (1968, 1969).

It is important to emphasise at this stage that isomer shift (I.S.) and quadrupole splitting (Q.S.) are sensitive to the following factors.

- a) Oxidation state.
- b) Covalence of the metal-ligand bond
- c) Co-ordination number.
- d) Site symmetry of the atom.

Thus for 6 co-ordinated (octahedral site)  $\text{Fe}^{2+}$ , the isomer shift and quadrupole splitting decrease with increasing distortion from octahedral symmetry. On the other hand for 6 co-ordinated  $\text{Fe}^{3+}$ , the splitting becomes larger and the shift smaller with increasing distortion of the nearby atoms from octahedral symmetry.

#### 9:4:3 HYPERFINE MAGNETIC INTERACTIONS

It has been shown previously (Quadrupole splitting) that in  $\text{Fe}^{57}$  the  $\pm 3/2$  level of the ground state is split into the  $\pm 3/2$  and  $\pm 1/2$  levels in the excited state. Each excited state has a set of sub levels which are normally degenerate. However, the degeneracy

of the sub-levels can be removed by an internal or external magnetic field. Thus on the removal of degeneracy it is possible to observe six absorption peaks.

In certain minerals a natural internal magnetic field can occur (ferromagnetic exchange interaction in metallic iron and antiferromagnetic interactions in  $\text{Fe}_2\text{O}_3$ ) and therefore a six line split can be observed. Normally a large applied external magnetic field is required to remove the degeneracy. Thus with an internal magnetic field certain minerals can be recognised by their six line pattern.

#### 9:4:4 RELATIVE INTENSITIES

The area under a Mossbauer absorption line is related to the number of absorbing nuclei per unit volume in the absorber. The shape of a single Mossbauer absorption curve is governed by the Lorentzian equation (Appendix I). The relationship between the intensity (or area A of an absorption line) and the number n of absorbing nuclei per unit area of the sample is given by the following equation.

$$A = \frac{1}{2} \pi n f \sigma_0 \Gamma \quad (\text{Hafemeister \& Shera 1966})$$

$\Gamma$  = line width

$\sigma_0$  = maximum (resonant) absorption cross section.

n = number of absorbing nuclei

A = Area of absorption line

f = fraction of absorbing nuclei that absorb without recoil.

As the iron content increases (or if the experiment proceeds too long), the relative intensity saturates, and the line shape is no longer Lorentzian. Hence, since the computer program assumes a

Lorentzian shape and statistical accuracy of the fitted curve is given by the chi-squared test, departure from the Lorentzian shape will result in a chi-squared value outside the statistically accepted range. A chi-squared value outside this range (Appendix I) could also be the result of an error in the assumption of the number of peaks, but this can be corrected by a new computer fit.

For a given absorber containing more than one distinguishable site for iron, the relative intensities of the Mossbauer peaks will give relative site populations provided the sample is thin. This has been used effectively by Bancroft, Maddock and Burns (1967a, b) and Bowen et al. (1969), Bancroft (1970).

Bowen et al. (1969) have also shown that knowing the total iron present in a sample, the determination of the amount of ferrous iron by the non destructive Mossbauer analysis is comparable with results from chemical methods. They suggest that Mossbauer Spectroscopy is more accurate and is improved by lengthening counting times, or by increasing the activity of the source. Lengthening counting times produce problems and is therefore not recommended for increasing precision.

#### 9:5 SAMPLE PREPARATION

There appears to be no uniform method of sample preparation. Sprenkel-Segal and Hanna (1964) mixed their samples with an equal amount of lucite powder and the mixture was thermally set under pressure into absorber discs 30mm in diameter and approximately 1mm thick. Other workers have mixed the samples with Vaseline and sandwiched the mixture between foil sheets. Equipment to produce thermally set discs was not available so in order to obtain a sample of uniform thickness and size, a perspex holder was designed to

fit the Mossbauer equipment. The recess was designed to hold one to two grams of sample and to have a thickness of approximately 1mm (Fig 9:5).

The size of 31mm for the diameter of the recess was determined by the cone of radiation emitted from the source and the position of the absorber. The recess diameter is 8mm less than the cone of radiation produced at the position of the absorber.

#### 9:6 CALIBRATION OF EQUIPMENT

A problem with Mossbauer Spectroscopy is the determination of the position of zero relative velocity and the situation is not helped by the confusion that exists in the literature as to a standard for the fixing of the zero relative velocity position. If the equipment uses a constant velocity drive the true zero velocity point can be determined by positioning the source at a reasonable intermediate point and determining the transmission rate at zero velocity. The majority of present day equipment uses the dual voice coil loudspeaker which is a constant acceleration drive unit. Thus, the use of a Mossbauer spectrum for the determination of the zero relative velocity position is necessary.

For iron using the gamma-rays emitted during the decay of  $\text{Co}^{57}$ , the radioactive nucleid is diffused into a suitable metal base such as steel, platinum, copper or palladium. A zero position can then be found using an absorber that is identical to the source base, i.e.  $\text{Co}^{57}$  in stainless steel with a stainless steel absorber, then the absorption peak obtained on the spectrum could be taken as zero relative velocity, (the position being obtained precisely by computer fitting).

There is at present no standard source or absorber, to which all measurements can be related. Attempts to obtain a standard

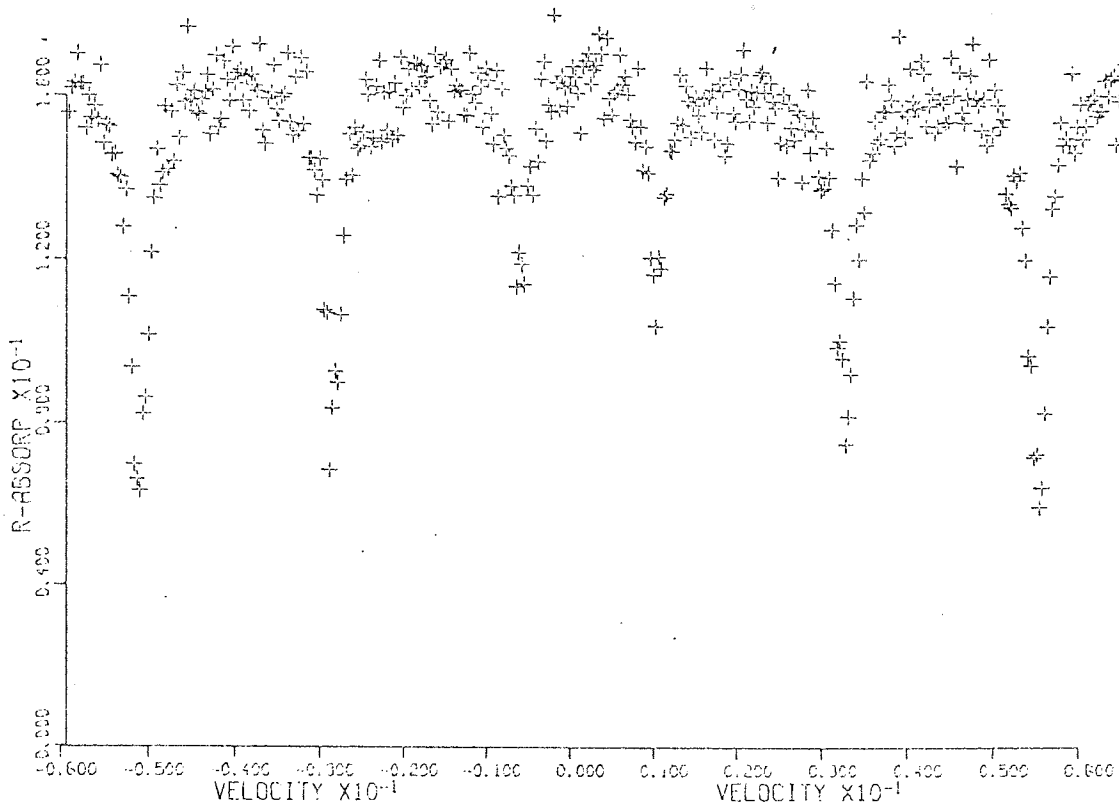
were made by Spijkerman et al. (1965) where they suggested sodium nitroprusside  $\text{Na}_2(\text{Fe}(\text{CN})_5\text{NO}) \cdot 2\text{H}_2\text{O}$ . The reason being that this substance produces a spectrum with large quadrupole splitting the energy of which is known and therefore the equipment can be calibrated. Natural iron has six absorption peaks (due to Hyperfine magnetic interaction), the split between which is known therefore it can be used for calibration and the centre of the spectrum can be taken as the zero relative velocity position. More recently workers have used stainless steel (which has a single peak) as the zero relative velocity position using either natural iron or sodium nitroprusside to calibrate the multichannel analyser.

The equipment used was a 20th Century Electronics voice coil and waveform generator, a xenon filled proportional counter coupled to a Laben multichannel analyser. It was set to produce approximately 0.03mm/sec per channel and was calibrated using natural iron, the zero relative velocity being the position of stainless steel peak.

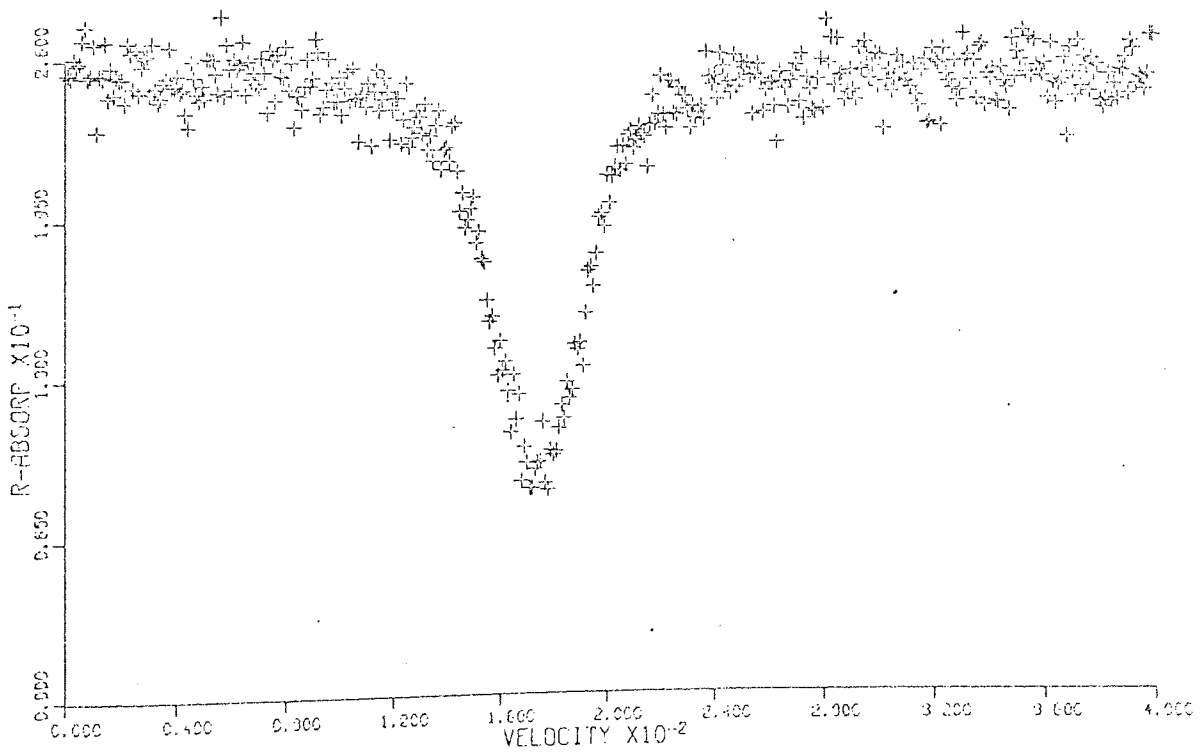
Other workers have used differing sources and standards. Therefore the results must be adjusted, the data for which are given in Table 9:1 .

TABLE 9:1

Source ( $\text{Co}^{57}$ ) in	Absorber	Standard	I.S.
Pt	Stainless Steel w.r.t	Sodium Nitroprusside	-0.607
Cu	" " "	" "	-0.483
Pd	" " "	" "	-0.442
Fe	" " "	" "	-0.348
Pd	" " "	Natural iron	-0.18
Pd	Natural Iron	Stainless Steel	0.18
Pd	" " "	Sodium Nitroprusside	-0.262



NAT-IRON



ST-STEEL

FIG 9:6

## 9:7 PREVIOUS WORK

Although Mossbauer Spectroscopy has been used extensively in chemistry its application in other fields has been neglected to a certain extent. The majority of research has been carried out on pure compounds or minerals, Bancroft et al. (1966, 1967a, b, c) have done extensive work on the iron silicates regarding site population, co-ordination number and the effects on Q.S. and I.S. At the present time no one has used Mossbauer spectroscopy on bulk sediments or soils.

Sprenkel-Segal and Hanna (1964) carried out Mossbauer measurements to identify the iron phases and the relative proportion in stoney meteorites. From this work has stemmed the study of the Apollo moon samples to provide similar information.

Clays and associated minerals have been investigated initially by Weaver et al. (1967) who demonstrated the advantages of Mossbauer spectroscopy over conventional analytical or X-ray methods for analysis of iron in clay minerals. This was enlarged by the work of Bowen et al. (1969) and Hogg and Meads (1970). Both sets of workers stated that Mossbauer Spectroscopy tended to show more ferrous iron ( $\text{Fe}^{2+}$ ) than chemical analysis and is just as accurate as the chemical methods. They also suggested that the method is much simpler and is able to give more information on the positioning of the iron ions.

Malathi et al. (1969) studied iron in illite and montmorillonite with a view to finding the oxidation state, co-ordination symmetry and site distortion of the iron ion. It is interesting to note that the illite used by Malathi et al. (1969) (Morris - Illinois:- Reference Clay mineral A.P.I. Research project

TABLE 9:2

REFERENCE	SAMPLE	IRON Fe <sup>2+</sup> *		IRON Fe <sup>3+</sup> *		STANDARD
		I.S.	Q.S.	I.S.	Q.S.	
WEAVER WAMPLER AND PECUIL (1968)	BIOTITE WEATHERED BIOTITE IRON KAOLIN ILLITE	1.15	2.4	0.35 0.37 0.35	0.6 0.44 0.6	NATURAL IRON
	BIOTITE WEATHERED BIOTITE IRON KAOLIN ILLITE	1.33 1.28	2.4 2.0	0.53 0.55 0.53	0.6 0.44 0.6	STAINLESS STEEL
BOWEN, WEED AND STEVENS (1969)	BIOTITE MUSCOVITE	1.37 1.39 ±0.06	2.46 2.93 ±0.12	0.73 ±0.02 0.62 ±0.05	0.66 ±0.02 0.68 ±0.02	SODIUM NITROPRUSSIDE
	BIOTITE MUSCOVITE	0.93 0.95	2.46 2.93	0.3 0.18	0.66 0.68	STAINLESS STEEL

\* At room temperature



TABLE 9:2 (cont.)

MALDEN AND MEADS (1967)	MUSCOVITE KAOLINITE GIBBSITE	1.20 $\pm$ 0.05	2.98 $\pm$ 0.05 2.25	0.48 $\pm$ 0.04 0.48 $\pm$ 0.04 0.47 $\pm$ 0.04	0.72 $\pm$ 0.05 0.50 $\pm$ 0.05 0.52 $\pm$ 0.05	STAINLESS STEEL
MALATHI <i>et al.</i> (1969)	NATURAL ILLITE			0.13 $\pm$ 0.03	0.54 $\pm$ 0.03	PALLADIUM SOURCE Co <sup>57</sup> in Pd
SOLOMON (1960)	PYRITE (FeS <sub>2</sub> )	0.33	0.30			NATURAL IRON
SPRENKEL-SEGEL AND HANNA (1964)	Fe <sub>2</sub> O <sub>3</sub>	SIX LINE SPLIT AT ROOM TEMPERATURE				NATURAL IRON
WERTHEIM (1961)	MAGNETITE Fe <sub>3</sub> O <sub>4</sub>	THREE SIX LINE PATTERNS SUPERIMPOSED EACH SIMILAR TO THAT OF Fe <sub>2</sub> O <sub>3</sub>				NATURAL IRON

49, Columbia University 1951) did not contain any ferrous iron, whereas illites used by all other workers have shown both ferrous and ferric iron present. They did however, show that the main exchange locations are the broken edges of clay minerals and that  $\text{Fe}^{3+}$  ions adsorbed on the broken edges form a complex having a cubic symmetry.

Malden and Meads (1967) working with kaolinite have also shown that substitution by iron ( $\text{Fe}^{3+}$ ) does occur and that a small amount of iron ( $\text{Fe}^{2+}$ ) is also present.

The isomer shift and the quadrupole split obtained by these workers are given in (Table 9:2).

#### 9:8 RESULTS

A representative selection of samples taken from Section One were used, each sample being taken as characteristic for the weathering zone encountered in the profile. It was felt that any major variations would be likely to occur in the weathering zones VI, V, (Chapter 4) and therefore all samples in this region except one (S4/1) were analysed.

The spectra obtained were then analysed by computer program (Appendix I) to obtain the best fit curve for the assumed peaks, the isomer shift and quadrupole splitting being calculated from the data obtained (Table 9:3)

Typical spectra of the standards stainless steel (single peak) and natural iron (six line split) are shown in (Fig 9:6). A selection of the spectra obtained are shown in Appendix J.

It is important to emphasise at this stage that work carried out by previous workers has tended to be on single minerals, often after purifying the specimens. Malathi et al. (1969) for example removed the impurities, pyrite, sericite, limonite etc., by treating

TABLE 9:3

SAMPLE	Fe <sup>2+</sup>		Fe <sup>3+</sup>		Fe <sup>3+</sup> /Fe <sup>2+</sup>
	I.S. (±0.015) *	Q.S. (±0.03) *	I.S. (±0.015) *	Q.S. (±0.03) *	
S1/1	1.357	2.65	0.55825	0.6061	7.2
S2/1	1.2919	2.7115	0.5423	0.5742	5.52
S3/1	1.37	2.74	0.5104	0.574	15.51
S5/1	1.32	2.839	0.59015	0.5423	2.86
S6/1	1.24	2.74	0.5104	0.5742	11.48
S10/1	1.355	2.71	0.5742	0.5742	8.14
S17/1	1.2919	2.7115	0.52635	0.6061	9.08
S18/1	1.5153	2.3925	0.5264	0.6699	6.85
S25/1	1.355	2.7115	0.5742	0.5742	2.24
S26/1	1.3398	2.6796	0.55825	0.5423	2.66
S36/1	1.292	2.6477	0.52635	0.6061	0.965
S40/1	1.3398	2.6796	0.52635	0.6061	1.173
S32/1	1.34	2.615	0.556	0.6061	
S32/1/ NAC	1.3398	2.6158	0.55825	0.6061	0.762
S32/1/ HCl	1.37170	2.8072	0.52635	0.6061	2.98

\* mm/sec

the illite with HCl (10%) and dilute  $\text{HNO}_3$  for three days. This removal of impurities rendered the absorption peaks sharper.

The samples in this present investigation have already been shown to contain a wide selection of minerals that contain iron, therefore the spectra obtained (depending on conditions) will be a combination of several spectra.

## 9:9 ANALYSIS OF RESULTS

### 9:9:1 SPECTRA AT ROOM TEMPERATURE

Of all the minerals present in the sample, the clays are in sufficient quantity with a suitable iron content to produce spectra. At room temperature, one would therefore expect a spectrum that indicates the positions of  $\text{Fe}^{2+}$  and  $\text{Fe}^{3+}$  in the clay lattice. Any pyrite or iron oxide ( $\text{Fe}_2\text{O}_3$ ) would be in insufficient quantity to produce a spectrum at room temperature (both minerals less than 10% of total sample). (See Spectra at  $77^\circ\text{K}$ , Appendix J).

Examination of the spectra (Table 9:3, Appendix J) indicate that two oxidation states of iron are present,  $\text{Fe}^{2+}$  and  $\text{Fe}^{3+}$ . The values of isomer shift and quadrupole splitting indicate that both ions are present in an octahedral environment probably due to substitution in the aluminium octahedral layer of the clay lattice (isomer shift and quadrupole splitting values corresponding to values obtained for iron in octahedral environments, Bancroft *et al.* 1968 ). This conclusion is further endorsed from the similarity in spectra that have been obtained by Weaver *et al.* (1967) and Bowen *et al.* (1969).

The actual values for the isomer shifts are slightly different from those quoted by other workers but it must be remembered that the investigation was carried out on a bulk sediment. Thus, the Lias clay containing both kaolinite and illite in varying proportions

shows an  $\text{Fe}^{3+}$  absorption peak but will in fact have two  $\text{Fe}^{3+}$  absorption peaks (one for kaolinite and one for illite). The isomer shift for  $\text{Fe}^{3+}$  will have slightly different values (Table 9:3) therefore the position of each peak will vary and the overlap would show up by overbroadening of the peaks themselves. \*

#### 9:9:1:1 VARIATION WITH DEPTH

##### $\text{Fe}^{3+}$

Examination of I.S. and Q.S. for  $\text{Fe}^{3+}$  (Table 9:3) show very little variation with changes of weathering, the values being very similar to those obtained by Weaver *et al.* (1967) for illite.

##### $\text{Fe}^{2+}$

The average values of I.S. and Q.S. for the unweathered material is 1.316 mm/sec and 2.66 mm/sec. Very little change is observed in I.S. as weathering increases except with sample S18/1 which has both a high I.S. (1.5153 mm/sec) and a low Q.S. (2.3925 mm/sec). There appears to be no explanation for this as there are no other indications of change at this level.

With regard to the Q.S. of  $\text{Fe}^{2+}$  there is an overall trend towards an increase in value with increasing weathering. The highest value being shown by sample S5/1 which reaches 2.839 mm/sec, this being almost as high as the value obtained by Malden and Meads (1967) for muscovite mica.

Even allowing for experimental error the results for quadrupole splitting of  $\text{Fe}^{2+}$  show an increase in value with increasing weathering.

---

\* This would have no effect on the curve fitting procedure since the  $\text{Fe}^{3+}$  absorption peaks for kaolinite and illite are sufficiently close for the peaks to be treated as one single peak.

Burns (1969) considered the crystal field splitting and stabilization energies for transition metal ions in silicate crystal structures, and their preference for different sites. He has shown that  $\text{Fe}^{2+}$  ions are more stable in tetragonally distorted octahedral sites. Burns (1968) has also shown that increasing distortion lowers the quadrupole splitting of the  $\text{Fe}^{2+}$  octahedral doublet.

Weathering results in progressing from a higher energy state to a low energy state, therefore unweathered clay (high energy state) should show more distortion of octahedral sites than weathered material. Hence there should be an increase of quadrupole splitting with weathering. This is observed from the results on Table 9:3.

It is well known that partial replacement of the aluminium ( $\text{Al}^{3+}$ ) octahedral ions by  $\text{Mg}^{2+}$ ,  $\text{Fe}^{2+}$  and  $\text{Fe}^{3+}$  ions takes place. However, it is not known to what degree these substitutions are possible.  $\text{Al}^{3+}$  has an ionic radius of 0.52 Å, comparison with the ions that can substitute for  $\text{Al}^{3+}$  show that they have greater ionic radii (Table 9:4).

TABLE 9:4

Element	Ionic Radius (Å)
$\text{Al}^{3+}$	0.52
$\text{Mg}^{2+}$	0.65
$\text{Fe}^{3+}$	0.64
$\text{Fe}^{2+}$	0.75

Although the principle of radius ratio is only strictly applicable to ionic compounds, and silicates are partially covalent, it can be used as an approximate guide to the degree of

substitution. The limiting radius ratio for an octahedral environment is 0.414 (i.e. where all the co-ordinating ions are touching). The radius ratio for oxides are given in Table 9:5.

TABLE 9:5

RADIUS RATIO OF AN OCTAHEDRAL SITE

Oxide	Radius Ratio
Al <sup>3+</sup>	0.42
Mg <sup>2+</sup>	0.59
Fe <sup>3+</sup>	0.58
Fe <sup>2+</sup>	0.68

It can be seen that Al<sup>3+</sup> has a radius ratio close to the limit and substitution by other ions would result in a distortion of the site.

Mg<sup>2+</sup> and Fe<sup>3+</sup> having similar ionic radii are more likely initially to substitute in the octahedral layer since they would cause less disturbance. However, having entered the structure distortion of adjacent sites becomes more important. Burns (1969) has shown that for a tetragonally distorted site, Fe<sup>2+</sup> possesses a greater crystal field stabilization energy than Fe<sup>3+</sup>, thus the Fe<sup>2+</sup> ion has a greater probability of being found in the distorted sites. Therefore the Fe<sup>2+</sup> ion will be found principally in the distorted sites but also in the normal sites.

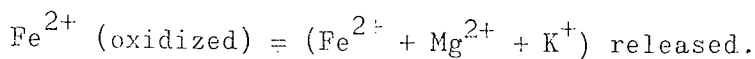
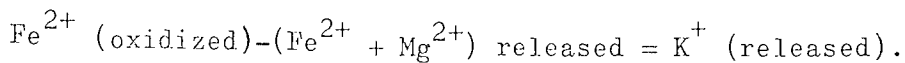
During weathering K<sup>+</sup>, Mg<sup>2+</sup>, Fe<sup>2+</sup> can be removed from the clays and since the crystal lattices of weathered minerals must maintain electric neutrality at all times, the following conditions must be met:

Changes in the internal charges = Changes in the external charges

OR

Changes in the octahedral charges = Changes in the surface charges.

i.e.



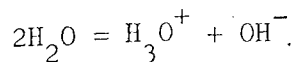
Once potassium is removed the electrical neutrality is preserved by the adsorption of other cations in particular  $\text{H}_3\text{O}^+$  and  $\text{Ca}^{2+}$  between the basic structural units. The hydroxonium ion ( $\text{H}_3\text{O}^+$ )\* and  $\text{Ca}^{2+}$  are much larger than the potassium ion and therefore expansion of the crystal lattice takes place altering the mineral illite towards a vermiculite type mineral. (This is noticed in the profile; see Chapter 7). This interchange of  $\text{K}^+$  with  $\text{H}_3\text{O}^+$  is a diffusion reaction.

The chemistry of hydroxonium ions show that they tend to react with layer lattice silicates to liberate octahedral cations. It is probable that  $\text{Fe}^{3+}$  and  $\text{Mg}^{2+}$  would be therefore susceptible to interchange reactions (i.e. diffusion of  $\text{H}^+$ ) and because of the stabilization energy imparted by  $\text{Fe}^{2+}$  to the site it occupies, there would be preferential removal of  $\text{Fe}^{3+}$  and  $\text{Mg}^{2+}$  during weathering.

---

\*

Since water itself is weakly ionized then the hydroxonium ion is present in water;



For convenience  $\text{H}_3\text{O}^+$  ion is written as  $\text{H}^+$  (hydrogen ion) and the concentration of the hydrogen ion is given in terms of pH.



On replacing  $\text{Fe}^{3+}$  or  $\text{Mg}^{2+}$  by  $\text{H}^+$  the adjacent sites would be distorted less and therefore the  $\text{Fe}^{2+}$  ion would now be less stable. This could then be replaced by  $\text{H}^+$ , the  $\text{Fe}^{2+}$  becoming oxidized, or as suggested by Ismail (1969), the  $\text{H}^+$  ions could act as acceptors for the electrons released from the ferrous iron during the oxidation process.

Once the  $\text{Mg}^{2+}$  and  $\text{Fe}^{3+}$  is removed there would be an increase in the quadrupole splitting particularly as more ions are removed. It should be emphasised that as the  $\text{Mg}^{2+}$  and  $\text{Fe}^{3+}$  is removed to form their respective oxides that the  $\text{Fe}^{2+}$  is also becoming oxidized and therefore although the quadrupole splitting increases the intensity of the  $\text{Fe}^{2+}$  doublet also decreases. This change of quadrupole splitting is observed from the results (Table 9:3).

A simple "weathering" test was carried out on an unweathered sample of Lias clay S32/1 by treating it with hydrochloric acid. A spectrum of both the unweathered and treated samples was obtained and analysed (Table 9:3). Again it showed this increase of quadrupole splitting from 2.615 mm/sec (unweathered) to 2.807 mm/sec (treated).

#### 9:9:1:2 INTENSITY OF PEAKS

The most noticeable difference due to weathering can be seen in the intensity changes of the peaks which in turn provide the  $\text{Fe}^{3+}/\text{Fe}^{2+}$  ratio. This ratio can be regarded as an indicator of the state of weathering of the clay (Chandler 1972), and to some extent is used in a visual manner in the engineering and pedological schemes of weathering.

Although samples throughout the complete profile were not examined, a broad picture is obtained that could be further investigated. The unweathered samples S36/1 and S40/1 show similar values for the  $\text{Fe}^{3+}/\text{Fe}^{2+}$  ratio (0.96, 1.17), the samples being

far enough apart to assume this to be a reasonable value for unweathered Lower Lias clay. As soon as weathering proceeds, i.e.

one II then a small amount of the ferrous ion is changed into ferric and is liable to be removed from the clay lattice, here the  $\text{Fe}^{3+}/\text{Fe}^{2+}$  ratio is approximately 2.45. There is then a gap in the data missing out part of Zone III (Sample S23/1 in this zone was analysed; see Spectra at 77°K). However, the change in value of the iron ratio is quite startling, jumping up to values ranging from 7.0 - 9.0 (Zone IV).

Above this level of weathering samples S6/1, S5/1, S3/1 are in the zone where we have iron enrichment and major variations in total and extractable iron. Again we have a similar variation, samples S3/1 and S6/1 show iron ratios of 15.5 and 11.48 respectively, but sample S5/1 has a ratio of only 2.86; a remarkable change over such a small distance where there are no other visual indications that anything is so radically different.

#### 9:9:2 SPECTRA AT 77°K

Certain minerals due to thermal factors, will not produce spectra at room temperature. However, by cooling the specimen the Mossbauer fraction is increased and a spectrum obtained. Since the equipment available did not have a cryostat, several selected samples were analysed by the Physicochemical Measurements Unit at Harwell. The spectra obtained are shown in Appendix J (computer evaluation of the spectra was not obtained). (All spectra are produced with respect to natural iron).

It can be seen by visual examination that many of these spectra are more complex than those at room temperature. Spectra

of samples S36/1 and S40/1 closely resemble the spectra produced at room temperature, each having  $\text{Fe}^{2+}$  and  $\text{Fe}^{3+}$  doublets in similar positions.

Pyrite is present in the unweathered clays (Chapter 7) in small quantities, either in concentrations or disseminated through the samples. Absorption by pyrite would result in a  $\text{Fe}^{2+}$  doublet in the region of the zero velocity position (Table 9:6) thus broadening the peak in this region and causing an inflexion point on the sides of the  $\text{Fe}^{2+}$  doublet from iron in an octahedral environment. No broadening is apparent and any distortion of the spectra by pyrite can be ignored. Iron oxide in the form of magnetite again can be ruled out since even appreciable amounts of disseminated magnetite would result in a substantial six-line component due to magnetic hyperfine interaction.

Thus the  $\text{Fe}^{2+}$  and  $\text{Fe}^{3+}$  doublets observed at room temperature and  $77^{\circ}\text{K}$  can be regarded as due almost entirely to  $\text{Fe}^{3+}$  and  $\text{Fe}^{2+}$  substitution the lattice of both kaolin and illite. From the evidence presented by Malden and Meads (1967) on their investigation into iron substitution in kaolin it is probable that the majority of  $\text{Fe}^{2+}$  lies in the octahedral sites of illite (mica), the  $\text{Fe}^{3+}$  being found in both illite and to a lesser extent kaolinite.

Sample S27/1 which was the least weathered Lias clay shows an increase in the number of peaks, compared to the spectra of S26/1 and S25/1 taken at room temperature. Neglecting the  $\text{Fe}^{2+}$ ,  $\text{Fe}^{3+}$  doublets due to iron in the clay lattice, it can be seen that there are six peaks (their approximate positions being given in Table 9:6). Since magnetite is not present in appreciable amounts it is safe to assume that the six peaks are due to the formation of

TABLE 9:6 \*

Reference	Sample	Energy (mm/sec)	I.S. mm/sec	Q.S. mm/sec
Sprenkel- Segel and Hanna (1964)	Fe <sub>2</sub> O <sub>3</sub> six line pattern	-8.27	+0.37 ±0.07	-0.09 ±0.04
		-4.63		
		-1.09		
		+1.50		
		+5.03		
		+8.31		
Sprenkel- Segel and Hanna (1964)	Pyrite	-0.26	+0.33	0.30
	FeS <sub>2</sub>	+0.34		
Present work	S17/1 six level split	-7.5	0.4	
		-4.0		
		-1.1		
		+1.5		
		+4.8		
		+7.4		
	S27/1	-7.5	0.5	
		-3.9		
		-0.8		
		+1.6		
		+4.7		
		+7.7		

\* Measurements with respect to natural iron.

$\alpha$ -Fe<sub>2</sub>O<sub>3</sub>, the internal magnetic interactions causing the six line split.

The possibility that the Fe<sup>3+</sup> doublet obtained at room temperature for all the weathered samples arises from small grains of  $\alpha$ -Fe<sub>2</sub>O<sub>3</sub> is rejected. At room temperature the spectrum of  $\alpha$ -Fe<sub>2</sub>O<sub>3</sub> particles large enough to give an observed quadrupole split should also contain the six-line component due to hyperfine magnetic interactions.

#### 9:9:2:1 INTENSITIES OF PEAKS

Again as with the spectrum observed at room temperature the intensities of the Fe<sup>2+</sup> and Fe<sup>3+</sup> peaks vary with weathering. The Fe<sup>2+</sup> peaks decreasing rapidly with increased weathering.

#### 9:10 CONCLUSIONS

The following conclusions can be drawn from the discussion of the spectra:

- i) In the unweathered clay of all the minerals present that contain iron, the resultant spectra obtained are due entirely to Fe<sup>3+</sup> & Fe<sup>2+</sup> substitution the octahedral sites of the clay lattice.
- ii) In the weathered clay the spectra at 77°K show Fe<sup>3+</sup> & Fe<sup>2+</sup> substitution in the clay and the formation of  $\alpha$ -Fe<sub>2</sub>O<sub>3</sub> resulting in the six-line split.
- iii) Spectra of the weathered clay at room temperature show only the Fe<sup>3+</sup>, Fe<sup>2+</sup> doublet as a result of substitution within the clay lattice.
- iv) Fe<sup>3+</sup> substitution in the octahedral layer of the clays will take place in both illite and kaolinite, but Fe<sup>2+</sup> substitution will be primarily be in the octahedral layer of illite.

v) The octahedral site for  $\text{Fe}^{2+}$  substitution is distorted by neighbouring ions, this distortion decreasing with increased weathering.

vi) There is a relationship between the  $\text{Fe}^{3+}/\text{Fe}^{2+}$  ratio and weathering (Chapter 10).

## CHAPTER 10

### ENGINEERING PROPERTIES

#### 10:1 INTRODUCTION

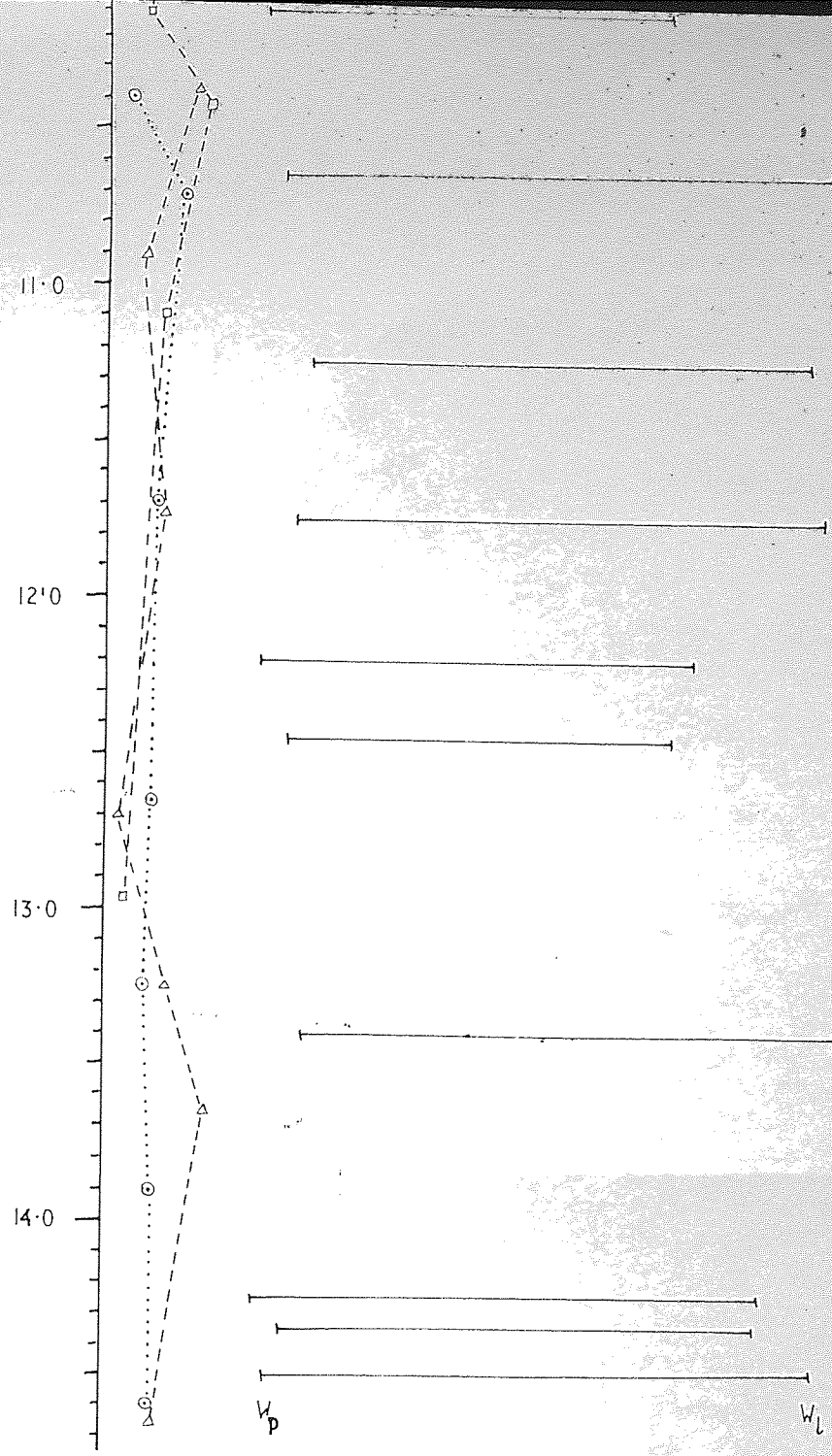
The engineering properties of soils depend essentially on the mineralogical composition, shape and size distribution of their particulate minerals, the fabric of the soil and the soil moisture. The way in which these factors interact is determined initially by the mode of origin of the soil but subsequent geological and pedological processes can modify a soil. Thus the geological history and subsequent weathering will alter the chemical, mineralogical and structural features of a soil causing its engineering properties to change.

The Lias clay samples obtained from the site at Blockley (Appendix A) were subjected to the normal engineering index tests. The unweathered cores and blocks (with the exception of those used for the fissure analysis; Chapter 5) were used for strength and compressibility tests (Thomas 1974). A series of in situ shear tests using a hand vane were also taken for the Sections examined in the Lias clay.

#### 10:2 ENGINEERING TESTS

##### 10:2:1 MOISTURE CONTENTS

In situ moisture contents were determined to a depth of 15m, however no determinations were made immediately above or below the calcareous beds (Pecten Bed and Mudstone band, Fig 3:4; Chapter 3). The variation of moisture content with depth for both Sections and the boreholes are shown in Fig 4:5, 4:6 and Fig 10:1. It can be seen that there is a gradual reduction of moisture content with depth (as is expected); though, this reduction is not very marked.

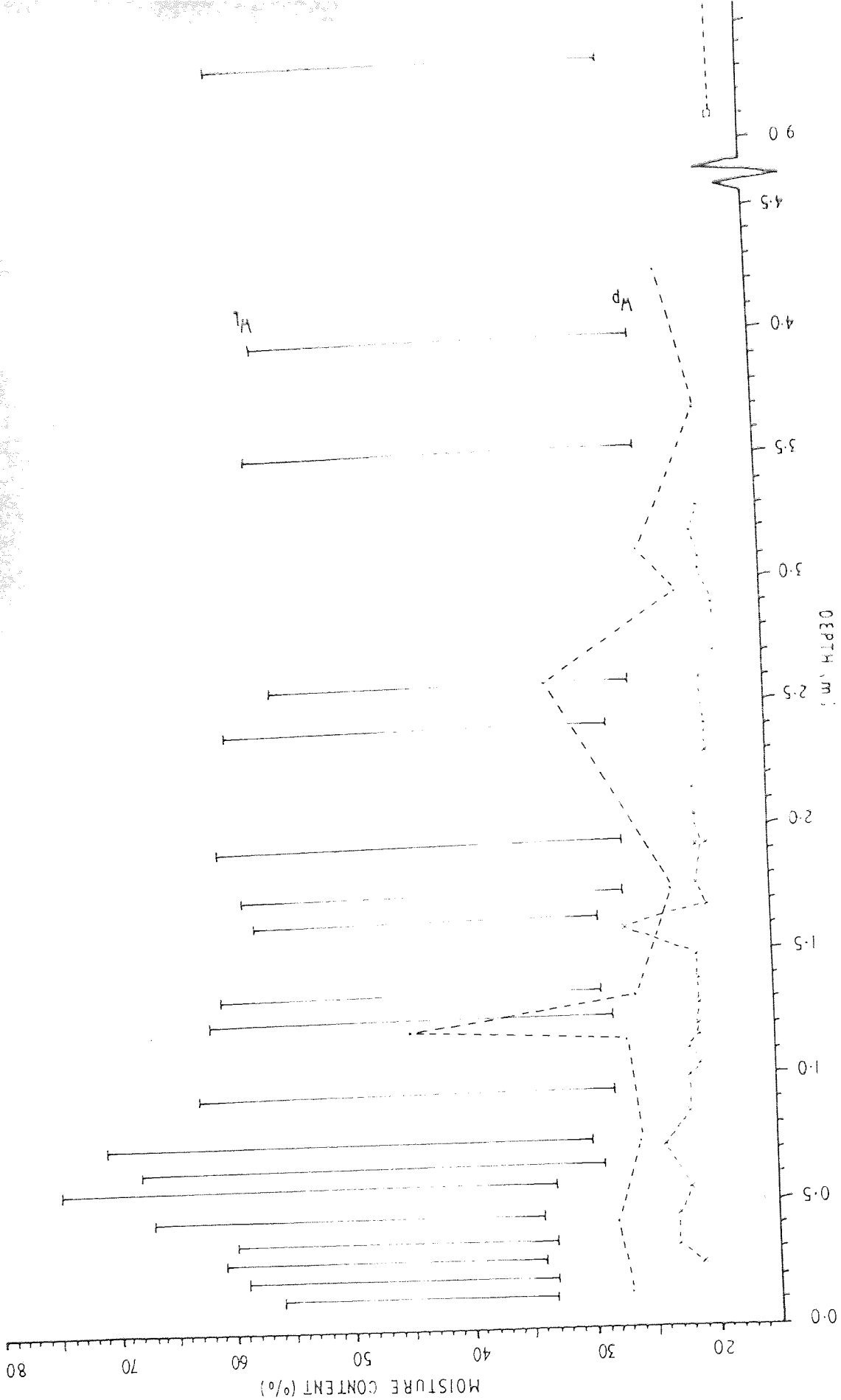


SECTION ONE      · - - - - ·  
 "    TWO        x - - - - x  
 BOREHOLE ONE    □ - - - - □  
 "    TWO        ⊙ ······ ⊙  
 "    THREE      △ - - - - △

W<sub>p</sub> = PLASTIC LIMIT  
 W<sub>l</sub> = LIQUID LIMIT



MOISTURE CONTENT / DEPTH RELATIONSHIP,  
BLOCKLEY



In the weathered material the in situ moisture content is close to the plastic limit of the soil (moisture content, 27% - 34%; plastic limit, 28% - 34%). With increasing depth (9m - 15m) the moisture content decreases to the range (16% - 22%), these values now being close to the shrinkage limit of unweathered Lias clay (shrinkage limit, average value 17%).

The in situ moisture contents of Section One were taken one day after a wet period and a very high moisture content was obtained at a depth of 1.2m below the ground surface. It was noticed subsequently that after heavy rain, water would issue from the fissures at this depth. This depth was classified as the upper section of the  $C_1(g)$  pedological weathering zone, where gleying is predominant and produces the mottling effect common to gleyed soils. Examination of the fissures showed a coating of pale grey argillaceous material (characteristic of gleyed zones) which was also apparent in thin sections (Chapter 6).

The pedological Zone  $C_1(g)$  was equated with engineering Zones IV and III of Fookes and Horswill (1969) in Chapter 4. It can therefore be suggested that Zone IV corresponds to the more intensely gleyed  $C_1(g)$  Zone, where fissures are more extensive and tend to be open. If Zone III corresponds to gleyed material where fissures are closed then the effective permeability will be reduced. Thus water will tend to collect in Zone IV resulting in the characteristic horizontal flow of water through the interconnecting fissures. The increase in moisture content therefore defines the base of a fissured zone, probably being caused by cyclic wetting and drying of the clay. It is important to note that even after a relatively dry period the base of Zone IV can still be identified from in situ moisture contents as determined for Section Two (N.B.

this Zone is at a slightly greater depth in this section due to variability of weathering).

#### 10:2:2 LIQUID AND PLASTIC LIMIT DETERMINATIONS

The mechanical properties of cohesive soils depend on their water content, particle size distribution (i.e. percentage of clay), the mineralogical composition of the clay fraction and the type of adsorbed cations. The last two factors also govern the amount of water adsorbed by the soil thus controlling the consistency limits (plastic and liquid limits) of the soil. Variations in mineralogy and chemistry should therefore be reflected in the plastic and liquid limits. Since the liquid limit is the boundary between a fluid (negligible shearing resistance) and a plastic state, the liquid limit will be more sensitive to any such changes than the plastic limit.

The B.S. 1377 (1967) procedure for liquid and plastic limit tests was carried out on a representative portion of air dried soil that had previously passed through a B.S. No. 36 sieve (440  $\mu\text{m}$ ), ensuring that only discrete particles remained on the sieve. It is significant that with the samples of Lias clay (weathered and unweathered) no more than 3% was ever retained on this sieve, the majority of material could be broken down to pass through the sieve. After sieving, the soil is mixed with distilled water on a glass plate by working with palette knives. This working should be continued for at least ten minutes in order to break down the aggregations of clays if any are present. Sherwood and Hollis (1966) investigated the effect of working on the liquid limit of Keuper Marl samples by means of a grease-worker (1000 pumps in the grease-worker being equivalent to approximately 60 minutes of working with palette knives). They showed that 10 minutes working with palette knives and 1000 pumps in the grease-worker gave no significant differences in the results for

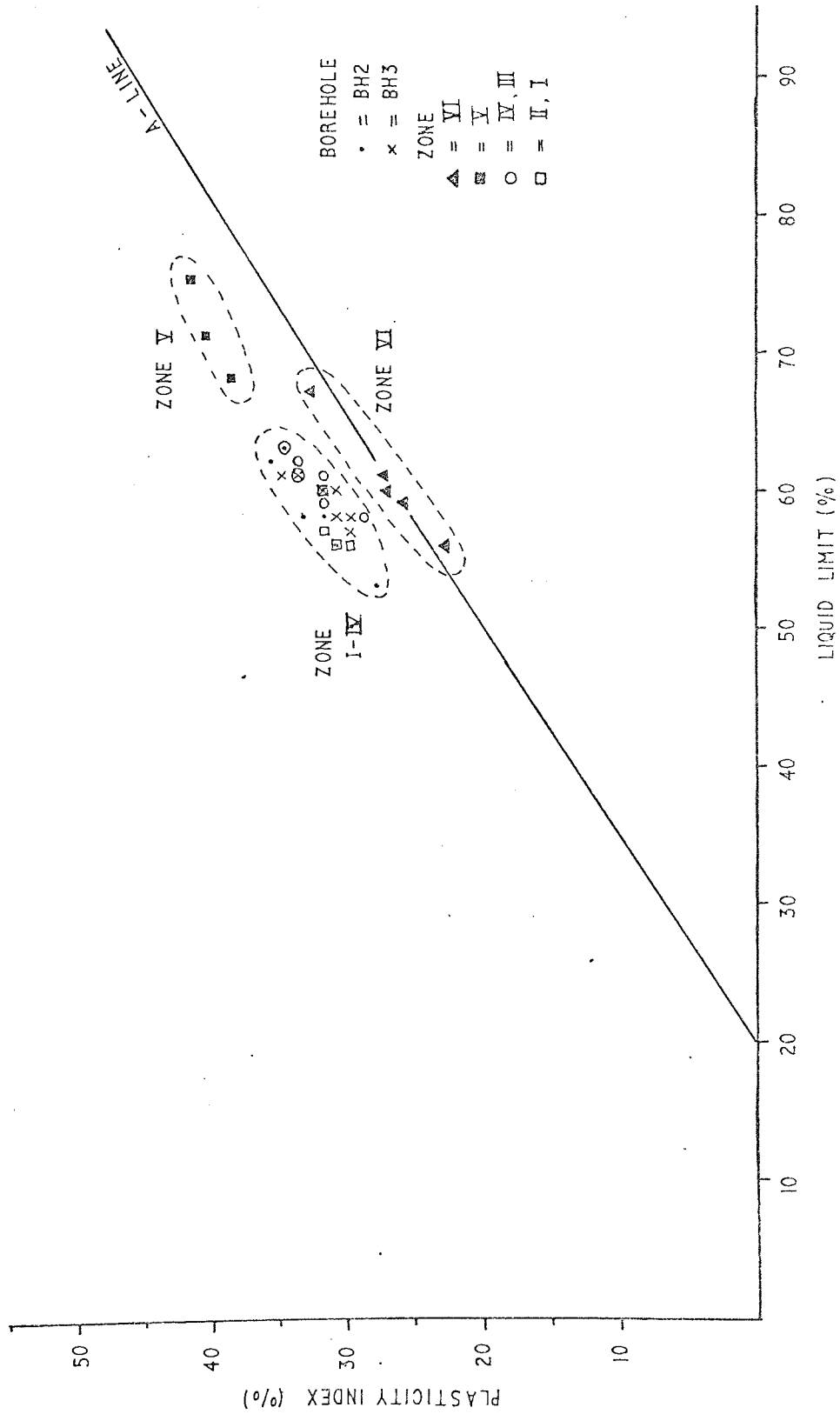
TABLE 10:1

<u>SAMPLE</u>	<u>DEPTH (m)</u>	<u>L.L.</u>	<u>P.L.</u>	<u>Ip</u>	<u>Activity (%)</u>
S1/1	0.15	56	33	23	59
S2/1	0.20	59	33	26	
S3/1	0.27	61	34	27	65
S4/1	0.35	60	33	27	
S5/1	0.44	67	34	33	
S6/1	0.57	75	33	42	95
S7/1	0.66	68	29	39	
S8/1	0.75	71	30	41	
S12/1	0.96	63	28	35	85
S16/1	1.25	62	28	34	97
S17/1	1.34	61	29	32	
S18/1	1.64	58	29	29	
S19/1	1.75	59	27	32	86
S21/1	1.95	61	27	34	
S25/1	2.40	60	28	32	120
S27/1	2.60	56	26	30	270
S32/1	3.56	57	25	32	
S35/1	4.00	56	25	31	

BOREHOLE  
SAMPLES

<u>DEPTH(m)</u>	<u>L.L.</u>	<u>P.L.</u>	<u>Ip.</u>	<u>ACTIVITY (%)</u>	<u>Gs</u>	
B2A	9.13	58	26	32	79	2.717
B2B	10.05	56	25	31	80	2.695
B2C	11.27	60	28	32	66	2.666
B2D	12.19	53	25	28	72	2.705
B2E	13.38	63	28	35	89	2.726
B2F	14.17	58	25	33	67	2.732
B2G	14.47	62	26	36	80	2.719
B3A	9.13	58	28	30	78	2.696
B3B	9.75	60	29	31	-	2.747
B3C	10.66	61	26	35	79	2.727
B3D	11.72	61	27	34	86	2.721
B3E	12.41	57	27	30	70	2.713
B3F	13.41	60	28	32	73	2.745
B3G	14.32	58	27	31	65	2.718

FIG 10:2 PLASTICITY INDEX/LIQUID LIMIT RELATIONSHIPS



the liquid limit of the Keuper Marl. There was however a significant difference if mixing was carried out for less than ten minutes such that the value of the liquid limit was found to decrease by as much as 10 percent of the ultimate liquid limit value.

The values of liquid and plastic limit are given in Table 10:1 and Fig 4:6, 10:1 .

On examining the liquid and plastic limit results for Section One, three divisions can be identified. These divisions are confirmed when plasticity index is plotted against liquid limit, (Fig 10:2, Table 10:2).

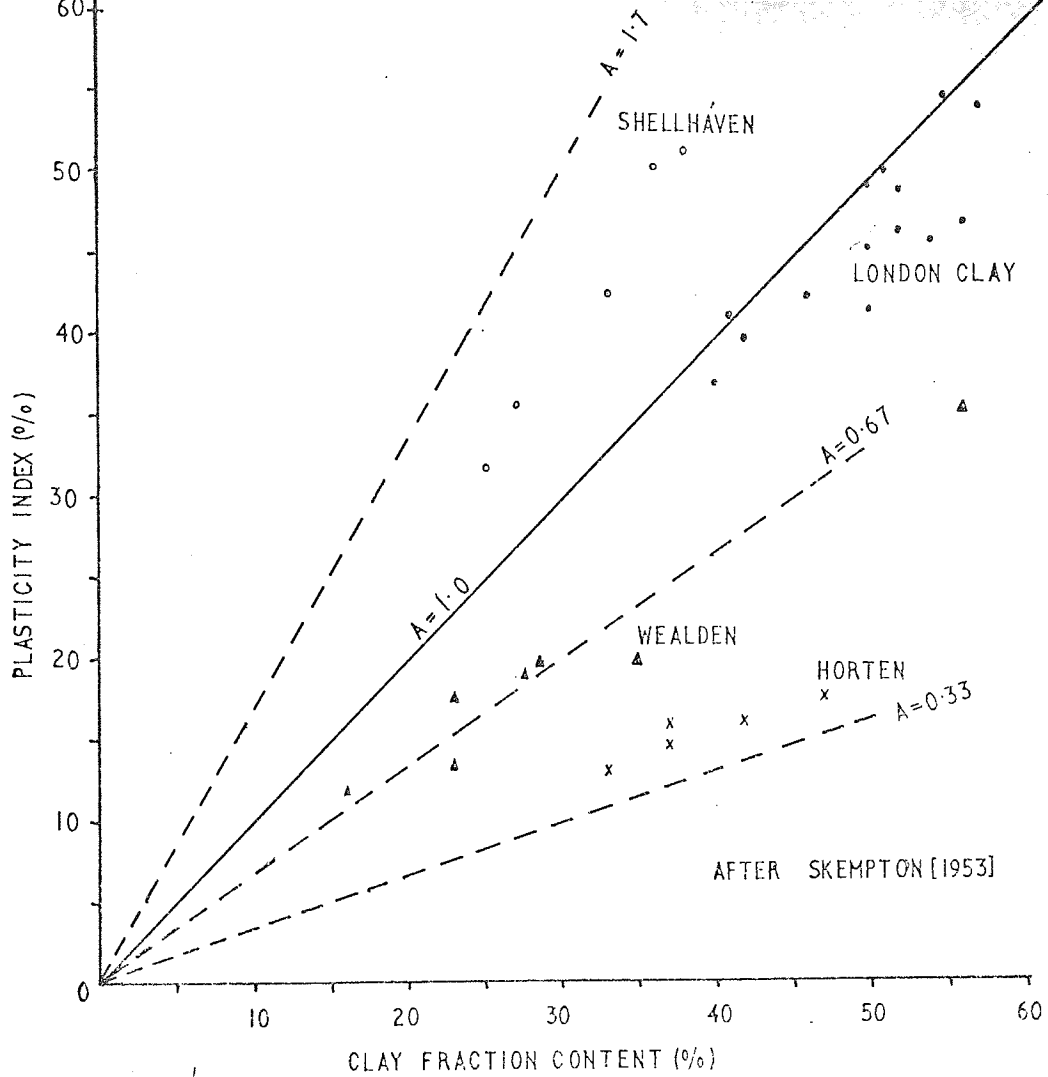
TABLE 10:2

DEPTH	RANGE	DIVISION	ENGINEERING ZONE
0 - 0.35	L.L. 56 - 60 P.L. 30	1.	VI
0.35 - 0.75	L.L. 66 - 75 P.L. 30	2.	V
0.75 - 2.60	L.L. 53 - 65 P.L. 25 - 29	3.	IV, III, II, I

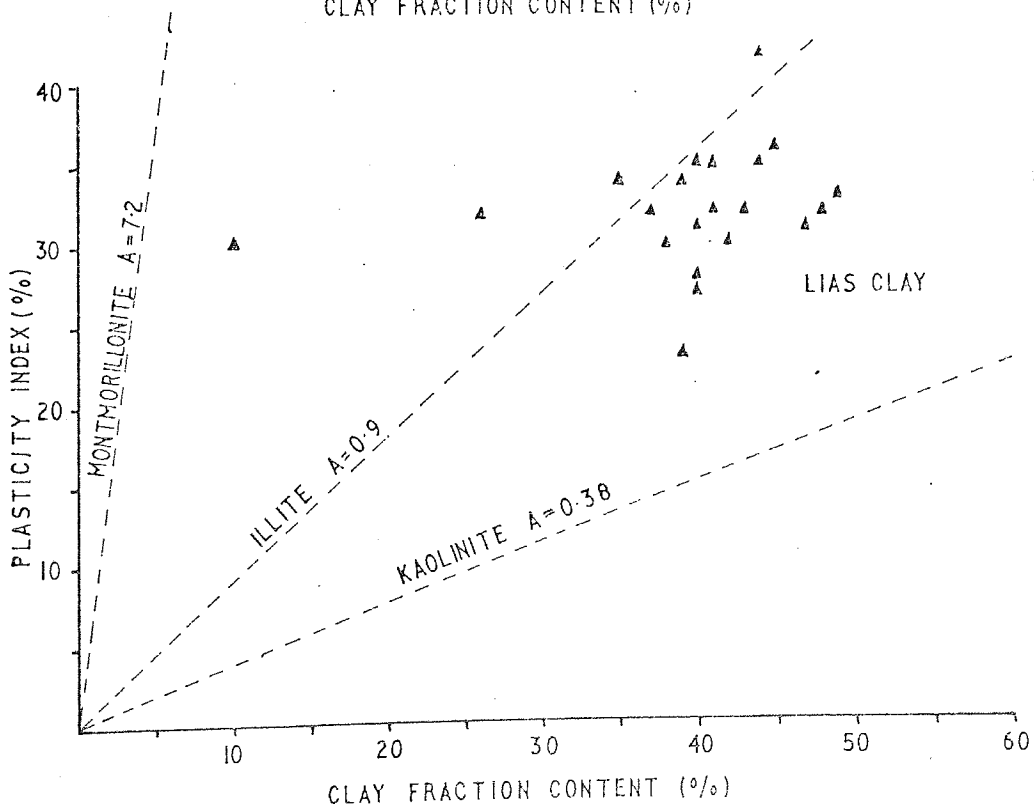
Division three corresponds to the engineering Zones IV, III, II, and I, and variations connected with changing mineralogy and weathering cannot be detected since these changes are so subtle as to have little or no effect on the liquid or plastic limit values.

Division two corresponds to Zone V where there is an increase in iron content and where the alteration of the clay minerals due to weathering is most intense, thus resulting in higher plasticity, (Fig 10:2).

For any particular type of soil a linear relationship usually exists between the percentage clay content and the liquid and plastic



(A)



(B)

PLASTICITY INDEX/CLAY FRACTION RELATIONSHIPS

FIG 10:3

limits, (Fig 10:3A after Skempton 1953). Sherwood and Hollis (1966) when studying the Keuper Marl proved that aggregations of clay minerals reduced the clay content as obtained by the British Standard procedure by up to 60%. When they plotted the plasticity index ( $I_p$ ), or liquid limit against clay content (B.S. 1377 procedure) no linear relationship was observed. Clay content as obtained by X-ray analysis did show this linear relationship. A plot of the clay content (B.S. 1377 procedure) against the plasticity index for the Lias clay (Fig 10:3B) does not show a definite linear trend. In fact, some samples have shown very low clay fraction contents, indicating aggregations of clay minerals possibly of coarse silt size. The liquid limits for the samples are indicative of soils with a fairly high clay content thus indicating that the aggregations were being broken down to some extent by working with palette knives.

It was previously stated that the liquid limit is very sensitive to clay mineralogy changes and therefore this test should respond to changes in the soil due to weathering. Changes in clay mineralogy are too small to be determined with any accuracy, but as the iron content can be used as a weathering indicator it is possible that a relationship exists between iron content and plasticity of a soil. Fig 10:4 shows a plot of liquid limit against iron content and it can be observed that there exists a good positive straight line correlation. A tentative linear correlation was also obtained from data for the Keuper Marl obtained by Sherwood and Hollis (1966). It should be pointed out that the samples of Keuper Marl came from a much wider area and clay mineralogy varied considerably. This suggests that not only clay mineralogy will affect liquid limit values, but also that



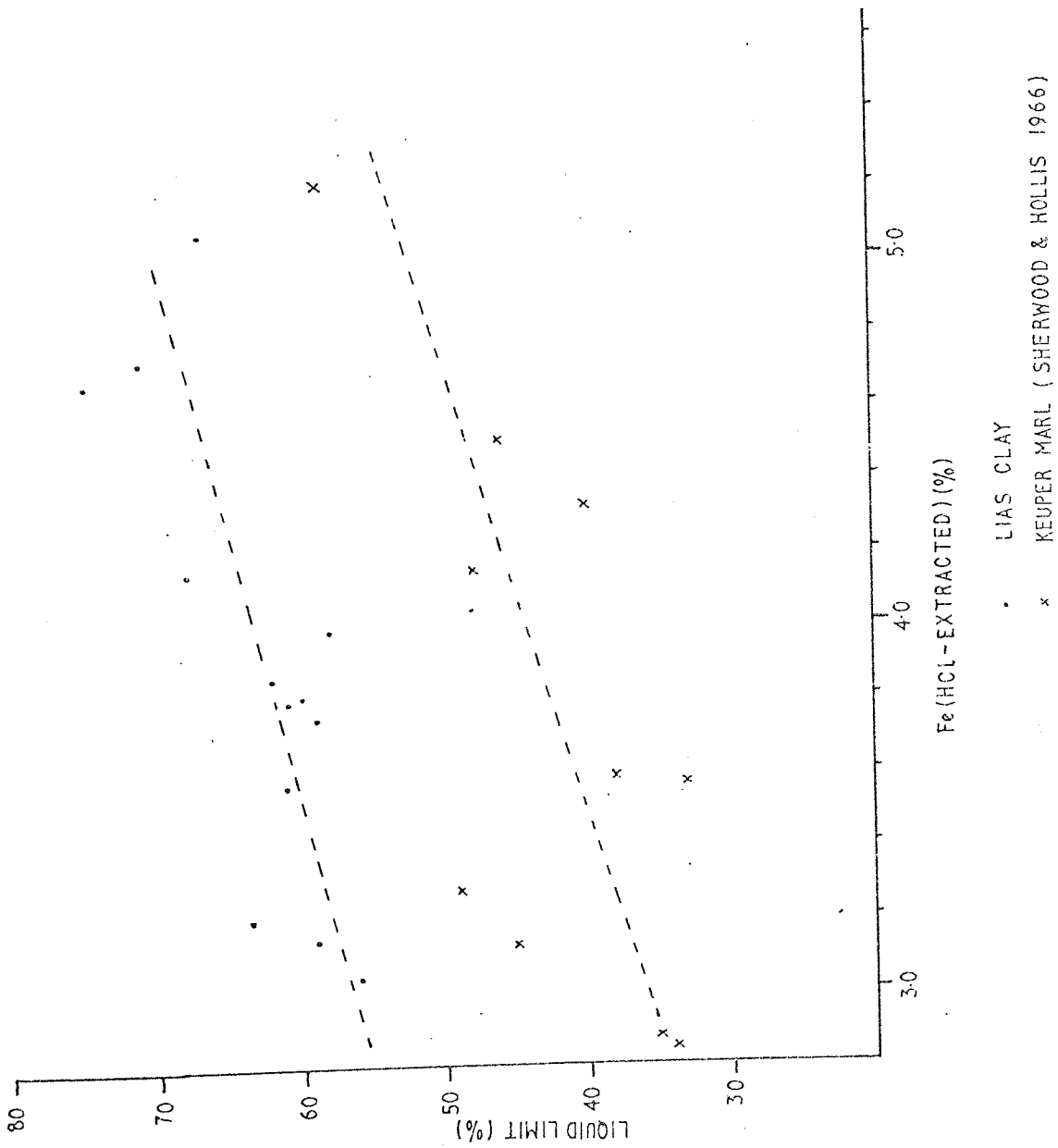


FIG 10:4 LIQUID LIMIT/Fe (HCl-EXTRACTED) CORRELATION

changes in iron content themselves might influence the results. The liquid limit will thus be sensitive to overall changes in mineralogy and chemistry.

### 10:2:3 PARTICLE SIZE DISTRIBUTION

The particle size distribution was carried out according to the B.S. 1377 (1967) procedure, the soil being treated to remove possible cementing agents. Organic matter being removed by oxidation with hydrogen peroxide ( $H_2O_2$ ) and carbonates by dilute hydrochloric acid. After pretreatment and dispersion of the soil in distilled water, sodium hexametaphosphate solution was added. This chemical is an excellent chelating agent and will remove any cations of any polyvalent metals such as calcium or iron which remain after acidification. Thus any iron oxides adhering to the clays should be effectively removed. Finally the soil suspension is further dispersed by a high speed stirrer.

Sherwood and Hollis (1966) and Davis (1967) working on the Keuper Marl proved that the clay content determined by the B.S. 1377 (1967) procedure, produced on average, clay content values that were 50% lower than those obtained by X-ray diffraction methods. An attempt was made to reduce this error by using ultra-sonic vibration on the samples for a period of ten minutes. A visual examination of the remaining coarse to medium silt size particles showed that they were in fact aggregations of smaller particles which could be broken down by cyclic wetting and drying.

The results of the particle size distribution analysis are shown in Table 10:3 and as it can be seen the percentage of clay sized material is much smaller than that obtained from thin section analysis. Coarse silt sized particles can be seen by the aid of a

TABLE 10:3

HAND SAMPLES	SIZE FRACTION			
	COARSE SILT	MEDIUM SILT	FINE SILT	CLAY
S1/1	30	21	10	39
S3/1	26	23	11	40
S6/1	17	27	12	44
S9/1	19	26	12	43
S12/1	19	27	13	41
S16/1	23	30	12	35
S19/1	13	35	15	37
S22/1	13	33	13	41
S25/1	30	30	14	26
S26/1	24	37	16	23
S27/1	32	43	15	10
S37/1	73	17	5	5
S38/1	21	37	21	21
S40/1	28	31	33	8
BOREHOLE SAMPLE				
B2A	11	33	15	41
B2B	10	29	21	40
B2C	5	32	15	48
B2D	17	29	14	40
B2E	8	28	24	40
B2F	7	31	12	50
B2G	10	29	16	45
B3A	10	31	20	39
B3C	13	28	15	44
B3D	20	28	13	39
B3E	17	27	13	43
B3F	11	31	14	44
B3G	7	27	18	48

hand lens and plates of mica were identified in the unweathered and weathered clay. Thus some clay minerals are of silt size but the percentage is indeterminable due to the presence of aggregates.

#### 10:2:4 SOIL pH

The measurements of soil pH were taken according to the B.S. 1377 (1967) procedure on a soil suspension of a standard concentration (Soil/Water:- 1/2.5). The suspension was then left for a minimum of two hours for equilibrium to be established and the measurements taken on a Pye Unicam Model 291 pH meter using a Pye Ingold E<sub>0</sub>7 electrode with automatic temperature compensation (accuracy  $\pm 0.02$  pH). The results are shown in Table 10:4 .

TABLE 10:4

#### SOIL pH

SAMPLE	DEPTH	pH ( $\pm 0.02$ )
S1/1	0.14	4.95
S2/1	0.20	5.25
S4/1	0.35	5.45
S5/1	0.43	5.69
S6/1	0.58	5.71
S9/1	0.79	6.41
S14/1	1.13	7.62
S20/1	1.88	8.03
S24/1	2.29	8.39
S26/1	2.50	8.41
S32/1	3.58	7.51
S37/1	4.25	7.54
Refined Kaolinite (St. Austell)		7.35

The results show that the hydrogen ion concentration increases with weathering. The soil becomes acidic in Zone V and VI and any carbonates or pyrite would be removed from the soil. It is interesting to note that samples from Zone IV, III and II give alkaline readings

yet measurable quantities of calcite could only be obtained from one sample S26/1. (Infra-red analysis of sample S19/1 from Zone III, also did not indicate the presence of calcite). Consideration of the oxidation-reduction potentials of  $Fe^{2+}$  and  $Fe^{3+}$  predict that the oxidation reaction would take place much more readily in an alkaline environment than in an acid environment. Thus although the oxidation of pyrite produces ferrous sulphate and sulphuric acid, the sulphuric acid reacts with the calcite to produce gypsum. This is either leached out or, if sufficient calcite is present it may crystallize out as selenite and thus the soil maintains an alkaline pH.

The change from acid to alkaline at sample S14/1 corresponds well with the base of Zone V and to the sudden drop in amount of kaolinite between samples S10/1 and S13/1. An overall increase in the proportion of three layer minerals tends to move the pH towards acidity.

10:2:5 STRENGTH

10:2:5:1 OVERBURDEN IN THE BLOCKLEY AREA

Since the time of deposition of the Lower Lias clay some 190 million years ago, the clay has been subjected to high preconsolidation pressures. From examination of the local geology and from consideration of the stratigraphy of the British Isles it is considered that both the Middle and Upper Jurassic rocks were deposited on top of the Lias in this area. Localized intra-Jurassic movements occurred causing broad folds to develop with local erosion, but the overburden present at the end of the Jurassic period is thought to have been of the order of 700m.

At the close of the Jurassic period the majority

of the Jurassic sediments in Britain were elevated above sea level and eroded. During the early Cretaceous period, removal of material reached 300m in specific areas. Towards the end of the Lower Cretaceous period, there was again subsidence of a large area of the British Isles below sea level. A shallow sea existed and chalk was deposited to an unknown thickness. At the close of the Cretaceous period there was again uplift of this area above sea level followed by erosion. There is no evidence that any further material was deposited during the Tertiary. It can therefore be assumed that the area has been subjected to erosion since the end of the Cretaceous period. Glaciation did extend to the south of Blockley although it is unlikely that this had any effect on the preconsolidation pressure.

It can therefore be assumed that the Lower Lias clay in the area has been subjected to an overburden in excess of 700m and may even have reached 1,000m in places. The Lower Lias clay is therefore a heavily overconsolidated clay with a stress history of loading and unloading. Consequently in its unweathered state the clay will have a natural water content well below its plastic limit, which has already been shown.

#### 10:2:5:2 IN SITU STRENGTH TESTS

In order to investigate the change of strength with weathering it was decided that initially in situ strength tests would be made on the profiles using a pocket shear vane (Torvane, Soil Test Ltd.).

The shear strength of a soil is the maximum resistance of the soil to shear stress at a point within the soil, thus when this resistance is reached continuous shear displacement takes place between two parts of the soil body. Shear displacements within a soil can take place across a well defined single rupture plane or across a wide shear zone (Morgenstern and Tchalenko; 1967c). Once sliding

(continuous shear displacement) occurs, the available resistance to shear (Shear strength) has been mobilized by the acting shear stress:

$$|\tau| = \tau_f$$

where  $|\tau|$  = absolute value of shear stress

$\tau_f$  = shear strength of the soil.

The magnitude of the resistance to shear is calculated from Coulomb's equation:

$$\tau_f = c + \sigma_n \tan \phi$$

where  $\tau_f$  = shear strength of soil ( $\text{kN/m}^2$ )

$\sigma_n$  = normal stress component (perpendicular to the shear plane).  $\text{kN/m}^2$ .

$\phi$  = angle of internal friction in degrees

$c$  = cohesive resistance in  $\text{kN/m}^2$

This equation is therefore used in modified forms for the determination of strength parameters in terms of effective stress (Skempton 1960) and the determination of true cohesion ( $c_e$ ) and true angle of friction ( $\phi_e$ ). Detailed discussion of the terms used in the various equations can be found in Lambe & Whitman (1969), Skempton (1960) and Hvorslev (1936).

Since a pocket shear vane was used to determine shear strength ( $\tau_f$ ) it is assumed that for soft cohesive soils sheared in an undrained manner\* the angle of internal friction  $\phi_u = 0^\circ$ . Therefore

---

\*

The vane test is a rapid test and therefore in material of low permeability drainage does not take place, i.e. the vane test can be considered to be an undrained test.

the shearing resistance is only due to cohesion  $c_u$  which is independent of the normal stress. On assuming that the soil shears along the surface of a cylinder whose diameter and height is equal to that of the vane and that shear resistance varies linearly across the ends of the cylinder, the following expression is obtained

$$c_u = \tau_f = \frac{T}{2\pi r^2(h + 2r/3)}$$

where  $T$  = maximum measured torque.

$r$  = radius of vane.

$h$  = height of vane.

Although the soil is not fully saturated and negative pore pressures were known to exist (Thomas 1974) it was thought that variation in capillary effects would be negligible over the major part of the profile. It is therefore possible, that part of the strength measured was due to capillary effects. Since it was probable that this was small the capillary effect was neglected.

#### 10:2:5:2:1 SHEAR VANE

The pocket shear vane used, a Torvane was obtained from Soil Test Ltd., U.S.A. is designed for the rapid determination of shear strength of cohesive soils. It is made of a standard vane with vane adaptors for use when working with extremely soft or very stiff sediments. The handle is attached to the vane through a precision helical spring. The calibrated dial on the handle converts the torque directly to  $\text{tons/ft}^2$ , which was then converted to  $\text{kN/m}^2$ . The Torvane adaptor for measured strengths from 0 - 268  $\text{kN/m}^2$  (0 - 2.5  $\text{tons/ft}^2$ ) was used during this investigations.

The surface of the clay was carefully prepared in situ with a



TABLE 10:6

## RESULTS (Section Two)

Shear Strength at failure

Depth(m)	kN/m <sup>2</sup>	Depth(m)	kN/m <sup>2</sup>
0.178	202.85	1.778	77.33
0.254	201.41	1.828	95.91
0.305	172.64	1.879	91.91
0.356	160.65	1.931	106.30
0.406	162.24	1.981	94.31
0.457	140.60	2.032	74.33
0.533	119.29	2.108	74.33
0.609	124.09	2.159	73.13
0.686	95.91	2.040	100.11
0.762	89.92	2.080	104.90
0.838	89.32	2.133	110.30
0.914	79.13	2.184	110.30
0.991	62.94	2.235	104.30
1.067	78.53	2.285	112.69
1.079	103.70	2.336	131.01
1.117	71.33	2.412	120.68
1.168	64.74	2.488	142.29
1.219	75.93	2.565	96.70
1.270	73.48	2.641	99.10
1.320	87.85	2.717	105.10
1.371	77.53	2.793	107.89
1.422	68.34	2.896	83.12
1.472	80.72	2.997	86.32
1.523	83.92	3.048	115.09
1.575	87.85	3.098	103.10
1.626	87.66	3.200	111.09
1.676	83.32	3.301	146.26
1.727	74.93		

palette knife. The Torvane blades were then carefully pressed into the sediment to their full depth. A slight vertical pressure was maintained on the handle which was then turned at a rate of rotation such that failure occurred in about 15 - 20 seconds. The maximum value attained by the pointer on the dial is the shear strength in tons/ft<sup>2</sup> subsequently converted to kN/m<sup>2</sup>.

Since the outside diameter of the vane was 20mm the volume of Lias clay tested was quite small and the vane was positioned away from any obvious fractures. Therefore, the strength of the clay is the intact strength. At each horizon four to five tests were taken and an average result calculated.

#### 10:2:5:3 RESULTS

The results of Section Two are shown in Table 10:6

#### 10:2:5:4 STRENGTH PARAMETERS FOR UNWEATHERED LOWER LIAS CLAY

From the borehole samples and the block samples a series of tests was carried out by Thomas (1974) and Nasserri (1972) as a general investigation of the Lias clay. The investigation included the standard triaxial (compression and extension tests) and shear box tests on both overconsolidated and normally consolidated Lower Lias clay. Residual strength parameters were also determined for the normally consolidated clay. A summary of the results are shown in Table 10:5.

TABLE 10:5

#### STRENGTH PARAMETERS FOR UNWEATHERED LOWER LIAS CLAY

TEST	MATERIAL	PARAMETERS
Triaxial	Undisturbed overconsolidated Lower Lias clay	$\phi_d = 30^\circ - 32^\circ$ $c_d = 20 \text{ kN/m}^2$
Triaxial	Normally consolidated Lower Lias clay - consolidated from a slurry in a tall oedometer.	$\phi' = 24^\circ$ $c' = 5 \text{ kN/m}^2$

TABLE 10:5 (cont)

TEST	MATERIAL	PARAMETERS
Shear Box	Normally consolidated in the shear box	$\phi' = 24.7$ $c' = 5.68$
Shear Box (Residual Tests)	Normally consolidated clay sheared along preformed slip planes.	$\phi_r = 18^\circ$ $c_r = 0$

10:2:5:5 MOISTURE CONTENT AND TORVANE TESTS

At regular intervals below the surface, moisture contents were determined at the positions where the Torvane tests were carried out. At deeper depths of 10.35m, Block 2B was taken which gave a moisture content on the front face of 17.2%. This block was returned to the laboratory and after a period of eight months the moisture content determined again on the front face was 16.5%, a difference of only 0.7%.

As Block 2B was being dissected for fissure analysis, moisture content samples and Torvane tests were carried out simultaneously on both prepared surfaces and joint surfaces. The average moisture content of eighteen samples was 15.2% ( $\pm 1.4\%$ ) a lower value than that which was revealed on the front face. This marked variation of moisture content within small distances was also noted by Thomas (1974) in the block samples used for hand carved triaxial and shear box samples.

A series of six combined Torvane tests with moisture contents were taken from Block 2B and the results shown in Table 10:7.

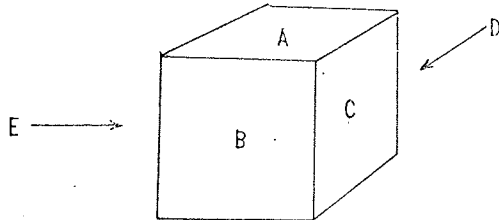
TABLE 10:7

## STRENGTH AND MOISTURE CONTENT OF VALUES FOR BLOCK 2B

Moisture Content (%)	kN/m <sup>2</sup>	
15.2	230.18	Prepared Surface
17.1	201.41	Prepared Surface
16.2	215.80	Side face (D)

TABLE 10:7 (cont)

Moisture Content (%)	kN/m <sup>2</sup>	
15.8	194.22	Joint surface
13.4	232.10	Side face (E)
16.5	177.43	Front face (B)
Average 15.7	Average 201.85	



A = Top surface  
B = Front surface

### 10:3 DISCUSSION OF RESULTS

The results of the Torvane tests are presented in Figs 10:7 and 11:1 where strength variation with depth is plotted and in Figs 10:5 and 10:6 where strength variation with moisture content is shown.

#### 10:3:1 STRENGTH/WATER CONTENT RELATIONSHIP

##### 10:3:1:1 INTRODUCTION

A clay, soon after deposition is subjected to increasing overburden by further sedimentation and therefore undergoes diagenetic changes. As soon as a sediment layer at the depositional interface is covered by a younger layer the physicochemical conditions in the interstitial water change, in particular the H<sup>+</sup> concentration and the 'Redox' potential. Compaction of the material is therefore accompanied by changes in the electrolyte concentration of the pore fluid and porosity decrease, with the overall effect of reorganising the clay mineral structure. The bringing together of clay particles depends on the attractive and repulsive forces that exist between clay particles (Table 10:8).

FIG 10:5

STRENGTH/WATER CONTENT RELATIONSHIP  
SECTION TWO

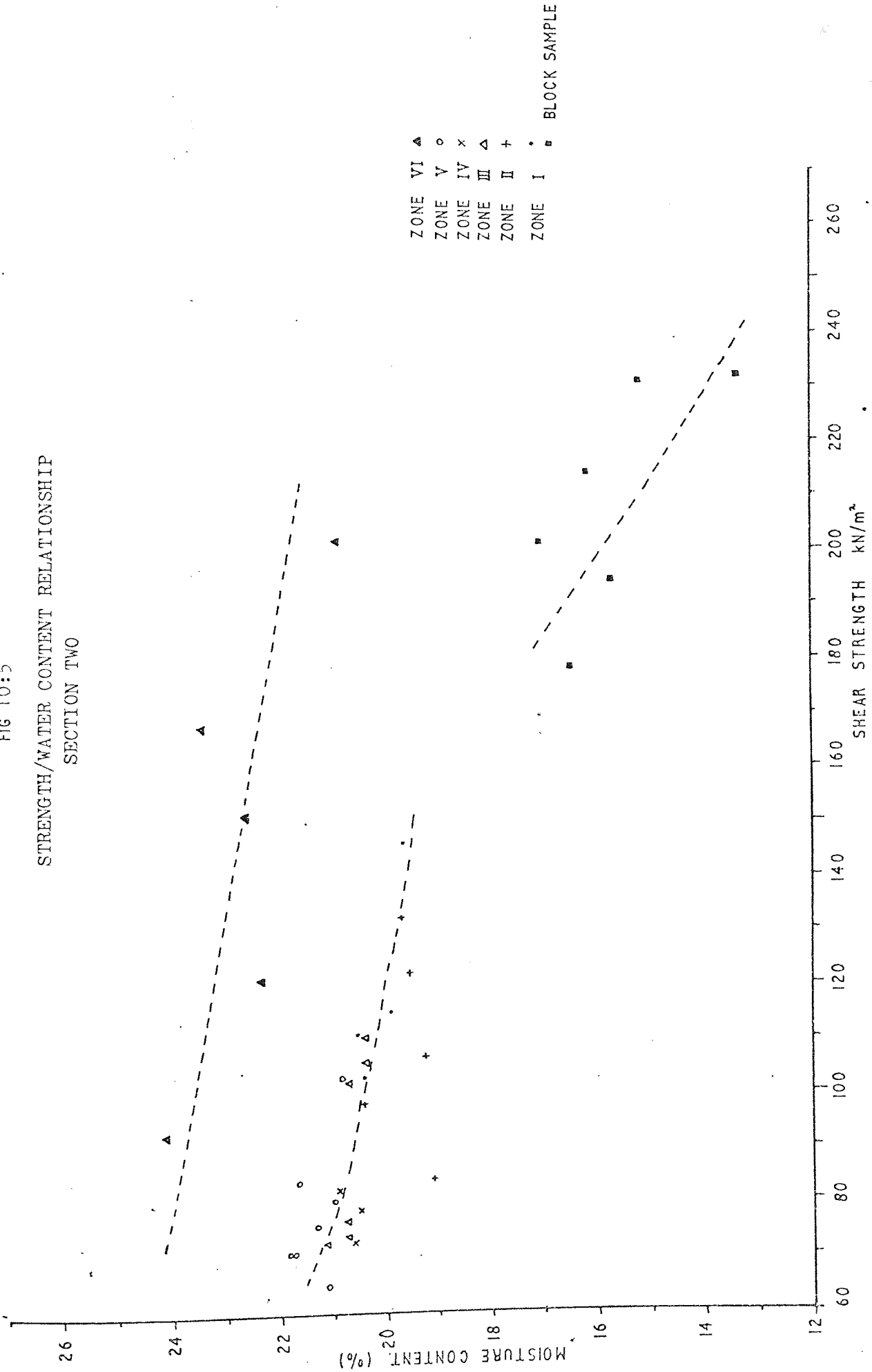
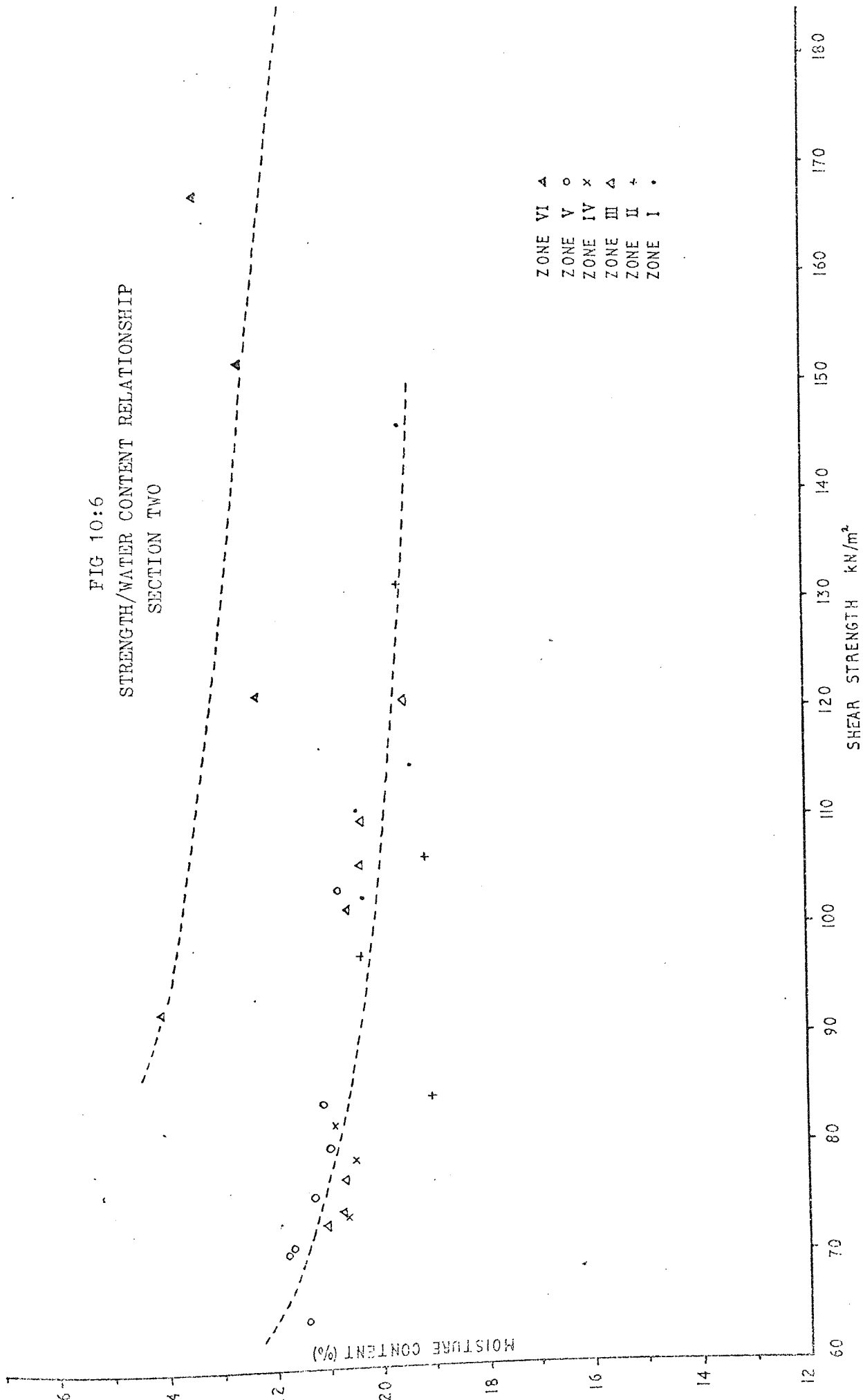
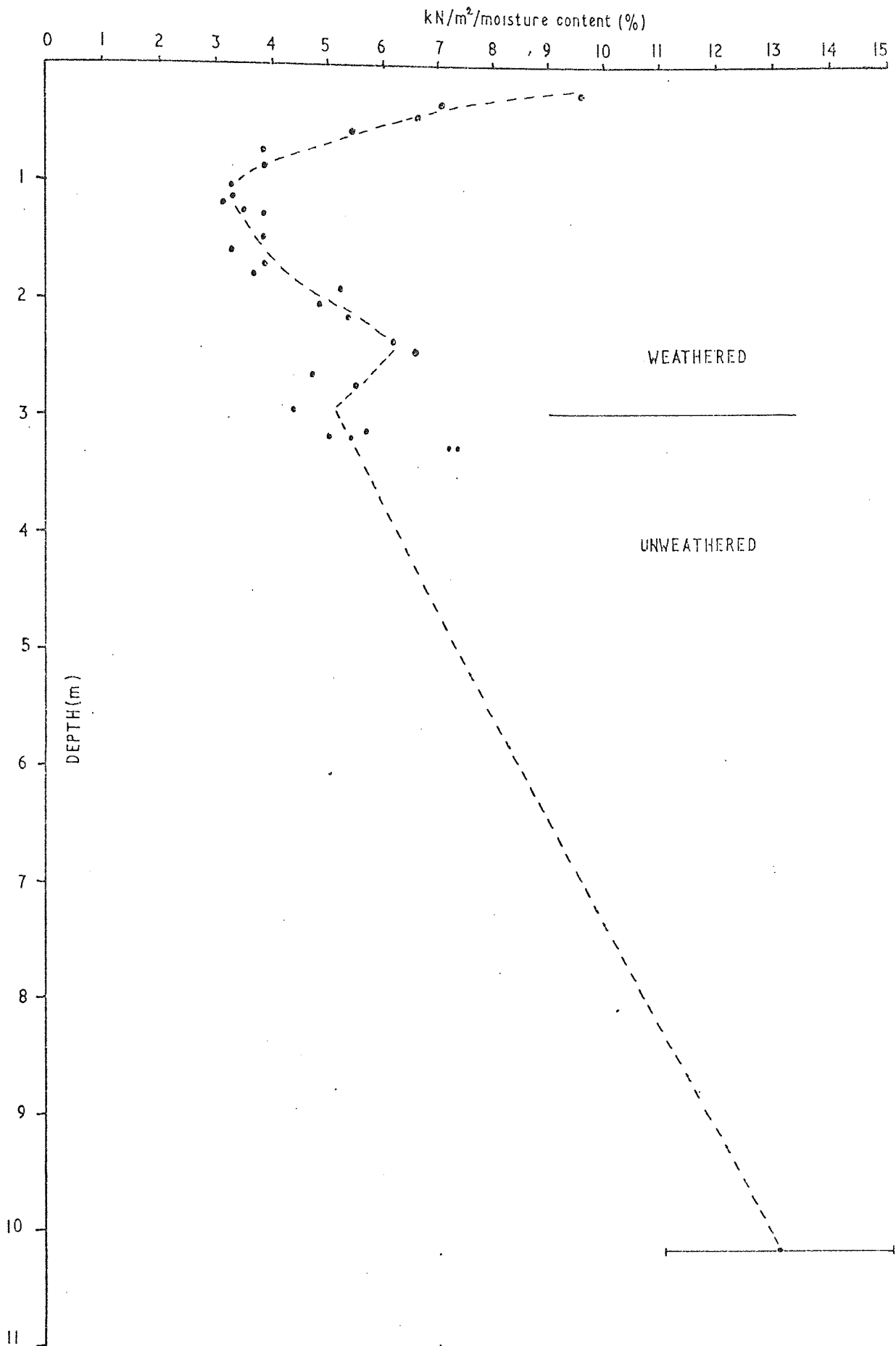


FIG 10:6  
STRENGTH/WATER CONTENT RELATIONSHIP  
SECTION TWO

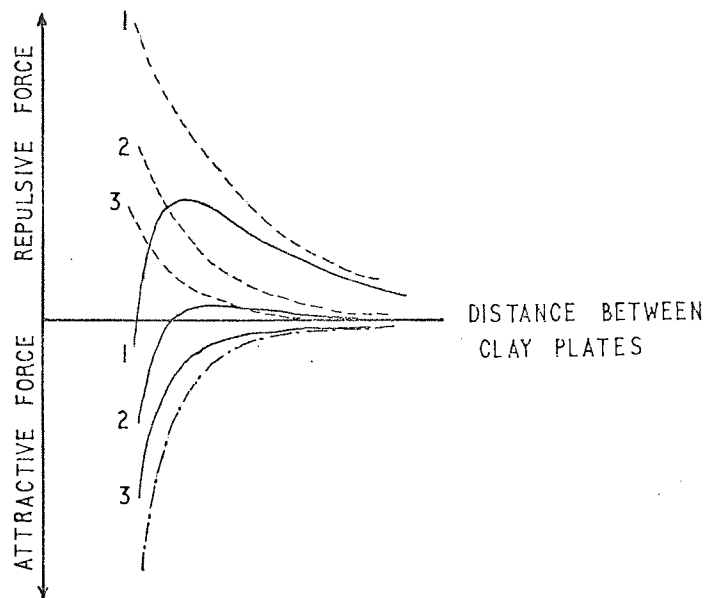




STRENGTH/DEPTH RELATIONSHIP  
SECTION TWO

FIG 10:7

FIG 10:8



- NET FORCE CURVES
- EXPONENTIAL REPULSIVE FORCE CURVES FOR VARYING CONCENTRATIONS OF ELECTROLYTE FROM DILUTE (1) TO STRONG (3)
- ..... VAN DER WAALS ATTRACTIVE FORCE CURVE

FORCES BETWEEN CLAY PARTICLES



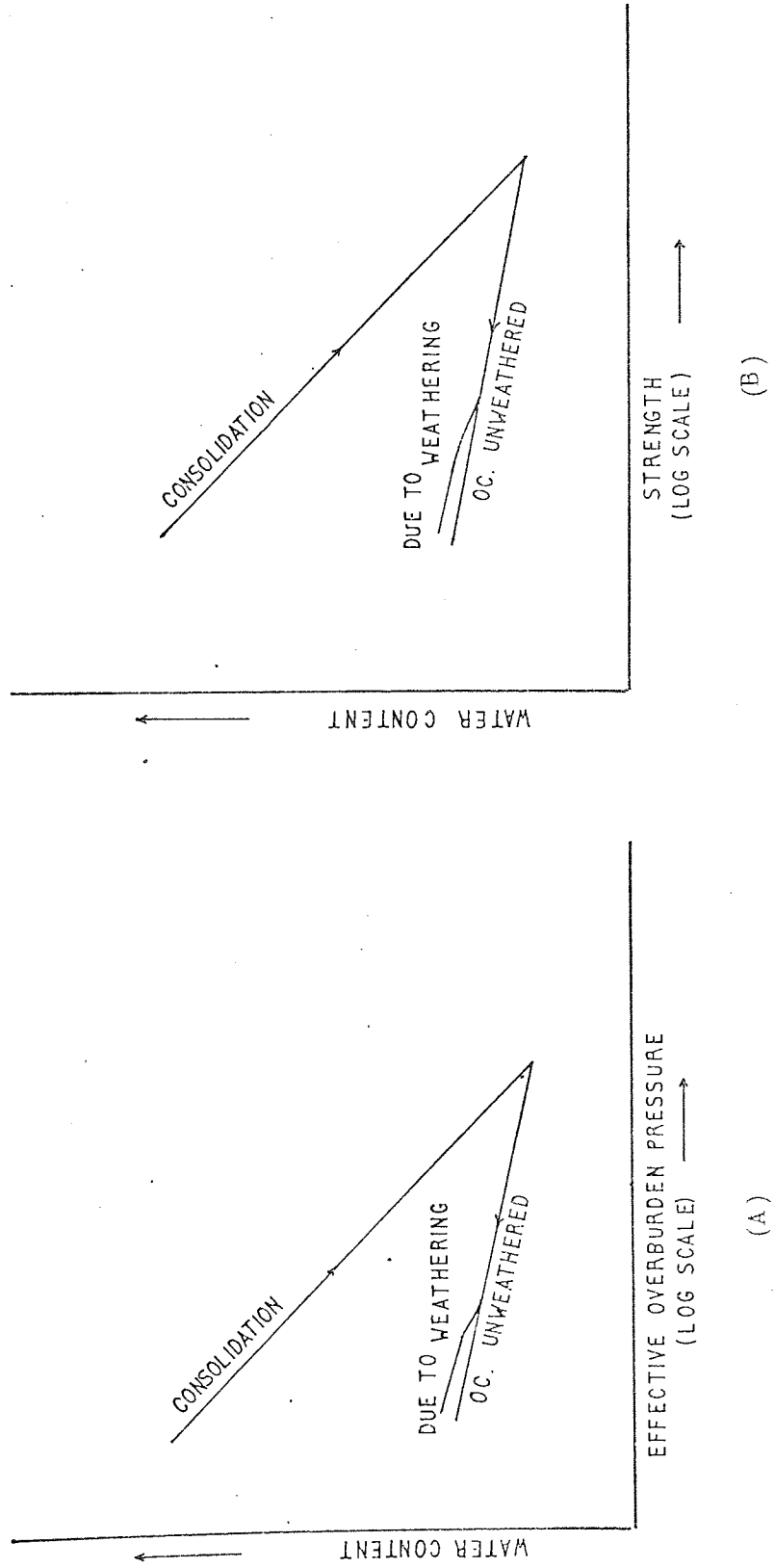
TABLE 10:8

FORCES BETWEEN CLAY PARTICLES

- Attractive force :- Van der Waals' force, an electrostatic force independent of pore fluid characteristics but dependant on the chemical composition of the clay mineral.
- Repulsive force :- The Coulombic electrical force between the particles that push like charges apart and is caused by the double layer of water surrounding the particles. Increase in the electrolyte concentration reduces this repulsive force thus allowing attraction of the particles to increase (Fig 10:8).

The void ratio at the time of deposition may exceed 70% but the majority of the trapped water is easily removed in the initial stages of compaction. As compaction takes place the void ratio and permeability is further reduced, thus water movement becomes restricted and chemical reactions between the pore fluid and the clay minerals can take place. This has the effect of increasing the electrolyte concentration in the pore fluid thus allowing the attractive forces (diagenetic bonding) to form. Hence diagenetic bonding is a function of time. Cementation by precipitation of a mineral during diagenesis is ruled out from the geochemical study (Chapters 7, 8, 9) and therefore bonding between the clay particles is primarily diagenetic with possibly some bonding resulting from the growth of clay material on the surface of existing clays (Chapter 6).

FIG 10:9 "SWELLING CURVES", BJERRUM 1967



Bjerrum (1967) pointed out the effects of weathering on the "swelling" curves exhibited by clays and clay-shales, as the overburden is removed by erosion. He suggested that weathering processes were responsible for the destruction of diagenetic bonds that had developed during the geological history of the deposit. Thus progressive breakdown of these bonds would result in the deposit having a range of water contents under the same effective overburden pressure, the elements with a high water content being those that are most weathered. This relationship is shown in Fig 10:9.

Removal of overburden will allow the clay to swell and increase its water content (Fig 10:9A). However, it will take more than swelling to destroy the diagenetic bonding altogether. Weathering will have an important effect on these bonds as weathering will bring into the system a new supply of ions in differing concentrations. Percolation of rain water along fissures that have been produced by overburden removal will enter the clay changing the pH of the pore water and lowering the electrolyte concentration, thus the reverse of diagenesis takes place. The effect of weathering therefore increases the water content and tends to increase the repulsive force between particles. This leads to a breakdown of the original fabric with remoulding of the material, rotating of lithorelicts and the formation of flame structures and shear planes within the weathered material.

It can be seen from Fig 10:9A,B that at a given water content it is possible for there to exist an unweathered overconsolidated clay and a weathered overconsolidated clay at different effective overburden pressures, with the weathered clay exhibiting the greater strength. This increase in strength being associated with the reorganisation of the original fabric and the change between the net

attractive and repulsive forces. Thus as weathering increases, water content should increase and strength decrease to give a uniform strength: water content relationship.

A plot of water content against strength for Section Two is shown in Fig 10:6, it can be seen that basically there are two linear correlations. The results have been plotted according to the weathering zones. For weathering Zones I - V there is an approximate linear relationship between strength and water content but show very little differentiation between zones. Zone VI the most oxidised of all zones, and the most weathered is differentiated from the other zones by having a higher strength for a given water content when compared with the other zones, again there is an approximate linear correlation with strength to water content.

In Fig 10:5 additional strength and water content data are included from a depth of 10.35m (unweathered clay). The clay here is under a greater effective overburden pressure and has not been subjected to the weathering agencies. Hence the different line of correlation. This difference in correlation is expected since the increase in water content that is a direct consequence of swelling under reduced effective stress will be much smaller than if weathering were to take place simultaneously. Since it is only water content that is changing for this unweathered material, then to produce the same degree of strength change as is observed in the weathered clay it would necessitate greater increases in water content (swelling) than is possible under the existing effective overburden pressure.

Chandler (1972) has shown similar correlations in the Upper Lias clay at Wothorpe, yet at the Rockingham and Gretton site, he

investigated he was able to show a definite strength/water content correlation for each zone\*. Chandler (1972) suggests that permafrost disturbance at the Wothorpe site has overwhelmed the effects of weathering. This may indeed be so since there is a layer of solifluction material on the surface down to a depth of 3m but the Rockingham and Gretton sites have a capping of boulder clay or slipped Lias. We can infer from this that weathering at these sites must have been restricted to the capping material from at least the end of the last ice-age. The depth of weathering at these sites is much greater than at Blockley and there is no evidence that any covering has existed at Blockley. It can therefore be assumed that the weathering profile at Blockley has developed since the last ice-age. This is supported by the depth of weathering (3 - 3.5m at the Blockley site) and by the  $Fe^{3+}/Fe^{2+}$  ratios.

10:3:2 STRENGTH: DEPTH RELATIONSHIP

A strength-depth plot for London Clay at Hendon, North London, by Marsland (1971) based on four sets of well spaced results indicates a break at the junction of the weathered brown clay and the unweathered blue clay. The bend or "kick back" inferred from the gradients of the

---

\* The correlation between the weathering zones of Chandler and Fookes & Horswill is given below:

	Chandler (1972)	Fookes & Horswill (1969)
Z	I	I
O	IIa	II
N	IIb	III
E	III	IV
S	IV	V & VI

strength/depth curve covering both the brown and blue clay.

Chandler (1972) suggested that where there is an abrupt change of the degree of weathering in a vertical profile then there may be a break or 'kick back) in the strength/depth curve. Such a break is suggested from consideration of Figs 10:7 and 11:1 with higher strengths at the base of the more weathered material than in the top of the underlying less weathered clay. A break of this type was suggested by Chandler (1972) at the junction between the solifluction material and the in situ Lias at the Gretton site.

The results of the strength/depth investigation are shown in Fig 10:7, Fig 11:1, with Fig 10:10 showing the full set of results obtained (N.B. each point represents an average of four to five tests at that level with an average standard deviation of  $\pm 10\text{kN/m}^2$ ). It can be seen that a distinct kick back does exist at the base of the weathered material indicating a lower strength in the top of the unweathered clay than in the overlying weathered clay. A comparison of the depths of the weathered zones suggests that each zone can be related to a different portion of the strength/depth and this is indicated in Fig 10:10.

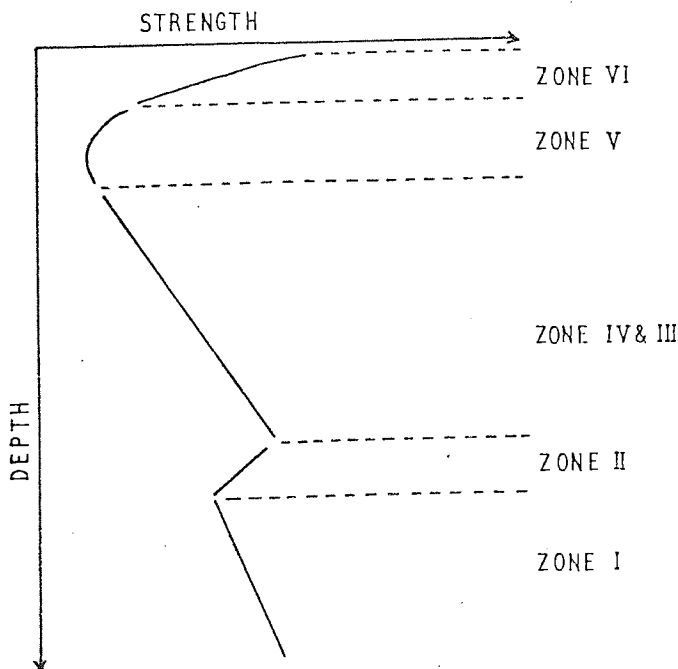


FIG 10:10

It can be seen that the "kick back" occurs in Zone II, alone where weathering is in its initial stages. This correlation between the Zones and the strength/depth curve may be coincidental and the generalizations in Fig 10:10 should await further evidence to establish this relationship.

## CHAPTER 11

### CONCLUSIONS

#### 11:1 INTRODUCTION

Throughout this investigation several topics have been explored and a variety of techniques used to provide a broad view of the Lower Lias clay at Blockley. In view of the object of the study as outlined in Chapter 1 it would be advantageous to outline the results and to emphasise specific points.

A summary of the results are given in Fig 11:1 (Profile Charts) Table 11:1.

#### 11:2 STRUCTURE

##### 11:2:1 MESOSTRUCTURAL CHANGES

As outlined in Chapter 5 the major mesostructural features are the fissures which when analysed resulted in the identification of five uniplanar sets;  $J_1$ ,  $(J_2, J_3)$ ,  $(J_4, J_5)$ .

The uniplanar set  $J_1$  is almost horizontal, paralleling the ground surface and the bedding planes. Statistically, it is significant and probably developed as a result of stress release parallel to the ground surface, but, will have been enhanced by the subhorizontal preferred orientation of the clay minerals (bedding).

The uniplanar sets  $J_2$  and  $J_3$  are a set of vertical conjugate fissures (Strikes  $042^\circ$  and  $127^\circ$  respectively). This system appears to bear no relationship with the ground surface or the exposure face. The acute dihedral angle of  $85^\circ$  between  $J_2$  and  $J_3$  has a bisectrix aligned almost E - W (bisectrix  $084.5^\circ$ ). This conjugate set of joints is similar to one found by Hancock (1968), working on the joints in the Middle Jurassic south of Blockley. He considered the region had suffered a single phase of subsidence, compression and uplift. This may be correct for the Middle Jurassic, but it is



TABLE 11:1

Zone	Description of hand specimen	Fabric (thin sections) and S.E.M.	Discontinuities	Chemical Observations
VI	Dark brown to grey brown in colour with reddish brown mottling. Gleying at shallow depths.	Remoulded random structure. Quartz concentrated in the upper regions.	1) Fissures produce a blocky structure becoming subangular to prismatic with depth. 2) None observed	1) None 2) 6.0 to 15.0 Shows great variation
V	Pale grey brown with extensive reddish brown to yellow brown mottling. Prismatic structure. Fissures gleyed.	Remoulded to random structure no trace of original bedding except in the few lithorelicts (<2cm in size) - iron stained with concentrations of iron oxides in the voids that act as a cement	1) Desiccation fissures produce the prismatic structure - grey argillaceous coatings on fissures. 2) Minor shears associated with remoulding	1) None 2) 4.0 to 12.0 (dependant on sample)

TABLE 11:1 (contd)

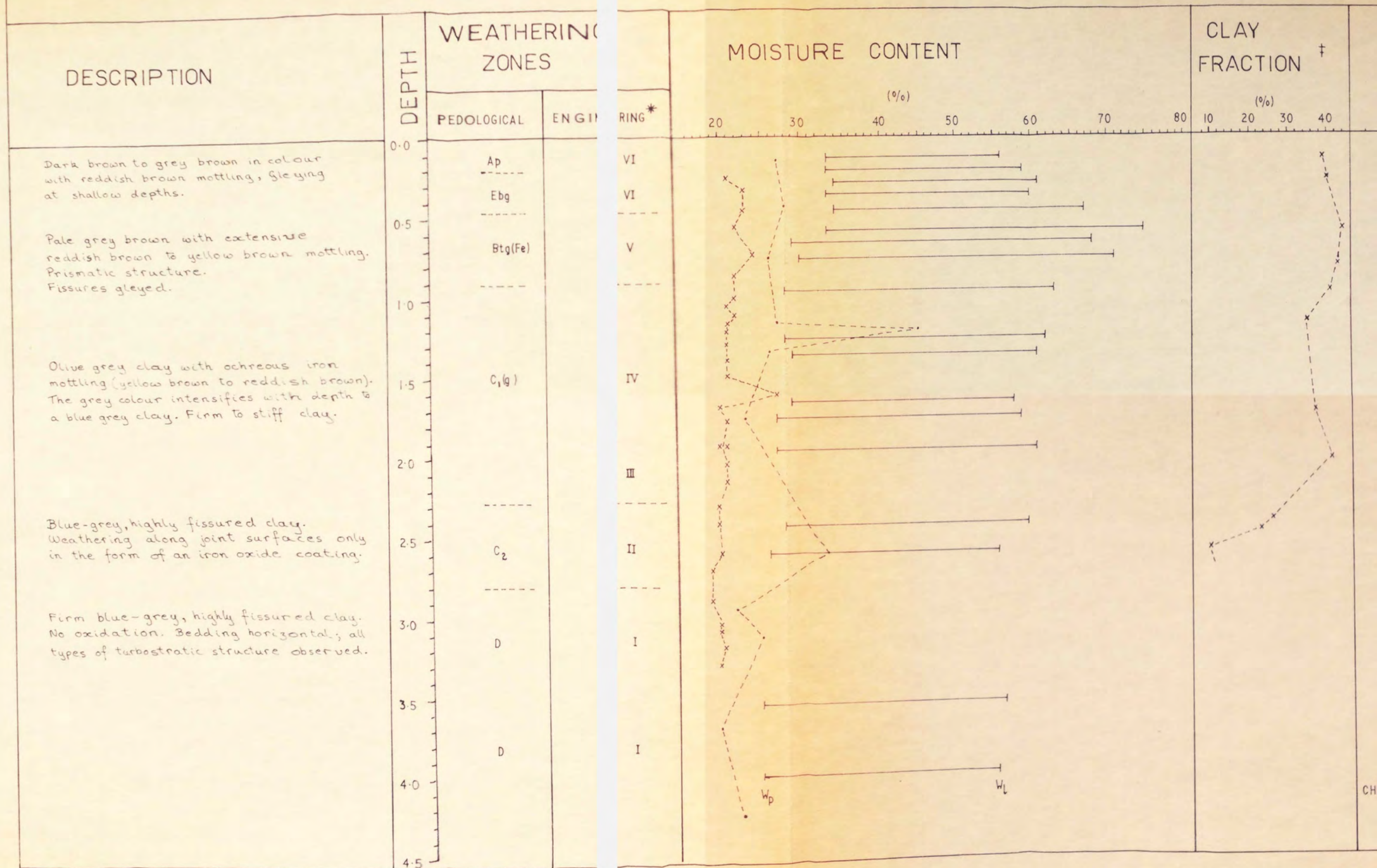
<p>IV III</p>	<p>Olive grey clay with ochreous iron mottling (yellow brown to reddish brown). The grey colour intensifies with depth to blue grey colour. Firm clay</p>	<p>Lithorelicts (up to 3cm) with horizontal bedding. Some however do show rotation. Size and number increases with depth. At depth matrix is less than 30% of material.</p>	<p>1) Grey argillaceous fissure and gradually change from apparent fissures in the upper region to true fissures at the base. 2) Shears and Plasmic separations often associated with remoulding and the development of flame structures</p>	<p>1) None 2) 2.0 to 8.0 decreases with depth, variations are small.</p>
<p>II</p>	<p>Blue grey highly fissured clay. Weathering being along joint surfaces only in the form of an iron oxide coating.</p>	<p>Bedding horizontal; Turbostratic structure</p>	<p>1) If. of low to medium. 2) No shears observed</p>	<p>1) 1% 2) 1.0 to 2.0</p>
<p>I</p>	<p>Firm blue grey fissured clay. No oxidation</p>	<p>Bedding horizontal; all types of turbostratic structures observed. Variations due to depositional changes.</p>	<p>1) If. Medium 2) Minor shear observed displacements of 1 -2mm</p>	<p>1) 2% 2) -1.0 to 1.0</p>

LOCATION :- Blockley (Northcot Brickworks)

Grid ref :- S 171372

Slope :- 1°

Altitude :- 350 ft. O.D.

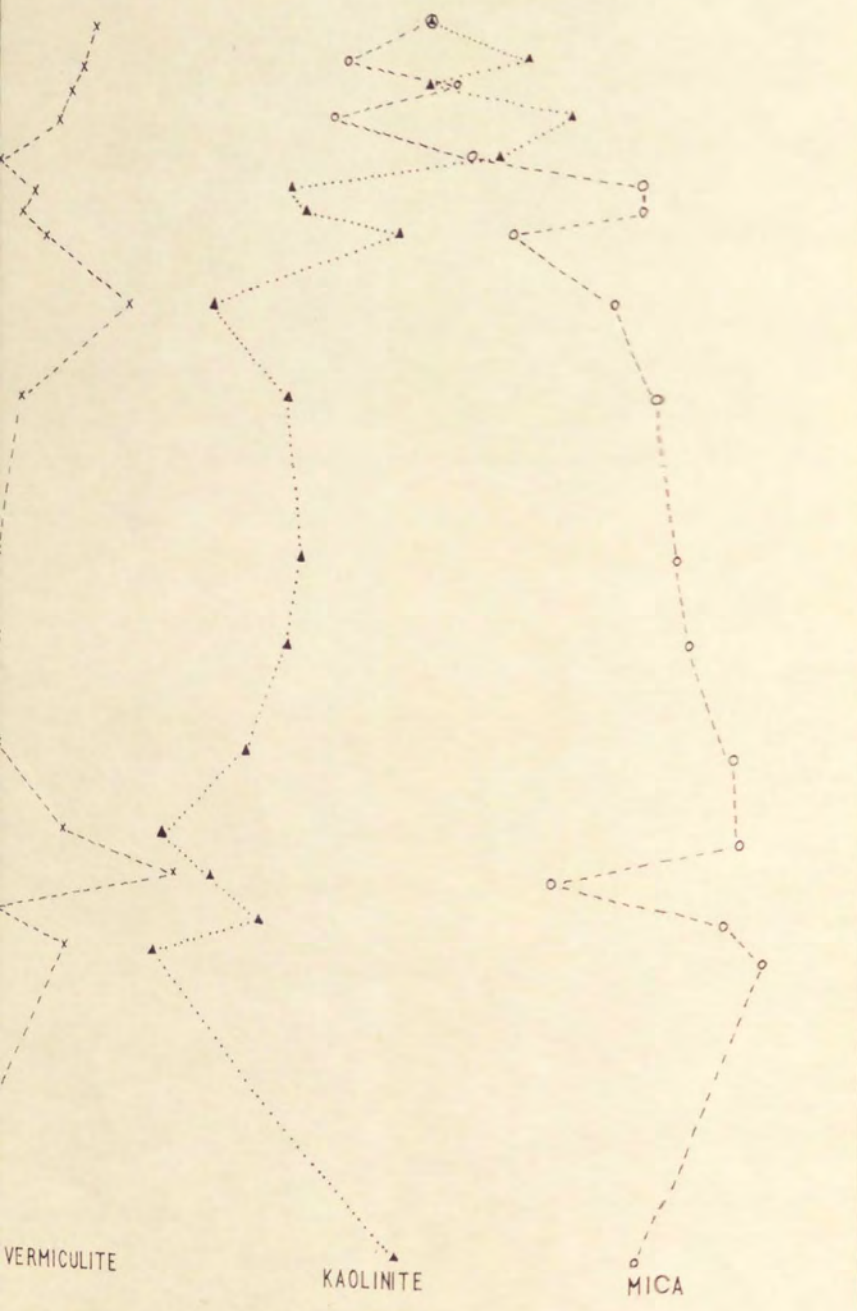


\* FOSTER & HORSWILL (1970)

† SEDIMENTATION ANALYSIS

CLAY MINERALS

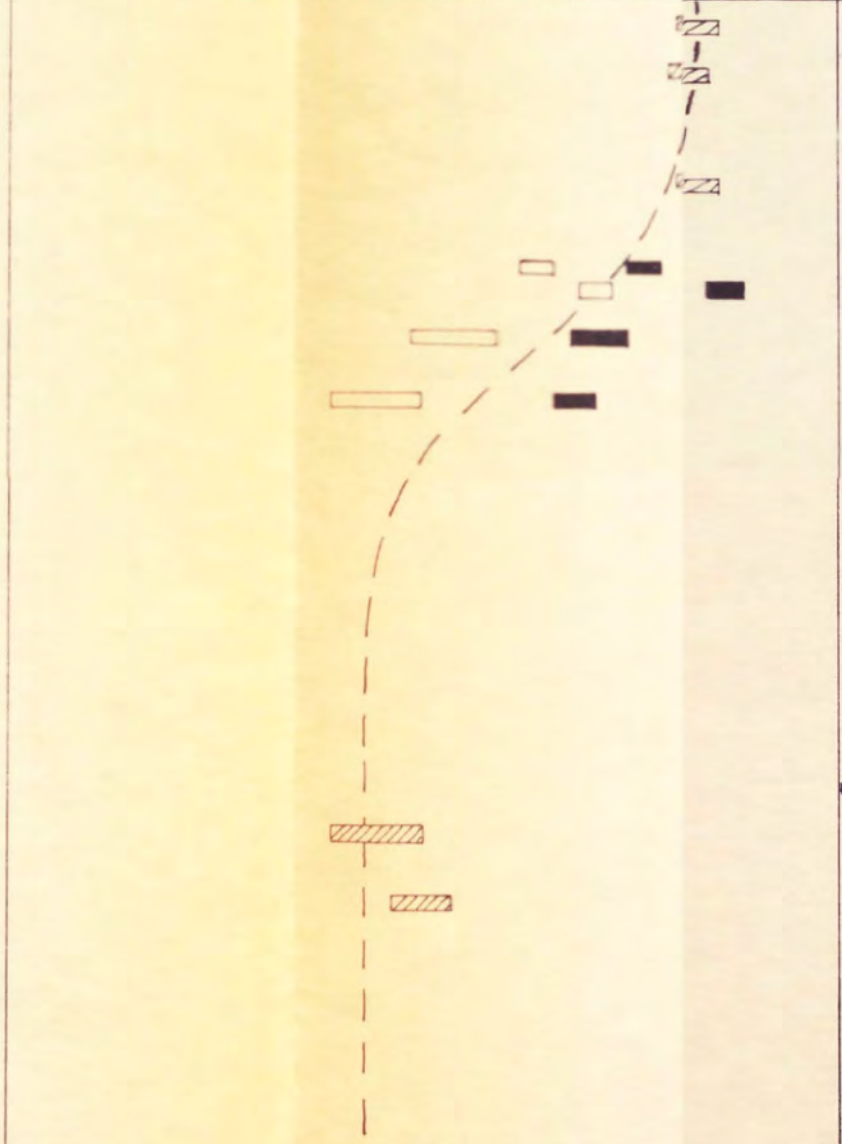
(%)  
10 20 30 40 50 60 70



VERMICULITE KAOLINITE MICA

BIREFRINGENCE RATIO  $\beta$

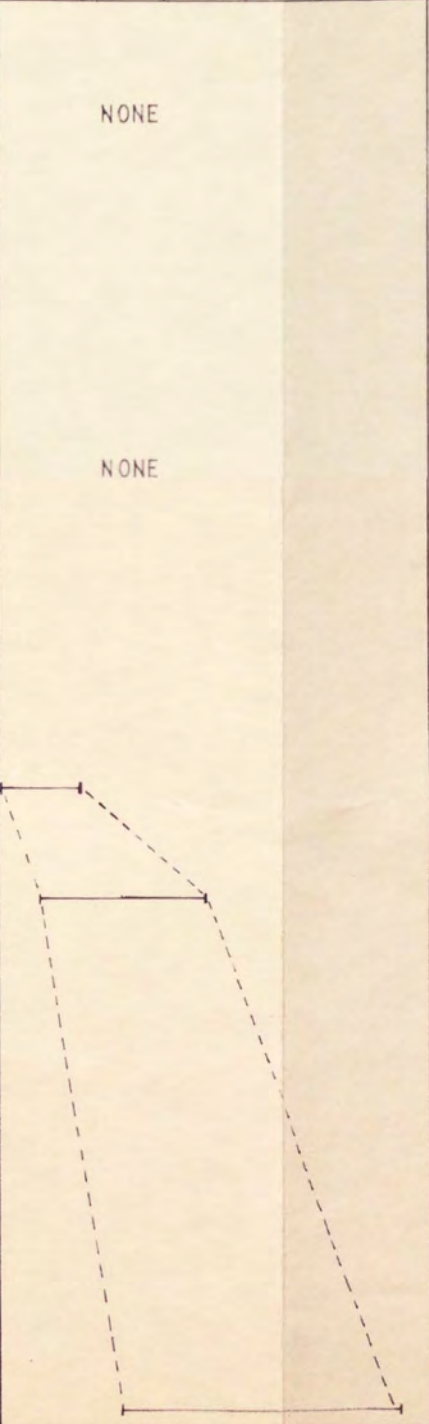
PERFECT STRUCTURE 0 0.1 0.2 0.3 0.4 0.5 0.6 0.7 0.8 0.9 1.0 RANDOM STRUCTURE



AVERAGE TEXTURE LITHORELIC REMOULDED

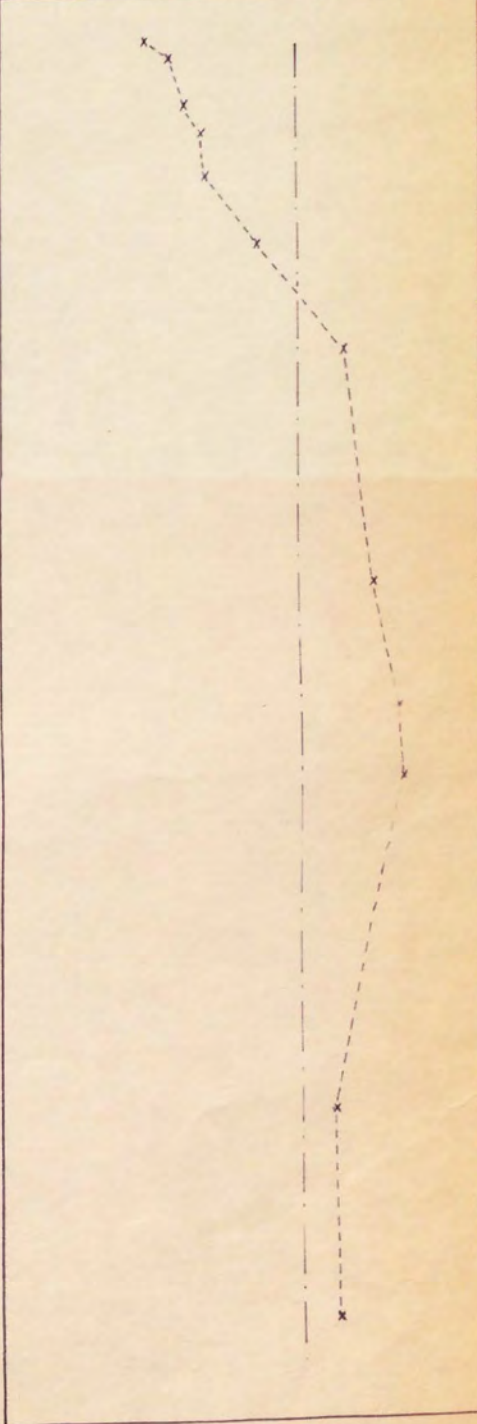
CaCO<sub>3</sub>

(%)  
2.0 4.0 6.0 8.0 10.0



pH

3.0 4.0 5.0 6.0 7.0 8.0 9.0

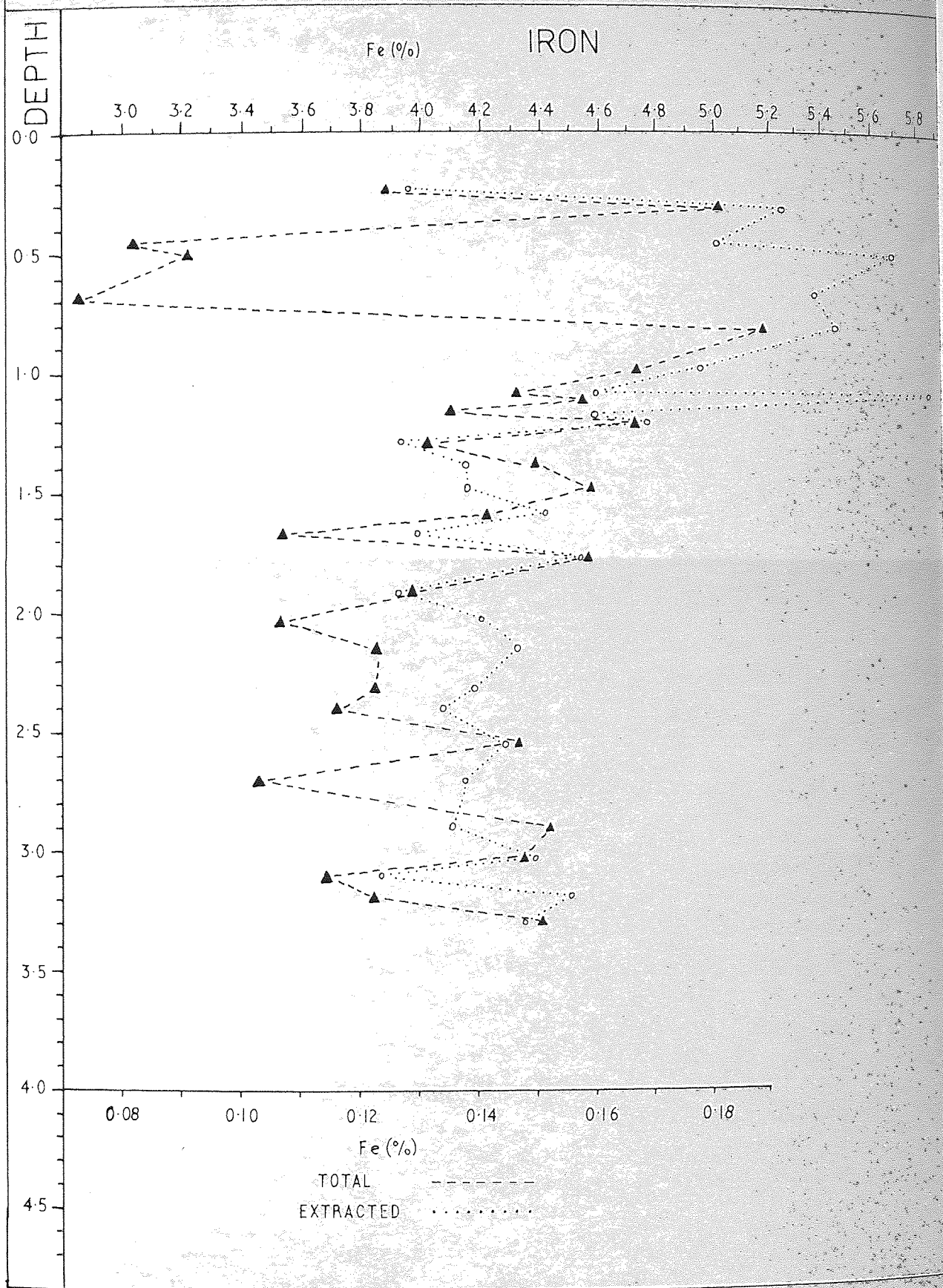


DEPTH  
0.0 0.5 1.0 1.5 2.0 2.5 3.0 3.5 4.0 4.5

FIG 11:1

LOCATION - Blockley (Northcot Brickworks)

Grid ref - SP. 171372



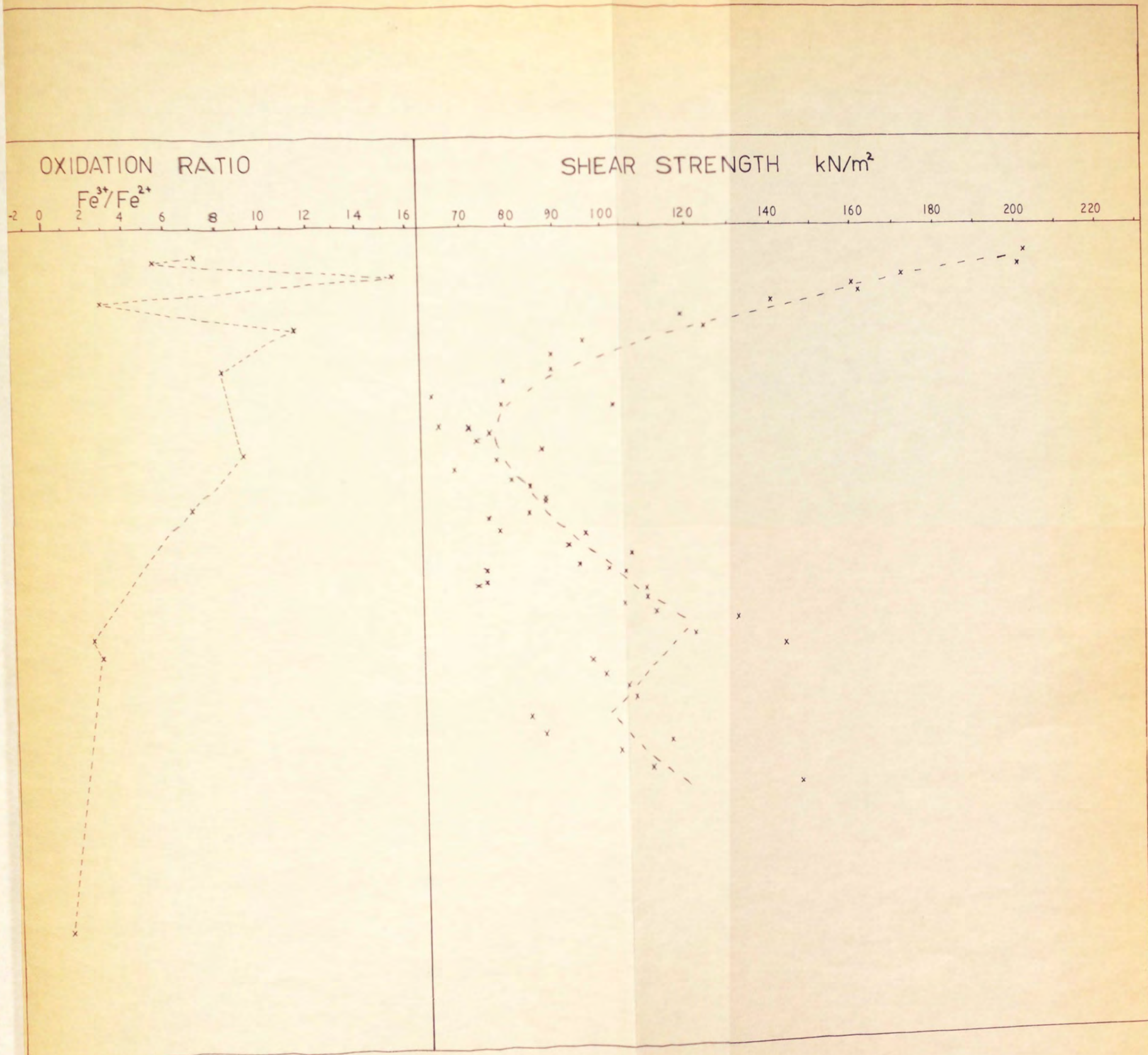


FIG II-1 (cont)

unacceptable for the Lower Lias. It is generally accepted that earth movements causing subsidence, compression and uplift of the Lower Lias occurred prior to the deposition of the Middle Jurassic.

The possibility that this system was produced by valley bulging stresses is ruled out as the position of the site in relation to the surrounding hills would produce shear joints (with slickensides) which would be inclined rather than vertical. It is therefore reasonable to assume that the  $J_1$ ,  $J_2$ ,  $J_3$  sets were formed during the first cycle of subsidence and uplift, an enhancement taking place during the second cycle, with the full development of  $J_1$  occurring with the removal of overburden. The development of  $J_2$  and  $J_3$  taking place in accordance with the decay of tectonic stress as postulated by Price (1966) (Chapter 5).

The inclined conjugate set  $J_4$  and  $J_5$  of which the uniplanar set  $J_5$  is poorly developed are more difficult to explain. The uniplanar set  $J_4$  (dip  $84^\circ - 90^\circ$ E, strike  $164^\circ$ ) are almost vertical in nature and appear both in block and cavity fissure analysis. It may be possible that this set is associated with set  $J_2$  and  $J_3$ . In other words joints  $J_3$  and  $J_4$  may be of the same set with a large variation in strike. To confirm this statistically would necessitate a stereographic plot of some 1000 joint planes. The idea that  $J_3$  and  $J_4$  are possibly associated is suggested since it was noticed that Block 2B (taken well back from the face) did not show any significant development of  $J_5$  joints. Therefore, the formation of  $J_5$  joints could be primarily due to stress release associated with the exposure face.

In the unweathered material fissure intensity is constant but it was very noticeable that the intensity increased in a narrow zone just below the weathering zones. Although there are no statistical figures,

the number of curved fissures also increased at this level. Their development is possibly due to the greater variations of moisture content to which this level is subjected, during seasonal fluctuations in ground-water levels. This state of intense fissuring continued into zone II (Fookes & Horswill 1969) where weathering is confined to the fissure surfaces.

Once weathering has set in to any degree then the fissures become less apparent due to weathering and remoulding occurring on the fissure surfaces. The lithorelicts are the weathered or unweathered cores of the fissure bound segments but they are not remoulded and still retain the structure of the parent material. Fissure analysis now becomes impossible since the stress system within a weathered mass is highly complex, and new systems of fissures may develop along with desiccation fractures. The stress system together with the nature of the material will define the structure of the highly weathered material for which the term ped (Brewer 1964) was originally defined. Fissures in the weathered material will still exist and possibly to some extent in a similar pattern to that in the unweathered material. However, their identification is a problem, and fissures in Zones III, IV could be termed apparent fissures.

The material in Zone V and VI exhibits a polygonal columnar structure often penetrating to 1.6m and a blocky, angular structure existing within these major columns. This structure is due to the desiccation of the surface material.

#### 11:2:2 MICROSTRUCTURE

The microstructures observable in the Lias clay are:

- i) The fabric of the clay.
- ii) structures due to sedimentary and weathering processes.



In the unweathered clay preferred orientation of the clay minerals results in a turbostratic fabric. This is a more realistic representation of a dispersed structure as defined by Aylmore and Quirk (1966). Yong (1971) suggests that a true dispersed structure based on the single plate theory is only applicable in dilute suspensions and therefore turbostratic is a more normal structure.

The turbostratic structure has been subdivided in this investigation into three categories (Fig 6:9, Chapter 6).

1) True Turbostratic.

This forms when the clay minerals are of similar composition and size, with the development of domains with perfect and random orientations.

2) Locked Turbostratic (or Flake Turbostratic).

Similar in form to the Brownian structure of Smart (1969). This forms when flakes of clay minerals (muscovite in the case of Lower Lias clay) of silt size are present in the material. The large flakes highlight the overall preferred orientation of the material and between the flakes exists true turbostratic structure.

3) Grain Turbostratic

This is where silt sized spherical to sub-spherical grains are present in the material. This results in the true turbostratic structure being bent round the grains due to compaction.

This is prevalent in the regions of Lower Lias clay containing a higher percentage of quartz.

The term locked turbostratic, refers to the theoretical way in which this material will behave. Turbostratic should show anisotropic behaviour as regards to strength, due to the preferred orientation of the clay particles. The strength in the case of the locked turbostratic structure will be greater normal to the flakes than for true turbostratic, due to the locking action of the larger silt sized flakes. Thus in terms of anisotropy;

Locked Turbostratic > True Turburbostratic > Grain Turbostratic.

#### 11:2:2:2 SEDIMENTARY STRUCTURES

Folding and remoulding of the unweathered clay as a result of density differences has occurred at specific horizons. The extent of these sedimentary structures is unknown since they were only observable in thin section. This remoulding may only take place in localised areas or specific horizons soon after deposition and this will result in zones and areas of weakness. Shear planes (the movements being observed by the displacement of silt layers) have formed in many horizons. These, together with the density structures could have developed as a result of differential consolidation resulting in movements of one area relative to another. Differential consolidation would be localized and therefore areas may be bounded by a series of small shears producing weakened zones.

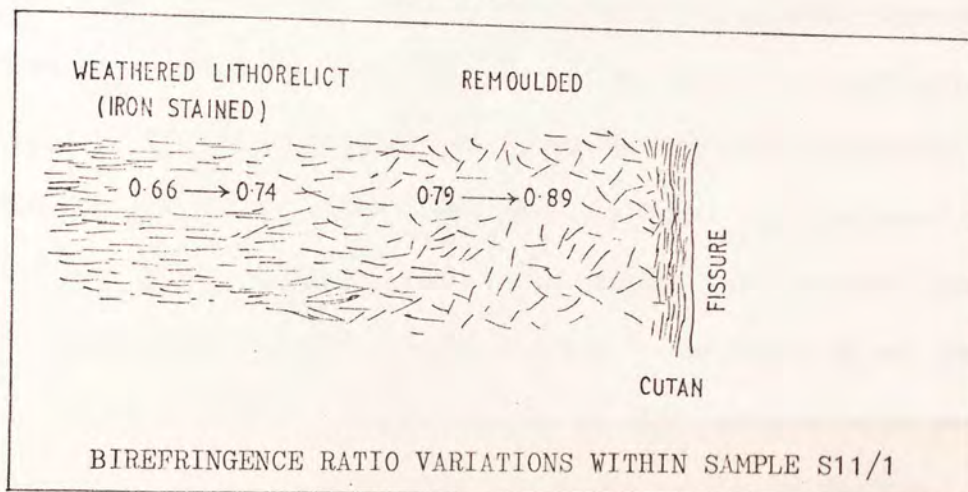
Thus although the material looks uniform in nature it is not; its apparent homogeneity is only due to the small size of the differences.

#### 11:2:2:3 RESULTS OF WEATHERING ON MICROSTRUCTURE

On weathering, the overall structure disappears as remoulding and movement of particles become more prevalent. This is noticeable

in the birefringence ratio which increases with weathering. (Fig 11:1). The lithorelicts (weathered or unweathered) in the weathered clay still retain a birefringence ratio similar to that of unweathered clay. The remoulded material shows marked increase in the birefringence ratio. This is shown well in slide S11/1 where the section shows a lithorelict passing into remoulded material and finally bounded by a fissure (clay cutan) (Fig 11:2).

FIG 11:2



This destruction of original fabric is also seen in the formation of the sedimentary structures where the birefringence ratio is as high as 0.7, whereas orientated unweathered material normally has a birefringence ratio of 0.53 - 0.6.

Remoulding in the weathered material is at its peak in Zones V and VI where the birefringence ratio is greater than 0.8, almost a fully random orientated material. The increase of remoulding with weathering should result in a reduction in anisotropy.

### 11:3 MINERALOGICAL AND CHEMICAL CHANGES

A summary of some of the results are shown in Fig 11:1. The analyses carried out to investigate those chemical changes which were thought most likely to have a significant effect on engineering properties.

### 11:3:1 MINERALOGY

The major minerals are the clays kaolinite and illite, making up 70% to 90% of the material with quartz, pyrite and calcite as subsidiary minerals. Throughout the unweathered material the proportions of clay minerals were relatively constant with minor fluctuations. It was not until the material had been subjected to weathering that variations became significant, especially at the onset of weathering in Zone II. Variations were considerable in Zones V and VI although changes were steady and gradual through Zones III and IV. Mineral counts and percentages are given in Chapter 7.

It was noticed during the scanning electron microscope investigation of the clays, that some clays had what appeared to be growths on their surfaces. These were shown by dispersive X-ray techniques to have a similar composition to the majority of the surrounding material. It is not known if these growths were present on the clays prior to deposition or formed during diagenesis.

### 11:3:2 CHEMISTRY

After the investigation of the mineralogy it was decided that the only possible cements that would affect the strength of the clay would be carbonates and iron compounds.

The carbonate was found associated with shell debris and pyrite. This is quite normal since pyrite and carbonate will precipitate out in similar pH and Eh conditions. The action of anaerobic bacteria produces the necessary sulphur for pyrite formation. During weathering of the clay the carbonate is removed by the percolating water which is mainly acid (Chapter 8). The acidic water often results from the oxidation of pyrite, the resultant sulphuric acid acting with calcite to produce calcium sulphate in solution. Precipitation of calcium sulphate (gypsum)

in the form of selenite was not observed in situ. However, if a piece of unweathered clay was allowed to air dry, the fissures opened and selenite roses formed on the fissure surfaces. This suggests that calcium sulphate was present in the pore water but not in sufficient concentration to allow precipitation. It is only the evaporation of the pore water that increases the concentration of calcium sulphate and thus the formation of selenite.

In the unweathered clay iron exists either in clay minerals, as a surface coating or in pyrite and is therefore present in the  $Fe^{2+}$  and/or  $Fe^{3+}$  state. Oxidation of  $Fe^{2+}$  produces a colour change, therefore it can be used as an indication to the state of weathering (i.e.  $Fe^{3+}/Fe^{2+}$  ratio) (Chapter 8 and 9).

A discussion on Chandler (1972) by Taylor & Spears (1973) suggested that carbonate percentages are subject to depositional rates when associated with argillaceous material; i.e.

- |     |                            |   |   |   |                                   |
|-----|----------------------------|---|---|---|-----------------------------------|
| i)  | slow rate of<br>deposition | → | increased<br>proportion of<br>fossil debris | → | more<br>calcite.                  |
| ii) | high rate of<br>deposition | → | more silt and<br>quartz                     | → | a decrease<br>in fossil<br>debris |

They also suggest that pyrite distribution throughout a profile is not constant, therefore the  $Fe_2O_3 : FeO$  as obtained by Chandler (1972) (by chemical means) could be misleading since the standard redox methods do not determine  $Fe^{2+}$  attributable to pyrite.

The results of the carbonate analyses could be subject to the variations as suggested by Taylor & Spears (1973). The  $Fe^{3+}/Fe^{2+}$  ratio is not as misleading since Mossbauer spectroscopy was

used (Chapter 9). The  $\text{Fe}^{2+}$  due to pyrite (if sufficient is present) can be recognised in the spectrum and accounted for. The  $\text{Fe}^{3+}/\text{Fe}^{2+}$  as identified here is that due to the weathering of the major constituents alone, i.e. the clays.

The use of Mossbauer spectroscopy for iron analysis has also led to a suggestion for the mechanism of weathering for the mica minerals although further work is required to confirm the theory. (Chapter 9).

Mossbauer analysis has also shown that iron oxides increase with weathering and that there are no iron oxide coatings in the unweathered clay. These iron oxides tend to concentrate in the voids and coat the clay flakes. Therefore, it is only in the highly weathered clay that iron oxides may have any effect on the engineering properties of the clay.

#### 11:4 ENGINEERING PROPERTIES

A summary of the properties and the changes with weathering are shown in Fig 11:1. It was unfortunate that  $c'$ ,  $\phi'$  and  $\phi'_r$  results were not available throughout the profile.

The use of shear strength of a soil as obtained by the pocket shear vane can be used to correlate the degree of weathering. A tentative correlation between weathering zones (degree of weathering) and the strength curve was described in Chapter 10, including the "kick back" where the degree of weathering changes dramatically (Fig 11:1).

The relationship between moisture content (controlled to a certain extent by weathering) and shear strength of the soil and suggested by Bjerrum (1967) has been shown to be true and supports the work carried out by Chandler (1972) (Chapter 10).

A correlation was also noted between liquid limit and iron content. The liquid limit increases as iron content increases in a

linear fashion. This increase was small and may be as a result of the changes in clay minerals. A similar linear correlation was obtained by replotting data from Sherwood and Hollis (1966).

#### 11:5 DISCUSSION

On looking back to the original terms of reference for the project, a certain amount of success regarding the degradation characteristics of the Lower Lias clay and the effect on its engineering properties has been achieved. In order to confirm the findings of this investigation the effects of weathering on Lower Lias clay should be examined for several sites in each basin of deposition to obtain an overall picture of the clay and its properties.

It is likely however, that with a clay formed in an environment radically different from that of the Lias clay, changes due to weathering will be either enhanced or reduced. At the present time very few studies of weathering and its effect on heavily overconsolidated clay material have been carried out and therefore further studies are necessary before valid comparisons and deductions can be made.

#### 11:6 FURTHER WORK AND THE VALUE OF TECHNIQUES USED

The majority of the techniques used in this investigation have been developed by other workers. However, modifications were often necessary to ensure results. This was especially so regarding thin sectioning of clay. An improved method of impregnation was achieved by using a special Araldite of very low viscosity under vacuum. This method is very successful for clays of very low permeability that exist in a natural state close to their shrinkage limit.

The use of an  $Fe^{3+}/Fe^{2+}$  ratio as a weathering index is ideal

for weathering studies since it results in a visual colour change which can be related to the ratio. Obtaining the  $\text{Fe}^{3+}/\text{Fe}^{2+}$  ratio by Mossbauer Spectroscopy although rather a sophisticated technique does have advantages over the traditional chemical methods (see 11:3:2 and Chapter 9).

The scanning electron microscope (S.E.M.) although essential for the study of clay fabric, can be restrictive with respect to sample preparation. The new generation of S.E.M. with the combined dispersive X-ray analysis equipment attached, provides the researcher with an excellent piece of equipment, since particles observed can now be analysed directly.

From this investigation several additional topics have been outlined below in which further work would be of value.

- a) A more extensive study of the Lower Lias clay covering every basin of deposition in Britain and obtaining the variations in their geotechnical properties.
- b) A detailed investigation of the weathered material using a scanning electron microscope fitted with dispersive X-ray analysis system.
- c) Further work on the mechanisms of weathering and the removal of elements.
- d) Controlled experiments on the effect and importance of surface coatings of iron oxides on the clay minerals and geotechnical properties of the clay. This could be coupled with controlled experiments on weathering of clays and the changes in geotechnical properties.



- e) The effectiveness of the sodium dithionate citrate system for the removal of iron oxide coatings. This could be investigated using Mossbauer Spectroscopy since  $\text{Fe}_2\text{O}_3$  will show on spectra obtained at  $77^\circ\text{K}$ .
- f) Further work on the neoformation of clays. Does it occur more often in nature than is thought at the present time and were the growths observed, typical?
- g) The subdivision of the turbostratic structure as described in Chapter 11 suggests that the anisotropy in the clay varies with type of structure. An investigation of the relationship between anisotropy and fabric could be carried out.
- h) The density structures observed in the profile may be more extensive than known and if this is so could result in lower observed strengths in these disturbed, remoulded areas. An investigation of the extent of these structures and their effect on properties would prove useful.



## REFERENCES

- Ager, D.V. 1956. The geographical distribution of Brachiopods in the British Middle Lias. *Q. Jl. Geol. Soc. Lond.* 112, p 157 -187.
- Allen, J.E. 1961. The use of organic solvents in atomic absorption spectrophotometry. *Spectrochim. Acta.* 17, p 467 -473.
- American Geological Institute. 1962. Dictionary of Geological Terms. Doubleday, New York.
- Anderson, B.J. & Jenne, E.A. 1970. Free-iron and manganese oxide contents of reference clays. *Soil Science.* 109, No. 3. p 163 - 169.
- Angino, E.E. & Billings, G.K. 1972. Atomic absorption spectrometry in Geology. Elsevier, Amsterdam.
- Arkell, W.J. 1933a. Jurassic System in Great Britain. Oxford University Press.
- Arkell, W.J. 1933b. Analysis of the Mesozoic and Cainozoic folding in England. *Int. Geol. Cong. Report on Session XVI*, p 937 - 952.
- Arkell, W.J. 1947. Geology of Oxford. Oxford University Press.
- Arkell, W.J. 1956. Jurassic Geology of the World. Oliver and Boyd, Edinburgh and London.
- Audley-Charles, M.G. 1970a. Triassic palaeogeography of the British Isles. *Q. Jl. Geol. Soc. Lond.* 126, p 49 - 89.
- Audley-Charles, M.G. 1970b. Stratigraphical correlation of the Triassic rocks of the British Isles. *Q. Jl. Geol. Soc. Lond.* 126, p 19.-47.

- Aylmore, L. and Quirk, J.P. 1966. Domain or turbostratic structure of clays. *Nature. Lond.* 187, p 1046.
- Badgley, P.C. 1965. *Structural and Tectonic Principles*. Harper and Row, New York.
- Bancroft, G.M., Maddock, A.G., Burns R.G. and Stens, R.G.J. 1966. Cation distribution in anthophyllite from Mossbauer and Infra-red Spectroscopy. *Nature, Lond.* 212, p 913 - 915.
- Bancroft, G.M., Maddock, A.G. and Burns, R.G. 1967a. Applications of the Mossbauer effect to silicate mineralogy - I. Iron silicates of known crystal structure. *Geochim. Cosmochim. Acta.* 31, p 2219 - 2246.
- Bancroft, G.M., Maddock, A.G. and Burns, R.G. 1967b. Determination of cation distribution in the cummingtonite - grunerite series. *Am. Mineral.* 52, p 1009 - 1026.
- Bancroft, G.M., Burns, R.G. and Howie, R.A. 1967c. Determination of cation distribution in orthopyroxene by the Mossbauer effect. *Nature, Lond.* 213, p 1221 - 1223.
- Bancroft, G.M., Maddock, A.G. and Burns, R.G. 1968. Application of Mossbauer effect to silicate mineralogy - II. Iron silicates of unknown and complex crystal structures. *Geochim. Cosmochim. Acta.* 32, p 547 - 559.
- Bancroft, G.M. 1970. Quantitative site population in silicate minerals by the Mossbauer effect. *Chem. Geol.* 5, p 255 - 258.
- Banwell, C.N. 1966. *Fundamentals of Molecular Spectroscopy*. McGraw-Hill, London.

- Barden, L. & Sides, G.R. 1970. The influence of weathering on the microstructure of Keuper Marl. *Q. Jl. Engng. Geol.* 3, p 259 - 261.
- Barden L. & Sides, G.R. 1971. Sample disturbance in the investigation of clay structure. *Geotechnique.* 21, p 211 - 222.
- Barden, L. 1972. The relation of soil structure to the engineering geology of clay soil. *Q. Jl. Engng. Geol.* 5, p 85 - 102.
- Berger, L. & Gnaedinger, J. 1949. Thixotropic Strength Regain of Clay. *Bull. Am. Soc. for Testing Materials*, No. 160. p 64 - 68.
- Birks, L.S. 1964. *Electron Probe Analysis.* Wiley, New York.
- Bitterli, J. 1963. Aspects of the genesis of bituminous rock sequences. *Geol. en Mijnbouw.* 42, p 183.
- Bjerrum, L. 1967. Progressive Failure in slopes of overconsolidated plastic clay and clay shales. *Jl. Soil. Mech. Fdn. Div. Am. Soc. Civ. Engrs.* 93, p 3 - 49.
- Boon, J.A. 1971. Mossbauer investigations in the system  $\text{Na}_2\text{O} - \text{FeO} - \text{SiO}_2$ . *Chem. Geol.* 7, p 153 - 169.
- Bowen, L.H., Weed, S.B. & Stevens, J.G. 1969. Mossbauer study of mica and their potassium depleted products. *Am. Mineral.* 54, p 72.
- Bradley, W.F. 1953. Analysis of mixed-layer clay mineral structures. *Analytical Chem.* 25, p 727 - 730.
- Braybrooke, J. 1966. The strength effects and measurements of discontinuities in rock masses. M.Sc. Thesis. University of London.
- Brewer, R. 1964. *Fabric and Mineral Analysis of Soil.* Wiley, New York.

- Bridges, E.M. 1970. World Soils. Cambridge University Press.
- British Standard Code of Practice. CP.2001. 1957. Site Investigations.
- British Standards Institution. BS 1377. 1967. Methods of testing soils for civil engineering purposes.
- Brown, G. 1953. Geological aspects of the St. Austell Granite. Clay Min. Bull. 9, p 17 - 21.
- Brown and Dufeu. 1956. see Perrin 1972.
- Brown, G. 1961. The X-ray identification and crystal structures of clay minerals. Mineralogical Society, London.
- Buckman, S.S. 1901. Bajocian and contiguous deep in the north Cotteswolds. Q. Jl. Geol. Soc. Lond. 57, p 126 - 154.
- Burns, R.G. 1968. Crystal field phenomena and iron enrichments in pyroxenes and amphiboles. Proc. 5th General meeting, Cambridge. I.M.A. Papers (1966). p 170 - 183.
- Burns, R.G. 1969. Site preferences of transition metal ions in silicate crystal structures. Chem. Geol. 5, p 275 - 283.
- Bush, P.R. 1970. A rapid method for the determination of carbonate carbon and organic carbon. Chem. Geol. 6, p 59 - 62.
- Butler, B.E. 1967. Soil periodicity in relation to landform development in south eastern Australia. in Landform studies from Australia and New Guinea; Ed. J.N. Jennings and J.A. Mabbutt. A.N.U., Canberra.
- Callomon, J.H. 1968. see Hallam 1968.
- Carroll, D. 1958. Role of clay minerals in the transportation of iron. Geochim. Cosmochim. Acta. 14, p 1 - 27.

- Casagrande, A. 1932. The structure of clay and its importance in foundation engineering. *Jl. Boston. Soc. Civil Engrs.* 19, p 168.
- Catt, J.A., Gad, M.A., Le Riche, H.H. and Lard, A.R. 1971. Geochemistry micropalaeontology and origin of the Middle Lias ironstones in north east Yorkshire. *Chem. Geol.* 8, p 61.
- Chandler, R.J. 1969. Effect of weathering on the shear strength properties of Keuper Marl. *Geotechnique.* 19, p 321 - 334.
- Chandler, R.J. 1971. Landsliding on the Jurassic escarpment near Rockingham, Northamptonshire. *Inst. Brit. Geogr. Spec. Pubn. No. 2.* p 111 - 128.
- Chandler, R.J. 1972. Lias clay: Weathering processes and their effect on shear strength. *Geotechnique.* 22, p 403 - 431.
- Chester, R. & Elderfield, H. 1971. An infra-red study of clay minerals. The identification of montmorillonite - type clays in marine sediments. *Chem. Geol.* 7, p 97 -105.
- Churchward, H.M. 1963. Soil studies at Swan Hill, Victoria. IV. Ground surface history and its expression in the array of soils. *Austral. Jl. Soil Res.* I, p 242 - 255.
- Coffin, D.E. 1963. A method for the determination of free-iron in soils and clays. *Can. Jl. Soil Science.* 43, p 7 - 17.
- Colbert, M. & Kay E.H. 1965. *Stratigraphy and Life History.* Wiley, New York.
- Compton, D.M.J. & Schoen, A.H. 1961. The Mossbauer Effect. *Proc. 2nd Int. Conf. on the Mossbauer Effect.*

- Davis, A.G. 1966. The mineralogy, structure and engineering properties of the Keuper Marl. Ph.D. Thesis, University of Birmingham.
- David, A.G. 1968. The Structure of the Keuper Marl. Q. Jl. Engng. Geol. 2, p 145 - 153.
- Deer, W.A., Howie, R.A. & Zussman, J. 1966. An introduction to the Rock forming minerals. Longmans, London.
- Denness, B. 1969. Fissures and related studies in selected Cretaceous rocks of south east England. Ph.D. Thesis, University of London.
- Dyer, J.R. 1965. Applications of Absorption Spectroscopy of Organic Compounds. Prentice-Hall, London.
- Dzulynski, St., Cegla, J. & Anketell, J.M. 1969. Unconformable surfaces formed in the absence of current erosion. Geol. Rom. VIII, p 41 - 46.
- Elderfield, H. 1970. Infra-red studies of marine minerals Instrument News, 21, p 14 - 15.
- Engineering Group Working Party, 1972. The preparation of maps and plans in terms of engineering geology. Geol. Soc. Lond. Q. Jl. Engng. Geol. 5, p 295 - 382.
- Fitton, J.G. & Gill, R.C.O. 1970. Oxidation of ferrous iron in rocks during mechanical grinding. Geochim. Cosmochim. Acta. 34, p 518 - 524.
- Fookes, P.G. 1965. Orientation of fissures in stiff overconsolidated clay of the Siwalik System. Geotechnique. 15, p 195 - 206.



- Fookes, P.G. & Wilson, D.D. 1966. The geometry of discontinuities and slope failures in Siwalik Clay. *Geotechnique*. 16, p 305 - 320.
- Fookes, P.G. & Denness, B. 1969. Observational studies on fissure patterns in Cretaceous sediments of south east England. *Geotechnique*. 19, p 453 - 477.
- Fookes, P.G. & Horswill, P. 1969. Discussion on engineering grade zones. Proc. Conf. In Situ Testing of soils and rocks. Instn. Civ. Eng. London. p 53 - 57.
- Fookes, P.G., Dearman, W.R. & Franklin, J.A. 1971. Some engineering aspects of rock weathering with field examples from Dartmoor and elsewhere. *A. Jl. Engng. Geol.* 4, p 139 - 185.
- Freeman, I.L. 1964. Mineralogy of ten British brick clays. *Clay Min. Bull.* 5, p 474 - 486.
- Fry, W.H. 1933. Petrographic methods for soil laboratories. United States Department of Agriculture, Washington, D.C. Technical Bulletin No. 344.
- Gillot, J.E. 1969. Study of the fabric of fine-grained sediments with the scanning electron microscope. *Jl. Sed. Pet.* 33, p 90 - 105.
- Glagolev-Chayes 1933. See Zussman 1967.
- Godwin-Austin, R. 1856. On the possible extension of the Coal Measures beneath the south eastern part of England. *Q. Jl. Geol. Soc. London.* XII, p 38 - 73.
- Goldanski, V.I. 1964. The Mossbauer effect and its applications in Chemistry. (Translation). Consultants Bureau, New York.

- Gramberg, J. 1966. A theory on the occurrence of various types of vertical and subvertical joints in the earths crust. Proc. 1st Congress Int. Soc. Rock Mech. (Lisbon) p 443 - 450.
- Greene-Kelly, R. 1963. Birefringence of clay mineral complexes. Proc. 10th Natn. Conf. on Clays, (London) p 469 - 475.
- Greene-Kelly R. & Chapman, S with Pettifer, K. 1970. The preparation of thin sections of soils using polyethylene glycols. in Micromorphological Techniques and Applications; Eds. D.A. Osmond & P. Bullock Agric. Res. Counc. Soil Survey Tech. Monogr. No. 2.
- Griggs, D. 1935. The strain ellipsoid as a theory of rupture. Am. Jl. Sci. 30, p 121 - 137.
- Grim, R.E. 1934. The petrographic study of clay minerals - A laboratory note. Nl. Sed. Pet. 4, p 45 - 46.
- Grim, R.E., Bray, R.H. & Bradley, W.F. 1937. The Mica in argillaceous sediments. Am. Mineral. 22, p 813 - 829.
- Grim, R.E. & Kulbicki, G. 1961. Montmorillonite. High-temperature reactions and classifications. Am. Mineral. 46, p 1329.
- Grim, R.E. 1968. Clay Mineralogy (2nd Edition). McGraw-Hill, London.
- Gruverman, I.J. Ed. Mossbauer Effect and Methodology, Plenum Press, New York, Vol. 1 (1965), Vol. 2 (1966), Vol. 3 (1967), Vol. 4 (1968).
- Hafemeister, D.W. & Shera, E.B. 1966. Calculation of Mossbauer absorption areas for thick absorbers. Nucl. Inst. Meth. 41, p 133 - 134.

- Hallam, A. 1960. A Sedimentary and faunal study of the Blue Lias of Dorset and Glamorgan. *Phil. Trans. Roy. Soc. B.* 243, p 1 - 94.
- Hallam, A. 1961. Cyclothems, transgressions and faunal changes in the Lias of north west Europe. *Trans. Edinb. Geol. Soc.* 18, p 124 - 174.
- Hallam, A. 1963. Eustatic control of major cyclic changes in Jurassic sedimentation. *Geol. Mag.* 100, p 444 - 450.
- Hallam, A. 1964a. Origin of the Limestone-Shale rhythm in the Blue Lias of England. *Jl. Geol.* 72, p 157 - 169.
- Hallam, A. 1964b. Liassic Sedimentary Cycles in western Europe and their relationships to changes in sea level. *in* *Developments in Sedimentology.* 1, Elsevier, Amsterdam p 517.
- Hallam, A. 1966. Depositional environment of British Liassic Ironstones considered in the context of their facies relationships. *Nature, Lond.* 209, p 1306 - 1309.
- Hallam, A. 1968. The Lias. *in* *The Geology of the East Midlands.* Eds. P.C. Sylvester-Bradley & T.D. Ford, Leicester.
- Hancock, P.L. 1968. Jointing in the Jurassic Limestones of the Cotswold Hills. *Proc. Geol. Ass.* 80, p 219 - 241.
- Harrison, J.L. & Murray, H.H. 1959. Clay mineral stability and formation during weathering, *Proc. 6th Natn. Conf. Clays and Clay Minerals.* (London). p 203 - 213.
- Hawkins, A.B. & Kellaway, G.A. 1971. Field Meeting at Bristol and Bath with special reference to new evidence of glaciation. *Proc. Geol. Ass.* 82, p 267 - 292.

- Hodgson, R.A. 1961. Regional study of jointing in Comb Ridge - Navajo Mountain Area, Arizona and Utah. Bull. Am. Ass. Petrol. Geol. 45, p 1 - 38.
- Honeyborne, D.B. 1951. The clay minerals in the Keuper Marl. Clay Min. Bull. 5, p 150 - 157.
- Hogg, C.S. & Meads, R.E. 1970. Mossbauer spectra of several micas and related minerals. Mineralog. Mag. 37, p 606 - 614.
- Holdrige & Keeling. 1953. See Perrin, R.M. 1972.
- Hudson, J.D. 1964. The petrology of the Great Estuarine Series and the Jurassic palaeogeography of Scotland. Proc. Geol. Ass. 75, p 499 - 528.
- Hull, E. 1855. On the physical geography phaenomena of the Cotteswold Hills. Q. Jl. Geol. Soc. Lond. 11, p 477 - 494.
- Hvorslev, M.J. 1936. Conditions of failure for emoulded cohesive soils. Proc. 1st Intl. Conf. on Soil Mechanics and Foundation Engineering V, p 51 - 53.
- Ismail, F.T. 1970. Oxidation - Reduction mechanism of octahedral iron in mica type structures. Soil Sci. 110, p 167 - 171.
- Kellaway, G.A., Horton, A. & Poole, E.G. 1971. Pleistocene Structures: Cotswolds and Upper Thames Basin. Bull. Geol. Surv. Gt. Britain. No. 37.
- Keller, W.D. 1957. The Principles of Chemical Weathering. Lucas, Columbia, Miss.
- Kendall, P.F. 1905. Sub-report on the Concealed Portion of the Coalfield of Yorkshire, Derbyshire and Nottinghamshire. Final report of the Royal Commission on Coal supplies. Part IX, p 188 - 205.

- Kent, P.E. 1937. Melton Mowbray Anticline. Geol. Mag. LXXIV, p 154 - 160.
- Kent, P.E. 1949. A structure contour map of the surface of the buried Pre-Permian rocks of England and Wales. Proc. Geol. Ass. 60, p 87 - 103.
- Kent, P.E. 1956. The Market Weighton structure. Proc. Yorks. Geol. Soc. XXX, p 197 - 224.
- Kiersch, G.A. & Asce, F. 1964. Vajont reservoir disaster. Civil Engineer. 34, p 32 - 39.
- Klupfel, W. 1917. Uber Die Sedimente der Flashsee in Lothringer Jura. Geol. Rundschau. 7, p 97 - 109.
- Knill, J.L. & Jones, K.S. 1965. The recording and interpretation of geological conditions in the foundations of the Roseires, Kariba and Latiyan dams. Geotechnique. 15, p 94 - 124.
- Krumbein, W.C. & Sloss, L.L. 1958. Stratigraphy and Sedimentation. Freeman, San Francisco.
- Krynine, D.P. & Judd, W.R. 1957. Principles of Engineering Geology and Geotechnics. McGraw-Hill, New York.
- Kuenen, Ph.H. 1953. Significant features of graded bedding. Am. Ass. Petrol. Geol. Bull. 37, p 1044 - 1066.
- Lambe, T.W. & Whitman, R.W. 1969. Soil Mechanics. Wiley, New York.
- Le Riche, H.H. 1959. Distribution of certain trace elements in the Lower Lias of south England. Geochim. Cosmochim. Acta. 16, p 101 - 122.
- Linton, D.L. 1955. The problem of Tors. Geog. Jl. 121, p 470 - 486

- Love, L.G. 1957. Micro Organisms and the presence of syngenetic pyrite. *Q. Jl. Geol. Soc. London.* 113, p 429 - 440
- Mabbut, J.A. 1961. Basal Surface or Weathering Front. *Proc. Geol. Ass. Lond.* 72, p 357 - 358.
- Malathi, N., Puri, S.P. & Saraswat, I.P. 1969. Mossbauer studies of iron in illite and montmorillonite. *Jl. Phys. Soc. Japan.* 26, p 680 - 683.
- Malden, P.J. & Meads, R.E. 1967. Substitution by iron in kaolinite. *Nature, Lond.* 215, p 844 - 846.
- Malpasset Report. 1960. Final report of the investigating committee on the Malpasset Dam. Trans. from the French, Ministerre de l'agriculture, Paris 1960, 2 vols.
- Marsland, A. 1971. Shear strength of stiff fissured clays. Building Research Station, Current Paper 21/71.
- Mehra, O.P. & Jackson, M.L. 1958. Iron oxide removal from soils and clays by a dithionate citrate system. *Proc. 7th Natn. Conf. Clays and Clay Min. (London).* p 317 - 327.
- Millar, C.E., Turk, L.M. & Foth, H.D. 1966. *Fundamentals of Soil Science.* Wiley, New York.
- Millot, G. 1964. *Geology of Clays.* (Trans, 1970), Chapman and Hall, London.
- Mitchell, J.K. 1956. The fabric of natural clays and its relation to engineering properties. *Proc. Highw. Res. Bd.* 35, p 693 - 713.
- Morgenstern, N.R. & Tchalenko, J.S. 1967a. Orientation of clay minerals by birefringence; I. *Proc. Roy. Soc. A.* 300, p 218 - 234.

- Morgenstern, N.R. & Tchalenko, J.S. 1967b. Orientation of clay minerals by birefringence; II. Proc. Roy. Soc. A. 300, p 234 - 250.
- Morgenstern, N.R. & Tchalenko, J.S. 1967c. Microscopic structures in kaolin subjected to direct shear. Geotechnique. 17, p 309 - 328.
- Moye, D.G. 1955. Engineering Geology for the Snowy Mountains Scheme. Jl. Int. Civ. Engrs. Austral. 30, p 287 - 298.
- Muehlberger, W.R. 1961. Conjugate joint sets of small dihedral angle. Jl. Geol. 69, p 211 - 219.
- Murray, H.H. & Leininger, R.K. 1956. Effect of weathering on clay minerals. Proc. 4th Natn. Conf. Clays and Clay Minerals. London. p 340 - 347.
- Nadai, A. 1950. Theory of flow and fracture of solids. McGraw-Hill, London.
- Nahin, P.G. 1955. Infra-red analysis of clays and related minerals. Bull. Div. Mines. California. 169, p 112.
- Nasseri, S. 1972. Laboratory Investigation of Residual Strength of Lias clay from Blockley, Gloucestershire. M.Sc in the Design of Foundation and Structure, University of Aston.
- Ollier, C. 1969. Weathering. Oliver and Boyd, Edinburgh.
- Parker, J.M. 1942. Regional systematic jointing in slightly deformed sedimentary rocks. Bull. Geol. Soc. Am. 53, p 381 - 408.
- Pawluck, S. 1967. Soil analyses by atomic absorption spectrophotometry. Atomic Absorption Newsletter. 6, p 53 - 56.

- Peltier, L. 1950. The geographic cycle in periglacial regions as it is related to climatic geomorphology. *Ann. Assoc. Am. Geog.* 40, p 214 - 236.
- Perrin, R.M.S. 1972. *The Clay Mineralogy of British Sediments.* Mineralogical Society, London.
- Pettijohn, F.J. 1957. *Sedimentary Rocks (2nd Ed.).* Harper, New York.
- Phillips, F.C. 1960. *The use of Sterographic Projections in Structural Geology (2nd edition).* Edward Arnold, London.
- Polynov, B.B. 1937. *Cycle of Weathering (Trans. A. Muir).* Murby, London.
- Pourton & Youell. 1969. see Perrin 1972.
- Price, N.J. 1966. *Fault and Joint Development in Brittle and Semi Brittle Rock.* Pergamon, New York.
- Pusch, R. 1966. Quick Clay Microstructure. *Engng. Geol.* 3, p 433 - 443.
- Quigley, R.M. & Thompson, G.D. 1966. The fabric of anisotropically consolidated sensitive marine clay. *Can. Geotech. Jl.* 3, p 61 - 73.
- Reiche, P. 1950. *A survey of weathering processes and products.* New Mexico University Publ.
- Roberts, J.C. 1961. Feather-fracture and the mechanics of rock jointing. *Am. Jl. Sci.* 259, p 481 - 492.
- Roscoe, K.H. 1967. Discussion of Session 2. *Proc. Geotech. Conf. Oslo.* 2, p 167 - 170
- Rosenqvist, I. Th. 1955. *Investigations in the clay-electrolyte-water system.* Norwegian Geotechnical Institute. Publ. 9. Oslo. p 83 - 87.



- Rosenqvist, I. Th. 1959. Physicochemical properties of soils.  
Proc. Am. Soc. Civ. Engrs. 85, p 31 - 53.
- Ross, C.S. & Hendricks, S.B. 1945. Minerals of the montmorillonite  
group. U.S. Geol. Surv. Prof. Pap. 205B.
- Rowe, P.W. 1972. The relevance of soil fabric to site investigation  
practice - 12th Rankine Lecture. Geotechnique. 22,  
p 195 - 300.
- Ruxton, B.P. & Berry, L. 1957. The weathering of granite and  
associated erosional features in Hong Kong. Bull. Geol.  
Soc. Am. 68, p 1263 - 1292.
- Saunders, M.K. & Fookes, P.G. 1970. A review of the relationship  
of rock weathering and climate and its significance to  
foundation engineering. Engng. Geol. 4, p 289 - 325.
- Schwarzbach, M. 1963. Climates of the Past. Van Nostrand,  
New York.
- Sellwood, B.W. 1972. Tidal-flat sedimentation in the Lower Jurassic  
of Bornholm Denmark. Palaeogeogr. Palaeoclimatology  
Palaeoecol. II, p 93 - 106.
- Sherwood, P.T. & Hollis, B.G. 1966. Studies of the Keuper Marl:  
Chemical properties and classification tests. Road  
Research Laboratory Report No. 41.
- Shotton, F.W. 1953. The pleistocene deposits of the area between  
Coventry, Rugby and Leamington and their bearing upon  
the topographic development of the Midlands. Phil.  
Trans. Roy. Soc. B. 237, p 209.
- Silva, S.R., Spiers, V.M. & Gross, K.A. 1965. Soil fabric study  
with the electron microscope. Report No. 282. Defence  
Standards Laboratory, Victoria, Australia.

- Simpson, S. 1956. On the trace-fossil Chondrites. *Q. Jl. Geol. Soc. Lond.* 112, p 475 - 499.
- Skempton, A.W. 1948. The rate of softening in stiff fissured clays, with special reference to London Clay. *Proc. 2nd Int. Conf. Soil Mech. Rotterdam.* 2, p 50 - 53.
- Skempton, A.W. & Northey, R.D. 1952. The sensitivity of clays. *Geotechnique.* 3, p 30 - 53.
- Skempton, A.W. 1953. The colloidal activity of clays. *Proc. 3rd Int. Conf. Soil Mech. and Found. Engng. Zurich.* 1, p 57 - 61.
- Skempton, A.W. 1960. Terzaghi's discovery of effective stress: from Theory to practice in Soil Mechanics. Wiley, New York.
- Skempton, A.W. 1964. Long-term stability of clay slopes. *Geotechnique.* 14, p 77 - 101.
- Skempton, A.W. & La Rochelle, P. 1965. The Bradwell slip: a short term failure in London Clay. *Geotechnique.* 15, p 221 - 242.
- Skempton, A.W. & Davis, A.G. 1966. see Davis 1966.
- Skempton, A.W., Schuster, R.L. & Petley, D.J. 1969. Joints and fissures in the London Clay at Wraysbury and Edgware. *Geotechnique.* 19, p 205 - 217.
- Smart, P. 1967. Soil structure, mechanical properties and electron microscopy. Ph.D. Thesis, University of Cambridge.
- Smart, P. 1969. Soil structure and the electron microscope. *Proc. Int. Conf. Struct. Solid Mechanics. Engng. Design. Civ. Engng. Mater.* University of Southampton.
- Solomon, I. 1960. Effect Mossbauer dans la pyrite et la marcassite. *C.R. Acad. Sci. Paris.* 250, p 3828 - 3830.

- Spijkerman, J.I., Ruegg, F.C. & DeVoe, J.R. 1965. Standardization of the differential chemical shift of Fe<sup>57</sup> in Mossbauer Effect Methodology. 1, p 115. Ed I.J. Gruverman, Plenum Press, New York.
- Sprenkel-Segel, E.L. & Hanna, S.S. 1964. Mossbauer analysis of iron in stone meteorites. Geochim. et Cosmochim. Acta. 28, p 1913 - 1931.
- Stauffer, M.R. 1966. An Empirical-Statistical study of three dimensional fabric diagrams as used in structural analysis. Can. Jl. Earth Sci. 3, p 473 - 498.
- Stone, 1967. See Bancroft 1967.
- Strakhov, N.M. 1962. Principles of Historical Geology (Part 2) Israel Prog. for Scientific Translations Ltd., Jerusalem.
- Strom, Kaare Munster. 1939. Land-locked water and black muds in Recent Marine Sediments. Ed P.D. Trask. p 356 - 372.
- Taylor, R.K. & Spears, D.A. 1973. Discussion on Lias Clay: Weathering processes and their effect on shear strength (Chandler 1972). Geotechnique. 23, p 131 - 132.
- Tchalenko, J.S. 1968. The microstructure of London Clay. Q. Jl. Engng. Geol. 1, p 155 - 168.
- Terzaghi, K.V. 1936. Stability of slopes of natural clay. Proc. 1st Int. Conf. Soil Mech. Cambridge, Mass. 1, p 161 - 165.
- Terzaghi, R.D. 1965. Sources of error in joint surveys. Geotechnique. 15, p 287 - 304
- Thomas, C.P. 1974. The Mechanical Properties of Heavily Overconsolidated Clay. Ph.D. Thesis, University of Aston.

- Togt, C.v.d. 1963. See Bitterli 1963.
- Tomlinson, M.E. 1963. The Pleistocene Chronology of the Midlands  
Proc. Geol. Ass. 74, p 187 - 202.
- Turner, F.J. & Verhoogen, J. 1960. Igneous and Metamorphic  
Petrology. McGraw-Hill, New York.
- Turner, F.J. & Weiss, L.E. 1963. Structural Analysis of  
Metamorphic Tectonites. McGraw-Hill, New York.
- Urey, H.C., Lowenstam, H.A., Epstein, S. & McKinney, C.R. 1951.  
Measurement of palaeotemperatures of the Upper Cretaceous  
of England, Denmark, and south eastern United States.  
Bull. Geol. Soc. Am. 62, p 399 - 416.
- Vivaldi, J.L.M. & Gallego, M.R. 1961. Some problems in the  
identification of clay minerals in mixtures by X-ray  
diffraction. Clay Min. Bull. 4, p 288 - 292.
- Walsh, A. 1955. The application of atomic absorption spectra to  
chemical analysis. Spectrochim. Acta. 7, p 108 - 117.
- Ward, W.H., Burland, J.B. & Gallois, R.W. 1968. Geotechnical  
assessment of a site at Mundford, Norfolk for a large  
proton accelerator. Geotechnique. 18, p 399 - 431.
- Weaver, C.E. 1956. The distribution and identification of mixed  
layer clays in sedimentary rocks. Am. Mineralog. 41,  
p 202 - 221.
- Weaver, C.E. 1958. A Discussion on the origin of clay minerals in  
sedimentary rocks. Proc. 5th Natn. Conf. Clays and  
Clay Minerals. London. p 159 - 173.
- Weaver, C.E., Wampler, J.M. & Pecuil, T.E. 1967. Mossbauer analysis  
of iron in clay minerals. Science. 156, p 504 - 508.

- Weinert, H.H. 1965. Climatic factors affecting the weathering of igneous rocks. *Agr. Meteor.* 2, p 27 - 42.
- Wertheim, G.K. 1964. *Mossbauer Effect: Principles and Applications.* Academic Press, London and New York.
- Whitaker, T. & Cooke, R.W. 1966. An investigation of the shaft and base resistance of large bored piles in London Clay. *Conf. on large bored piles, London.* Institution of Civil Engineers. p 7 - 49.
- Wobber, F.J. 1967. Post depositional structures in the Lias, south Wales. *Jl. Sed. Pet.* 37, p 166 - 174.
- Wood, A. & Woodland, A.W. 1968. Borehole at Mochras, west of Llanbedr, Merionethshire. *Nature.* 219, p 1352 - 1354.
- Woodland, A.W. 1971. The Llanbedr (Mochras Farm) Borehole. *Inst. Geol. Sci. Rep. No. 71/18.*
- Yong, R.N. 1971. General Report to Session 5. *Soil Technology and Stabilisation. Proc. 4th Asian Reg. Conf. Soil. Mech. Bangkok.* 2,
- Zussman, J. Ed 1967. *Physical Methods in Determinative Mineralogy* Academic Press, London and New York.



APPENDICES

## APPENDIX A

### SAMPLES

Sampling was carried out using a variety of different sampling techniques to assess disturbance factors (examined by Thomas 1974) and secondly to provide samples that gave a representative cover for the soil profile to be examined.

#### A:1 HAND SAMPLES

These were taken throughout the weathered profile and into the unweathered, the sampling interval being very small in order to cover the weathering profile in detail. Two Sections were sampled separated by 100 m. All samples were sealed in foil and placed in plastic bags, water content samples being taken on site.

SECTION ONE (Fig 4:5 Chapter 4).

Sample	Mean Depth (m)	Sample	Mean Depth (m)
S1/1	0.14	S21/1	1.95
S2/1	0.20	S22/1	2.05
S3/1	0.27	S23/1	2.14
S4/1	0.35	S24/1	2.29
S5/1	0.43	S25/1	2.40
S6/1	0.58	S26/1	2.50
S7/1	0.66	S27/1	2.60
S8/1	0.74	S28/1	2.77
S9/1	0.79	S29/1	2.95
S10/1	0.83	S30/1	3.04
S11/1	0.89	S31/1	3.13
S12/1	0.97	S32/1	3.58
S13/1	1.05	S33/1	3.69
S14/1	1.13	S34/1	3.88
S15/1	1.19	S35/1	4.00
S16/1	1.25	S36/1	4.11
S17/1	1.33	S37/1	4.25
S18/1	1.64	S38/1	11.25
S19/1	1.75	S39/1	13.91
S20/1	1.88	S40/1	15.15



## SECTION 2

Sample No	%w	Mean Depth (m)	Gs	Sample No.	%w	Mean Depth (m)	Gs
S1/2	21.00	0.25	2.524	S17/2	20.77	1.78	2.674
S2/2	23.50	0.33	2.590	S18/2	21.13	1.93	2.654
S3/2	22.70	0.43	2.665	S19/2	19.73	1.93	2.687
S4/2	22.40	0.53	2.681	S20/2	20.74	2.03	2.697
S5/2	24.15	0.69	2.825	S21/2	21.15	2.16	2.702
S6/2	21.70	0.84	2.639	S22/2	20.75	2.06	2.681
S7/2	21.80	0.99	2.692	S23/2	20.42	2.18	2.679
S8/2	20.85	1.08	2.657	S24/2	19.60	2.31	2.719
S9/2	21.77	1.12	2.659	S25/2	19.75	2.45	2.702
S10/2	21.14	1.17	2.650	S26/2	20.43	2.60	2.684
S11/2	21.35	1.22	2.620	S27/2	19.22	2.75	2.673
S12/2	21.00	1.30	2.666	S28/2	19.08	2.94	2.659
S13/2	20.65	1.40	2.620	S29/2	19.95	3.05	2.680
S14/2	20.95	1.50	2.696	S30/2	20.44	3.09	2.679
S15/2	26.65	1.60	2.702	S31/2	20.49	3.20	2.658
S16/2	20.48	1.68	2.697	S32/2	19.70	3.30	2.664

w = moisture content

Gs = specific gravity

A:2 BOREHOLE SAMPLES

Three boreholes were drilled by Geotechnical Engineering Limited, Gloucester to investigate the Lias clay. Sampling started at a depth of 8.83 m below the surface, using both diamond coring (mud flush) and hydraulically driven U70s. Core samples were sealed in a similar manner to the hand cut block samples (Chapter 5 ).

A:2:1 BOREHOLE 1

Water Content	Depth (m)	Sample Type
17.25	9.06	Core
17.50	10.04	"
21.30	10.43	"
18.60	11.04	"
16.35	12.95	"

A:2:2 BOREHOLE 2

Water Content	Depth (m)	Sample Type	Gs
16.20	10.38	U70	2.717
19.60	10.70	Core	2.695
18.00	11.67	U70	2.666
18.10	12.63	Core	2.705
17.65	13.26	U70	2.726
18.40	13.89	Core	2.732
18.40	14.57	U70	2.719

Index Test Sample	Depth (m)
B2A	9.13
B2B	10.05
B2C	11.27
B2D	12.19
B2E	13.38
B2F	14.17
B2G	14.47

A:2:3 BOREHOLE 3

Water Content	Depth(m)	Sample Type	Gs
20.5	10.37	U70	2.696
17.3	10.89	Core	2.747
18.6	11.71	U70	2.727
15.9	12.65	Core	2.721
19.1	13.25	U70	2.713
21.8	13.70	Core	2.745
18.6	14.65	U70	2.718

Index Test Sample	Depth(m)
B3A	9.13
B3B	9.75
B3C	10.66
B3D	11.72
B3E	12.41
B3F	13.41
B3G	14.32

A:3 BLOCK SAMPLES

Hand cut block samples were taken at various depths to provide undisturbed samples for strength testing (Thomas 1974) and fissure analysis (Chapter 5).

Block	Water Content	Depth (To Top)
1A	(Base) 18.1, 17.4, 19.0	9.90
1B	not determined	9.90
2A	(Face) 19.4, Base 19.0	10.34
2B	(Face) 17.2	10.35
3A	(Base) 17.7, 19.2	10.91
3B	(Base) 17.7, 17.8	10.92

## APPENDIX B

### A METHOD OF OBTAINING THE OPTIMUM SAMPLE SIZE FOR A TRULY REPRESENTATIVE FISSURE FABRIC PROPOSED BY STAUFFER, M.R. (1966)

#### B:1 SIMPLE FABRICS (WITH ONE CONCENTRATION).

1. First plot and contour 100 points
2. If no preferred-orientation is apparent, plot an additional 300 points and contour all 400. If the diagram still shows no preferred-orientation it probably is a random distribution. Many workers claim an interest only in strongly preferred-orientations. In such cases, 100 points are sufficient to indicate a fabric of interest.
3. If step 1 yields a single point maximum with a 20% or higher value the fabric probably is truly representative and little could be gained by plotting more data.
4. If step 1 results in a single point maximum with a maximum contour value between 12% and 20% then 100 more points making a total of 200 should be sufficient
5. If step 1 results in a fabric with a single point maximum and a value between 8% and 12% then about 200 more points making a total of 300 are required.
6. If the maximum contour is between 4% and 8% but low value contours have at least a crude axial symmetry then a total number of between 600 and 1,000 points will probably be required.
7. If a result similar to step 6. but with a maximum contour value of 4% or less is obtained, then 1,000 points are probably necessary.
8. Should step 1 yield a diagram with several point maxima lying approximately in a girdle arrangement then the procedure is more complex and depends on the value of the scattered point maxima as well as on the angular distance between the 1% contours. It would therefore be best to plot at least another 100 points before one attempts to determine the optimum sample size.

9. If step 8 yields a fabric with 1% contours less than  $15^{\circ}$  apart and with no point maxima larger than twice the value of the highest girdle contour then the fabric probably is truly representative, although the point maxima must be ignored unless they are duplicated almost exactly on three or more successive diagrams.
10. If step 8 results in a diagram with the 1% contours fairly smooth and about  $20^{\circ}$  apart but with several 3% to 6% point maxima then another 200 points may be sufficient.
11. If after adding the second 200 points, the values of the point maxima decrease and they change position then 400 points are sufficient but the point maxima must be ignored.
12. Should the point maxima, however, remain in their original positions after step 10 then another 200 points, making a total of 600 points, must be plotted to ensure that they are real and not a function of sampling.
13. After step 8 is completed should the diagram contain several point maxima between 3% and 6% but with very irregular 1% contours then at least another 400 points must be added.
14. Depending on what changes in the fabric step 13 causes, operation of either step 11 or 12 will hold. In the case of step 12 another 400 rather than 200 points must be added.
15. If after step 8, the 1% contour is very irregular and no point maxima are greater than 3%, especially if they are extremely scattered, then a total of at least 1,000 points and possibly 2,000 points will be required, and any point maxima of less than 2% must be ignored.

B:2 COMBINED FABRICS (fabric with more than one concentration or type of concentration).

In general, combined fabrics require at least twice as many points as do simple fabrics for similar concentration strengths. For

combined fabrics, however, the maximum contour value is not a direct indication of the concentration strength; the various components of such diagrams affect each other so that concentrations similar to those in simple fabrics are represented by lower contour values. The simplest way to treat combined fabrics is to plot sub-fabrics of 100 points or more, depending on the apparent strength of the fabric. If after plotting 400 points, the addition of 200 more still produces changes in the fabric, then at least another 400 points will be required. If these last 400 points are themselves any different from the original 400 then 400 points may be necessary, making a total of 1,400.

A fabric with two girdles, each with a concentration strength similar to the model girdle population, was found to require at least 2,000 and preferably 4,000 points for differentiation. It is doubtful, of course, if such fabrics are worth studying, especially with reference to engineering significance. They would probably appear to be random distributions for sample sizes up to 400 points.

## APPENDIX C

### X-RAY ANALYSIS

As it has previously been stated the identification of clays by X-ray diffraction is now a standard technique although still specialized. The techniques used will be outlined here and one is referred to the articles by Grim (1968), Brown (1961), Millot (1964) etc., for further and additional details.

#### C:1 X-RAY PRODUCTION

X-rays are produced when a rapidly moving stream of electrons impinges upon atoms of matter placed in its path. The character of the X-rays emitted being dependant upon the initial velocity and nature of the target material. The strongest X-rays are produced by collision of electrons with the electrons in the K shells of the atoms of the target material, and are of two types  $K_{\alpha}$  and  $K_{\beta}$ . For clay mineral identification a copper target is normally used and the  $K_{\alpha}$  X-rays being directed to the sample, thus the  $CuK_{\beta}$  must be screened off by the use of a filter (Nickel in the case of copper) (Table C:1).

TABLE C:1

Target	Wavelength		Filter
	$K_{\alpha}$	$K_{\beta}$	
Cu	1.5418	1.39217	Nickel
Co	1.7902	1.62073	Fe (Iron)
Fe	1.9373	1.75654	Mn (Manganes)

The X-rays on striking the sample are reflected from lattice planes according to the Bragg Law.

$$n\lambda = 2d(hkl) \sin \theta$$

where  $d$  = lattice spacing for the planes (hkl)  
(hkl) = indices for the lattice plane  
 $\lambda$  = wave length of X-rays  
 $\theta$  = glancing angle of reflection (Bragg angle)  
 $n$  = the order of the reflection.

N.B. For clays the basal spacings (001 planes) are used for identification.

$\text{CuK}_{\alpha}$  radiation does have the effect of causing fluorescence of iron, thus increasing the level of background radiation with the resultant effect of obscuring peaks of low intensity. This can be overcome by using either  $\text{Fe K}_{\alpha}$  or  $\text{CoK}_{\alpha}$  radiation or by removing excess iron and iron oxides by the Mehra and Jackson (1958) sodium citrate method.

## C:2 RECORDING TECHNIQUES

Clay minerals can be identified by recording the reflections either photographically or using a diffractometer. Both techniques have advantages but special modifications are necessary with most powder cameras Davis (1966).

Clay minerals have basal spacings from  $7\text{\AA}$  -  $30\text{\AA}$ . Cameras that can measure up to  $30\text{\AA}$  are suitable but the majority cannot measure above  $15\text{\AA}$  and are therefore useless and must be modified. The problem is that the Bragg angle of clays is very small and therefore scattering near the collimeter (exit and entrance point) obscures the evidence on the photographic plate unless a semi-focusing camera is employed.

Diffractometers are easier and more rapid since the trace for an identification can be obtained in less than 30 minutes.

The equipment used during this investigation was a Siemens and a Jeol X-ray diffractometer both capable of measuring from



$2^{\circ}(2\theta)$  upwards. A scan rate of  $1^{\circ}(2\theta)$  per minute was used for general survey work and initial results with a rate of  $2^{\circ}(2\theta)$  per minute for detailed examinations.

### C:3 TYPES OF POWDER SPECIMEN

Clays are platy minerals and the first step is the identification of the 001 basal reflections and a sample where the 001 planes are orientated in a specific direction enhances the diffraction peaks. Thus for identification work orientated samples are the best but for quantitative work the samples must be random.

#### C:3:1 ORIENTATED FLAT-LAYER SPECIMENS

A thin clay layer deposited on a glass slide can be ideal for diffractometers. They can also be heated and treated directly. These slides can be produced by several means:

- (a) Centrifuging
- (b) Sedimenting
- (c) Suspension, evaporation

Glass slides will produce a large background swell at  $25^{\circ}$  to  $30^{\circ}(2\theta)$ . This can be almost eliminated using a low scattering quartz specimen plate. This could also be eliminated by the use of a porous ceramic plate.

#### C:3:2 ORIENTATED AND NON-ORIENTATED ROD-TYPE SPECIMENS

These are mainly used with powder cameras (but can be used with diffractometers) and can be produced by several methods.

##### Orientated.

- (a) External coating of a thin capillary tube.
- (b) Mixing clay with glue and rolling into a thin rod.

### Non-orientated.

- (a) Pouring dry powder into a thin-walled capillary and tapping gently to consolidate the powder.
- (b) Extruding clay paste through a hypodermic needle gives a well formed cylinder with only slight orientation of the 001 planes parallel to the axis of the cylinder.

### C:3:3 NON-ORIENTATED PLATE SPECIMENS

These are produced by having a cavity in a glass plate, the cavity being filled with sufficient powder so that one smoothing action will produce a flat surface flush with the glass.

If sufficient material is available a cavity 1-3mm deep can be used and the material tamped down gently without any shearing motion or undue pressure, and any excess removed. Absence of orientation is not guaranteed but it is probably at a minimum. This was the method used for this investigation.

### C:4 SAMPLE PREPARATION AND SIZE

The analysis can be carried out on either the whole rock sample or on a specific size fraction i.e.  $< 2\mu$ . Pourton and Youell (1969) stress that rocks containing clay minerals should be subjected to the absolute minimum pretreatment which should if possible be restricted to grinding to produce a homogenous sample.

In this study a large sample of 5 gms was ground and then sampled statistically by using a Glen Creston Sample Divider (Model PT.) to obtain a representative sample. This

sample was then used for both X-ray and chemical analysis, no further pretreatment was carried out.

With many rocks it is common to concentrate clay minerals into a suitable size fraction by dispersion and sedimentation. In some cases eg. limestones, one must remove carbonates using a mild reagent such as buffered acetic acid. In any such analyses where one has only examined a specific size fraction, the proportion of rock which the fraction represents, must always be stated. Analysis without this proportion is useless. Where clays constitute 50% to 90% of the rock, concentration of a particular mineral group is unnecessary.

#### C:5 QUANTITATIVE ANALYSIS

There is no special system for the routine quantitative analysis of clay mineral mixtures. For highly accurate determinations the use of standard clay minerals is recommended. However one is dependant on obtaining pure minerals similar to the components in the mixture to be analysed. This is particularly difficult because clays are so variable.

For special situations it may be possible to use a precise method which involves the extraction of individual clay minerals from the samples themselves.

Here a method proposed by Shaw et al. (1970) has been used in which the following assumptions are inherent.

a) The clay minerals comprise 100% of the sample, whereas in many cases, there are other minerals present as well as amorphous material.

b) That the refracting ability of the clay minerals, which is generally dependent on the composition, polytype and degree of crystallinity is consistent.

c) That there is a 1:1 linear relationship between the ratio of the 3.58Å kaolinite peak to the 3.54Å chlorite peak.

X-ray diffraction traces of the original untreated sample, and after ethylene glycol treatment and heating to 180°C for 1 hour are required.

a) On the 180°C trace, measure the heights of the 7Å and 10Å peaks. Calculate the total percent kaolinite (K) and/or chlorite (C) as follows:-

$$\frac{h_{7\text{\AA}} (180^\circ)}{2.5}$$

$$\% K + C = \frac{\frac{h_{7\text{\AA}} (180^\circ)}{2.5}}{\frac{h_{7\text{\AA}} (180^\circ)}{2.5} + h_{10\text{\AA}} (180^\circ)} \times 100$$

b) On the 180°C trace measure the heights of the 3.54Å and 3.59Å peaks. These heights are used to apportion the 7Å peaks into % kaolinite and % chlorite as follows:-

$$\% K = \frac{h_{3.59\text{\AA}} (180)}{h_{3.59\text{\AA}} (180) + h_{3.54\text{\AA}} (180)} \times \% K + C$$

$$\% C = \% (K+C) - \% K$$

c) Calculate total percent illite (I) and/or montmorillonite (M) as follows using peak heights from the 180°C trace.

$$\% I + M = \frac{h \ 10\overset{\circ}{\text{A}} (180)}{\frac{h \ 7\overset{\circ}{\text{A}} (180)}{2.5} + h \ 10\overset{\circ}{\text{A}} (180)} \times 100$$

d) Measure the 7Å and 10Å peak heights on the ethylene glycol trace. Use these measurements and those above from the 180°C trace to calculate percentages of illite and montmorillonite as follows:-

$$\% I = \frac{h \ 10\overset{\circ}{\text{A}} (\text{EG}) \left( \frac{h \ 7\overset{\circ}{\text{A}} (180)}{h \ 7\overset{\circ}{\text{A}} (\text{EG})} \right)}{h \ 10\overset{\circ}{\text{A}} (180)} \times \% (I + M)$$

$$\% M = (\% I + M) - \% I$$

## APPENDIX D

### CHEMICAL ANALYSIS

#### D:1 CALCITE ANALYSIS

In the analysis, calcite,  $\text{CaCO}_3$  is calculated from the amount of carbon dioxide,  $\text{CO}_2$ , that is evolved from a sample treated as described.

#### D:2 SAMPLE PREPARATION

A sample weighing 20 - 25 gms is taken and dried and then ground to pass a British Standard Sieve No.120 (125  $\mu\text{m}$ ). This ground sample was then placed in a sample splitter (Glen Creston Sample Splitter) and the sample split into six. One of the sub-samples was split into thirds thus yielding approximately 1 g which was weighed and placed in flask A (Fig D:1). A second 1 g sample was also tested and unless the results were not reproducible the third gram was discarded.

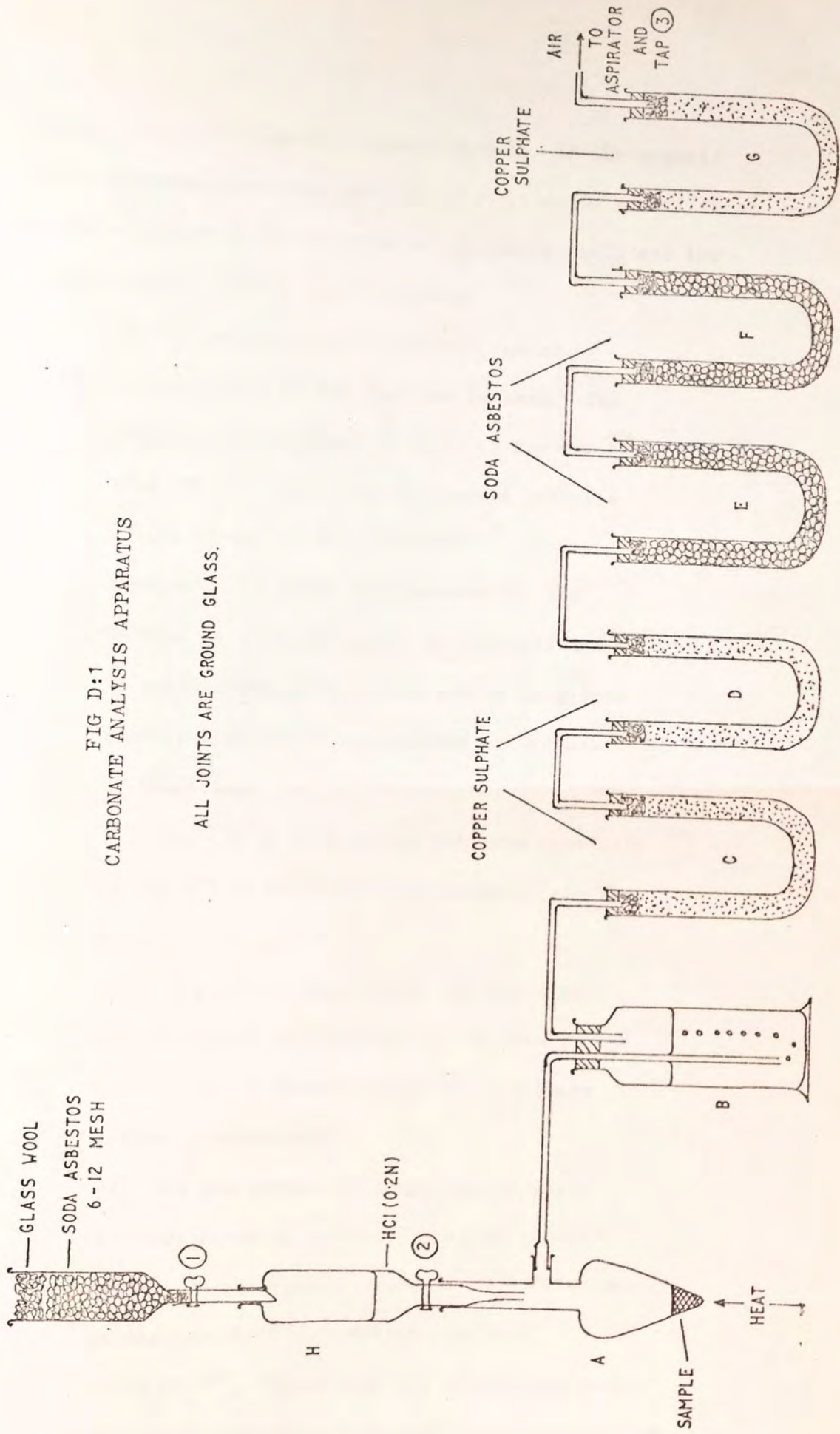
#### D:3 PROCEDURE

The apparatus and set up is as shown in Fig D:1 all joints and connections being ground glass. Initially all taps are closed and the joints sealed and the sample in flask A is placed in position. The U-tubes E and F which contain the soda asbestos (6 - 12 mesh) are weighed prior to the experiment since it is here that the carbon dioxide evolved from the sample will be retained by absorption. The funnel H is then filled with 10 ml of 0.2N HCl or 10 ml of syrupy ortho-phosphoric acid. Either can be used although ortho-phosphoric is recommended if metals are being tested.

This method can also be used to obtain the organic carbon content in which case phosphoric acid with the addition of 2 ml of 150% w/v chromium trioxide solution to the phosphoric acid

FIG D:1  
CARBONATE ANALYSIS APPARATUS

ALL JOINTS ARE GROUND GLASS.



must be used to oxidise the organic carbon. If the organic carbon is being determined then all the carbonate should first be removed prior to the addition of phosphoric acid and the solution must be boiled for 15 minutes.

i) The aspirator is filled with water or alternatively an air pump can be used. The tap (3) is opened and if there is any leakage from the aspirator then this would indicate a leak in one of the connections. It is advisable to place taps between all the U-tubes in order to ensure no leakages and to prevent taking the whole set up to pieces since a leak can be pinpointed by the use of these taps.

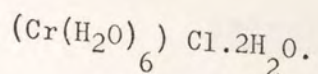
ii) Tap (2) is then opened followed carefully by tap (1) to allow the acid to drip onto the sample.

iii) Tap (2) is then closed and the sample heated. After boiling, tap (2) is then opened and the gas is drawn through the following series of containers.

iv) The gas bubbles through flask B which contains chromium trioxide in ortho-phosphoric acid. The chromium trioxide ( $\text{Cr}_2\text{O}_3$ ) dissolves in the acid to form hydrated ions i.e.

$(\text{Cr}(\text{H}_2\text{O})_6)^{3+}$ . These ions are strong complexing agents and therefore will remove gaseous HCl and  $\text{H}_2\text{O}$  from the  $\text{CO}_2$  gas by forming complexes i.e.





In case all the water is not removed the gas passes through a U-tube C containing anhydrous copper sulphate. During the experiments this hardly changed colour showing that the chromium trioxide in ortho-phosphoric acid was very efficient.

v) The  $\text{CO}_2$  carbon dioxide is collected in U-tubes, D and E and to ensure that all the  $\text{CO}_2$  is collected, air, (removed of  $\text{CO}_2$ ) is passed through the apparatus for 1 - 2 hours.

vi) All the taps are then closed and the U-tubes D and E are removed and weighed.

Any increase in weight is due to  $\text{CO}_2$  which is then expressed as a percentage of the oven-dry weight.

#### D:4 CALIBRATION

In order to check the equipment 1gm of Analar calcium carbonate was used. This should evolve 44 percent by weight of carbon dioxide. The apparatus when tested was accurate to within one percent.

#### D:5 CALCULATION

The percentage of calcite ( $\text{CaCO}_3$ ) in the sample is found by the following calculation.

$$\% \text{CaCO}_3 = \frac{2.3 \times \text{Wt. CO}_2}{\text{Sample Wt.}} \times 100$$

## APPENDIX E

### INFRA-RED SPECTROSCOPY

#### E:1 INTRODUCTION

The field of Spectroscopy is divided into emission and absorption spectroscopy, Infra-Red Spectroscopy being an absorption method.

An absorption spectrum is obtained by placing the substance between the spectrometer and some source of energy that provides electromagnetic radiation in the frequency range being studied. The atoms are excited by this bombardment of energy from their ground state to a state of higher energy, to reach this higher energy state they must therefore absorb energy. The spectrometer analyzes the transmitted energy relative to the incident energy for a given frequency. In the case of infra-red spectroscopy the wavelength of the electromagnetic radiation use is shown below.

0.8  $\mu\text{m}$  to 2.5  $\mu\text{m}$  (12,500 - 4000  $\text{cm}^{-1}$ ) near infra-red

2.5  $\mu\text{m}$  to 15  $\mu\text{m}$  ( 4,000 - 667  $\text{cm}^{-1}$ ) infra-red

15  $\mu\text{m}$  to 200  $\mu\text{m}$  ( 667 - 50  $\text{cm}^{-1}$ ) far infra-red

For a more detailed description of the infra-red technique one is referred to Banwell (1966) where he described the types of vibration (stretching, bending and rotation) and for the wavelengths necessary to provide the given energy to Zussman (1967) and Dyer (1965).

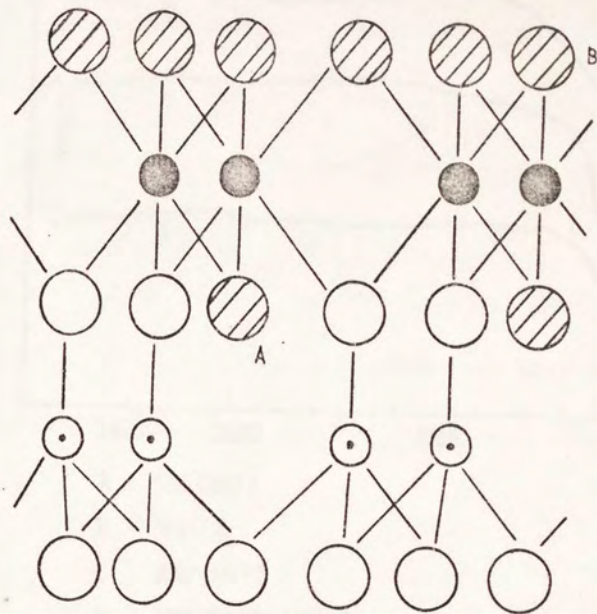
#### E:2 SAMPLE PREPARATION





To provide satisfactory infra-red spectra the samples are diluted by an almost inert medium, each medium having certain advantages with regard to the absorption range and its spectrum.

The most common medium is KBr and a 10mg sample is mixed with KBr and ground together with 10 drops of absolute alcohol and finally pressed into a disc. Pregrinding to give 90% of the sample less than  $2\mu\text{m}$  in size is recommended, but with clays this brings in the added danger of altering the clay structure through stress and heat generated during the grinding process. Therefore grinding by hand to less than  $75\mu\text{m}$  is adequate. KBr has the disadvantage of having an absorption range in the infra-red i.e.  $2.5\mu\text{m} - 15\mu\text{m}$ . It was therefore decided to use CsI as the diluent and produce CsI discs, CsI having a range from  $2.5\mu\text{m} - 40\mu\text{m}$  Elderfield (1970) Zussman (1967). The use of halide discs and pellets allows quantitative sample preparation. The absorption peaks in a spectrum are quoted either as the wavelength of the infra-red in microns ( $\mu\text{m}$ ) or as the wavenumber ( $\text{cm}^{-1}$ ) (the number of waves per centimetre).

Infra-red studies of clays and minerals have been carried on for some time Elderfield (1970), Grim and Kulbicki (1961), Chester and Elderfield (1971), Nahin (1955). In some cases accurate determinations were possible for example Grim and Kulbicki were able to differentiate between dioctahedral and trioctahedral clays on the basis of the sensitivity of their infra-red spectra to incidence angle of the sample in the infra-red beam. However, because of the complex nature of sediments, practical limitations are placed on the usefulness of infra-red techniques.

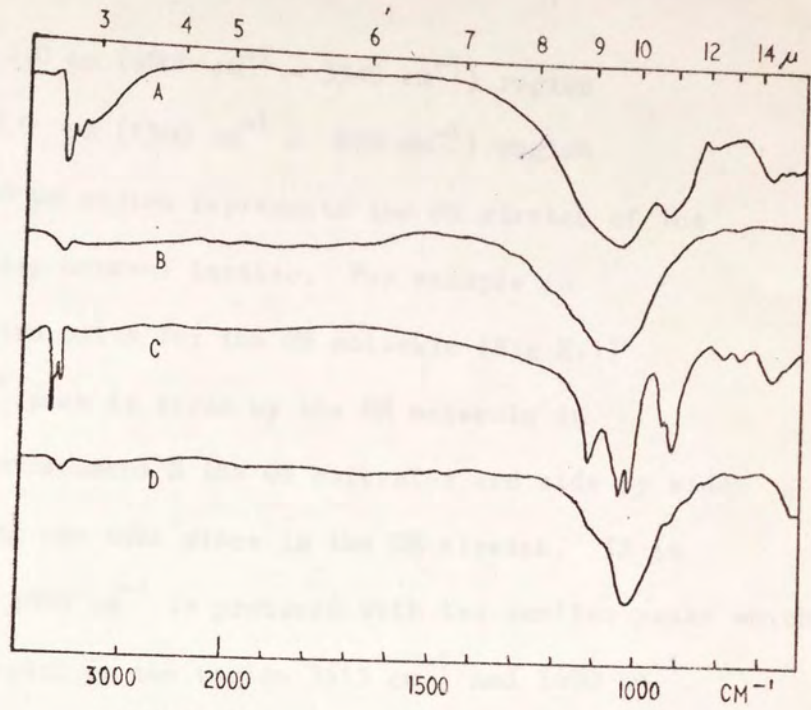
A prime example is the identification of clay minerals by infra-red spectroscopy. Clay minerals show two main regions of absorption:



-  OH group.
-  Oxygen.
-  Aluminium.
-  Silicon.

Crystal Structure of Kaolinite.

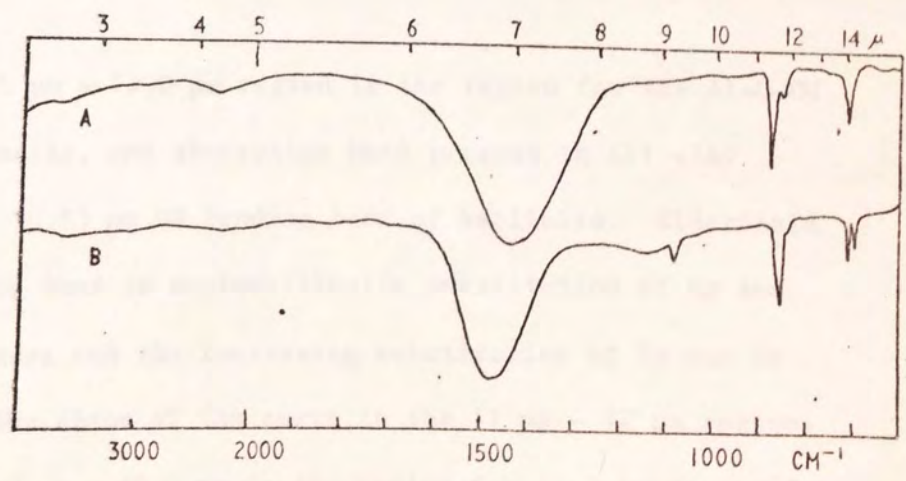
FIG E:1



- A : CHLORITE
- B : ILLITE
- C : KAOLINITE
- D : MONTMORILLONITE

TYPICAL INFRA-RED SPECTRA OF CLAY MINERALS  
AFTER ELDERFIELD 1970

(a)



- A : CALCITE
- B : ARAGONITE.

AFTER ELDERFIELD 1970.

(b)

FIG E:2

- a) 2.5 - 3.0  $\mu\text{m}$  ( $4000\text{ cm}^{-1}$  -  $3340\text{ cm}^{-1}$ ) region
- c) 8 - 40.0  $\mu\text{m}$  ( $1300\text{ cm}^{-1}$  -  $870\text{ cm}^{-1}$ ) region

The 2.5 - 3.0  $\mu\text{m}$  region represents the OH stretch of the OH molecule in the clay mineral lattice. For example in kaolinite there are two sites for the OH molecule (Fig E:1)

The  $3615\text{ cm}^{-1}$  peak is given by the OH molecule in environment A. In environment B the OH molecules are side by side and therefore coupling can take place in the OH stretch. If in phase then a peak at  $3690\text{ cm}^{-1}$  is produced with two smaller peaks which show out of phase stretch in the region  $3615\text{ cm}^{-1}$  and  $3690\text{ cm}^{-1}$ . (Nahin 1955).

The infra-red spectrum of the main clay minerals are shown in Fig E:2 (Elderfield 1970). It can be seen from these that the variations in spectra for identification purposes can if more than one clay variety is present cause problems that can be resolved more accurately using x-ray diffraction. However the infra-red spectrum can give us an indication of the minerals present.

The 8.0  $\mu\text{m}$  - 12.0  $\mu\text{m}$  region is the region for the Al-O-OH bending frequencies, one absorption band present in all clay spectra is the 10.93  $\mu\text{m}$  OH bending band of kaolinite. Elderfield (1970) has shown that in montmorillonite substitution of Mg and  $\text{Fe}^{3+}$  for Al occurs and the increasing substitution of Fe can be detected from the shape of the curve in the 11  $\mu\text{m}$  - 12  $\mu\text{m}$  region.

The 12.0  $\mu\text{m}$  - 40.0  $\mu\text{m}$  is the region for Si-O bending and Si-O-Si bending and stretching since these require less energy.

### E:3 RESULTS

Prior to any serious work, an infra-red spectrum of a sample

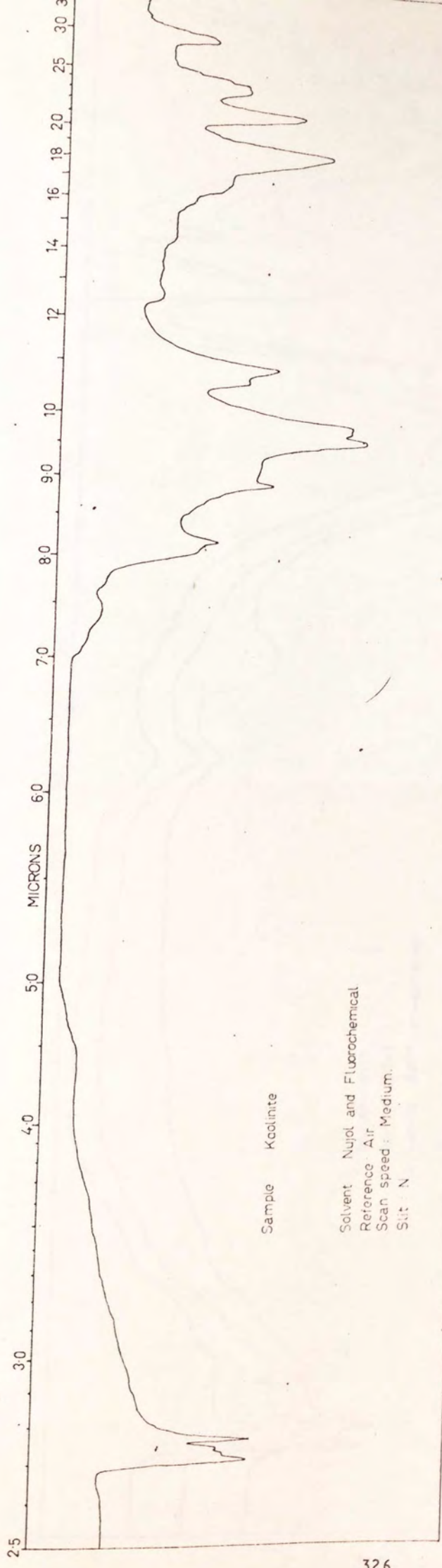


FIG E:3 IR-SPECTRUM OF KAOLINITE

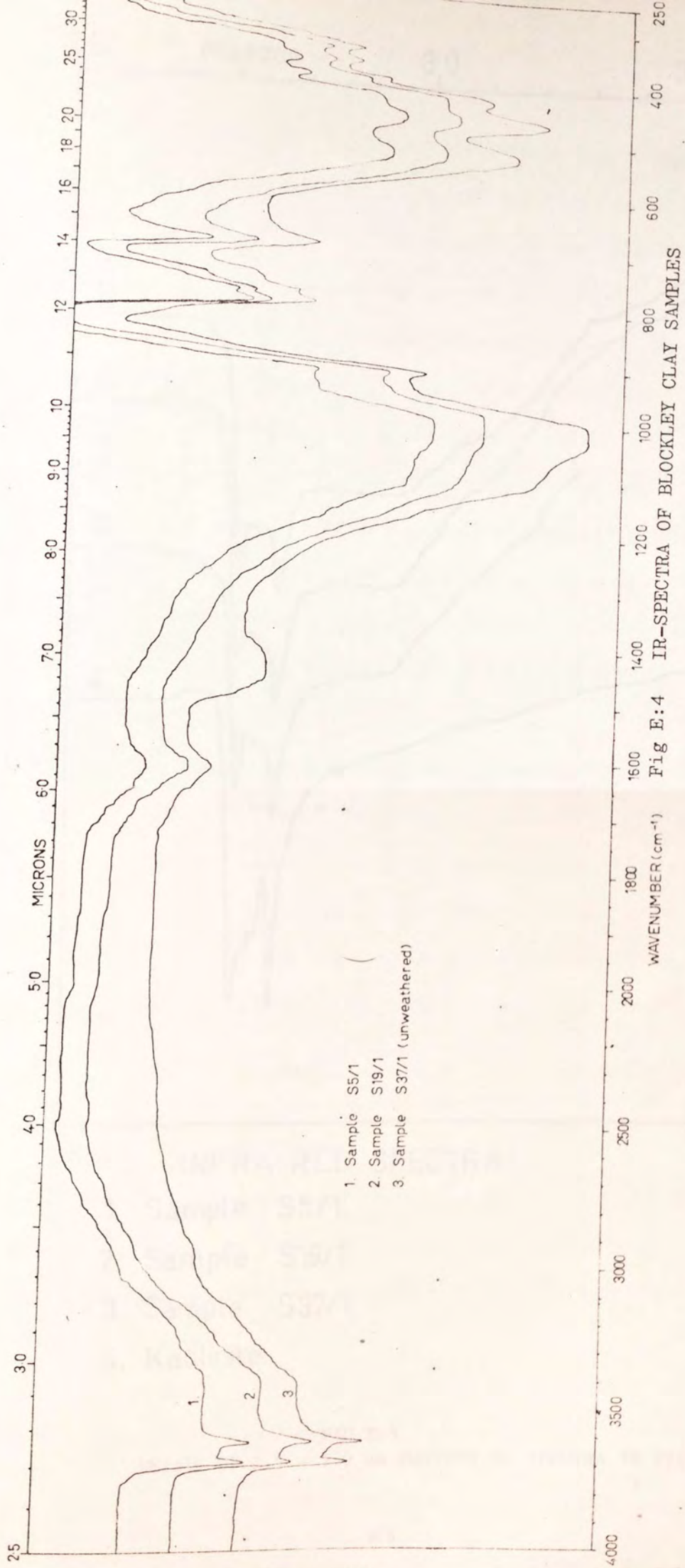
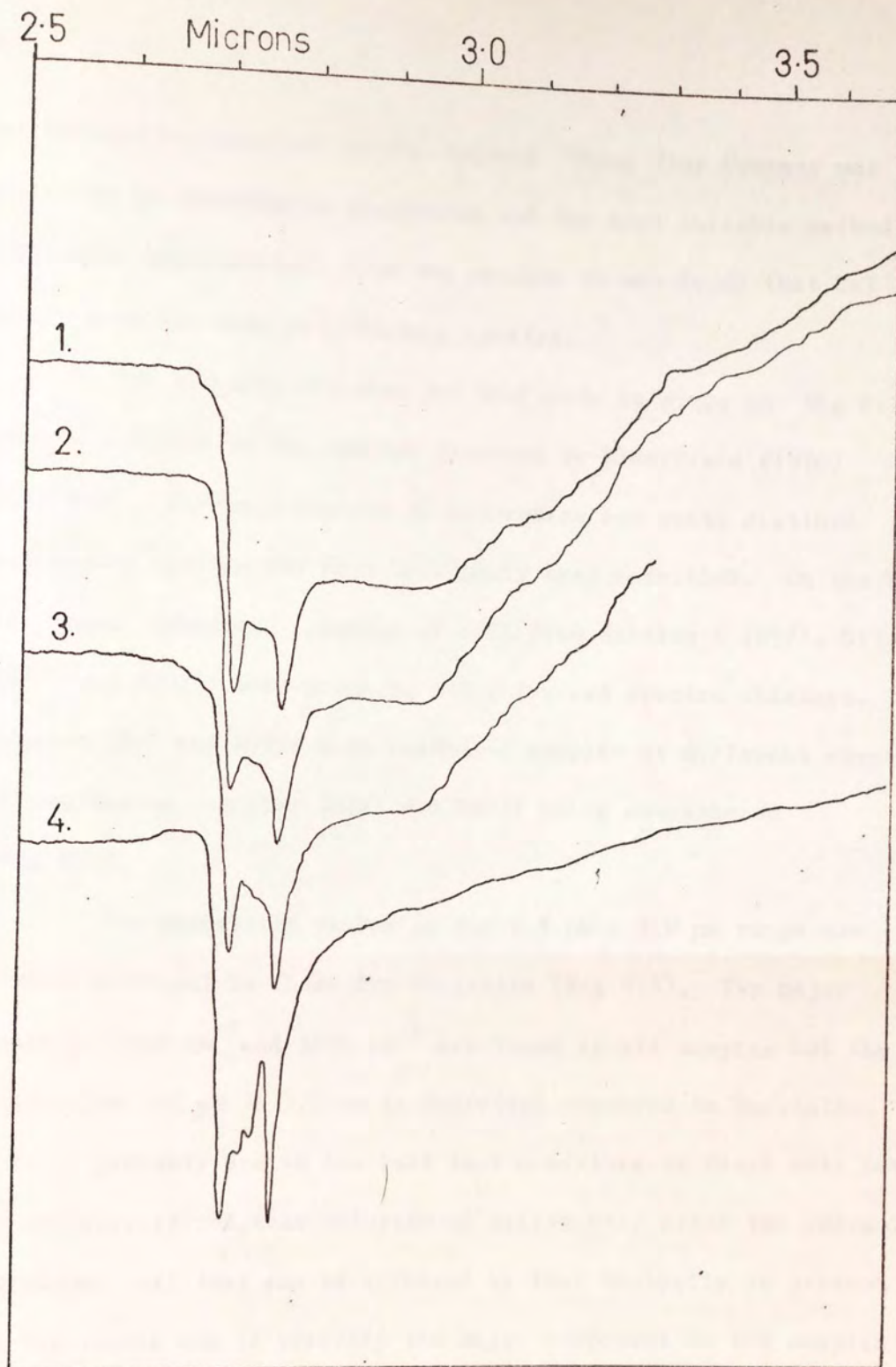


Fig E:4 IR-SPECTRA OF BLOCKLEY CLAY SAMPLES





INFRA-RED SPECTRA

- 1. Sample S5/1.
- 2. Sample S19/1.
- 3. Sample S37/1.
- 4. Kaolinite.

FIG E:5  
 DETAIL OF 2.5 - 3.0  $\mu$ m PORTION OF SPECTRA IN FIGS E:3, E:4

of refined kaolin from the St. Austell China Clay Company was obtained to investigate resolution and the most suitable method of sample preparation. From the results it was found that CsI discs gave the most satisfactory spectra.

The spectrum obtained for kaolinite is given in Fig E:3 and is compared to the spectra produced by Elderfield (1970) (Fig E:2). The main regions of absorption are quite distinct and easily visible and have previously been described. On the basis of these results, samples of soil from section 1 (S5/1, S19/1, S37/1 and S40/1) were prepared and infra-red spectra obtained. Samples S5/1 and S19/1 were weathered samples at different stages of weathering, samples S37/1 and S40/1 being unweathered (Fig E:4).

The absorption peaks in the  $2.5 \mu\text{m} - 3.0 \mu\text{m}$  range are almost identical to those for kaolinite (Fig E:5). Two major peaks at  $3690 \text{ cm}^{-1}$  and  $3615 \text{ cm}^{-1}$  are found in all samples but the region from  $2.8 \mu\text{m}$  to  $3.0 \mu\text{m}$  is depressed compared to kaolinite. This is probably due to the fact that a mixture of clays will have an additive effect, thus chlorite or illite will alter the infra-red spectrum. All that can be inferred is that kaolinite is present in the sample and is possibly the major component in the samples examined.

The only other major difference between the samples is the broad absorption peak in the  $1400 \text{ cm}^{-1}$  region for samples S37/1 & S40/1 (Fig E:4), which indicates the presence of some compound that is removed by weathering.

The carbonate group of minerals (Table E:1) do show absorption peaks in the  $1400 \text{ cm}^{-1}$  region, the peaks showing variation with the bonded metal. Therefore, a carbonate is present

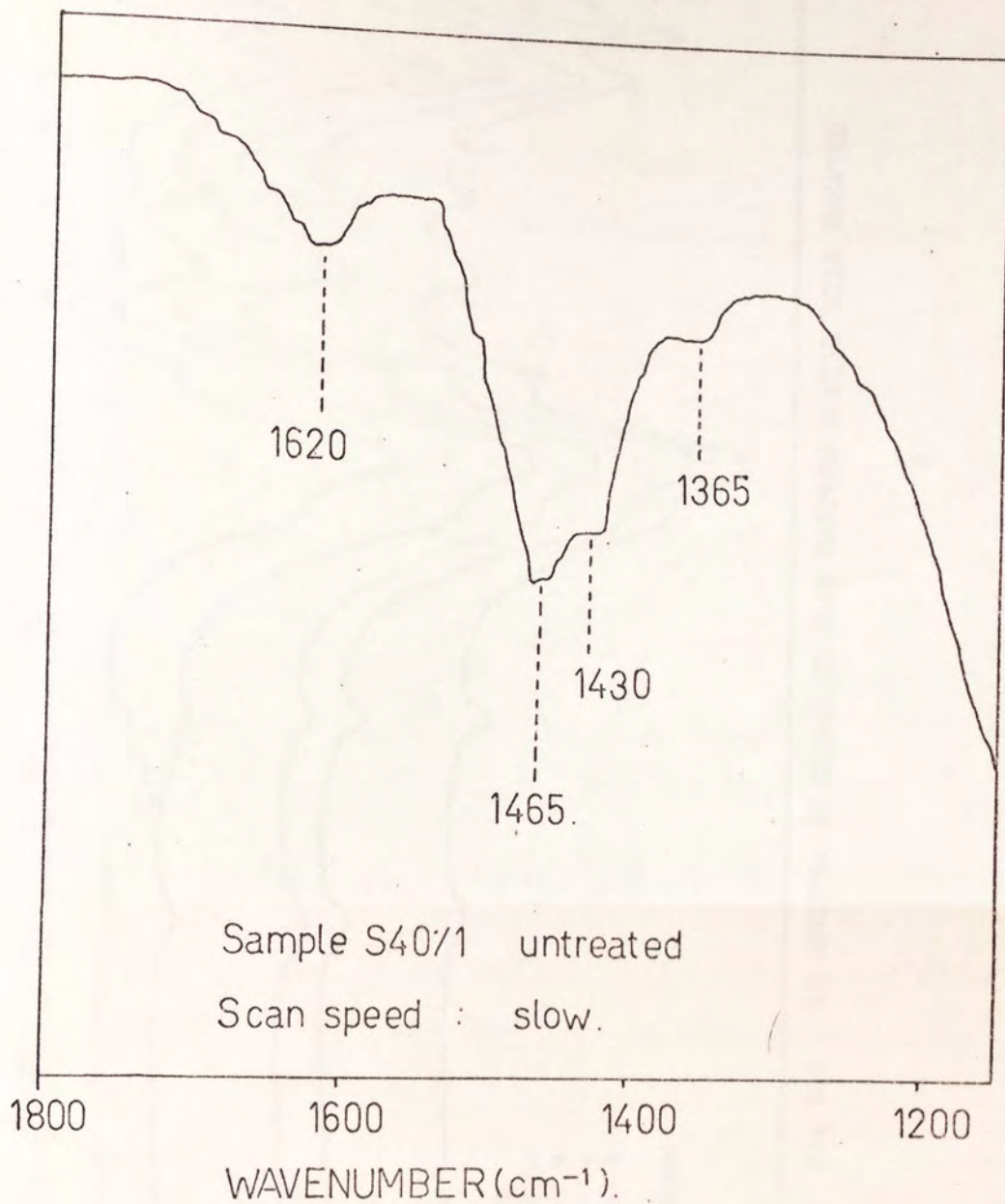


FIG E:6  
DETAIL OF 5.5 to 8.5  $\mu\text{m}$  PORTION. SAMPLE S40/1

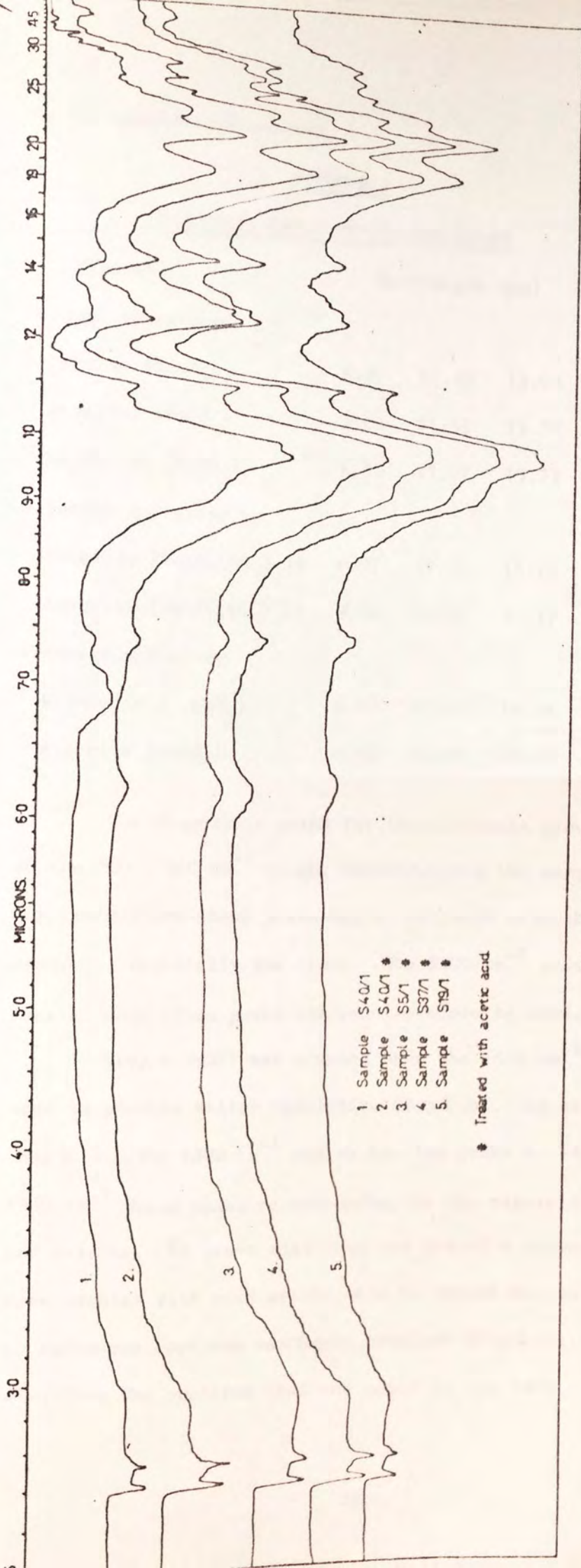


Fig E:7 IR SPECTRA OF BLOCKLEY CLAY SAMPLES ACETIC ACID TREATED

in the unweathered samples.

TABLE E:1

CARBONATE GROUP ABSORPTION PEAKS

Mineral	Wavelength ( $\mu\text{m}$ )			Wave Number ( $\text{cm}^{-1}$ )		
Calcite sub-group						
Calcite ( $\text{CaCO}_3$ )	6.97	11.45	14.04	1435	873	712
Siderite ( $\text{FeCO}_3$ )	7.03	11.55	13.57	1422	866	737
Magnesite ( $\text{MgCO}_3$ )	6.90	11.27	13.37	1450	887	748
Dolomite sub-group						
Dolomite ( $\text{Ca}(\text{Mg}(\text{CO}_3)_2)$ )	6.97	11.35	13.70	1435	881	730
Ankerite ( $\text{Ca}(\text{Fe}(\text{CO}_3)_2)$ )	6.90	11.27	13.77	1450	877	726
Argonite sub-group						
Witherite ( $\text{BaCO}_3$ )	6.92	11.61	14.41	1445	860	693
Argonite ( $\text{CaCO}_3$ )	6.90	11.61	14.04	1450	860	712

The diagnostic peaks for the carbonate groups are those peaks in the  $700 - 760 \text{ cm}^{-1}$  range. However, since the sample analysed is a complex mixture these peaks may be confused with those of other minerals, especially the clays. The  $1400 \text{ cm}^{-1}$  area is relatively free of absorption peaks and can therefore be used.

Sample S40/1 was scanned over the  $1400 \text{ cm}^{-1}$  area on a slow scan to provide better resolution (Fig E:6). As can be seen from Fig E:6 the  $1400 \text{ cm}^{-1}$  region has two peaks at  $1465 \text{ cm}^{-1}$  and  $1430 \text{ cm}^{-1}$  these peaks corresponding to the minerals aragonite and calcite. To prove that this was indeed a carbonate the samples were treated with weak acetic acid to remove any carbonates and an infra-red spectrum was again obtained (Fig E:7). It can be seen from the spectrum that the peaks in the  $1400 - 1450 \text{ cm}^{-1}$  range

were destroyed thus confirming the presence of calcite and aragonite.

The presence of the small  $1355 \text{ cm}^{-1}$  peak in the untreated S40/1 and treated samples is due to retention of a small amount of alcohol which is used when preparing the sample prior to producing the disc.

The appearance of the  $1600 \text{ cm}^{-1}$  peak in the treated samples is due to insufficient drying of the sample after treatment thus the absorbed water produces a peak in this region.

#### E:4 CONCLUSIONS

The major result of this analysis shows that although clays can be partially recognised by infra-red spectroscopy, the carbonate minerals can be identified. Since the quantity of calcite in the samples varies considerably then the presence of calcite in the weathered samples can easily be ascertained prior to any lengthy quantitative analysis.

## APPENDIX F

### F:1 ATOMIC ABSORPTION ANALYSIS

Atomic absorption was first introduced by Walsh (1955) as an instrumental technique and since then it has become a standard method for the quantitative chemical analysis of various materials. The determination of the percentage of an element in a sample is carried out by preparing known standards containing accurate amounts of the pure element and comparing the absorption due to the element in the sample with the standards.

### F:2 THEORY

Assume that we have a cloud of atoms which are free of any molecular bonding forces and energy is applied to the atomic cloud (i.e. in the form of heat) then some of the atoms will be excited to higher energy levels by the transition of electrons to different orbits. When the atoms return to their lower, more stable state the energy acquired from the thermal source must be released. This energy appears as light and therefore an emission spectrum is obtained for the atoms. Each atom will have one or more higher energy levels and Walsh (1955) showed that although the majority of atoms (96%) are in the ground state the population for the various energy levels is highly dependant on temperature changes. Light energy can also cause the excitation of atoms.

In atomic absorption the material to be analysed is dissolved (by various methods) and a dilute solution sprayed into a burner. The heat energy from the flame raises 4% of the atoms to a higher energy state, the remaining atoms (if an ideal case) are merely stripped of their chemical bonds and remain in the ground state. These atoms are capable of absorbing radiation in a few extremely narrow bands of  $10^{-4}$  Å in width, the wavelength

of the radiation being characteristic of the atoms. If a light beam is passed through this cloud of atoms then the absorption of light can be monitored. Atomic absorption is more sensitive because the amount of atoms causing this effect is orders of magnitude larger than for emission. The predominance of atoms in the lower energy state assures higher precision since variations in flame temperature produce negligible changes in the number of atoms in the ground state.

Due to strong absorption by air at short wavelengths ( $2000\text{\AA}$ ) atomic absorption is restricted to the elements whose absorption lies in the  $2000 - 10,000\text{\AA}$ , this therefore precludes the majority of the non metals.

### F:3 METHOD AND TECHNIQUES

The basic apparatus consists of a hollow-cathode emission lamp that is chosen to emit light in a narrow band width at the same wavelength as that of the metal being analysed. This radiation is passed through a flame into which the sample (in solution) is aspirated. The radiation is focused at the central portion of the flame, some of this radiation is absorbed by the atoms of the metal being analysed which are excited to the higher energy state. On returning to the ground state fluorescent radiation is emitted in all directions and at a wavelength corresponding to the source, thus absorption occurs in this case at the same wavelength as emission. The narrow bands where absorption and emission coincide are termed resonance lines.

The absorption of the source radiation is proportional to the amount of atoms present in the ground state, thus Beer's Law is applicable. The concentration of the element in the aspirated



sample is approximately equal to absorbance (A), which is proportional to the log of the reciprocal of sample transmittance T;

$$A = \log \left( \frac{1}{T} \right) = -\log T.$$

The radiation that is passed through the flame is refocused onto a slit and passed through a monochromator to filter the background. The intensity or transmission of this radiation is measured using a photo-detector read out. Double-beam instruments in which the beam is split such that one beam suffers absorbance while the other is by-passed, eliminates apparent changes in absorbance due to fluctuations in beam intensity. The normal type of equipment employs liquid that is aspirated into the flame although new apparatus is available to analyse solids. This, however, is a rather specialized and expensive technique at the present time.

A Perkin Elmer 303 atomic absorption spectrometer with chart recorder output was used for the quantitative chemical analysis on all the Lias clay samples. This instrument requires a liquid that is aspirated into the flame after prior mixing with acetylene/air, the Lias clay samples must therefore be rendered soluble.

#### F:4 INTERFERENCES

The majority of interferences are mainly chemical, these being:

- a) Overlapping of the resonance lines of atoms; this is unlikely and the few coincidences that have been investigated are noted in the users handbook for the particular instrument being used.

- b) Ionization suppression owing to one element interfering with another, which can be eliminated by using a hotter flame. It can also be overcome by using extraction methods i.e. APDTC or EDTA to remove the element under investigation and at the same time concentrate it, or, the offending element. A releasing agent such as lanthanum can also be added to the solution to overcome this problem.
- c) Some elements produce refractory oxides in the burner and these particles scatter the resonance beams and can cause serious problems (Allen 1961), e.g. such elements as aluminium, tungsten, vanadium and titanium. The use of a complexing agent such as EDTA helps to prevent refractory compounds forming.

#### F:5 METHOD OF ANALYSIS

The determination depends upon the comparison of the absorbance of the unknown sample with the absorbance of known samples, thus standard solutions are required. These are made by dissolving the pure element ('Spec. pure') to produce a solution that can be further diluted by differing amounts to give several standards that will be in the optimum analytical range of 20% - 80% absorption.

The standards are aspirated into the flame and the percentage absorbance is obtained which is then converted into absorbance using the manufacturers tables, a plot of absorbance against  $\mu\text{g/ml}$  being obtained for the standard. The ideal plot should

be linear through the origin but in some cases due to interferences the plot departs from linear in the lower concentrations (Angino & Billings 1972). The unknowns can then be aspirated into the flame, the absorbance found, and the concentration in  $\mu\text{g/ml}$  for the unknown solution read from the graph. The amount of the element in the sample can then be calculated.

The method of addition can also be used when the element under investigation exists in small amounts and is subjected to interferences from the matrix. A known amount of the element whose concentration is sought is added to the sample solution and the solution tested as before. Since a known amount of the element was added any increase is due to the sample itself.

The standards should be analysed initially and after every four to six samples to ensure no variation in the standards or instrumental drift. To enable samples to be processed quickly and to eliminate drawing of graphs, a program was written for a Hewlett-Packard Model 10 programmable calculator that took the standard results produced a line of least squares fit through the points and then calculated the concentration in the solutions and the percentage present in the sample analysed (Appendix G). This enabled 15 - 20 samples to be analysed per day with the results being available on the same day.

If a rough estimate of the amount of element present in the sample is known this aids in the dilution of the sample solution. Otherwise tests on different dilutions are often required to ensure that the diluted sample solutions tested are not below the detection limit of the element under investigation. Table (F:1) gives the elements for which determinations were made together with the running conditions.

TABLE F:1

ELEMENT	RADIATION WAVELENGTH Å	SLIT	OXIDISER AND FLOW	FUEL AND FLOW	DETECTION LIMIT (µg/ml)
Fe	2483	3	AIR 9	A9*	0.01
Co	2407	3	AIR 9	A9*	0.01
Cu	3247	4	AIR 9	A9*	0.005
Ni	2320	3	AIR 9	A9*	0.01
Pb	2833	4	AIR 9	A9*	0.03

\* A = Acetylene

Detection Limits for the Perkin-Elmer

303 Atomic Absorption Spectrometer.

## APPENDIX G

### ATOMIC ABSORPTION PROGRAM

#### G:1 INTRODUCTION

This program enables rapid data processing of raw experimental data from the atomic absorption laboratory. Data is entered via the keyboard, processed (see text), and then printed out in the following form:

- a)  $\mu\text{g/ml}$  in test solution
- b)  $\mu\text{g/ml}$  in sample
- c) p.p.m. in sample
- d) percentage in sample

It can be seen from the output and program instructions that the program was written with powdered rock samples in mind since the weight of material is necessary to calculate p.p.m. in the sample. However if one is dealing with liquid samples (i.e. natural waters) one can ignore the last three values of the output and use the first value of  $\mu\text{g/ml}$  of the test solution. This can then be either taken as the actual value provided no extraction or concentration processes have been carried out on the sample, or it can be multiplied by the appropriate factor to take into account any of these processes to produce the  $\mu\text{g/ml}$  in the sample taken.

#### G:2 PROGRAM DESCRIPTION

The program is written for a Hewlett-Packard 9810A calculator, the necessary ancillary equipment being the printer and mathematical ROM. The total number of steps fits the standard 500 Total Program Step unit and the number of registers used is 51, which again fits the standard storage register module.

The method of determining concentration depends upon the instrument used. With atomic absorption instruments reading in

absorbance or concentration, the readout may be calibrated to read directly in concentration if the concentrations of the samples and standards are within the linear working range. Calibration can then be made with only a reagent blank and a standard at the upper end of the linear concentration range.

With machines which read out in percentage absorption (i.e. the Perkin Elmer 303), the readings for each sample and standard should be converted to net absorbance, this is done in the program using the following formula.

$$\text{Absorbance} = -\log (100 - \text{Absorption}).$$

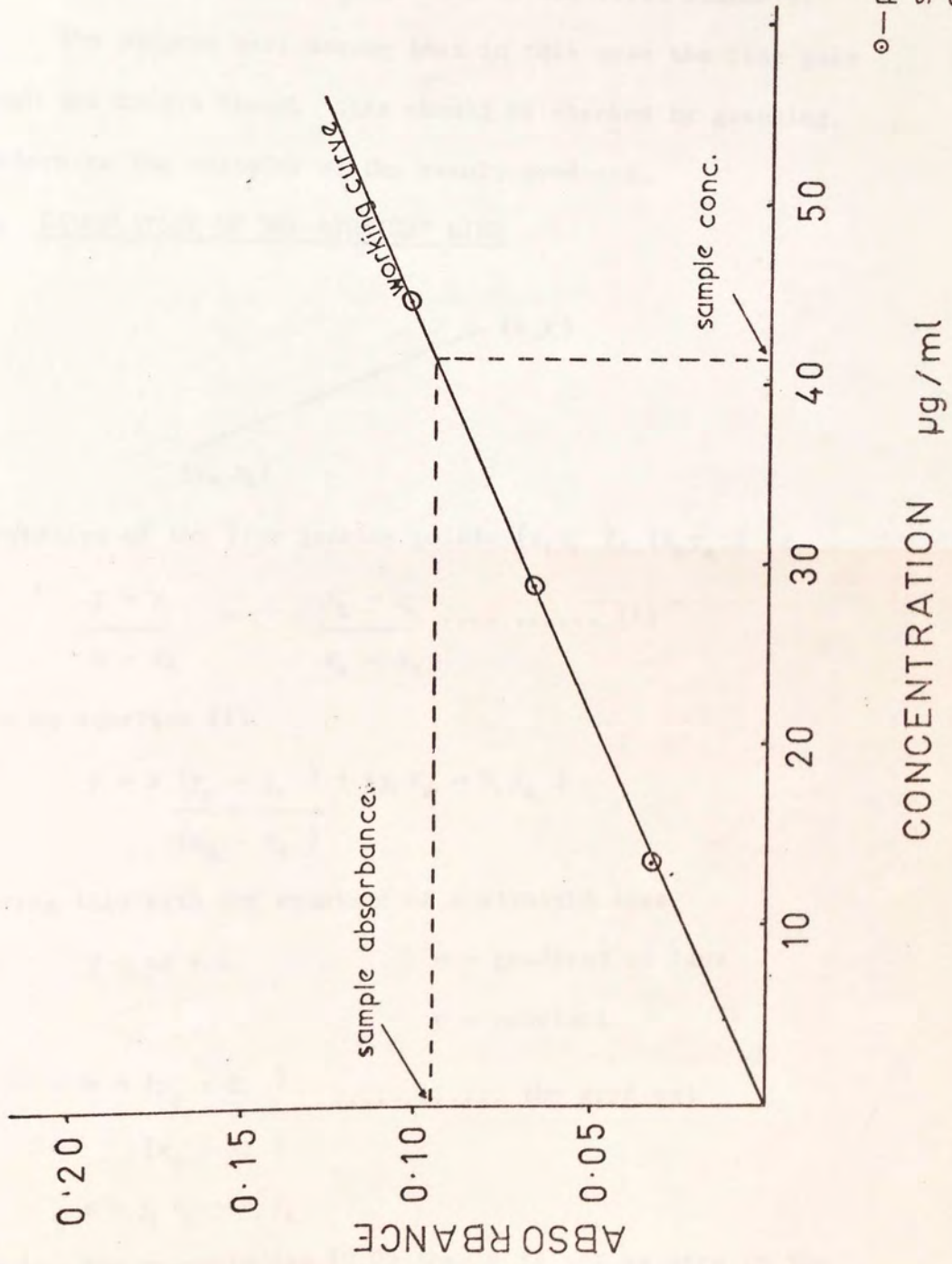
If the data was to be hand calculated a calibration curve can then be prepared, plotting absorbance versus concentration (Fig G:1).

For determinations where the concentrations of the sample and standard solutions are within the linear concentration range, only one standard and a reagent blank need be used, although the linearity of the curve should be checked periodically with intermediate standards. If the calibration curve extends beyond the linear working range, additional standards must be used. The working curve may change from day to day and should therefore be checked with every batch of samples.

In many cases however, the points do not lie on a straight line through the origin, hence one has to establish a line of best fit. This can lead to a sample and standard giving the same absorption reading but different concentrations.

The program therefore first searches with a sample to determine which standards the sample is between, it then calculates the

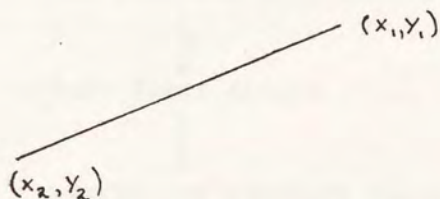
FIG G:1



equation of the line between these points. If the sample concentration is outside the upper standard concentration then the program prints out  $\pi^2$ . Ideally all samples should be between the first and last standard but in some cases they can be below the first one, in the range zero to the first standard.

The program will assume that in this case the line goes through the origin though this should be checked by graphing, to determine the validity of the result produced.

G:2:1 CALCULATION OF THE STRAIGHT LINE



the equation of the line joining points  $(x_1, y_1)$ ,  $(x_2, y_2)$  is

$$\frac{y - y_1}{x - x_1} = \frac{y_2 - y_1}{x_2 - x_1} \dots\dots\dots (1)$$

expanding equation (1)

$$y = x \frac{(y_2 - y_1)}{(x_2 - x_1)} + (y_1 x_2 - x_1 y_2)$$

comparing this with the equation of a straight line

$$y = mx + c \quad m = \text{gradient of line} \\ c = \text{constant}$$

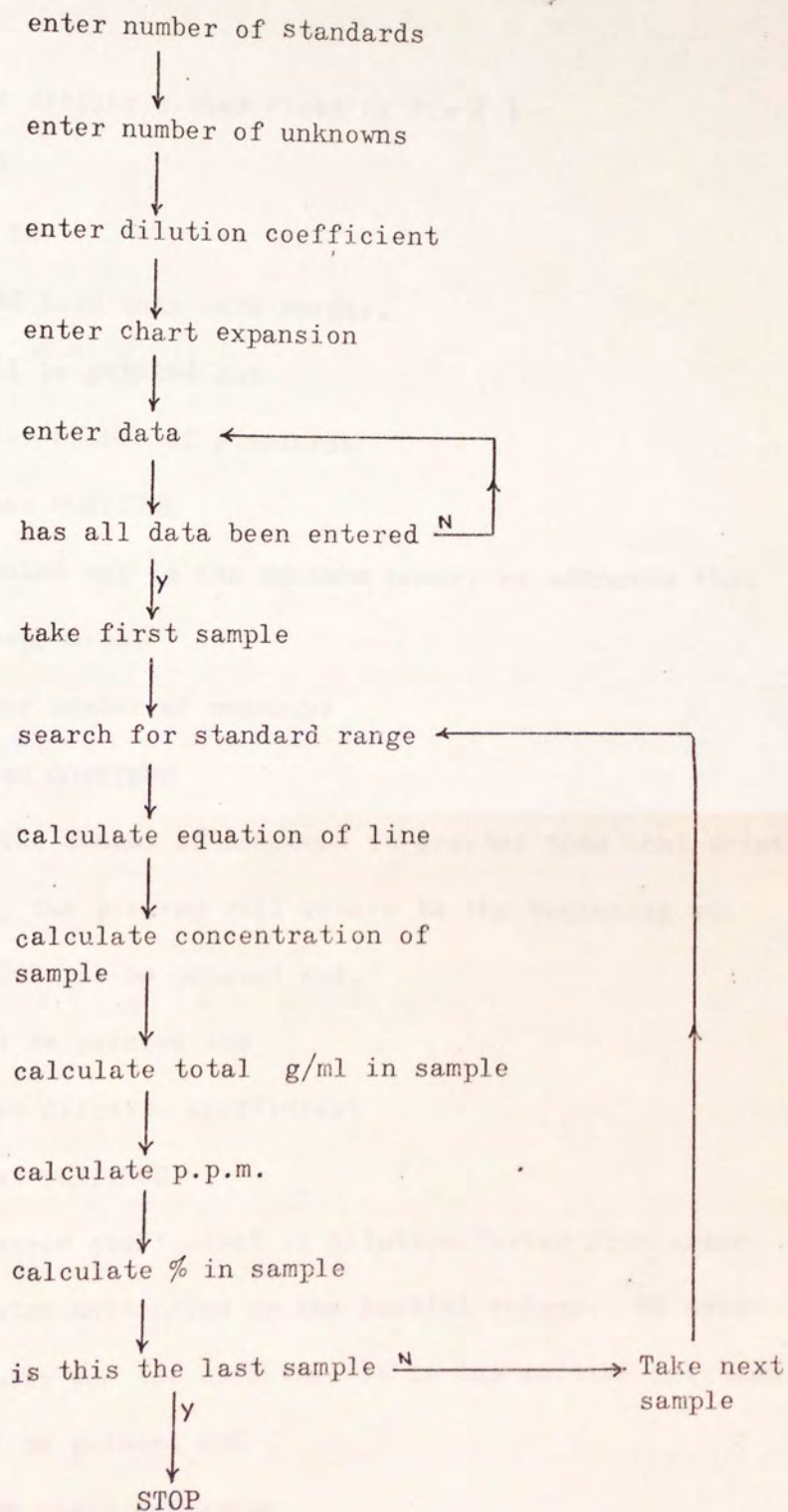
$$m = \frac{(y_2 - y_1)}{(x_2 - x_1)} \dots\dots\dots \text{the gradient}$$

$$c = y_1 x_2 - x_1 y_2$$

If  $x_1, y_1$  has the co-ordinates (0,0) then c is set as zero in the program. Once the equation has been calculated the sample data is inserted and the concentration is worked out.



G:3 FLOW DIAGRAM



G:4 PROGRAMMING INSTRUCTIONS

G:4:1 SIDE ONE

Choose display either Float or Fix ( )

a) Press FMT

GO TO

load card into card reader.

b) 1.000 will be printed out

enter number of standards

press CONTINUE

c) The number printed out is the maximum number of unknowns that the program will cope with.

enter number of unknowns

press CONTINUE

N.B. if the number of unknowns is greater than that printed out, the program will return to the beginning and 1.000 will be printed out.

d) 2.000 will be printed out

enter dilution coefficient

press CONTINUE

N.B. dilution coefficient is dilution factor from auto-diluter multiplied by the initial volume. If auto-diluter was not used then it is the initial dilution.

e) 3.000 will be printed out

enter chart expansion

press CONTINUE

f) 4.000 will be printed out

enter standards and concentrations - unknowns and sample weight in the following order.

```

1. Absorption )
                )
2.  $\mu\text{g/ml}$  )
                )
3. Absorption ) Standards (entered with the lowest
                ) concentration first)
4.  $\mu\text{g/ml}$  )

:

Absorption )
                )
Sample Wt. )
                )
Absorption ) Unknowns
                )
Sample Wt. )

:

```

Standards and unknowns are printed out for checking.

g) 5.000 is printed out only if all the data you specified has been entered and the program is being executed.

h) Data is printed out in sets of four results the values of which correspond to the following

1.  $\mu\text{g/ml}$  in tested solution
2.  $\mu\text{g/ml}$  in sample
3. p.p.m. in sample
4. percentage in sample

i) To re-run the program repeat steps b to f (program returns to the beginning at the end of each run).

#### G:4:2 SIDE TWO

In certain cases when one is using a blank other than distilled water together with a large scale expansion, the background will fluctuate and so the percent absorption for the sample or standard must be background corrected. This is done by taking background readings before and after the sample or standard, averaging the result and removing this from the sample or standard absorption.

For the program on side two the data is fed in, in batches of three; background-peak-background, and the corrected peak is then printed out. These corrected peaks are then entered into the program to obtain the concentrations in the sample

1) Press FMT  
GO TO  
load program

2) 1.000 will be printed out

Press GO TO  
LABEL  
A  
CONTINUE

3) 9.000 is shown on the display  
enter data in the following manner

```
Background )  
           )  
Peak       ) 1  
           )  
Background ) )  
           )  
Peak       ) 2  
           )  
Background )
```

4) When all data has been entered and the corrected percentage absorptions printed out;

Press RUN  
END  
CONTINUE

5) 1.000 is printed out  
enter data as for side one, steps b) to i)

PROGRAM LISTING

```

Clear
  1
Print
Print
Stop
  ↑
  ↑
  2
  X
  1
  0
  +
y → ( )
  2
x → ( )
  4
  ↓
  ↑
  7
x ↻ y
  ↓
  ↑
Print
Print
Stop
  enter number of unknowns
X > Y
  0
  0
  0
  0
  ↑
  ↑
  1
  -
  2
  X
x ← ( )
  2
  +
y → ( )
  1
  ↓
  2
  *
  * = Multiply
x ← ( )
  2
  +
y → ( )
  b
x ↻ Y
  2
  -
y → ( )
  0
Clear x
  ↑
  ↑

```

```

8
x ->( )
3
↓
1
0
0
x ->( )
5
↓
2
Print
Stop          enter dilution coefficient
x ->( )
6
↓
3
Print
Print
Stop          enter chart expansion
x ->( )
7
↓
x ->( )
8
y ->( )
9
↓
10
x ->( )
a
4
Print
Print
Stop          enter data
Print
x ->( )
IND
a
1
x ->( )
+
a
↓
↓
a
↑
b
X=Y
0
1
1
7
GO TO
0
0
9
3
5
Print

```

Print  
Clear

x ← ( )  
3  
x → ( )  
a  
x ← ( )  
4  
x → ( )  
b  
x ← ( )  
IND  
2  
↑  
x ← ( )  
IND  
b  
X=Y  
0  
1  
8  
3  
X>Y  
0  
1  
8  
3  
↓  
b  
↑  
x ← ( )  
0  
X=Y  
0  
1  
6  
8  
2  
↑  
E  
Clear x  
↑  
↑  
GO TO  
0  
1  
2  
9  
↓  
x ← ( )  
2  
↑  
x ← ( )  
1  
X=Y  
0  
3  
8  
9  
GO TO  
0  
4  
3

State of shift calculation

```

9
Clear x - Start of main calculation
↑
↑
x ← ( )
IND
b
↑
GO TO
S/R
0
4
0
5
y → ( )
4
8
↓
x ← ( )
IND
a
↑
GO TO
S/R
0
4
0
5
y → ( )
4
7
↓
b
↑
1
+
y → ( )
4
6
x ← ( )
IND
4
6
x → ( )
4
6
↓
a
↑
1
+
y → ( )
4
5
x ← ( )
IND
4
5
x → ( )
4
5
↓

```



```

x← ( )
4
8
↑
x← ( )
4
7
-
x← ( )
4
6
↑ roll
x← ( )
4
5
-
↑ roll
↑ roll
÷
y →( )
a
x →( )
b

```

Calculation of gradient  
of line

```

Clear x
↑
↑
x← ( )
4
7
↑
↑
+
x← ( )
4
5
↑
1
+
↓
X=Y
0
3
9
4

```

Testing if both x ,y are  
zero and if so setting  
c=0

```

Clear x
↑
↑
x← ( )
4
7
↑
x← ( )
4
6
*
x← ( )
4
8
↑ roll

```

Calculation of c, if x ,y  
are not zero

```

x← ( )
4
5
*
↑ roll
↑ roll
-
b
÷
y →( )
4
4
Clear x
↑
↑
x← ( )
IND
2
↑
GO TO
S/R
0
4
0
5
x← ( )
4
4
-
a
÷
↓
Print
↑
x← ( )
6
*
↓
Print
↑
x← ( )
2
↑
1
+
y →( )
4
3
x← ( )
IND
4
3
x← y
↓
÷
↓
Print
↑
1
Enter Exp.
CHG SIGN
4

```



Entering sample into  
equation of line

g/ml in test solution

Total g/ml in sample

p.p.m. in sample

```

*
↓
Print
Print
x ← ( )
2
↑
x ← ( )
1
X=Y
0
0
0
0
↓
2
x → ( )
+
2
GO TO
0
1
2
0
π
x2
Print
PRINT
Stop
Clear x
↑
↑
x → ( )
4
4
GO TO
0
2
8
8
1
+
X=Y
0
4
3
3
-
x ← ( )
7
÷
x ← ( )
5
x ← y
-
↓
K
4
↑
INT x
-
x ← y
-
GO TO

```

% in Sample

Storing c=0.0

Subroutine for converting  
absorption to absorbance

```

0
4
3
7
CONTINUE
Clear x
↑
↑
CONTINUE
S/R
CONTINUE
6
9
K
8
Print
Print
↓
2
x ->( )
+
2
GO TO
0
1
2
0
GO TO
LABEL
B
LABEL
A
Clear
9
Stop
x ->( )
a
Stop
x ->( )
b
Stop
↑
a
+
2
÷
b
x y
-
↓
Print
GO TO
LABEL
A
LABEL
B
END

```

Printing out factorial 69

Program for background  
correction

G:6 STORE REGISTERS USED

<u>Store</u>	<u>Data in Store</u>
000	)
001	)
002	)
	) Counters dependant on data, entered automatically
003	8
004	10
005	100
006	Dilution coefficient
007	Chart expansion
008	)
009	) Zero entered automatically
	)
010	)
.	)
.	) Data Storage
.	)
043	)
044	)
.	)
.	)
.	) Temporary Stores
048	)
a	)
b	)

## APPENDIX H

### H:1 MOSSBAUER SPECTROSCOPY

Iron compounds are amenable to study by gamma-ray nuclear resonance fluorescence which depends on the phenomenon known as the Mossbauer Effect. This effect has been observed with some 28 nucleides besides iron, (i.e. tin) however, with certain nucleides the information obtained tends to be more limited than is the case with iron.

The basic idea of Mossbauer Spectroscopy, nuclear resonant scattering of gamma radiation is not new, since Kuhr<sup>\*</sup> in 1929 first suggested that this might be observed. It was not however until 1951 that Moon<sup>\*</sup> completed the first successful observations of gamma-ray nuclear resonance and even then it took until 1958 for Mossbauer<sup>\*</sup> to finally provide the key to further work. Since then there has been a surge forward both in equipment and techniques, and it is now a sophisticated tool that is mainly used by physicists and chemists.

### H:2 THEORY

#### H:2:1 RESONANCE AND RESONANT ABSORPTION

Acoustic resonance can be demonstrated with two tuning forks having the same frequency. If one is struck, the sound waves emanating will cause the second fork to vibrate. If the tuning forks are not accurately tuned then the sound waves will be out of phase and a beat note will be detected.

Resonance in atomic systems at an optical level can be shown by the yellow light of sodium. If we had two bulbs filled with sodium vapour, and one of these bulbs was heated to above room temperature, energy in the form of photons of light would be given off. If this light was focused on the second bulb the

---

\* See Goldanski (1964)

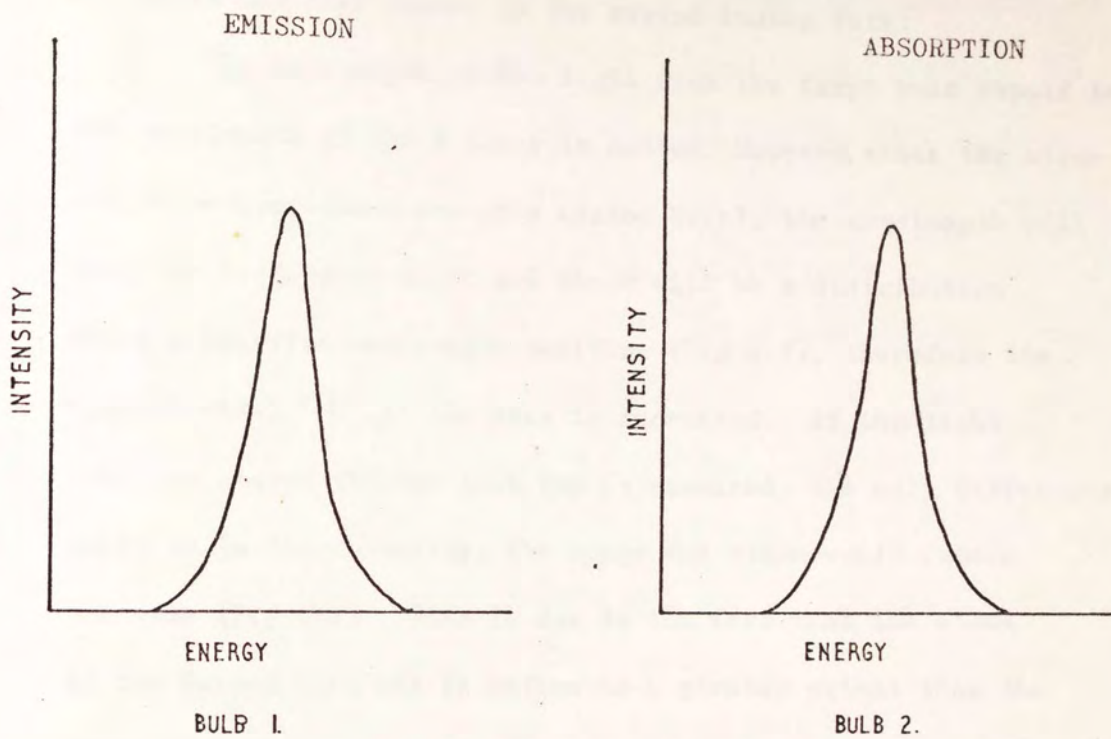


FIG H:1 OPTICAL EMISSION AND ABSORPTION SPECTRA

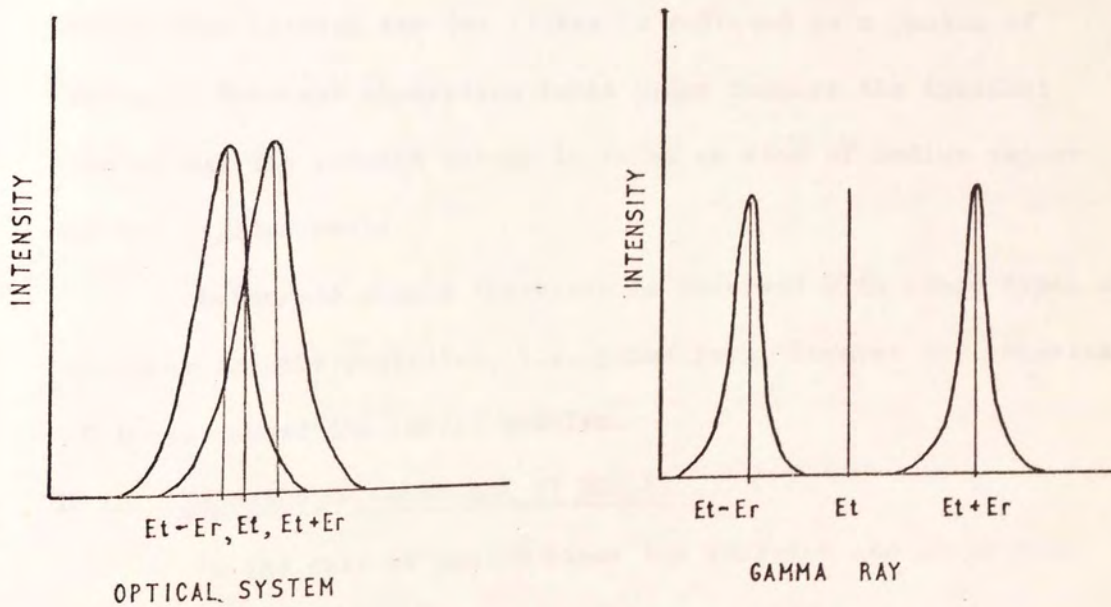


FIG H:2 OPTICAL AND GAMMA RAY SPECTRA

sodium vapour would extract energy and glow, in effect acting in the same manner as the second tuning fork.

The wavelength of the light from the first bulb should be the wavelength of the D lines in sodium. However, since the atoms are in motion (atoms are in a heated bulb), the wavelength will vary due to Doppler shift and there will be a distribution about a specific wavelength position (Fig H:1), therefore the natural width  $\Gamma$  of the line is increased. If the light that has passed through bulb two is examined, the only difference would be in the intensity, the shape and width would remain the same (Fig H:1). This is due to the fact that the atoms in the heated bulb are in motion to a greater extent than the atoms in bulb two.

The characteristic light emitted by the sodium atoms is in fact the result of an electronic transition between the ground state and an excited state of the sodium atom. The energy difference between the two states is radiated as a photon of energy. Resonant absorption takes place because the incident photon has the correct energy to raise an atom of sodium vapour to the excited state.

Resonance should therefore be observed with other types of electromagnetic radiation, i.e. gamma rays, however the emission of these caused the initial problem.

#### H:2:2 EMISSION OF GAMMA-RAY BY NUCLEI.

In the case of sodium atoms the emission and absorption lines overlap to some extent and resonance will occur (Fig H:2a).

Let us assume that the energy required to raise the nucleus from its ground state to the excited state is  $E_t$  (energy of



transition). When a nucleus releases a gamma-ray, a velocity of recoil is imparted to the nucleus by the gamma-ray thus the energy of the gamma-ray is reduced by an amount equal to the energy of recoil ( $E_r$ ). The inverse happens when a gamma-ray impinges on a nucleus in the ground state, some of the energy of the gamma-ray is taken up in recoil. Therefore in order to raise a nucleus to its excited state, the gamma-ray will require an energy greater than the energy of transition (Fig H:2b).

Since the energy of emission is smaller than  $E_t$ , and the energy required for absorption is larger than  $E_t$ , as it stands these peaks will never overlap.

With sodium atoms the line widths of emission are sufficient to overcome this recoil loss therefore the lines overlap. Line width is a result of the uncertainty of energy and time, thus half life and line width are interconnected. For a gamma-ray, if a typical value of half life is taken ( $\approx 10^{-7}$ s) then the resultant line width is  $4.6 \times 10^{-9}$  eV. This is much smaller than the energy lost in nuclear recoil and as a result the gamma-ray emission line does not overlap the absorption line and therefore nuclear resonance is not observable. The line widths can however, be broadened by an increase of temperature (Thermal Doppler Broadening), and some resonance can be observed.

In 1957 Rudolf Mossbauer was examining gamma-radiation from the decay of  $\text{Os}^{191}$ , which even at room temperature has overlap of the emission and absorption lines for gamma-rays. He attempted to reduce the overlap in order to measure the "background" of his apparatus in the absence of resonance absorption, so both emitter and absorber were cooled down to 77°K. In the absence of resonance his counter behind the absorber

should have shown an increased counting rate. What in fact actually happened was that the counter gave fewer (counts than without cooling) indicating that gamma absorption had increased.

The theory behind this unexpected result had been worked out by Lambe<sup>\*</sup> (1939) and Mossbauer was quick to realise this. Lambe, who was working with slow neutrons which also impart a recoil energy, showed that the recoil energy could be absorbed by the solid containing the nuclei.

Extensive calculations by Mossbauer based on Lambe's concept showed that the free recoil is eliminated in a fraction of the gamma-ray emissions and absorptions. This fraction of nuclei where the energy of recoil is not dissipated throughout the crystal lattice is known as the Mossbauer fraction.

Thus the emission spectrum for a nuclear transition contains an undisplaced line of natural width accompanied by a thermal Doppler distribution. The absorption line has a similar structure and there is therefore exact resonance between the narrow lines in the two distributions.

Mossbauer carried out further experiments to show that resonant absorption can occur by relative movement of the source and absorber. If the source is moving towards the absorber, the gamma-rays have a slightly higher frequency (Doppler Effect), i.e. a shorter wavelength (higher energy) than if both source and absorber were kept stationary. With the source moving away from the absorber a lower energy gamma-ray would result. When the energy of the gamma radiation matches the energy of the lowest lying state of the nuclei in the absorber, the radiation is absorbed and almost instantly (within  $10^{-9}$  seconds) re-emitted in all directions (i.e. resonant fluorescence). Therefore

\* See page 357

radiation is no longer transmitted through the sample and hence does not reach the detector.

Thus by using a source that has a relatively high fraction of recoilless emissions of gamma-rays in conjunction with relative movement of the source and absorber, gamma-ray nuclear resonance can be observed. If necessary both the source and absorber can be cooled to increase the Mossbauer fraction.

For further details one is referred to the articles by Gruverman (1965 et seq.), Goldanski (1964), Compton and Schoen (1961), Wertheim (1964).

## APPENDIX I

### I:1 ANALYSIS OF MOSSBAUER SPECTRA BY COMPUTER

The computer program written and developed during this work produces a line of best fit using the least-squares method. Initial assumptions are made on line shape, the number of peaks and approximate position values which are supplied to the program. The results are printed out and a graph is drawn on a graph plotter. The program is written in Fortran for an ICL 1905 Computer, but it can easily be altered for different computers.

Computer programs for Mossbauer spectral analysis have been written. The majority of programs have been produced in the U.S.A. with the exception of Stone (see Bancroft et al. 1967a). It was impossible to obtain this program. The following program is written as a series of subroutines with a small main control section, enabling new control sections to be written to suit the requirements of the individual.

### I:2 MOSSBAUER SPECTRUM

The initial assumption is on the shape of a single emission or absorption. If a particle is set oscillating it will radiate energy and the amplitude of its oscillation will steadily decrease. The radiation is not monochromatic but has an intensity distribution which is a function of frequency  $\nu$  (Fig I:1) and is given by the following equation;

$$I_{\nu} = \frac{C}{(x - x_0)^2 + \beta^2/4}$$

$I$  = intensity of frequency  $\nu$

$\beta$  = damping constant or line width

$x_0$  = oscillating frequency

$C$  = constant

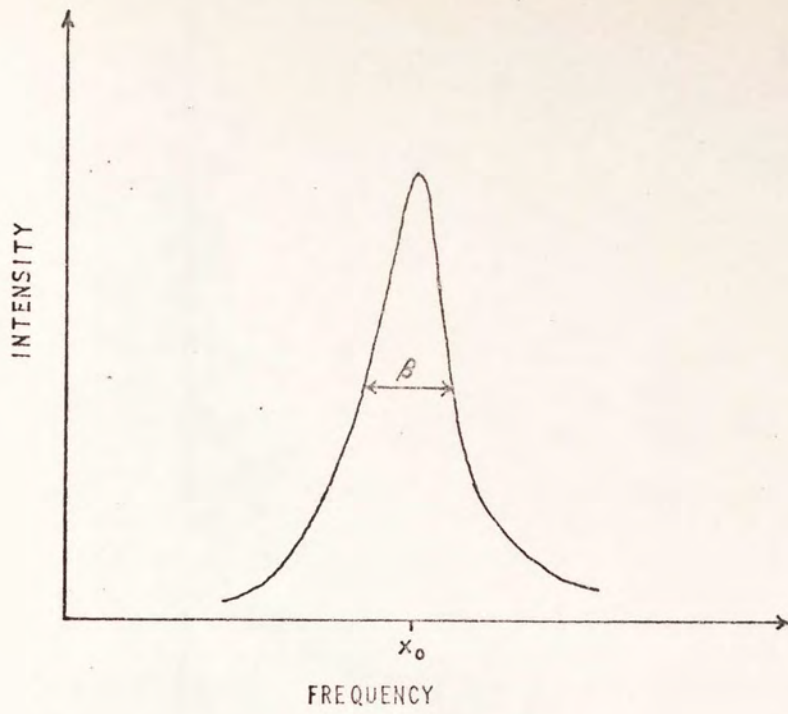


FIG I:1  
THE LORENTZIAN DISTRIBUTION

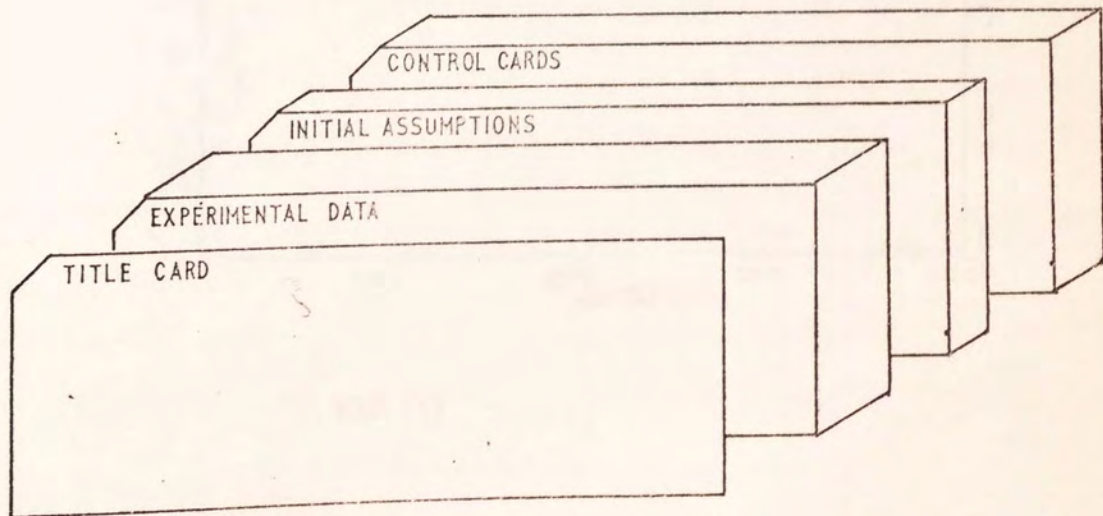
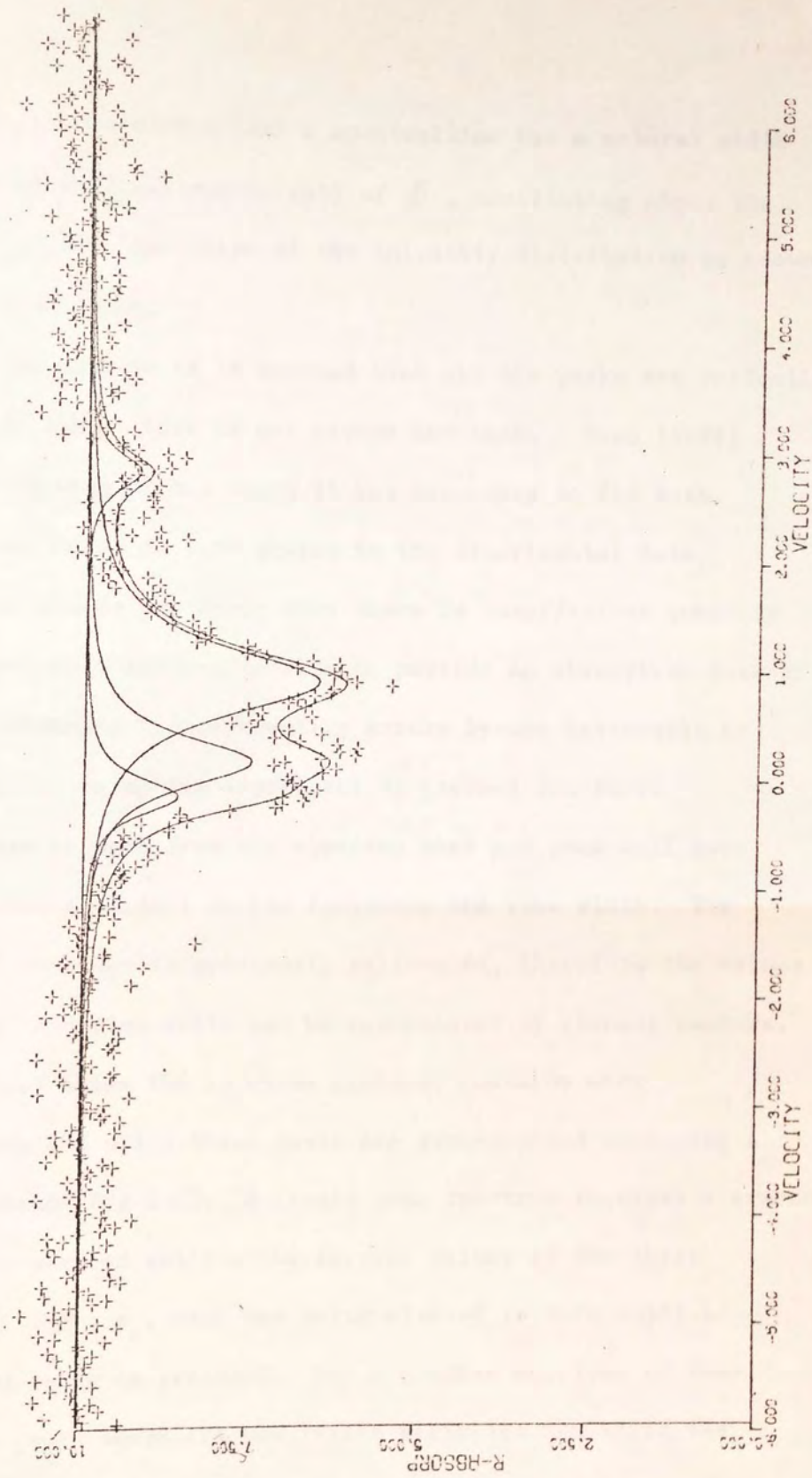


FIG I:3  
COMPUTER PROGRAM STRUCTURE



MICA

FIG I:2

The formula states that a spectralline has a natural width (full width at half maximum height) of  $\beta$ , oscillating about the frequency  $x_0$ . The line shape of the intensity distribution is known as a Lorentzian shape.

In the program it is assumed that all the peaks are perfectly Lorentzian in shape; this is not always the case. Boon (1971) showed that in many of his cases it was necessary to fit both Lorentzian and Gaussian line shapes to the experimental data. Gaussian line shapes can occur when there is insufficient quantity of the element in a particular site to provide an absorption peak of sufficient intensity before counting errors become noticeable by overcounting (allowing the experiment to proceed too far).

It can be seen from the equation that any peak will have specific values dependant on its frequency and line width. The multichannel analyser is previously calibrated, therefore the values of frequency and line width can be represented by channel numbers.

In most cases the spectrum produced contains more than one peak and often these peaks are superimposed producing a complex spectrum (Fig I:2). A single peak spectrum requires a search routine to be carried out for the correct values of the three variables  $I_r$ ,  $\beta$ ,  $x_0$ , each one being altered in turn until a least squared curve is produced. For a complex spectrum of four superimposed peaks there are now twelve variables for which the search must be carried out.

Two search routines are incorporated in the program; SEARCH and PSEARCH.

The SEARCH routine examines all the variables independantly and treats each peak as independant from all the others. The PSEARCH

routine will search for quadrupole split peaks and if no acceptable least squares curve (using the subroutine PSSQ) is found then it will pass on, through the SEARCH routine before terminating the program.

When the final theoretical curve has been calculated the degree of fit with the experimental data is calculated. This is represented by the statistical value chi-squared  $\chi^2$ . For curves with four peaks and hence twelve variables the chi-squared value is:

$$325.02 < \text{CHI-SQUARED} < 455.17$$

and for single peaks;

$$333.45 < \text{CHI-SQUARED} < 464.95$$

The value is dependant on the number of data points and the number of peaks and the limiting values are calculated in the program using the following formula:

$$\begin{array}{ll} 1\% & ( \chi + 2.2 - 3.3 \sqrt{\chi} ) & \chi = \text{No. of degrees of freedom} \\ 99\% & ( \chi + 2.2 + 3.3 \sqrt{\chi} ) & = \text{No. of channels used minus} \\ & & \text{the number of adjustable} \\ & & \text{parameters. (Bancroft et al} \\ & & \text{1968).} \end{array}$$

Both the chi-squared value calculated and the limiting values are printed out. If the chi-squared value is not statistically valid then this is stated in the print out and no conclusions should be drawn from the results. If this happens, then one should examine the data, the print out and the graph produced for an explanation. In the majority of cases it was found that the data was at fault either by incorrect punching or a channel dropping counts during the experiment resulting in a point well outside the range of the curve. In such an instance it is often profitable to examine the oscilloscope for such points before the data is punched out.



For ratio and quantitative analysis the area under the curves are calculated and printed out.

### I:3 HARDWARE REQUIREMENTS

Core Size 11K

Card Reader

Line Printer

Graph Plotter

The graph plotter used above had a step size of 0.1 mm hence all the graphs and the call routines are in

### I:4 INPUT

The input data necessary for this program is shown in (Fig I:3)

#### I:4:1 TITLE CARD

This is a single card in alpha numeric format and is used to title both the print out and the graph. The title of both print out and graph should be no longer than eight characters. However, the rest of the card can be used for further identification when the data is stored.

#### I:4:2 EXPERIMENTAL DATA

This consists of a number of cards, the exact number being dependant on the format used. The first two columns of each card are reserved for a numbering system in case the cards become disarranged. The format used in this program is fixed at ten channels per card giving a total of forty cards in this section. The format in the final program will however, be able to be changed by the use of an object time format statement.

#### I:4:3 INITIAL ASSUMPTIONS

This consists of four cards giving approximate values for the specific variables.

I:4:3:1 CARD 1: NUMBER OF PEAKS

This is an integer and is punched right justified in the first three columns.

I:4:3:2 CARD 2: LINE WIDTHS

This consists of real numbers of the format F7.2, the decimal point being taken as read between the fifth and sixth column and should not be punched. The line widths are in numbers of channels.

I:4:3:3 CARD 3: PEAK INTENSITIES

Again these are real numbers with the same format as the previous card, the intensities being in percent below background.

I:4:3:4 CARD 4: PEAK POSITIONS

These are real numbers with the same format as card 2, again, these are represented in channel numbers.

I:4:4 CONTROL CARDS

This is the final section of the input data and consists of five cards which give additional information to control the output and type of graph produced.

I:4:4:1 CARD 1: This contains the following values.

PAIR: if greater than zero i.e. +1 then peaks are paired,  
if zero or negative there are no paired peaks.

Format F3.0

NPAIR: integer, gives the number of paired peaks, format I3.

VEL: real number, format F6.4 gives the true velocity in  
mm/s per channel.

I:4:4:2 CARD 2: This card contains two integers with the format I3,  
JPLOT and IPLOT

JPLOT: if this is negative then the Mossplot subroutine

is not executed and a graph is not drawn nor are the areas beneath the curves calculated.

I:PLOT: if the Mossplot subroutine is used then this value governs the type of x-axis on the graph.

I:PLOT = 1: the x-axis shows the positions of the channels

I:PLOT  $\neq$  1: the x-axis or the velocity scale is drawn with reference to the zero velocity position that is being used as a reference point and is scaled according to the velocity calibration value VEL.

I:4:4:3 CARD 3: This contains a single value ABMAX (real number, format F6.2) which gives the maximum value of the y-axis, the axis being scaled accordingly.

I:4:4:4 CARD 4: The size of the x and y axes in centimetres are punched on this card, SIZEX and SIZEY in that order with the format F6.2.

I:4:4:5 CARD 5: If the multichannel analyser has been calibrated and the reference position found then this is punched on this card with the format F6.2.

#### I:5 OUTPUT

An example of the type of graph obtained is shown in

Fig I:2.

#### I:6 EXAMPLE

A sample having the number 32/1/HCL produces a spectrum with four peaks, each pair being produced by a quadrupole split. A graph 16 x 5 inches is required with the true velocity scale. A velocity calibration gives a value of 0.0319 mm/s channel the reference point being channel 186. The cards and values needed would be punched in the following manner.

32/1/HCL

00 057470 057799 -----

DATA CARDS

39 057145 057704 -----

4

14 14 14 14

25 25 5 5

211 193 271 185

1 20.0319

2 2

10.00

10 5

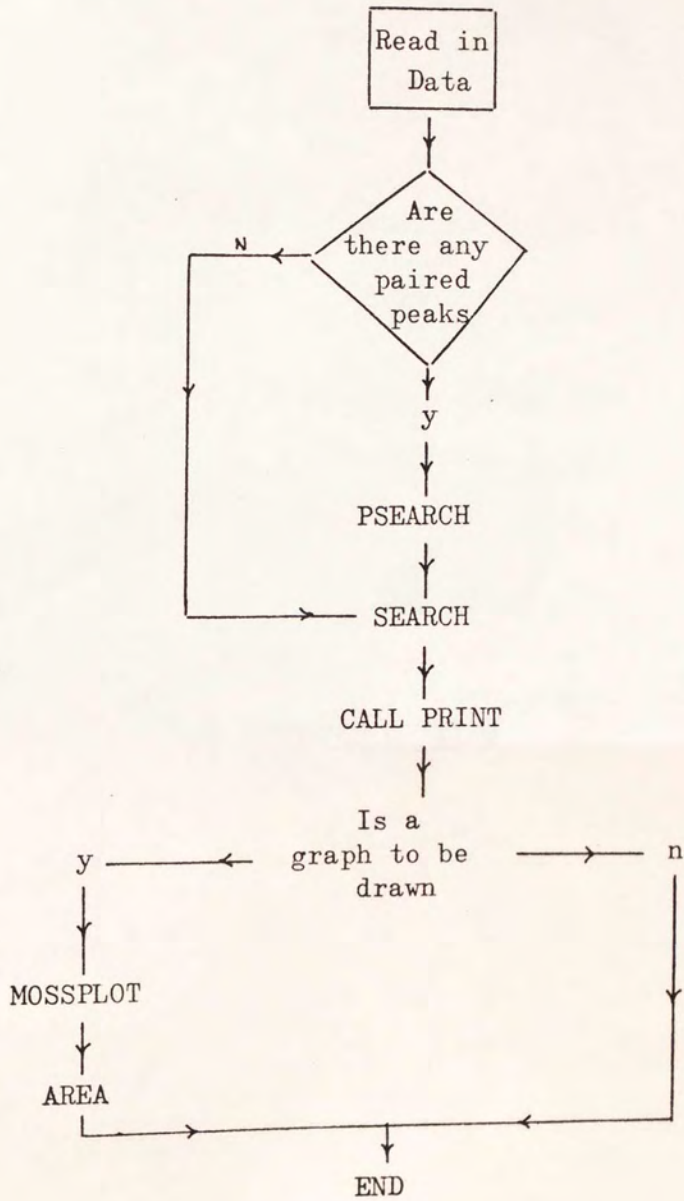
186

I:7 MAJOR NAMES USED IN THE PROGRAM

- ABMAX : maximum size of the y-axis.
- ALPHA : The constant C of the Lorentzian equation.
- AREA : Area under the curve calculated by Simpsons Rule.
- B : Array that contains the text for the graph, this is automatically entered in the Block Data section.
- BETA : Array; contains the line widths for the peaks.
- CHISQ : Chi-squared value.
- IPLLOT : Integer to specify type of graph drawn.
- JPLOT : Integer to specify whether the graphing routine is carried out or not.
- M : Integer: the number of peaks.
- NPAIR : Number of paired peaks.
- PAIR : Specified whether paired peaks are present or not.

SFX : Scale factor for the x-axis.  
 SFY : Scale factor for the y-axis.  
 SSQI : Initial sum of the square.  
 SSQ : Sum of the squares calculated after a search has  
 been carried out.  
 TH : Array; containing the theoretical calculated values.  
 VAR 1 : Lower Limit for chi-squared value.  
 VAR 2 : Upper Limit for chi-squared value.  
 VEL : Velocity in mm/s per channel.  
 XO : Array; contains the positions of the peaks  
 XX : Array; containing the number of channels  
 YO : Array; containing the intensities of the peaks.  
 YY : Array; containing the counts per channel, i.e.  
 the experimental data.  
 ZERO : Reference position from which all shifts and  
 quadrupole splits are measured

I:8 FLOW DIAGRAM (simplified).



I:9 PROGRAM LISTING

MASTER MFIT

```

C *****
C THIS PROGRAM FITS LORENTZIAN CURVES TO
C EXPERIMENTAL MOSSBAUER DATA.
C DATA IS OBTAINED FOM A 400 CHANNEL
C MULTI-CHANNEL ANALYSER.
C THE PROGRAM CAN COPE WITH UP TO TEN
C PEAKS, APPROXIMATE VALUES OF BETA,XO,
C YO ARE ENTERED,THE NUMBER OF PEAKS(M)
C IS ASSUMED AND THE BEST FIT CURVE IS
C CALCULATED
C *****
C M      = NUMBER OF PEAKS
C BETA   = LINE WIDTH
C YO     = MAXIMUM INTENSITY
C XO     = POSITION OF MAXIMUM INTENSITY
C PAIR   = IF +1 PAIRED PEAKS
C         IF -1 NO PAIRED PEAKS
C NPAIR  = NUMBER OF PAIRED PEAKS
C VEL    = VELOCITY/CHANNEL
C JPLOT  = IF NEGATIVE NO GAPH WILL BE
C         DRAWN
C IPLOT  = IF EQUAL TO 1 THEN THE GRAPH
C         DRAWN WILL BE IN CHANNELS,
C         OTHERWISE THE ZERO REFERENCE
C         POSITION WILL BE REQUIRED.
C ABMAX  = VALUE > MAXIMUM INTENSITY.
C SIZEX  = SIZE OF X-AXIS.
C SIZEY  = SIZE OF Y-AXIS.
C ALPHA  = CONSTANT DEPENDANT ON BETA,
C         YO,XO.
C CHISQ  = CHI SQUARED VALUE.
C SSQ    = SUM OF SQUARES.
C SSQI   = INITIAL SUM OF SQUARES.
C *****

```

```

DIMENSION XXP(400)
DIMENSION YN(40)
DIMENSION BCD(2),B(1)
COMMON/MOSSA/XX(400),YY(400),TH(400),ALPHA(10)
COMMON/MOSSB/BETA(10),YO(10),XO(10),BASE,M,SSQ
COMMON/MOSSC/L,SEX,SFY,AREA,B,BCD,CHISQ,DX,ABMAX
COMMON /CPRINT/ VEL,SSQI
COMMON /CPLOT/JPLOT,IPLOT
COMMON/CSYMB/XXP
READ (1,111) B

```

```

C-EAD IN YY-VALUES
I=1
N=10
DO 1 L=1,40
READ(1,100) YM,(YY(J),J=I,N)
YN(L)=YM
I=I+10
N=N+10
1 CONTINUE
READ (1,101) M
READ(1,102) (BETA(I),I=1,10)
READ(1,102) (YO(I),I=1,10)
READ(1,102) (XO(I),I=1,10)
READ (1,103) PAIR,NPAIR,VEL
READ(1,109) JPLOT,IPLOT
DO 200 I=1,M
IF (40-BETA(I))201,200,200
201 WITE (2,300)

```



```

GO TO 18
200 CONTINUE
DO 202 I=1,M
IF (30-YO(I)) 203,202,202
203 WRITE (2,300)
GO TO 18
202 CONTINUE
DO 204 I=1,M
IF (400-XO(I))205,205,204
205 WRITE (2,300)
300 FORMAT(52H PLEASE CHECK IF DATA HAS BEEN PUNCHED CORECTLY )
GO TO 18
204 CONTINUE
DO 12 I=1,M
IF(XO(I)-30)20,12,12
20 WRITE(2,112)
112 FORMAT (49H PEAK TOO CLOSE TO AXIS FOR PROGRAM TO BE VALID)
GO TO 18
12 CONTINUE
C-ENTER X-VALUES INTO ARRAY
C *****
SUM=0
DO 3 I=1,400
SUM=SUM+1.0
3 XX(I)=SUM
C-CALCULATE BASE LINE
C *****
SUM=0
DO 7 I=1,10
7 SUM=SUM+YY(I)
BASE=SUM/10
WRITE (2,101) M
WRITE(2,106) (BETA(I),I=1,10)
WRITE(2,106) (XO(I),I=1,10)
WRITE(2,106) (YO(I),I=1,10)
WRITE (2,103) PAIR,NPAIR,VEL
VAR=M*3.0
VAR=400-VAR
RAV=SQRT(VAR)
VAR1=(VAR+2.2)-(3.3*RAV)
VAR2=(VAR+2.2)+(3.3*RAV)
C-ARE THERE ANY PAIRS
C *****
IF (PAIR.GE.0.0) GOTO 90
IF (PAIR.LE.0.0) GOTO 80
90 CONTINUE
NNPAIR=NPAIR+1
DO 17 K=1,2
DO 5 L=1,NNPAIR,2
CALL PSEARCH
WRITE(2,106) (BETA(I),I=1,10)
WRITE(2,106) (XO(I),I=1,10)
WRITE(2,106) (YO(I),I=1,10)
WRITE(2,105) SSQ
WRITE(2,107) CHISQ
5 CONTINUE
IF(CHISQ.LT.VAR2.AND.CHISQ.GT.VAR1)GO TO 19
17 CONTINUE
GOTO 80
80 CONTINUE
DO 9 K=1,3
DO 11 L=1,M
CALL SEARCH

```

```

WRITE(2,106) (BETA(I),I=1,10)
WRITE(2,106) (XO(I),I=1,10)
WRITE(2,106) (YO(I),I=1,10)
WRITE(2,105) SSQ
WRITE(2,107) CHISQ
11 CONTINUE
IF(CHISQ.LT.VAR2.AND.CHISQ.GT.VAR1)GO TO 19
9 CONTINUE
19 CONTINUE
CALL PRINT
IF(JPLOT.LT.0.0)GO TO 18
CALL HG PLOT (0.0,0.0,6,1)
CALL MOSSPLOT
CALL HG PLOT (0.0,0.0,0,2)
18 CONTINUE
C-*****
100 FORMAT (F2.0,10(F7.0))
101 FORMAT(I3)
102 FORMAT(10F7.2)
103 FORMAT(F3.0,I3,F6.4)
105 FORMAT(F15.2)
106 FORMAT(10(F7.2,2X))
107 FORMAT (F15.1)
109 FORMAT (2I3)
111 FORMAT(A8)
STOP
END
SUBROUTINE PSSQ
C SUBROUTINE FOR CALCULATING SSQ
C *****
DIMENSION BCD(2),B(1)
COMMON/MOSSA/XX(400),YY(400),TH(400),ALPHA(10)
COMMON/MOSSB/BETA(10),YO(10),XO(10),BASE,M,SSQ
COMMON/MOSSC/L,SEX,SFY,AREA,B,BCD,CHISQ,DX,ABMAX
SSQ=0.0
DO 2 J=1,400
TH(J)=0.0
DO 3 I=1,M
ALPHA(I)=(BETA(I)*BETA(I)*0.25)*YO(I)
PEM=XX(J)-XO(I)
EMP=PEM*PEM
ETA=(BETA(I)*BETA(I))*0.25
TEMP=ALPHA(I)/(EMP+ETA)
3 TH(J)=TH(J)+TEMP
TH(J)=TH(J)*0.01*BASE
TH(J)=BASE-TH(J)
ERROR=YY(J)-TH(J)
SUM=ERROR*ERROR
SSQ=SSQ+SUM
2 CONTINUE
RETUN
END
SUBROUTINE SEARCH
C-LEAST SQUARES LOENTZIAN BEST FIT SEARCH
C *****
DIMENSION BCD(2),B(1)
COMMON/MOSSA/XX(400),YY(400),TH(400),ALPHA(10)
COMMON/MOSSB/BETA(10),YO(10),XO(10),BASE,M,SSQ
COMMON/MOSSC/L,SEX,SFY,AREA,B,BCD,CHISQ,DX,ABMAX
CALL PSSQ
SSQI=SSQ
220 BETA(L)=BETA(L)+1

```

```

CALL PSSQ
IF (SSQ.LE.SSQI)GO TO 100
200 BETA(L)=BETA(L)-1
SSQI=SSQ
CALL PSSQ
IF (SSQ.LE.SSQI)GO TO 200
210 BETA(L)=BETA(L)+1
CALL PSSQ
GO TO 300
100 BETA(L)=BETA(L)+1
SSQI=SSQ
CALL PSSQ
IF (SSQ.LE.SSQI)GO TO 100
110 BETA(L)=BETA(L)-1
CALL PSSQ
GO TO 300
300 SSQI=SSQ
YO(L)=YO(L)+0.2
CALL PSSQ
IF (SSQ.LE.SSQI)GO TO 300
310 SSQI=SSQ
YO(L)=YO(L)-0.2
CALL PSSQ
IF (SSQ.LE.SSQI)GO TO 310
YO(L)=YO(L)+0.2
CALL PSSQ
400 SSQI=SSQ
XO(L)=XO(L)+1
CALL PSSQ
IF (SSQ.LE.SSQI)GO TO 400
410 XO(L)=XO(L)-1
SSQI=SSQ
CALL PSSQ
IF (SSQ.LE.SSQI)GO TO 410
XO(L)=XO(L)+1
CALL PSSQ
SSQI=SSQ
CHISQ=0
DO 15 I=1,400
TEMPS=YY(I)-TH(I)
PEMT=(TEMPS*TEMPS)/TH(I)
CHISQ=CHISQ+PEMT
15 CONTINUE
RETURN
END

```

SUBROUTINE PSEARCH  
C-LEAST SQUARES LORENTZIAN FIT FOR QUAD. SPLIT PEAKS

C

```

*****
DIMENSION BCD(2),B(1)
COMMON/MOSSA/XX(400),YY(400),TH(400),ALPHA(10)
COMMON/MOSSB/BETA(10),YO(10),XO(10),BASE,M,SSQ
COMMON/MOSSC/L,SEX,SFY,AREA,B,BCD,CHISQ,DX,ABMAX
CALL PSSQ
SSQI=SSQ
220 BETA(L)=BETA(L)+1
BETA(L+1)=BETA(L)
CALL PSSQ
IF (SSQ.LE.SSQI)GO TO 100
200 BETA(L)=BETA(L)-1
BETA(L+1)=BETA(L)
SSQI=SSQ
CALL PSSQ
IF (SSQ.LE.SSQI)GO TO 200
210 BETA(L)=BETA(L)+1

```

```

      BETA(L+1)=BETA(L)
      CALL PSSQ
      GO TO 300
100  BETA(L)=BETA(L)+1
      BETA(L+1)=BETA(L)
      SSQI=SSQ
      CALL PSSQ
      IF (SSQ.LE.SSQI)GO TO 100
110  BETA(L)=BETA(L)-1
      BETA(L+1)=BETA(L)
      CALL PSSQ
      GO TO 300
300  SSQI=SSQ
      YO(L)=YO(L)+0.2
      YO(L+1)=YO(L)
      CALL PSSQ
      IF (SSQ.LE.SSQI)GO TO 300
310  SSQI=SSQ
      YO(L)=YO(L)-0.2
      YO(L+1)=YO(L)
      CALL PSSQ
      IF (SSQ.LE.SSQI)GO TO 310
      YO(L)=YO(L)+0.2
      YO(L+1)=YO(L)
      CALL PSSQ
400  SSQI=SSQ
      DO 500 I=1,M
405  SSQI=SSQ
      XO(I)=XO(I)+1
      CALL PSSQ
      IF (SSQ.LE.SSQI)GO TO 405
410  XO(I)=XO(I)-1
      SSQI=SSQ
      CALL PSSQ
      IF (SSQ.LE.SSQI)GO TO 410
      XO(I)=XO(I)+1
      CALL PSSQ
      SSQI=SSQ
500  CONTINUE
      CHISQ=0.0
      DO 15 I=1,400
      TEMPS=YY(I)-TH(I)
      PEMT=(TEMPS*TEMPS)/TH(I)
      CHISQ=CHISQ+PEMT
      15 CONTINUE
      RETURN
      END
      SUBROUTINE MOSSPLOT
C SUBROUTINE FOR PLOTTING CALCULATED FIT
C *****
      DIMENSION BCD(2),B(1)
      DIMENSION XXP(400)
      COMMON/MOSSA/XX(400),YY(400),TH(400),ALPHA(10)
      COMMON/MOSSB/BETA(10),YO(10),XO(10),BASE,M,SSQ
      COMMON/MOSSC/L,SEX,SPY,AREA,B,BCD,CHISQ,DX,ABMAX
      COMMON /CPRINT/ VEL,SSQI
      COMMON /CPLOT/JPLOT,IPLOT
      COMMON/CSYMB/XXP
      READ(1,104) ABMAX
104  FORMAT (F6.2)
      READ (1,105) SIZEX,SIZEY

```

```

105 FORMAT (2F6.2)
DY=ABMAX/4
DX=40.0
SFX=SIZEX/400
SFY=SIZEY/ABMAX
GAPY=SIZEY/4
GAPX=(SIZEX/400)*DX
IF (GAPY.GT.3.0) NH=4
IF (GAPY.LT.3.0) NH=3
C PLOT EXPERIMENTAL POINTS
DO 1 I=1,400
YY(I)={ (BASE-YY(I)) / BASE } * 100
YY(I)={ ABMAX+YY(I) } - (2*YY(I))
YY(I)=YY(I)*SFY
XXP(I)=XX(I)*SFX
1 CONTINUE
CALL HGXPLOT (0.0,25.0,0,4)
CALL SYMBPLOT
CALL HGPAXISV (0.0,0.0,BCD(1),8,SIZEY,90.0,0.0,DY,GAPY,NH)
CALL HGPSYMBL (4.0,-2.0,0.6,B,0.0,8)
C PLOT THE WHOLE CURVE
DO 2 J=1,400
TH(J)=0.0
DO 3 I=1,M
PEM=XX(J)-XO(I)
EMP=PEM*PEM
ETA=BETA(I)*BETA(I)/4.0
TEMP=ALPHA(I)/(EMP+ETA)
TH(J)=TH(J)+TEMP
3 CONTINUE
2 CONTINUE
DO 4 I=1,400
TH(I)={ ABMAX+TH(I) } - (2*TH(I))
TH(I)=TH(I)*SFY
4 CONTINUE
CALL HGPLINE (XXP,TH,400,1)
C-PLOT INDIVIDUAL CURVES
DO 5 I=1,M
DO 6 J=1,400
TH(J)=0.0
PEM=XX(J)-XO(I)
EMP=PEM*PEM
ETA=BETA(I)*BETA(I)/4.0
TEMP=ALPHA(I)/(EMP+ETA)
TH(J)=TH(J)+TEMP
6 CONTINUE
CALL CALAREA
IF(JPLOT.E.2)GO TO 8
DO 7 K=1,400
TH(K)={ ABMAX+TH(K) } - (2*TH(K))
TH(K)=TH(K)*SFY
7 CONTINUE
CALL HGPLINE (XXP,TH,400,1)
8 CONTINUE
5 CONTINUE
IF(IPLOT.EQ.1)GO TO 9
C- VELOCITY SCALE PLOT
C- ZERO= POSITION OF ZERO REF. POINT
READ(1,106) ZERO
106 FORMAT(F6.2)
GAPZ=SIZEX/(400*VEL)
CENT=(400*VEL)/2

```

```

TEC=ANINT(CENT)
SIZEZ=GAPZ*TEC
DZ=1.0
XZ=SFX*ZERO
CET=TEC*GAPZ
0 IF (GAPZ.GT.3.0) NH=4
  IF (GAPZ.LT.3.0) NH=3
  CALL HGPlot(0.0,0.0,3,0)
  CALL HGPlot(-XZ,0.0,0,4)
  CALL HGPAXISV(0.0,0.0,BCD(2),-8,SIZEZ,0.0,0.0,DZ,GAPZ,NH)
  CALL HGPAXISV(-CET,0.0,BCD(2),-8,SIZEZ,0.0,-TEC,DZ,GAPZ,NH)
  GO TO 10
9 CONTINUE
  IF (GAPX.LT.3.0) NH=3
  IF (GAPX.GT.3.0) NH=4
  CALL HGPAXISV(0.0,0.0,BCD(2),-8,SIZEZ,0.0,0.0,DX,GAPX,NH)
10 CONTINUE
  RETURN
  END
  SUBROUTINE CALAREA

```

C- AREA UNDER CURVE BY SIMPSONS RULE

C \*\*\*\*\*

```

DIMENSION BCD(2),B(1)
COMMON/MOSSA/XX(400),YY(400),TH(400),ALPHA(10)
COMMON/MOSSB/BETA(10),YO(10),XO(10),BASE,M,SSQ
COMMON/MOSSC/L,SEX,SFY,AREA,B,BCD,CHISQ,DX,ABMAX
H=1.0
EVEN=0.0
DO 1 I=2,388,2
  EVEN=EVEN+TH(I)
1 CONTINUE
  ODD=0.0
  DO 2 I=3,387,2
    ODD=ODD+TH(I)
2 CONTINUE
  ODD=ODD*2.0
  EVEN=EVEN*4.0
  AREA=(H/3.0)*(TH(1)+EVEN+ODD+TH(399))
  WITE(2,3) AREA
3 FORMAT(14H      AREA = ,F10.2)
  RETURN
  END
  SUBROUTINE SYMBPLOT

```

C-SUB/R FOR PLOTTING 400 POINTS IN FORM OF +

C \*\*\*\*\*

```

DIMENSION XXP(400)
COMMON/MOSSA/XX(400),YY(400),TH(400),ALPHA(10)
COMMON/MOSSB/BETA(10),YO(10),XO(10),BASE,M,SSQ
COMMON/MOSSC/L,SEX,SFY,AREA,B,BCD,CHISQ,DX,ABMAX
COMMON/CSYMB/XXP
DO 10 I=1,400
  X=XXP(I)
  Y=YY(I)
  CALL HGPlot(X,Y,3,0)
  CALL HGPlot(X+0.1,Y,2,0)
  CALL HGPlot(X-0.1,Y,1,0)
  CALL HGPlot(X,Y,1,0)
  CALL HGPlot(X,Y+0.1,1,0)
  CALL HGPlot(X,Y-0.1,1,0)
  CALL HGPlot(X,Y,1,0)
10 CONTINUE
  RETURN
  END

```

## SUBROUTINE PRINT

## C-PRINTING SUBROUTINE

C

\*\*\*\*\*

```

DIMENSION BCD(2),B(1)
COMMON/MOSSA/XX(400),YY(400),TH(400),ALPHA(10)
COMMON/MOSSB/BETA(10),YO(10),XO(10),BASE,M,SSQ
COMMON/MOSSC/L,SEX,SPY,AREA,B,BCD,CHISQ,DX,ABMAX
COMMON/CPRINT/VEL,SSQI
CALL DATE(DAT)
WRITE(2,1) B,DAT
1 FORMAT(1H1,30X,48HMOSSBAUER SPECTRUM ANALYSIS ( J.M.COULTHARD
1///10X,30H CURVE FITTED FOR SAMPLE ,A8,20X,7H DATE ,A8//)
WRITE(2,9)M,VEL
9 FORMAT(27H NUMBER OF PEAKS = ,I3,10X,12HVELOCITY = ,F6.1
1,21H MM/SEC PER CHANNEL ///,23X,12H ALPHA ,5X18H BETA LINE
2WIDTH,5X,14H YO INTENSITY,5X,22H XO POSITION OF PEAK///)
DO 20 I=1,M
WRITE(2,3)I,ALPHA(I),BETA(I),YO(I),XO(I)
3 FORMAT (10H CURVE ,I3,7X,4(F10.2,12X))
20 CONTINUE
WRITE(2,4)
4 FORMAT(///)
CALL PSSQ
SSQI=SSQ
CHISQ=0.0
DO 15 I=1,400
TEMP=YY(I)-TH(I)
PEMT=(TEMP*TEMP)/TH(I)
CHISQ=CHISQ+PEMT
15 CONTINUE
WRITE(2,7)CHISQ
7 FORMAT (40H DEGREE OF FIT (CHI-SQUARED TEST ) = ,F15.1//)
WRITE (2,8) SSQI
8 FORMAT (27H FINAL SUM OF SQUARES = ,F15.1,///)
VAR=M*3.0
VAR=400-VAR
RAV=SQRT(VAR)
VAR1=(VAR+2.2)-(3.3*RAV)
VAR2=(VAR+2.2)+(3.3*RAV)
WRITE(2,5) VAR1,VAR2
5 FORMAT (4X,F7.2,11H < CHISQ < ,F7.2///)
IF(CHISQ.LT.VAR2.AND.CHISQ.GT.VAR1) GO TO 16
WRITE (2,6)
6 FORMAT (45H CHI-SQUARED RESULT NOT STATISTICALLY VALID ///)
16 CONTINUE
RETURN
END
BLOCK DATA
DIMENSION BCD(2),B(1)
COMMON/MOSSA/XX(400),YY(400),TH(400),ALPHA(10)
COMMON/MOSSB/BETA(10),YO(10),XO(10),BASE,M,SSQ
COMMON/MOSSC/L,SEX,SPY,AREA,B,BCD,CHISQ,DX,ABMAX
DATA BCD(1)/16HR-ABSORPVELOCITY/
END
FINISH

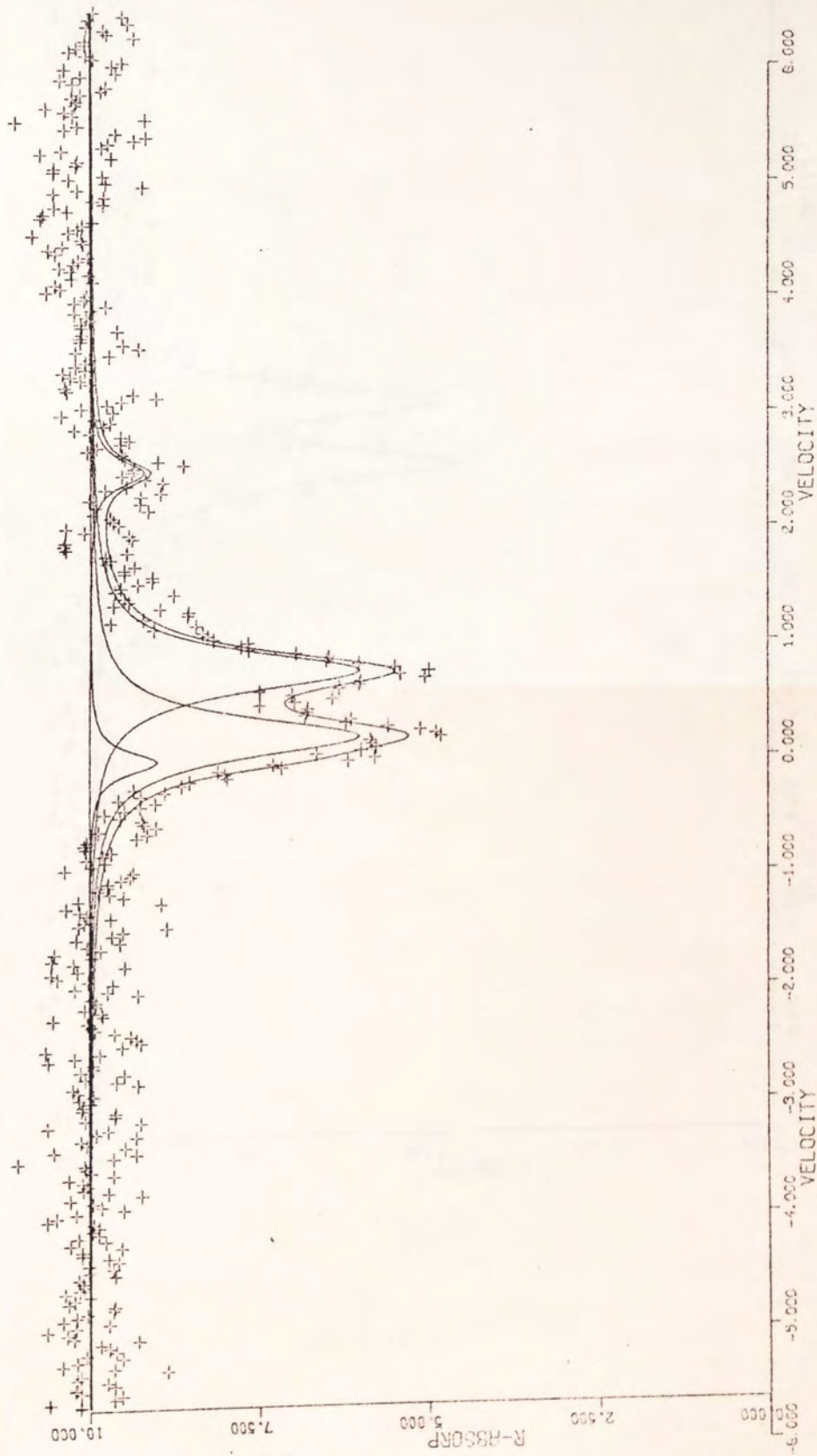
```

\*\*\*\*

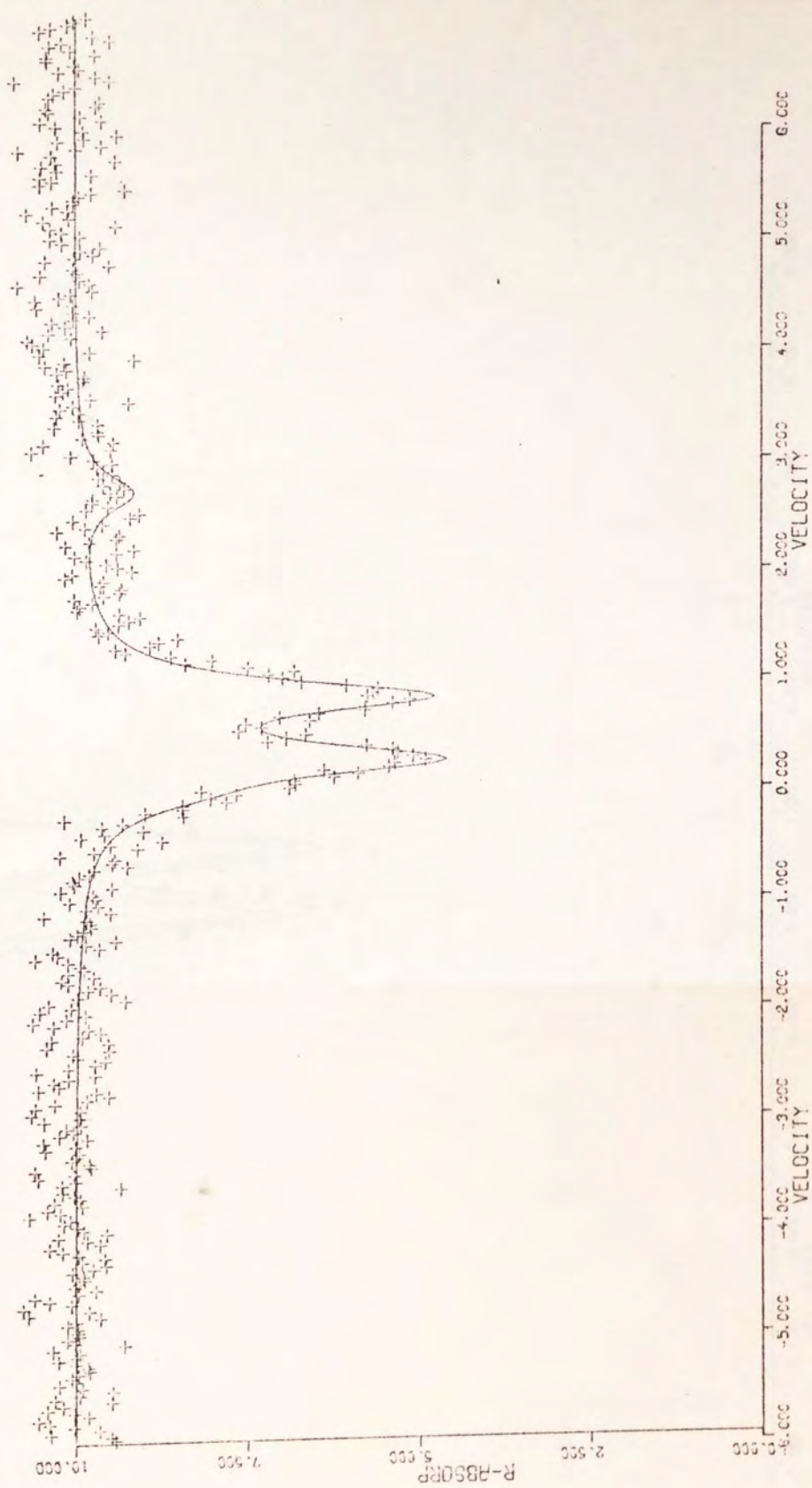
APPENDIX J

I. MOSSBAUER SPECTRA AT ROOM TEMPERATURE

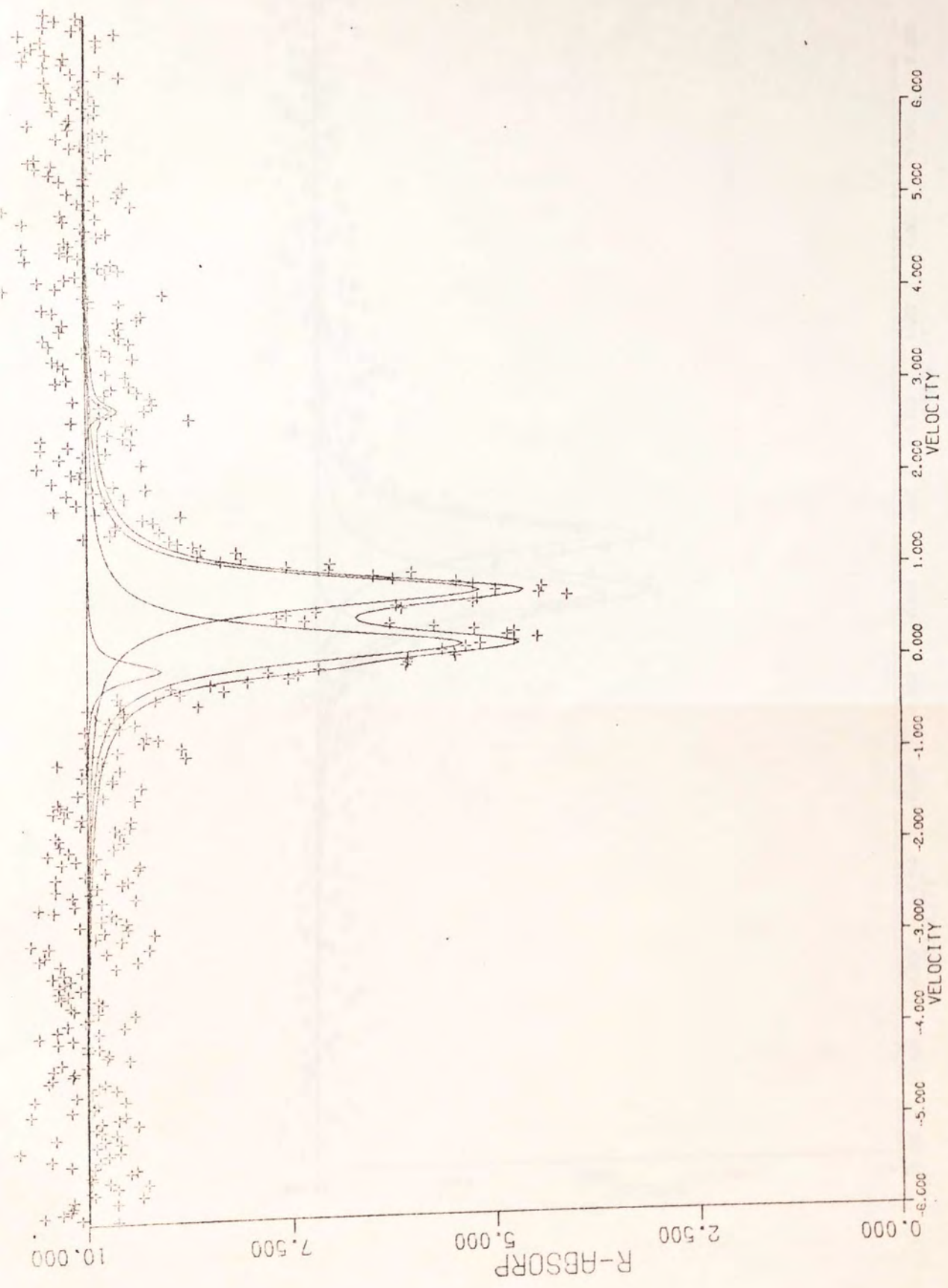




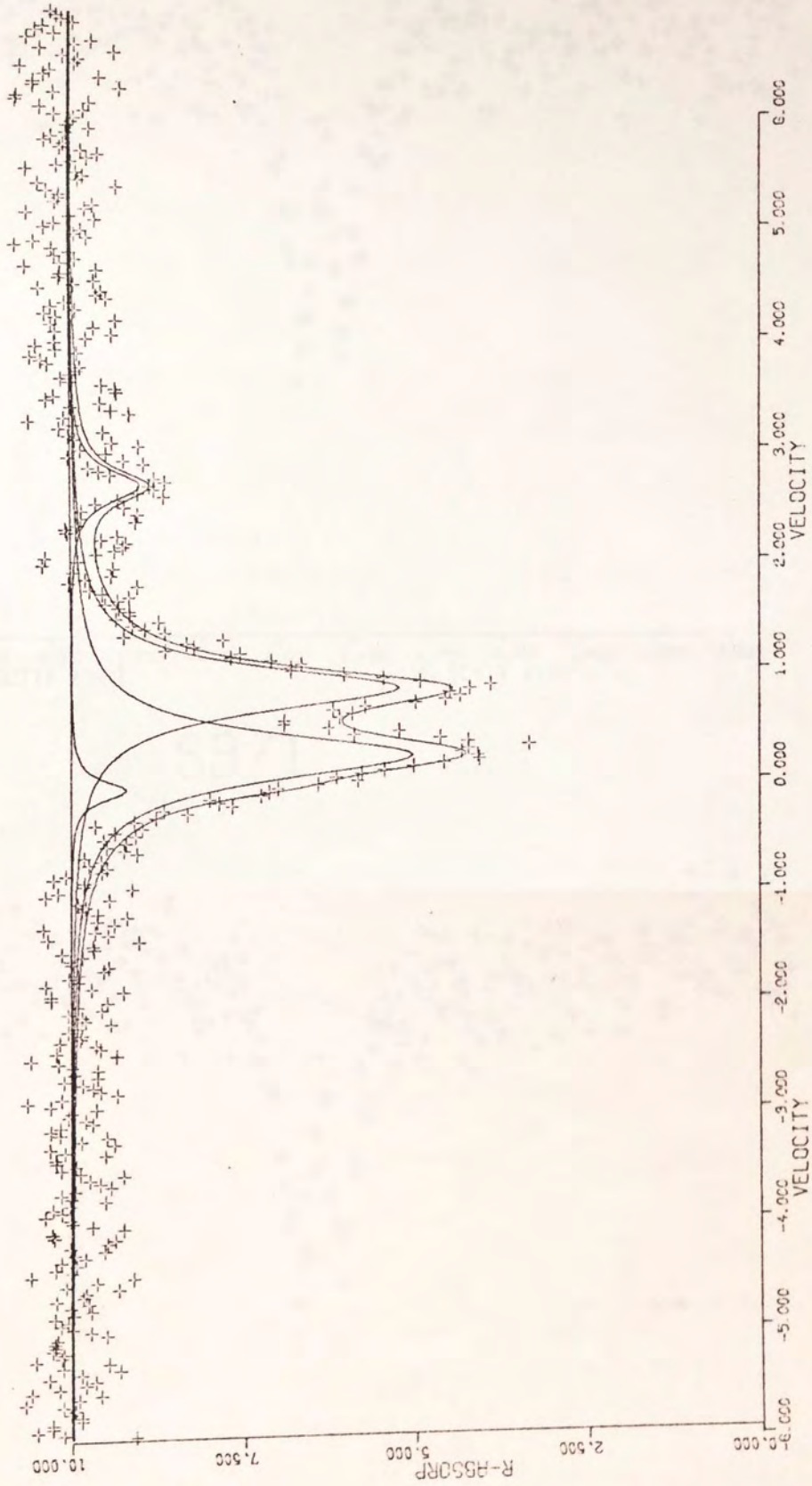
S1/1



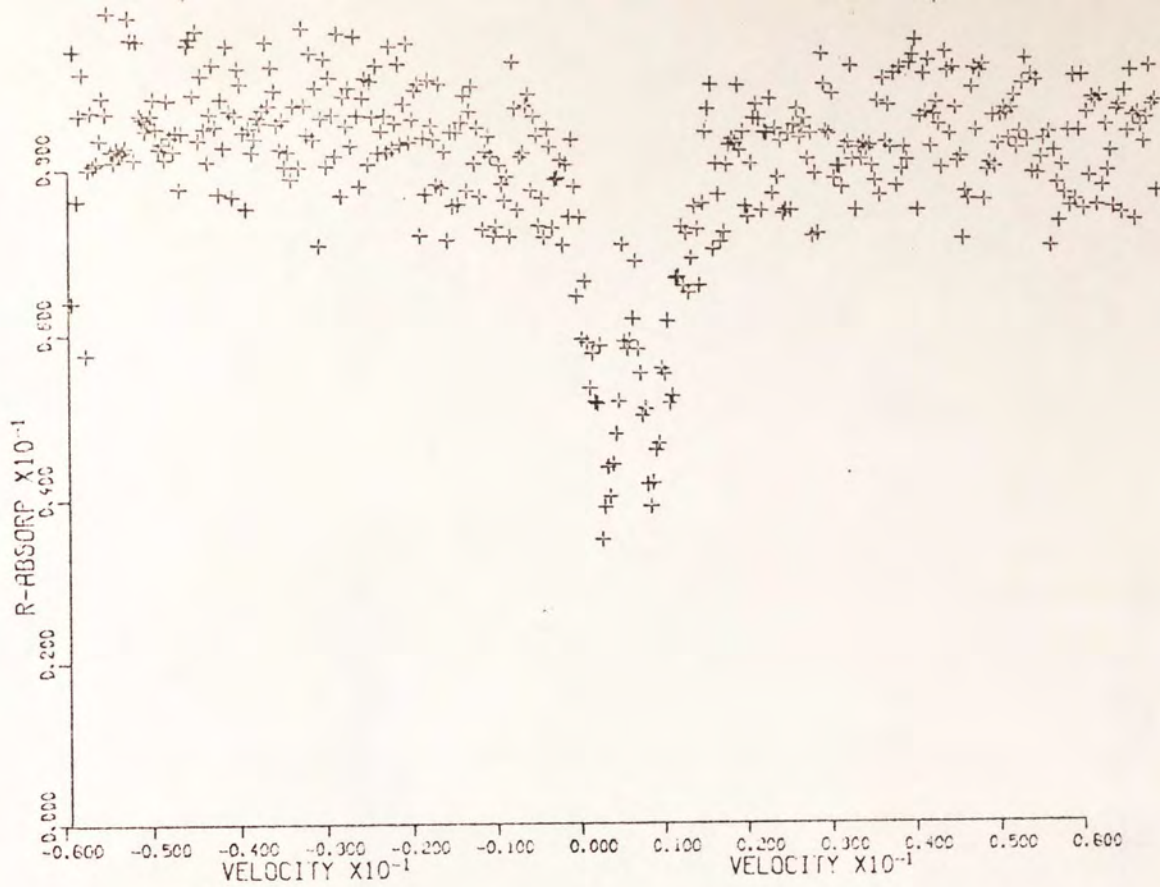
39/1 S2/1



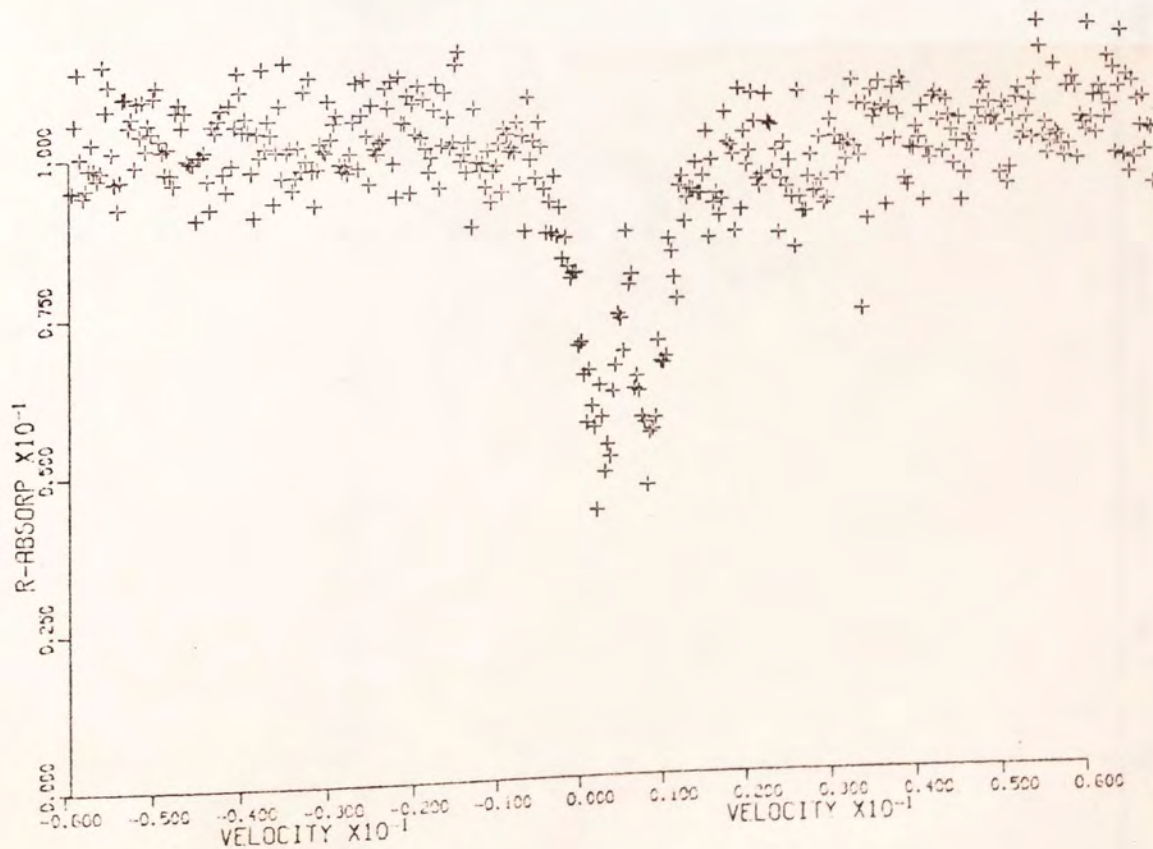
S3/1



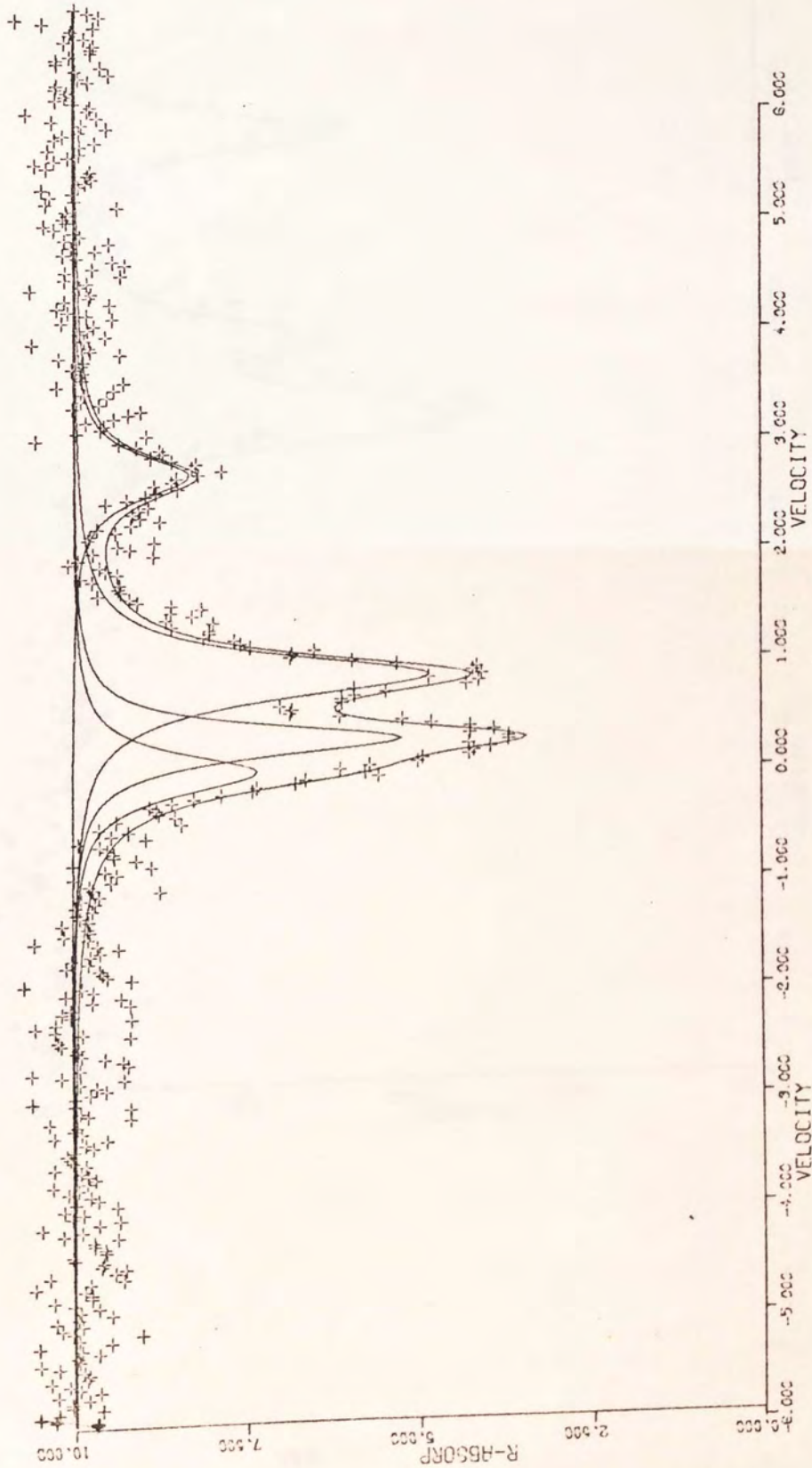
S17/1



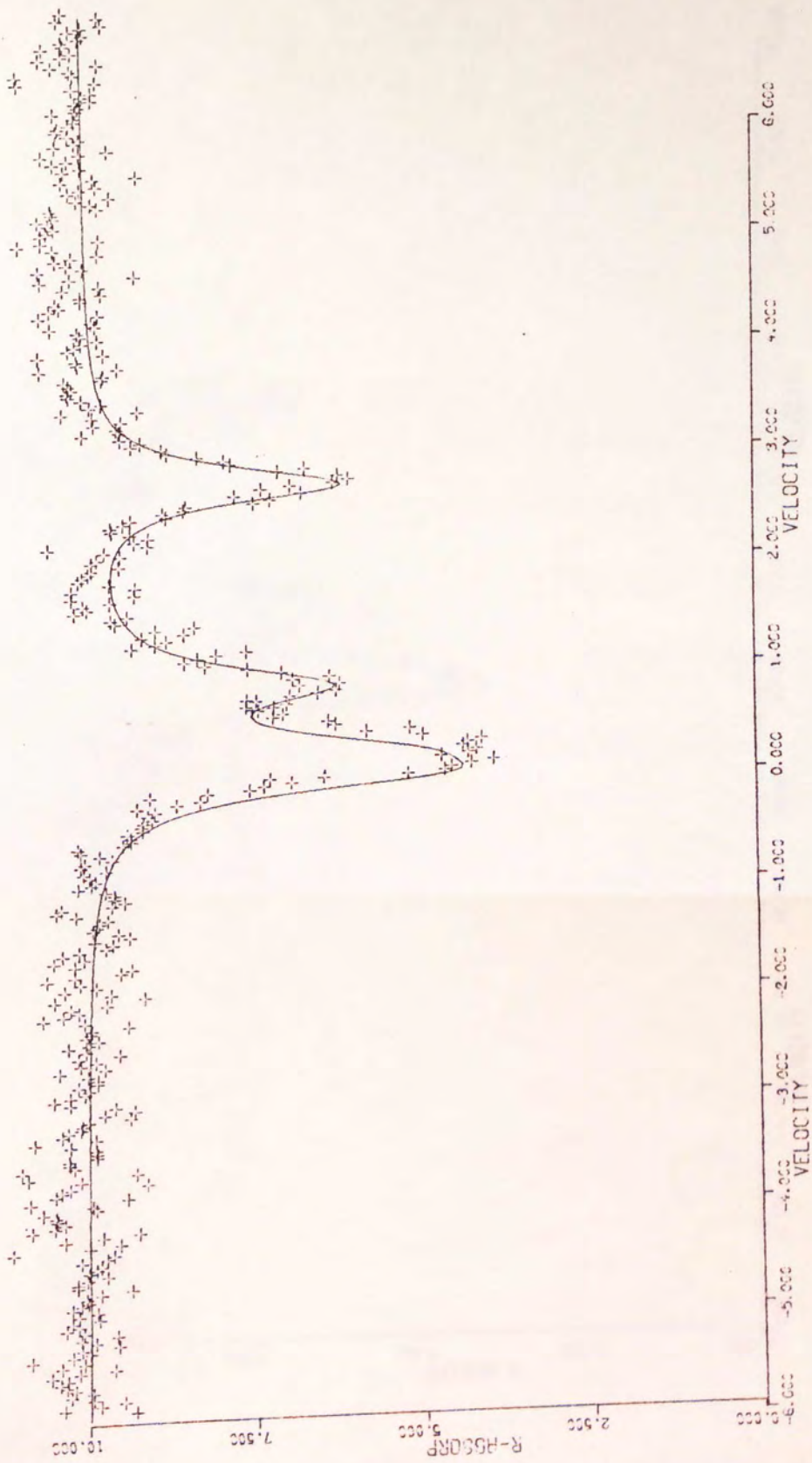
S3/1



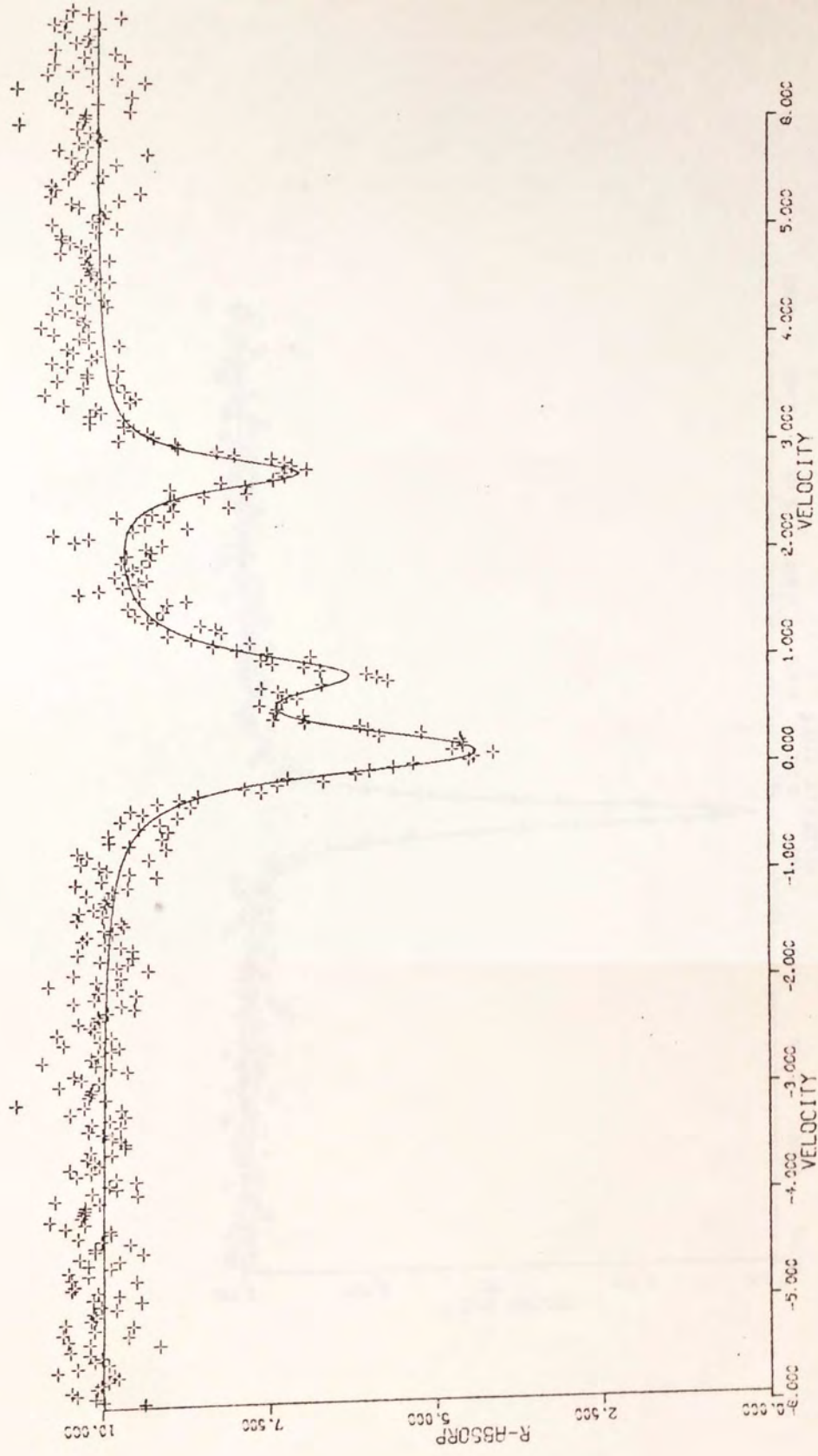
S18/1



S25/1

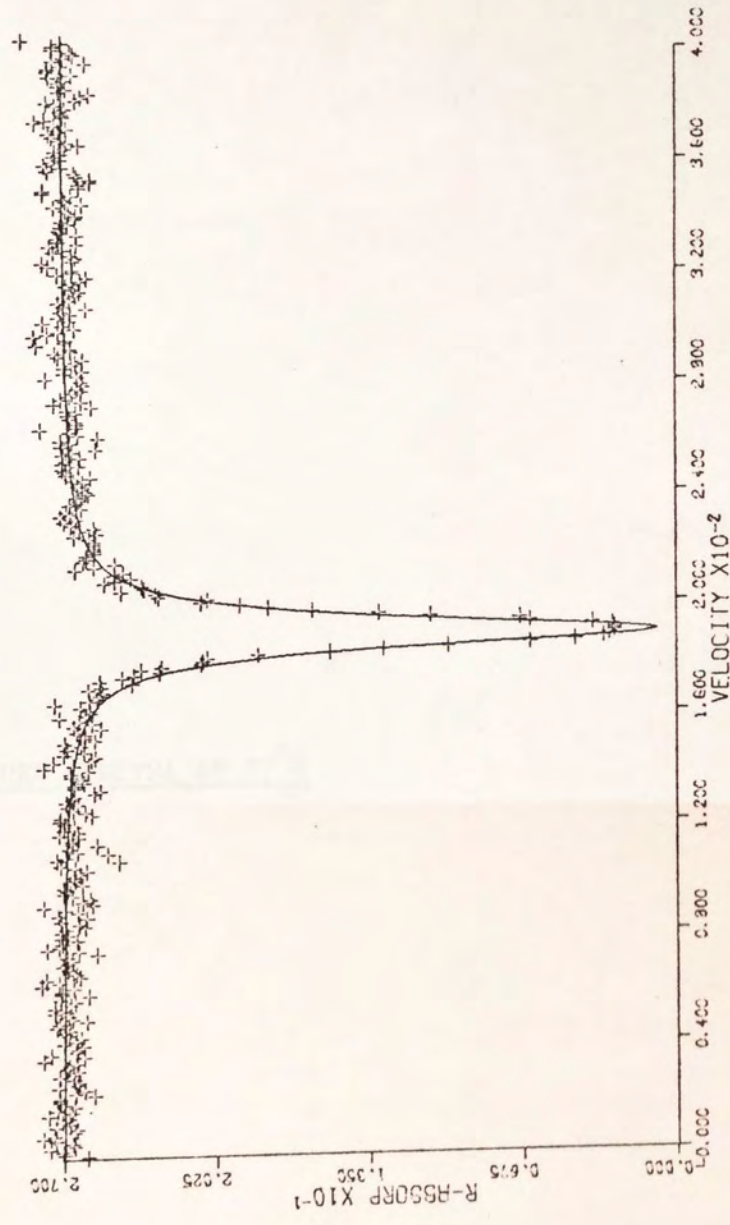


S36/1



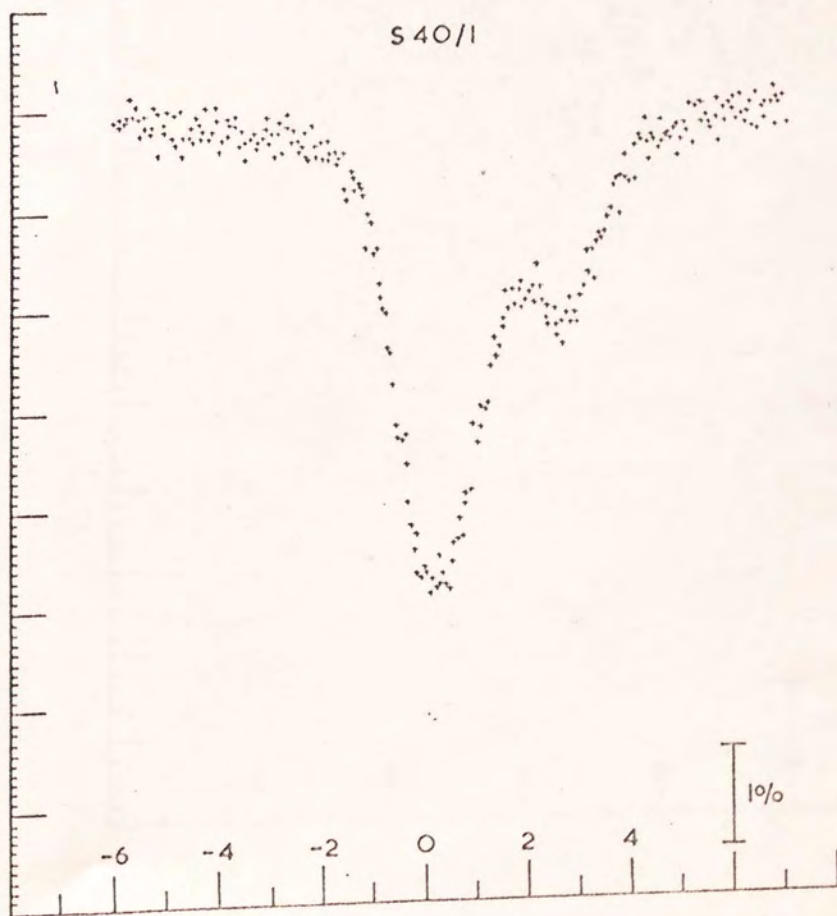
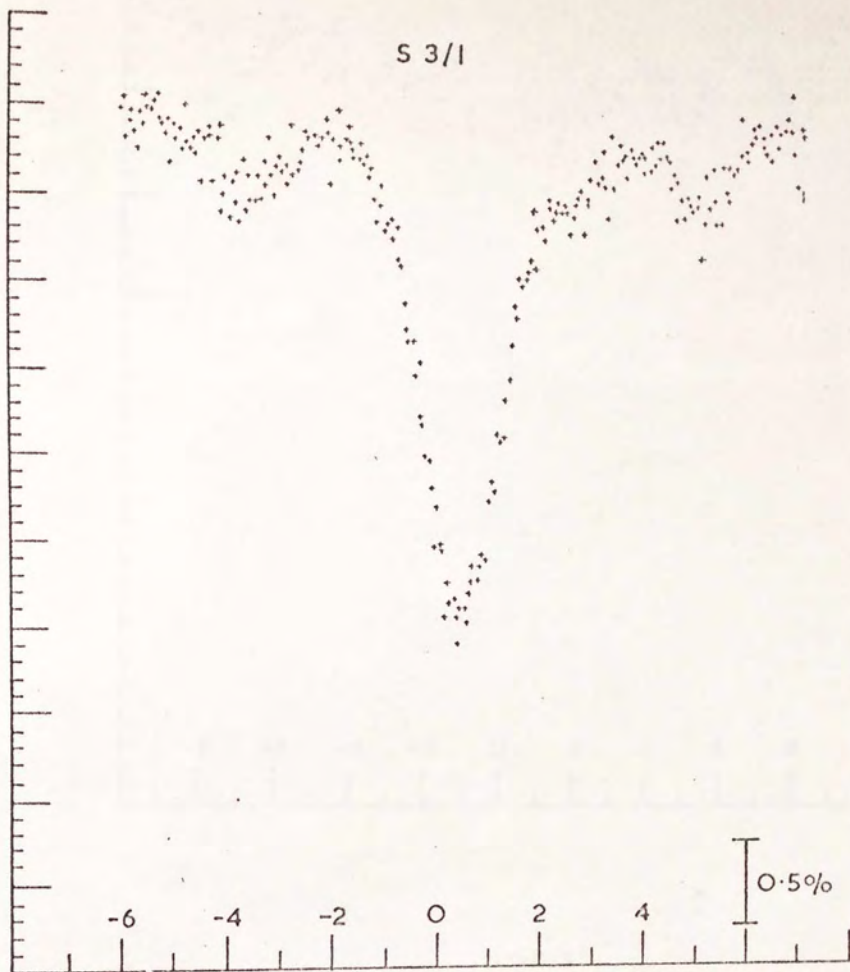
S40/1



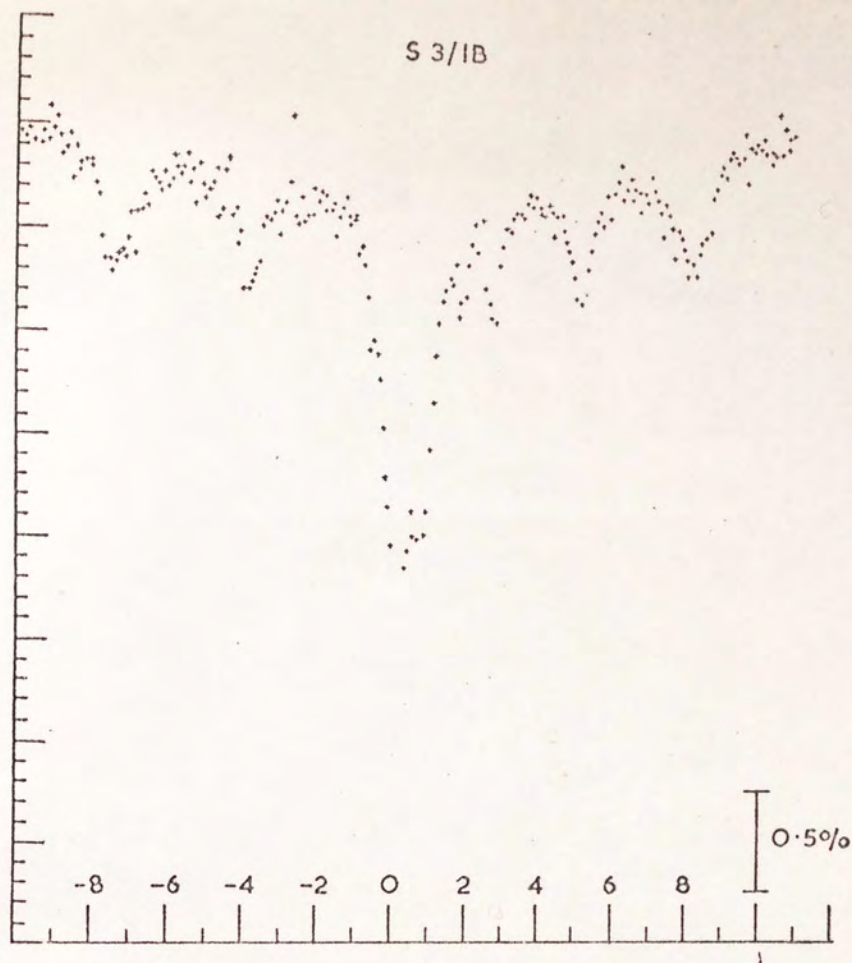


ST-STEEL

II. MOSSBAUER SPECTRA AT 77°K



S 3/1B



S8/1

